

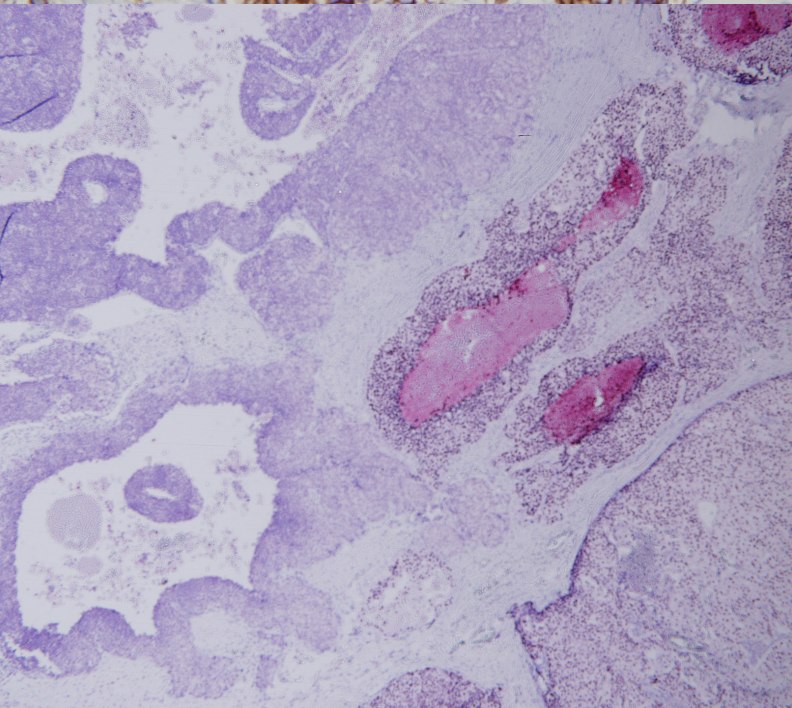
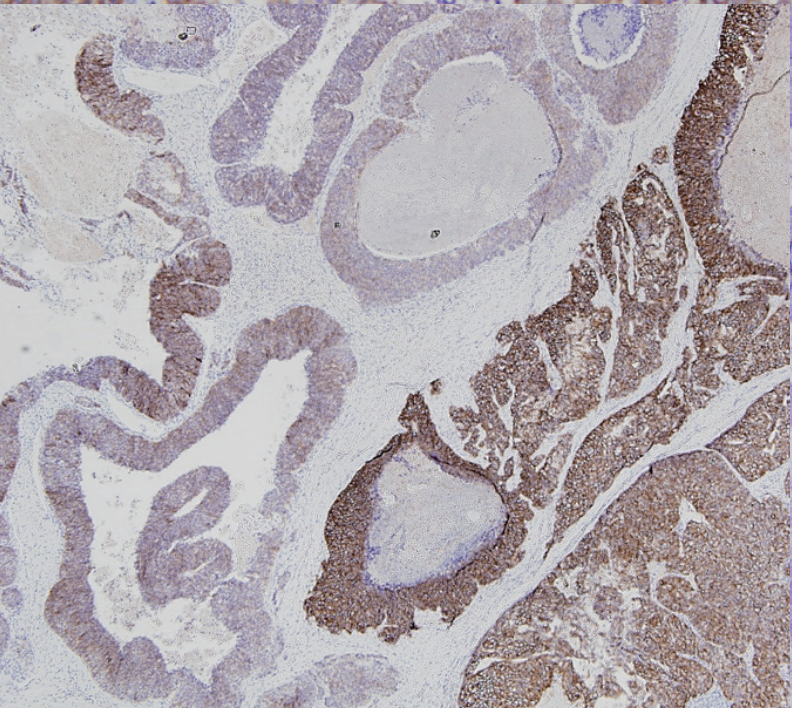
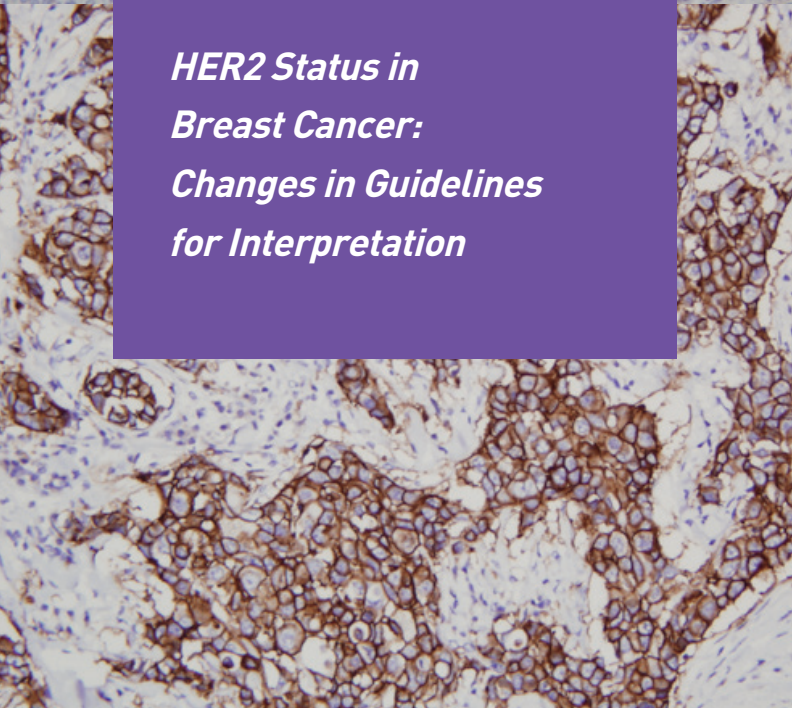
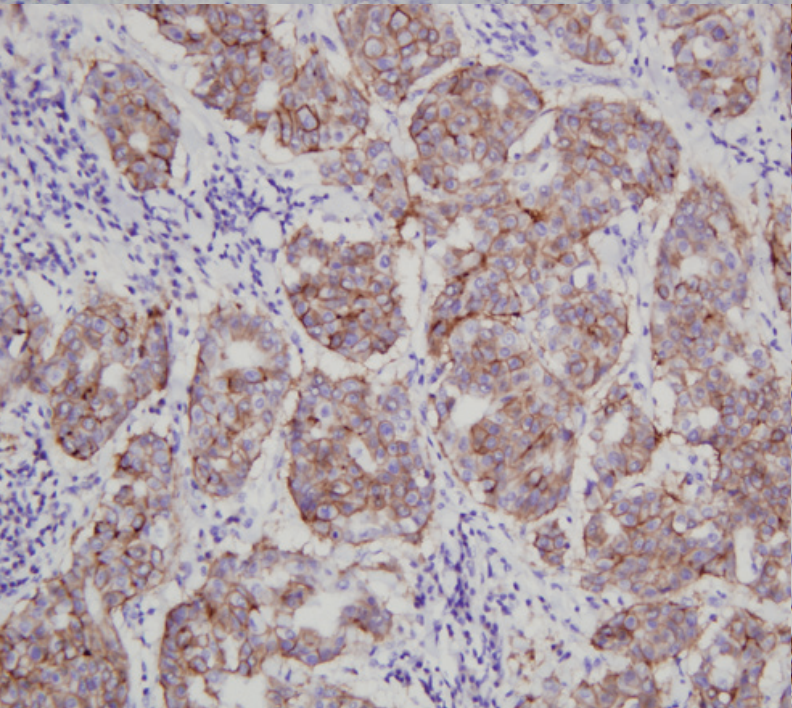
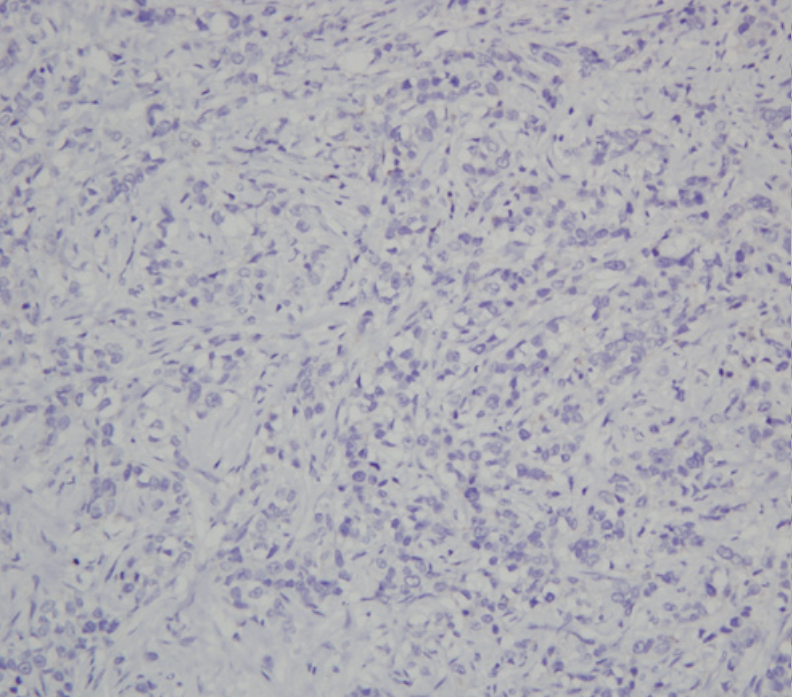
# JPTM

Journal of Pathology  
and Translational Medicine

January 2020  
Vol. 54 / No.1  
jpatholtm.org  
pISSN: 2383-7837  
eISSN: 2383-7845



*HER2 Status in  
Breast Cancer:  
Changes in Guidelines  
for Interpretation*



## Aims & Scope

The *Journal of Pathology and Translational Medicine* is an open venue for the rapid publication of major achievements in various fields of pathology, cytopathology, and biomedical and translational research. The Journal aims to share new insights into the molecular and cellular mechanisms of human diseases and to report major advances in both experimental and clinical medicine, with a particular emphasis on translational research. The investigations of human cells and tissues using high-dimensional biology techniques such as genomics and proteomics will be given a high priority. Articles on stem cell biology are also welcome. The categories of manuscript include original articles, review and perspective articles, case studies, brief case reports, and letters to the editor.

## Subscription Information

To subscribe to this journal, please contact the Korean Society of Pathologists/the Korean Society for Cytopathology. Full text PDF files are also available at the official website (<http://jpatholtm.org>). *Journal of Pathology and Translational Medicine* is indexed by Emerging Sources Citation Index (ESCI), PubMed, PubMed Central, Scopus, KoreaMed, KoMCI, WPRIM, Directory of Open Access Journals (DOAJ), and CrossRef. Circulation number per issue is 700.

## Editors-in-Chief

Jung, Chan Kwon, MD (*The Catholic University of Korea, Korea*) <https://orcid.org/0000-0001-6843-3708>  
Park, So Yeon, MD (*Seoul National University, Korea*) <https://orcid.org/0000-0002-0299-7268>

## Senior Editors

Hong, Soon Won, MD (*Yonsei University, Korea*) <https://orcid.org/0000-0002-0324-2414>  
Kim, Chong Jai, MD (*University of Ulsan, Korea*) <https://orcid.org/0000-0002-2844-9446>

## Associate Editors

Shin, Eunah, MD (*Yongin Severance Hospital, Yonsei University, Korea*) <https://orcid.org/0000-0001-5961-3563>  
Kim, Haeryoung, MD (*Seoul National University, Korea*) <https://orcid.org/0000-0002-4205-9081>

## Editorial Board

Avila-Casado, Maria del Carmen (*University of Toronto, Toronto General Hospital UHN, Canada*)

Bae, Young Kyung (*Yeungnam University, Korea*)

Bongiovanni, Massimo (*Lausanne University Hospital, Switzerland*)

Bychkov, Andrey (*Chulalongkorn University, Thailand Kameda Medical Center, Japan Nagasaki University Hospital, Japan*)

Choi, Yeong-Jin (*The Catholic University of Korea, Korea*)

Chong, Yo Sep (*The Catholic University of Korea, Korea*)

Chung, Jin-Haeng (*Seoul National University, Korea*)

Fadda, Guido (*Catholic University of Rome-Foundation Agostino Gemelli University Hospital, Italy*)

Gong, Gyungyub (*University of Ulsan, Korea*)

Ha, Seung Yeon (*Gachon University, Korea*)

Han, Jee Young (*Inha University, Korea*)

Jain, Deepali (*All India Institute of Medical Sciences, India*)

Jang, Se Jin (*University of Ulsan, Korea*)

Jeong, Jin Sook (*Dong-A University, Korea*)

Jun, Sun-Young (*The Catholic University of Korea, Korea*)

Kang, Gyeong Hoon (*Seoul National University, Korea*)

Kim, Aeree (*Korea University, Korea*)

Kim, Jang-Hee (*Ajou University, Korea*)

Kim, Jung Ho (*Seoul National University, Korea*)

Kim, Kyu Rae (*University of Ulsan, Korea*)

Kim, Se Hoon (*Yonsei University, Korea*)

Kim, Woo Ho (*Seoul National University, Korea*)

Ko, Young Hye (*Sungkyunkwan University, Korea*)

Koo, Ja Seung (*Yonsei University, Korea*)

Lai, Chiung-Ru (*Taipei Veterans General Hospital, Taiwan*)

Lee, C. Soon (*University of Western Sydney, Australia*)

Lee, Hye Seung (*Seoul National University, Korea*)

Liu, Zhiyan (*Shandong University, China*)

Lkhagvadorj, Sayamaa (*Mongolian National University of Medical Sciences, Mongolia*)

Moon, Woo Sung (*Chonbuk University, Korea*)

Paik, Jin Ho (*Seoul National University, Korea*)

Park, Chan-Sik (*University of Ulsan, Korea*)

Park, Young Nyun (*Yonsei University, Korea*)

Shahid, Pervez (*Aga Khan University, Pakistan*)

Song, Joon Seon (*University of Ulsan, Korea*)

Sung, Chang Ohk (*University of Ulsan, Korea*)

Tan, Puay Hoon (*National University of Singapore, Singapore*)

Than, Nandor Gabor (*Semmelweis University, Hungary*)

Tse, Gary M. (*The Chinese University of Hong Kong, Hong Kong*)

Yatabe, Yasushi (*Aichi Cancer Center, Japan*)

Yoon, Sun Och (*Yonsei University, Korea*)

Zhu, Yun (*Jiangsu Institution of Nuclear Medicine, China*)

## Consulting Editors

Huh, Sun (*Hallym University, Korea*)

Kakudo, Kennichi (*Kindai University, Japan*)

Ro, Jae Y. (*Cornell University, The Methodist Hospital, U.S.A.*)

## Ethic Editor

Choi, In-Hong (*Yonsei University, Korea*)

## Statistics Editors

Kim, Dong Wook (*National Health Insurance Service Ilsan Hospital, Korea*)

Lee, Hye Sun (*Yonsei University, Korea*)

## Manuscript Editor

Chang, Soo-Hee (*InfoLumi Co., Korea*)

## Layout Editor

Kim, Haeja (*iMiS Company Co., Ltd., Korea*)

## Website and JATS XML File Producers

Cho, Yoonsang (*M2Community Co., Korea*)

Im, Jeonghee (*M2Community Co., Korea*)

## Administrative Assistants

Jung, Ji Young (*The Korean Society of Pathologists*)

Jeon, Anmi (*The Korean Society for Cytopathology*)

## Contact the Korean Society of Pathologists/the Korean Society for Cytopathology

**Publishers:** Choi, Chan, MD, Hong, Soon Won, MD

**Editors-in-Chief:** Jung, Chan Kwon, MD, Park, So Yeon, MD

**Published by the Korean Society of Pathologists/the Korean Society for Cytopathology**

## Editorial Office

Room 1209 Gwanghwamun Officia, 92 Saemunan-ro, Jongno-gu, Seoul 03186, Korea  
Tel: +82-2-795-3094 Fax: +82-2-790-6635 E-mail: [office@jpatholtm.org](mailto:office@jpatholtm.org)

#1508 Renaissancetower, 14 Mallijae-ro, Mapo-gu, Seoul 04195, Korea  
Tel: +82-2-593-6943 Fax: +82-2-593-6944 E-mail: [office@jpatholtm.org](mailto:office@jpatholtm.org)

**Printed by** iMiS Company Co., Ltd. (JMC)

Jungang Bldg. 18-8 Wonhyo-ro 89-gil, Yongsan-gu, Seoul 04314, Korea  
Tel: +82-2-717-5511 Fax: +82-2-717-5515 E-mail: [ml@smileml.com](mailto:ml@smileml.com)

**Manuscript Editing by** InfoLumi Co.

210-202, 421 Pangyo-ro, Bundang-gu, Seongnam 13522, Korea  
Tel: +82-70-8839-8800 E-mail: [infolumi.chang@gmail.com](mailto:infolumi.chang@gmail.com)

Front cover image: Representative examples of HER2 protein expression and HER2 heterogeneity in breast cancer (Figs. 1 and 2). p35, p38.

© Copyright 2020 by the Korean Society of Pathologists/the Korean Society for Cytopathology

© Journal of Pathology and Translational Medicine is an Open Access journal under the terms of the Creative Commons Attribution Non-Commercial License (<https://creativecommons.org/licenses/by-nc/4.0>).

© This paper meets the requirements of KS X ISO 9706, ISO 9706-1994 and ANSI/NISO Z.39.48-1992 (Permanence of Paper).

This journal was supported by the Korean Federation of Science and Technology Societies Grant funded by the Korean Government.

## CONTENTS

---

### REVIEWS

- 1 **Standardized Pathology Report for Colorectal Cancer, 2nd Edition**  
Baek-hui Kim, Joon Mee Kim, Gyeong Hoon Kang, Hee Jin Chang, Dong Wook Kang, Jung Ho Kim, Jeong Mo Bae, An Na Seo, Ho Sung Park, Yun Kyung Kang, Kyung-Hwa Lee, Mee Yon Cho, In-Gu Do, Hye Seung Lee, Hee Kyung Chang, Do Youn Park, Hyo Jeong Kang, Jin Hee Sohn, Mee Soo Chang, Eun Sun Jung, So-Young Jin, Eunsil Yu, Hye Seung Han, Youn Wha Kim, The Gastrointestinal Pathology Study Group of the Korean Society of Pathologists
- 20 **Tumor immune response and immunotherapy in gastric cancer**  
Yoonjin Kwak, An Na Seo, Hee Eun Lee, Hye Seung Lee
- 34 **HER2 status in breast cancer: changes in guidelines and complicating factors for interpretation**  
Soomin Ahn, Ji Won Woo, Kyoungyul Lee, So Yeon Park
- 45 **Molecular characteristics of meningiomas**  
Young Suk Lee, Youn Soo Lee
- 64 **2019 Practice guidelines for thyroid core needle biopsy: a report of the Clinical Practice Guidelines Development Committee of the Korean Thyroid Association**  
Chan Kwon Jung, Jung Hwan Baek, Dong Gyu Na, Young Lyun Oh, Ka Hee Yi, Ho-Cheol Kang, Clinical Practice Guidelines Development Committee of the Korean Thyroid Association

### ORIGINAL ARTICLES

- 87 **Analysis of the molecular subtypes of preoperative core needle biopsy and surgical specimens in invasive breast cancer**  
Ye Sul Jeong, Jun Kang, Jieun Lee, Tae-Kyung Yoo, Sung Hun Kim, Ahwon Lee
- 95 **Clinicopathologic characteristics of HER2-positive pure mucinous carcinoma of the breast**  
Yunjeong Jang, Hera Jung, Han-Na Kim, Youjeong Seo, Emad Alsharif, Seok Jin Nam, Seok Won Kim, Jeong Eon Lee, Yeon Hee Park, Eun Yoon Cho, Soo Youn Cho
- 103 **Expression of female sex hormone receptors and its relation to clinicopathological characteristics and prognosis of lung adenocarcinoma**  
Jin Hwan Lee, Han Kyeom Kim, Bong Kyung Shin

- 
- 112 Comparison of papanicolaou smear and human papillomavirus (HPV) test as cervical screening tools: can we rely on HPV test alone as a screening method? An 11-year retrospective experience at a single institution  
Myunghee Kang, Seung Yeon Ha, Hyun Yee Cho, Dong Hae Chung, Na Rae Kim, Jungsuk An, Sangho Lee, Jae Yeon Seok, Juhyeon Jeong

## CASE REPORT

- 119 Morule-like features in pulmonary adenocarcinoma associated with epidermal growth factor receptor mutations: two case reports with targeted next-generation sequencing analysis  
Yoo Jin Lee, Harim Oh, Eojin Kim, Bokyung Ahn, Jeong Hyeon Lee, Youngseok Lee, Yang Seok Chae, Chul Hwan Kim

## EDITORIAL

- 123 Papillary thyroid carcinoma variants with tall columnar cells  
Chan Kwon Jung

**Instructions for Authors** for *Journal of Pathology and Translational Medicine* are available at <http://jpatholm.org/authors/authors.php>

## Standardized Pathology Report for Colorectal Cancer, 2nd Edition

Baek-hui Kim<sup>1</sup>, Joon Mee Kim<sup>2</sup>, Gyeong Hoon Kang<sup>3</sup>, Hee Jin Chang<sup>4</sup>, Dong Wook Kang<sup>5</sup>, Jung Ho Kim<sup>3</sup>, Jeong Mo Bae<sup>3</sup>, An Na Seo<sup>6</sup>, Ho Sung Park<sup>7</sup>, Yun Kyung Kang<sup>8</sup>, Kyung-Hwa Lee<sup>9</sup>, Mee Yon Cho<sup>10</sup>, In-Gu Do<sup>11</sup>, Hye Seung Lee<sup>12</sup>, Hee Kyung Chang<sup>13</sup>, Do Youn Park<sup>14</sup>, Hyo Jeong Kang<sup>15</sup>, Jin Hee Sohn<sup>11</sup>, Mee Soo Chang<sup>16</sup>, Eun Sun Jung<sup>17</sup>, So-Young Jin<sup>18</sup>, Eunsil Yu<sup>15</sup>, Hye Seung Han<sup>19</sup>, Youn Wha Kim<sup>20</sup>,  
 The Gastrointestinal Pathology Study Group of the Korean Society of Pathologists

<sup>1</sup>Department of Pathology, Korea University Guro Hospital, Seoul; <sup>2</sup>Department of Pathology, Inha University School of Medicine, Incheon;

<sup>3</sup>Department of Pathology, Seoul National University Hospital, Seoul National University College of Medicine, Seoul;

<sup>4</sup>Department of Pathology, Research Institute and Hospital, National Cancer Center, Goyang; <sup>5</sup>Department of Pathology, Eulji University Hospital, Eulji University School of Medicine, Daejeon; <sup>6</sup>Department of Pathology, School of Medicine, Kyungpook National University, Daegu;

<sup>7</sup>Department of Pathology, Chonbuk National University Medical School, Jeonju; <sup>8</sup>Department of Pathology, Seoul Paik Hospital, Inje University College of Medicine, Seoul;

<sup>9</sup>Department of Pathology, Chonnam National University Medical School, Gwangju; <sup>10</sup>Department of Pathology, Yonsei University Wonju College of Medicine, Wonju;

<sup>11</sup>Department of Pathology, Kangbuk Samsung Hospital, Sungkyunkwan University School of Medicine, Seoul; <sup>12</sup>Department of Pathology, Seoul National University Bundang Hospital, Seongnam; <sup>13</sup>Department of Pathology, Kosin University College of Medicine, Busan; <sup>14</sup>Department of Pathology, Pusan National University Hospital, Pusan National University School of Medicine, Busan; <sup>15</sup>Department of Pathology, Asan Medical Center, University of Ulsan College of Medicine, Seoul;

<sup>16</sup>Department of Pathology, Seoul National University Boramae Hospital, Seoul National University College of Medicine, Seoul; <sup>17</sup>Department of Hospital Pathology, College of Medicine, The Catholic University of Korea, Seoul; <sup>18</sup>Department of Pathology, Soonchunhyang University Seoul Hospital, Soonchunhyang University College of Medicine, Seoul; <sup>19</sup>Department of Pathology, Konkuk University Medical Center, Konkuk University School of Medicine, Seoul;

<sup>20</sup>Department of Pathology, Kyung Hee University College of Medicine, Seoul, Korea

The first edition of the ‘Standardized Pathology Report for Colorectal Cancer,’ which was developed by the Gastrointestinal Pathology Study Group (GIP) of the Korean Society of Pathologists, was published 13 years ago. Meanwhile, there have been many changes in the pathologic diagnosis of colorectal cancer (CRC), pathologic findings included in the pathology report, and immunohistochemical and molecular pathology required for the diagnosis and treatment of colorectal cancer. In order to reflect these changes, we (GIP) decided to make the second edition of the report. The purpose of this standardized pathology report is to provide a practical protocol for Korean pathologists, which could help diagnose and treat CRC patients. This report consists of “standard data elements” and “conditional data elements.” Basic pathologic findings and parts necessary for prognostication of CRC patients are classified as “standard data elements,” while other prognostic factors and factors related to adjuvant therapy are classified as “conditional data elements” so that each institution could select the contents according to the characteristics of the institution. The Korean version is also provided separately so that Korean pathologists can easily understand and use this report. We hope that this report will be helpful in the daily practice of CRC diagnosis.

**Key Words:** Colorectal neoplasms; Pathology report; Standardization; Protocol

**Received:** August 17, 2019 **Revised:** September 24, 2019 **Accepted:** September 26, 2019

**Corresponding Author:** Joon Mee Kim, MD, PhD, Department of Pathology, Inha University School of Medicine, 27 Inhang-ro, Jung-gu, Incheon 22332, Korea  
 Tel: +82-32-890-3987, Fax: +82-32-890-3464, E-mail: jmkpath@inha.ac.kr

The first edition of the ‘Standardized Pathology Report for Colorectal Cancer’ was developed by the Gastrointestinal Pathology Study Group of the Korean Society of Pathologists and published in the Korean Journal of Pathology (predecessor of the Journal of Pathology and Translational Medicine) in 2006 [1]. Colorectal cancer (CRC), which was the fourth most common cancer in Korea at the time, is now the second most common cancer in Korea. Meanwhile, there have been many changes in the

pathologic diagnosis of CRC, such as the diagnostic criteria for carcinoma, and pathologic findings included in the pathology report [1,2]. Molecular pathology tests for CRC have also become necessary tests, as targeted therapy and immunotherapy were introduced into the treatment of CRC. The existing standardization report does not reflect the recent changes in colon cancer diagnosis.

There has been considerable demand for the revision of the

standardized pathology report, which is used by many Korean pathologists. From September 2017 to October 2018, the committee for the revision of the report was organized, and after several discussions and meetings, the second edition of the ‘Standardized Pathology Report for Colorectal Cancer’ was completed. This new report is based on the previous report with reference to the College of American Pathologists (CAP) protocol, American Joint Committee on Cancer (AJCC) 8th edition, World Health Organization (WHO) classification of tumors of the digestive system 5th edition, and International Classification of Diseases for Oncology (ICD-O) [3-6].

The purpose of this standardized pathology report is to enable standardized diagnosis and treatment of CRC patients and, furthermore, to help select the same patient group and exchange information in multicenter clinical trials or international studies. It would be desirable to include all the latest findings up to now in this report, but this would lead to an increase in the workload of the pathologist. In the current medical system of Korea, increased workloads cannot be appropriately reflected in the medical fee, which may lead this report to be unpractical for Korean pathologists. Therefore, the basic pathologic findings and parts necessary for prognostication of CRC patients are classified as “standard data elements,” and other prognostic factors and factors related to adjuvant therapy are classified as “conditional data elements” so that each institution can select the contents according to the characteristics of the institution. As with the first edition, we have written this in English for the internationalization of pathology reports. We also have restricted the use of abbreviations or numerical taxonomy so that we can keep track of future data elements even if the diagnostic criteria and classification methods change.

As The Korean Journal of Pathology has become an English-language journal named The Journal of Pathology and Translational Medicine, this report was written in English, but the Korean version is also provided separately so that Korean pathologists can easily understand and use this report (Supplementary Material 1).

## STANDARD DATA ELEMENTS FOR RESECTED COLORECTUM

All report forms mentioned in this document are shown in Table 1. If there are two or more tumors, the data elements should be listed for each tumor, starting with the tumor that has the deepest level of invasion. ‘Regional lymph node metastasis,’ ‘Associated findings,’ and ‘Separate lesions’ are noted only in the deepest tumor.

## Histopathologic type of invasive carcinoma

Histologic classification of tumors is based on WHO classification (5th edition) [5]. Although most CRCs are “adenocarcinoma, not otherwise specified (NOS),” if there are other histologic variants, it is recommended to mention them separately. This is because some histologic variants may be associated with specific molecular alteration or patient prognosis [5,7]. Representative histologic types of CRC described in WHO classification and AJCC 8th edition are shown in Table 1 [4,5].

Mucinous adenocarcinoma and signet ring cell carcinoma can be diagnosed when extracellular mucins are over 50% of tumor areas and signet ring cells are over 50% of tumor component, respectively. At levels of 50% or less, it is recommended to describe the ratio of mucin or signet ring cells along with histologic type [5]. When patients received preoperative neo-adjuvant therapy, which may produce mucin, it is advisable to describe the diagnosis of the preoperative specimen [8]. Medullary carcinoma is a rare histologic type that requires differentiation from undifferentiated carcinoma and it is diagnosed when cancer cells appear as solid or sheet-like structures and lymphocytic infiltration is prominent with intraepithelial (tumor-infiltrating) lymphocytes and neutrophils [5,7]. Tumor cells of medullary carcinoma usually show abundant eosinophilic cytoplasm, vesicular nuclei, and prominent nucleoli [5]. Another rare histologic type, micropapillary adenocarcinoma, can be diagnosed when small tumor cell clusters are surrounded by empty spaces, resembling lymphatic or small vessel invasion [9-11]. Micropapillary adenocarcinoma has a high risk of lymph node metastasis and is frequently accompanied with poor prognostic factors such as lymphatic and vascular invasion [9-13]. However, CRC with pure micropapillary patterns are extremely rare and most micropapillary lesions coexist with another histologic type [5,14]. The WHO classification suggests that tumors consisting of 5% or more micropapillary component should be diagnosed as micropapillary adenocarcinoma [5]. However, the minimal proportion of micropapillary components required for the diagnosis of micropapillary adenocarcinoma is controversial, and our committee could not reach a consensus. Serrated adenocarcinoma is also a special subtype of CRC that is morphologically similar to serrated polyps and is characterized by neoplastic glands with prominent epithelial serrations, low nucleus-to-cytoplasm ratio, eosinophilic and abundant cytoplasm, and vesicular nuclei [5,15,16]. Although some studies have suggested diagnostic criteria for serrated adenocarcinoma [17], a consensus has not yet been reached. Adenosquamous carcinoma is diagnosed when an area of definite squamous differentiation is present in the tumor. Although the WHO classification sug-

**Table 1.** Report form of pathologic diagnosis for resected colorectal cancer

Standard data elements
<p><b>Specimen type</b></p> <input type="checkbox"/> Right hemicolectomy <input type="checkbox"/> Transverse hemicolectomy <input type="checkbox"/> Left hemicolectomy <input type="checkbox"/> Anterior resection <input type="checkbox"/> Low anterior resection <input type="checkbox"/> Abdominoperineal resection <input type="checkbox"/> Subtotal/total colectomy <input type="checkbox"/> Total proctocolectomy <input type="checkbox"/> Transanal excision <input type="checkbox"/> Endoscopic mucosal resection <input type="checkbox"/> Other: (specify: _____ )
<p><b>Histopathologic type of invasive carcinoma</b></p> <input type="checkbox"/> Adenocarcinoma, NOS <input type="checkbox"/> Low-grade (well differentiated and moderately differentiated) <input type="checkbox"/> High-grade (poorly differentiated) <input type="checkbox"/> Mucinous adenocarcinoma <input type="checkbox"/> Signet ring cell carcinoma <input type="checkbox"/> Medullary carcinoma <input type="checkbox"/> Serrated adenocarcinoma <input type="checkbox"/> Micropapillary adenocarcinoma <input type="checkbox"/> Squamous cell (epidermoid) carcinoma (excluding upwardly spreading anal tumors) <input type="checkbox"/> Adenosquamous carcinoma <input type="checkbox"/> Small cell neuroendocrine carcinoma <input type="checkbox"/> Large cell neuroendocrine carcinoma <input type="checkbox"/> Mixed neuroendocrine-non-neuroendocrine neoplasm <input type="checkbox"/> Undifferentiated carcinoma <input type="checkbox"/> Other: (specify: _____ )
<p><b>Location</b></p> <input type="checkbox"/> Cecum <input type="checkbox"/> Ascending colon <input type="checkbox"/> Hepatic flexure <input type="checkbox"/> Transverse colon <input type="checkbox"/> Splenic flexure <input type="checkbox"/> Descending colon <input type="checkbox"/> Sigmoid colon <input type="checkbox"/> Rectosigmoid junction <input type="checkbox"/> Rectum <input type="checkbox"/> Other: (specify: _____ )
<p><b>Gross type</b></p> <input type="checkbox"/> Fungating/polypoid <input type="checkbox"/> Ulcerofungating <input type="checkbox"/> Ulceroinfiltrative <input type="checkbox"/> Infiltrative <input type="checkbox"/> Unclassifiable
<p><b>Tumor size</b></p> <p>_____ x _____ x _____ cm</p>

(Continued)

Standard data elements
<p><b>Depth of invasion</b></p> <input type="checkbox"/> Intramucosal carcinoma (pTis) <input type="checkbox"/> Tumor invades the submucosa (pT1) <input type="checkbox"/> Tumor invades the muscularis propria (pT2) <input type="checkbox"/> Tumor invades through the muscularis propria into pericolorectal tissue (pT3) <input type="checkbox"/> Tumor invades through the visceral peritoneum (pT4a) <input type="checkbox"/> Tumor directly invades or adheres to adjacent organs or structures (pT4b)
<p><b>- [Endoscopic excision (Endoscopic submucosal dissection/polypectomy) or transanal excision]</b></p> <input type="checkbox"/> Tumor invades the lamina propria with no extension through muscularis mucosae (pTis) <input type="checkbox"/> Tumor invades the submucosa (pT1) For sessile lesion: Distance of tumor from muscularis mucosae: _____ mm For pedunculated lesion: Haggitt level (head, neck, stalk, beyond stalk) Distance of tumor invasion in stalk: _____ mm
<p><b>Resection margin</b></p> Proximal margin <input type="checkbox"/> Free from carcinoma <input type="checkbox"/> Involved by carcinoma Distal margin <input type="checkbox"/> Free from carcinoma <input type="checkbox"/> Involved by carcinoma Circumferential margin (rectum only) <input type="checkbox"/> Free from carcinoma <input type="checkbox"/> Involved by carcinoma Safety margin: proximal _____ cm, distal _____ cm, circumferential _____ cm
<p><b>- [Endoscopic excision (Endoscopic mucosal resection/submucosal dissection/polypectomy) or transanal excision]</b></p> Deep margin <input type="checkbox"/> Free from carcinoma <input type="checkbox"/> Involved by carcinoma <input type="checkbox"/> Not applicable Horizontal margin <input type="checkbox"/> Free from carcinoma <input type="checkbox"/> Involved by carcinoma <input type="checkbox"/> Involved by adenoma: (specify grade: _____ ) <input type="checkbox"/> Not applicable Safety margin: deep _____ cm, horizontal _____ cm
<p><b>Regional lymph node metastasis</b></p> <input type="checkbox"/> No metastasis in all _____ regional lymph nodes (pN0) <input type="checkbox"/> Metastasis to _____ out of _____ regional lymph nodes pN _____
<p><b>Lymphatic (small vessel) invasion</b></p> <input type="checkbox"/> Not identified <input type="checkbox"/> Present
<p><b>Venous invasion</b></p> <input type="checkbox"/> Not identified <input type="checkbox"/> Present <input type="checkbox"/> Intramural <input type="checkbox"/> Extramural

(Continued to the next page)

Table 1. Continued

Standard data elements
<b>Perineural invasion</b> <input type="checkbox"/> Not identified <input type="checkbox"/> Present
<b>Pre-existing adenoma</b> <input type="checkbox"/> Absent <input type="checkbox"/> Tubular/Tubulovillous/Villous adenoma Low grade dysplasia/High grade dysplasia <input type="checkbox"/> Sessile serrated lesion (sessile serrated adenoma/polyp) <input type="checkbox"/> Sessile serrated lesion (sessile serrated adenoma/polyp) with dysplasia <input type="checkbox"/> Traditional serrated adenoma <input type="checkbox"/> Other (specify: _____)
<b>Associated findings</b> <input type="checkbox"/> Absent <input type="checkbox"/> Tumor perforation (pT4a) <input type="checkbox"/> Perforation (non-tumor perforation) <input type="checkbox"/> Metastasis to one site or organ without peritoneal metastasis (pM1a) <input type="checkbox"/> Metastasis to two or more sites or organs without peritoneal metastasis (pM1b) <input type="checkbox"/> Metastasis to the peritoneal surface with or without other site or organ metastasis (pM1c) Specify metastatic sites or organs: _____
<b>Separate lesions</b> <input type="checkbox"/> Absent <input type="checkbox"/> Adenoma <input type="checkbox"/> Polyp <input type="checkbox"/> GIST <input type="checkbox"/> Ulcerative colitis/Crohn's disease <input type="checkbox"/> Others Specify: _____
Conditional data elements
<b>Tumor budding</b> <input type="checkbox"/> Not identified <input type="checkbox"/> Present <input type="checkbox"/> ≤4 buds (low) <input type="checkbox"/> 5–9 buds (intermediate) <input type="checkbox"/> ≥10 buds (high) <input type="checkbox"/> Cannot be assessed (specify: _____)
<b>Completeness of total mesorectal excision</b> <input type="checkbox"/> Complete <input type="checkbox"/> Nearly complete <input type="checkbox"/> Incomplete <input type="checkbox"/> Cannot be determined
<b>Preoperative chemoradiotherapy</b> <input type="checkbox"/> Yes <input type="checkbox"/> No <input type="checkbox"/> Not known <b>If yes) Tumor regression grade</b> <input type="checkbox"/> Grade 0: No viable cancer cells (complete response) <input type="checkbox"/> Grade 1: Single cells or rare small groups of cancer cells (near-complete response) <input type="checkbox"/> Grade 2: Residual cancer with evident tumor regression, but more than single cells or rare small groups of cancer cells (partial response) <input type="checkbox"/> Grade 3: Extensive residual cancer with no evident tumor regression (poor or no response)

(Continued)

Conditional data elements
<b>DNA mismatch repair immunohistochemistry</b> MLH1: <input type="checkbox"/> Positive (retained expression) <input type="checkbox"/> Negative (loss of expression) MSH2: <input type="checkbox"/> Positive (retained expression) <input type="checkbox"/> Negative (loss of expression) PMS2: <input type="checkbox"/> Positive (retained expression) <input type="checkbox"/> Negative (loss of expression) MSH6: <input type="checkbox"/> Positive (retained expression) <input type="checkbox"/> Negative (loss of expression) Summary: DNA mismatch repair deficiency (was/was not) observed
<b>Microsatellite instability (MSI)</b> Summary: <input type="checkbox"/> MSI-stable (MSS) <input type="checkbox"/> MSI-low (MSI-L) <input type="checkbox"/> MSI-high (MSI-H)
<b>KRAS mutation analysis</b> <input type="checkbox"/> No mutation detected <input type="checkbox"/> Mutation detected (specify: <i>example: c.35G&gt;A, p.Gly12Asp</i> _____)
<b>NRAS mutation analysis</b> <input type="checkbox"/> No mutation detected <input type="checkbox"/> Mutation detected (specify: <i>example: c.35G&gt;A, p.Gly12Asp</i> _____)
<b>BRAF mutation analysis</b> <input type="checkbox"/> No mutation detected <input type="checkbox"/> BRAF V600E (c.1799T>A) mutation <input type="checkbox"/> Other BRAF mutation (specify: _____)

Comment: This report is intended to be applicable to endoscopic resection or transanal excision specimens as well as surgical resection of CRC. NOS, not otherwise specified; CRC, colorectal cancer.

gests a greater than 20% and 25% adenocarcinoma component or squamous cell carcinoma component, respectively, for the diagnosis of adenosquamous carcinoma in esophageal and gastric cancer, respectively, there is no standardized diagnostic criteria for adenosquamous carcinoma in terms of the squamous cell carcinoma component [5]. We recommend diagnosing adenosquamous carcinoma when the squamous cell carcinoma component is clearly seen in “more than occasional small foci” as described in the previous report [1]. Undifferentiated carcinoma is diagnosed when the epithelial tumor lacks morphological, immunohistochemical, and molecular evidence of specific differentiation [5]. Adenoma-like adenocarcinoma, also called villous adenocarcinoma, was first introduced as a histological subtype of CRC in the WHO 5th edition [5]. Adenoma-like adenocarcinoma is composed of villous adenoma-like well differentiated tumors in the invasive portion, showing pushing border and minimal dysplasia [5]. Whether adenoma-like adenocarcinoma should be classified as a specific subtype of CRC is still controversial and has not been added as a subtype in this report.

Differentiation of tumors is determined by the area ratio of gland or tubule formation by tumor cells [7]. The degree of differentiation of the tumor is applicable to adenocarcinoma, NOS. This is because other histologic types show their own prognosis [7]. Recently, tumor differentiation has been shown to affect the prognosis of patients with mucinous adenocarcinoma [5,18]. However, standardized tumor grading of mucinous adenocarcinoma has not been presented yet. Tumor grading is preferably performed using a two-tiered system with low-grade and high-grade [5]. In the 3-tiered grading system, tumor differentiation is graded as well differentiated (> 95% gland formation), moderately differentiated (50%–95% gland formation), or poorly differentiated (< 50% gland formation). The “well- and moderately differentiated” grades correspond to low-grade, while “poorly differentiated” corresponds to high-grade of the two-tiered grading system [5,19].

### Location

The location of the tumor follows the ICD-O classification [6]. The length of the cecum is approximately 6 cm and the length of the sigmoid colon is approximately 40 cm. The rectum begins at 1–2 cm above the dentate line and is 12–15 cm long. The upper third of the rectum is covered by peritoneum on the anterior and lateral sides, the middle third is covered by peritoneum on the anterior side, and the lower third is not covered by peritoneum. In this revision, “overlapping lesion of the colon” was removed from the tumor location section because it is practically not used in most institutions. When tumors are involved in two locations of the colon, the tumor epicenter and more involved area should be considered in the determination of tumor location.

### Gross type

Superficial type is not recommended for describing tumor gross morphology, because superficial type could be defined by microscopic examination. Fungating/polypoid type can substitute most gross morphology of the previously established superficial type. Nevertheless, if superficial type is used, it should be applied to tumors that are confined to mucosa or submucosa and with tumor thickness of no more than two-fold thickness of adjacent mucosa. Other criteria for tumor gross types are the same as in the previous version. Fungating/polypoid, ulcerofungating, ulceroinfiltrative, and infiltrative gross types correspond to the Borrmann classification of gastric cancer.

### Tumor size

The tumor size is expressed as the product of the longest axis and the length perpendicular to it. The depth of the tumor is measured with a microscope at the thickest point.

### Depth of invasion

According to the AJCC 8th edition, “intraepithelial carcinoma” that is confined to the crypt epithelium and lacks invasion beyond the basement membrane is considered synonymous to high-grade dysplasia and is excluded from the pTis category. Intramucosal carcinoma that shows invasion into lamina propria with no penetration through the muscularis mucosae into the submucosa is assigned to pTis considering the negligible risk for metastasis [4]. The histopathologic features of intramucosal carcinoma are defined as follows: (1) infiltration of the stroma by either single or small clusters of tumor cells with basement membrane disruption; (2) a stromal response such as desmoplasia or inflammatory cell infiltrates around the invasion front; (3) definite nuclear anaplasia and severe glandular structural abnormality including marked glandular crowding or excessive branching and budding that endows high suspicion of basement membrane destruction (Fig. 1A, B) [20]. In comparison, high-grade dysplasia is diagnosed when the tumor gland shows (1) nuclear pleomorphism with loss of polarity, (2) architectural complexity of intraluminal cribriforming or necrosis, and (3) back-to-back fusion of multiple glands without lamina propria invasion. Low-grade dysplasia is used when the pseudostratified nucleus is seen without complex architectural change of the glands, regardless of the nuclear ratio to the cell length (Fig. 1C) (refer to ‘Pre-existing adenoma’). However, intraepithelial carcinoma of the colorectum had been classified as pTis in the AJCC 7th or earlier editions, while intraepithelial carcinoma of other gastrointestinal tracts except the colorectum is still diagnosed as pTis [4]. Therefore, we recommend minimizing the use of intraepithelial carcinoma or adenocarcinoma in situ in order to reduce confusion and suggest using high-grade dysplasia or intramucosal carcinoma for the diagnosis of mucosal high-grade lesions.

If there is a tumor at the site where the proper muscle has disappeared by ulceration, it is defined as subserosal infiltration of the tumor (pT3). If tumor cells approach the serosal surface by a gap of  $\leq 1$  mm with a fibroinflammatory reaction, scrupulous examinations using deeper sections and/or additional tissue blocks are needed to uncover serosal surface involvement [4,21]. In colorectal tumors, similar to other gastrointestinal organs, pT4 is subcategorized into pT4a and pT4b. Although pT4a is basically defined as direct involvement of the serosal surface (visceral peri-

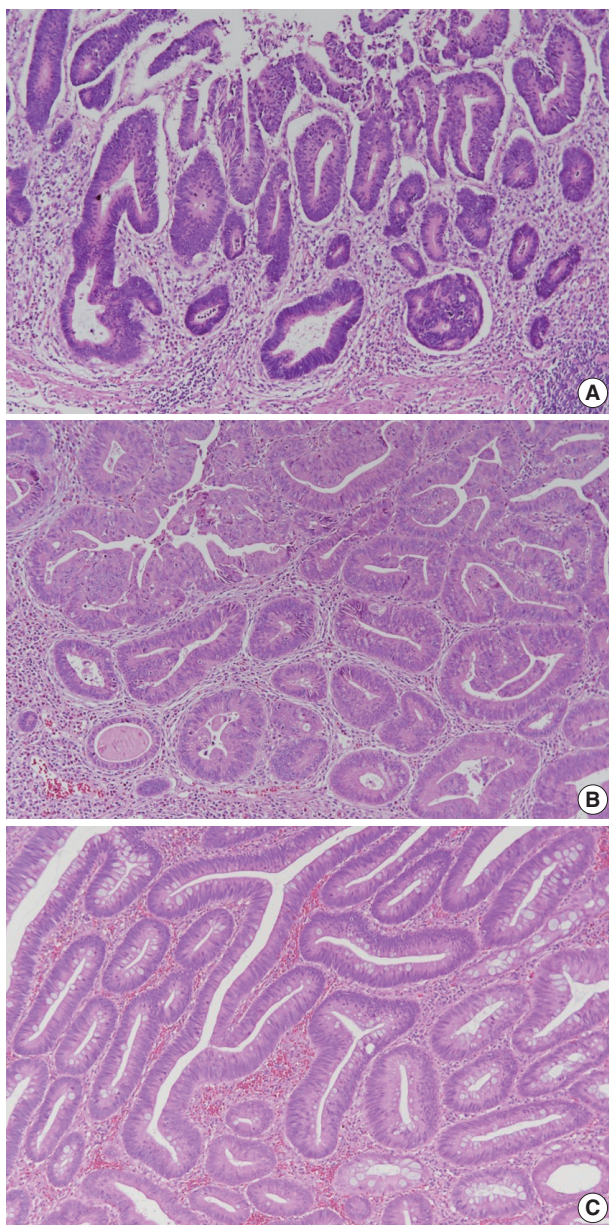


**Fig. 1.** Histologic features of intramucosal carcinoma. (A) The intramucosal carcinoma shows irregular invasive glands accompanied by desmoplasia. (B) The glands show excessive budding and luminal serration, which is highly suspicious for disruption of the basement membrane. (C) The elongated nuclei are seen in low-grade dysplasia, regardless of the ratio to the cell length.

toneum) by tumor invasion, pT4a encompasses the cases in which tumors with perforation display carcinoma cells running through inflammation to the serosal surface and are accompanied by mesothelial proliferation. The pT4a category is not applicable in nonperitonealized portions of the colorectum, including posterior aspects of the ascending and descending colon and lower portion of the rectum. The pT4b category is assigned when the

tumor directly invades the adjacent organs or structures. For distal rectal tumors, tumors with involvement of the external sphincter are assigned to pT3, whereas those with the involvement of the levator ani muscle are assigned to pT4b.

The presence of tumor cells within the lymphatic or venous vessels is not considered when determining the depth of invasion. The presence of vascular invasion should be recorded in parentheses separately (e.g., invades proper muscle [involvement of subserosa by lymphatic emboli]). The skip metastasis of multiple lesions in mucosa or submucosa of the adjacent bowel is not classified as distant metastasis. The presence of a peritumoral abscess or acellular mucin pool in cancers with preoperative chemoradiotherapy has been known to be unrelated to patients' prognosis in CRC, and also is not considered in determining the depth of invasion [22-24].

#### Endoscopic excision (endoscopic submucosal dissection/polypectomy) or transanal excision

Invasive adenocarcinomas arising in colorectal adenomas have been called "malignant polyps," in which tumor cells penetrate through the muscularis mucosae into the submucosa. Independent prognostic factors that prompt further surgical treatment of endoscopically resected polyps are as follows: (1) poorly differentiated carcinoma, (2) tumors at or less than 1 mm from the resection margin, and (3) presence of lymphatic and/or venous vessel involvement. Submucosal invasion depth is also an important factor in determining subsequent surgical treatment, since a submucosal invasion depth of  $\geq 1,000$   $\mu\text{m}$  in malignant polyps of sessile (non-pedunculated) morphology indicates a significantly increased risk for lymph node metastasis [25,26].

In this committee, measurement methods were discussed to reduce measurement error in submucosal invasion depth. Polyps are classified into pedunculated and nonpedunculated polyps. For pedunculated polyps, submucosal invasion is classified as 'head,' 'neck,' 'stalk,' and 'beyond stalk' according to the Haggitt classification, in which the neck of the polyp (level 2) is the reference point for measuring stalk invasion (Fig. 2A, B) [27,28]. In nonpedunculated polyps, when the muscularis mucosae is preserved, submucosal invasion depth is measured vertically from the lowest part of the muscularis mucosae. When the muscularis mucosae has been disrupted or has disappeared, the depth of submucosa invasion is measured from the imaginary line that is continuous from the residual muscularis mucosae of the neighboring mucosa (Fig. 2C, D) [29].

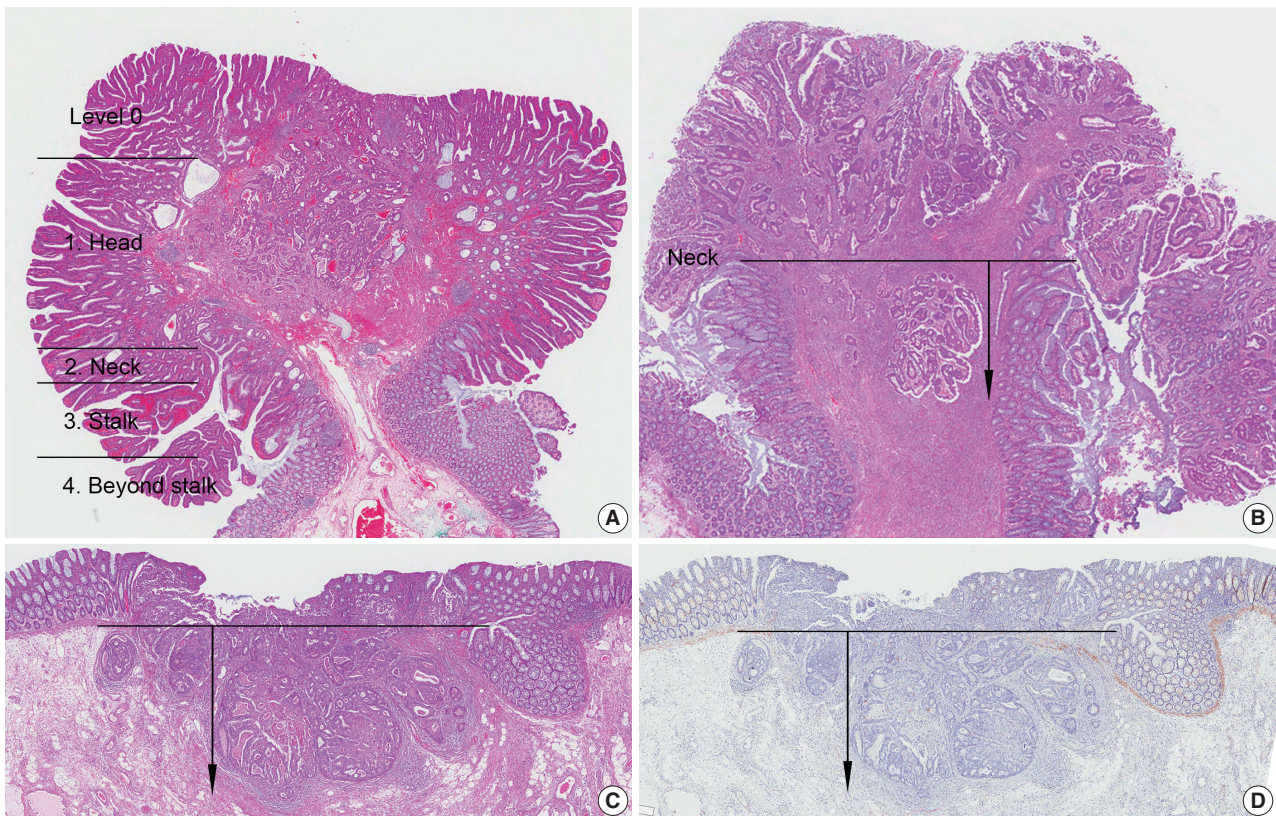


**Fig. 2.** Measuring depth of invasion in tumors with submucosal invasion. (A) Haggitt level of invasion is composed of head, neck, stalk, and beyond stalk in pedunculated tumors. (B) The depth of invasion should be measured from the neck of the polyp (Haggitt level 2). (C) In cases with disrupted muscularis mucosae, the depth of submucosa invasion is measured from a continuous line of the residual muscularis mucosae. (D) To highlight indistinct muscularis mucosae, immunohistochemistry for desmin may be performed.

### Resection margin

The distance from the proximal and distal resection margins is the length from the edge of the carcinoma to the nearest resection margin. In rectal cancer, the circumferential resection margin should be measured in the areas uncovered by peritoneum. After confirming the circumferential resection margin of the resected specimen, mark the margin with ink, and obtain sections including the site where the tumor is most deeply infiltrated. The involvement of carcinoma in the margin is finally assessed by microscopic examination. If the distance between circumferential resection margin and carcinoma (including lymph node, neural invasion, and intravascular tumor emboli) is 0.1 cm or less than 0.1 cm, the resection margin is regarded as positive [3,4]. Circumferential margins of colon cancers other than rectal cancers can be reported when necessary.

### Endoscopic excision (endoscopic mucosal resection/submucosal dissection/polypectomy) or transanal excision

This form is applied to the endoscopic resection (polypectomy,

mucosal resection, and submucosal dissection) and trans-anal resection. The deep and horizontal margins are examined microscopically. Margin involvement by adenoma is reported in the horizontal margin. When it is impossible to evaluate the resection margins, such as in specimen fragmentation, it shall be marked as 'not applicable.'

### Regional lymph node metastasis

Diagnosis of regional lymph node metastasis is made according to the AJCC 8th edition [4]. Although it is recommended to examine 12 or more lymph nodes for determination of accurate prognosis, pN0 can be used if fewer lymph nodes are available, but no lymph node metastasis is observed. Preoperative chemotherapy and radiotherapy can cause fewer lymph nodes to be harvested. Metastasis to lymph nodes other than regional lymph nodes should be diagnosed as distant metastasis and should not be included in lymph node metastasis numbers.

If the size of the metastatic tumor is less than 2 mm and more than 0.2 mm, it is classified as micrometastasis. If it is less than

0.2 mm, it is classified as isolated tumor cell [4]. A lymph node with micrometastasis is counted as a metastatic lymph node. Although isolated tumor cells are known to be associated with poor prognosis in some stages, pN0 is recommended in AJCC [4]. However, this is controversial and difficult to apply in routine pathologic diagnosis. Thus, we recommend that isolated tumor cells found on hematoxylin and eosin (H&E) slides are considered to be lymph node metastasis and included in the metastatic lymph node numbers, as in the first edition of this report [1].

Tumor deposits are tumor nodules observed separately from the primary tumor in the subserosa, mesentery, and perirectal tissues, regardless of size, shape, and border. Lymph node, vessel, and neural invasions are excluded from tumor deposits [4]. If a blood vessel or nerve structure is observed within the tumor nodule, it should be regarded as a blood vessel invasion or a neural invasion. Elastic stain or immunohistochemical stain (IHC), such as smooth muscle actin, may be helpful in differentiating tumor deposits. pN1c is used when there is no lymph node metastasis, regardless of the invasion depth of the primary tumor, and when there is a tumor deposit. If there are metastatic lymph nodes, tumor deposits are not included in the number of positive lymph nodes. Care should be taken if the patient received preoperative therapy, because regressed residual tumor in subserosa or perirectal soft tissue can be seen as a tumor deposit.

#### Lymphatic (small vessel) invasion and venous invasion

Identification of lymphatic invasion by the tumor has been recognized as a predictor of lymph node metastasis [26], and identification of venous invasion is a well-known independent prognostic indicator [30]. IHC for D2-40 may be performed additionally to identify endothelial cells because it can be difficult to differentiate the lymphatic vessel from retraction artifacts on H&E sections (Fig. 3A). It is commonly difficult to distinguish lymphatic vessels from blood vessels on H&E sections. Thus, it is considered as lymphatic (small vessel) invasion when the tumor cells involve small vessels, such as lymphatics, capillaries, and postcapillary venules (Fig. 3B), whereas venous invasion is when the tumor cells involve large vessels with an identifiable smooth muscle layer or elastic lamina (Fig. 3C) [31]. This should be considered lymphatic (small vessel) invasion if the size of the involved vessel corresponds to that of small vessel, even though there are red blood cells in the involved vessel. Additionally, special stains for elastic fiber or IHCs for CD31, D2-40, and smooth muscle actin can be used if necessary. It is recommended extramural venous invasion be reported separately from the intramural venous invasion, because the former is an adverse prognostic factor

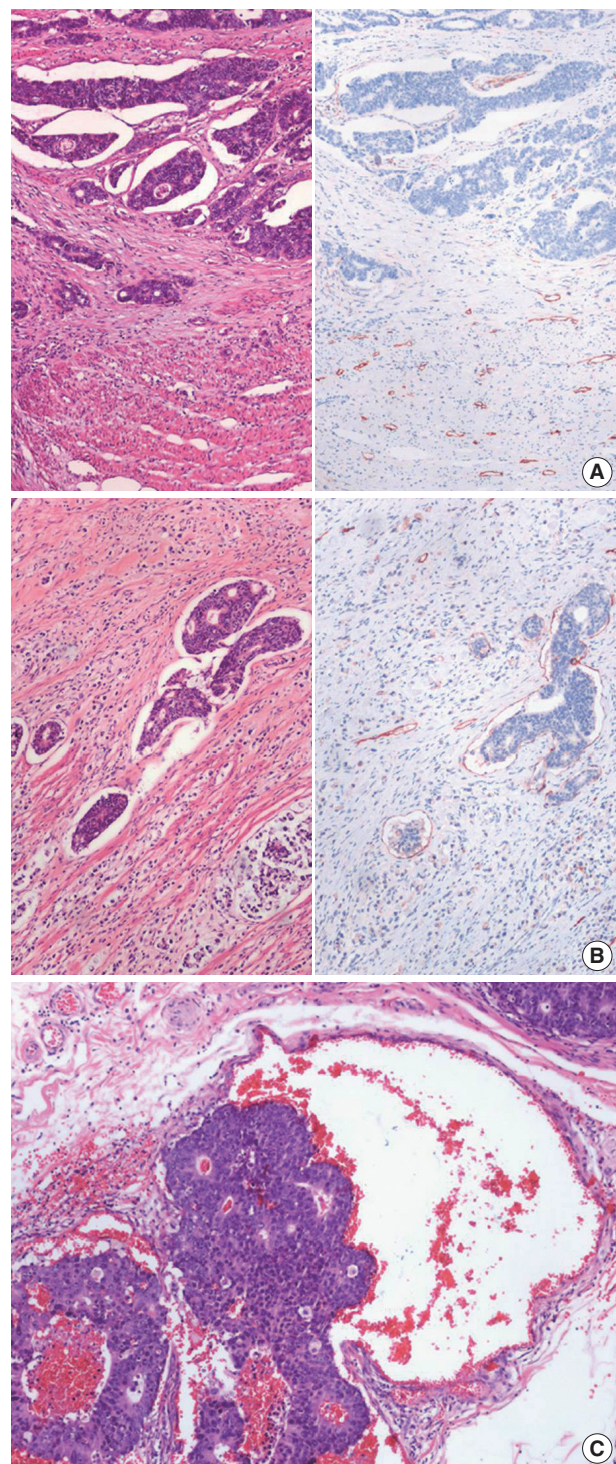


**Fig. 3.** Histologic features of lymphatic invasion and venous invasion. (A) Tumor clusters with retraction artifacts can be misinterpreted as lymphatic invasion (H&E stain and D2-40 immunohistochemical stain). (B) Tumor invasion of small vessels is considered as lymphatic invasion (H&E stain and D2-40 immunohistochemical stain). (C) Tumors involving vessels with identifiable smooth muscle layer or elastic lamina are considered as venous invasion.

and an independent risk factor for liver metastasis [30].

### Perineural invasion

Perineural invasion has been known as an independent predictor of poor prognosis in CRC [32]. Perineural invasion is an essential element of the pathologic report for CRC and it can be assessed on routine H&E sections. Although there is no clear definition of perineural invasion, it is considered as perineural invasion when the tumor cells invade any of the three layers of nerve sheath, around the nerve, as well as into the nerve [33].

### Pre-existing adenoma

Two major categories of CRC precursor lesions include conventional adenomas and serrated lesions [34]. According to the latest WHO classification of tumors of the digestive system, conventional adenomas are morphologically classified into tubular (villous component < 25%), tubulovillous (villous component 25%–75%), or villous (villous component > 75%) adenomas based on the proportion of tubular and villous architectures in an adenoma [5]. By definition, all conventional adenomas show dysplastic epithelium, and dysplasia in conventional adenomas can be graded as low-grade or high-grade [5]. High-grade dysplasia is characterized by architectural complexities (e.g., intraluminal cribriforming or necrosis, or back-to-back fusion of multiple glands), nuclear pleomorphisms, loss of nuclear polarity, and increased nuclear-to-cytoplasmic ratio (Fig. 4A). Features of low-grade dysplasia include non-complex architecture, pseudostratified/elongated nuclei with hyperchromasia, and preserved cellular polarization (Fig. 4B). The most important part of the distinction between high-grade and low-grade dysplasia is a complex glandular structure formation of tumor glands without invasion of lamina propria. Dysplastic glands only showing cytologic atypia without complex structural change are not diagnosed as high-grade dysplasia. In the previous edition, we recommended the diagnosis of high-grade dysplasia when there are three contiguous dysplastic gland structures showing high-grade features, which include cytologic atypia. According to the previous edition, there was a tendency to diagnose high-grade dysplasia with only focal cytologic atypia, but tumors with glandular structural abnormalities were sometimes missed as low-grade dysplasia. So, in this edition, complex structural abnormality is described as an essential part of the diagnosis of high-grade dysplasia. When high-grade and low-grade dysplasia components are mixed in a conventional adenoma, the adenoma should be diagnosed as high-grade dysplasia [1].

Serrated lesions include hyperplastic polyps (HPs), sessile ser-

rated lesions (SSLs, formerly called sessile serrated adenoma/polyp), and traditional serrated adenomas (TSAs), according to the latest WHO classification [5]. However, the classification and diagnostic criteria of serrated lesions have continuously changed [35,36]. Based on a comprehensive review of the latest WHO classification (2019) [5], expert panel recommendations from the US (2012) [35], and UK guidance (2015) [36], we recommend the use of three diagnostic terms for serrated lesions as pre-existing adenomas in CRC: SSL, SSL with dysplasia (SSLD), and TSA. Because HP is regarded as a benign, non-precancerous lesion, it is excluded from serrated lesions as a pre-existing adenoma of CRC.

All SSLs are regarded as premalignant lesions, and morphologic dysplasia in SSLs can be present or absent. In comparison to SSL without dysplasia, SSLD is regarded to have a higher risk of progression into carcinoma. SSL is morphologically characterized by crypt luminal serrations extending to the crypt base, horizontal growth of the crypt, and asymmetrical proliferation with typical dilated/branching bases of crypts (Fig 4C). The diagnosis of SSL can be made when there is at least one typical architecturally distorted crypt [5,35]. Morphologic changes in SSLD can be diverse, and multiple morphologic patterns can be seen in a single lesion. Structural changes in SSLD include villous change, elongation of crypts, crowding of crypts, cribriform formation, and excessive decrease of luminal serration. Cytologically, dysplastic cells can show conventional adenoma-like dysplasia (so-called intestinal dysplasia) or round atypical nuclei with prominent nucleoli (serrated dysplasia) [5]. Loss of MLH1 expression is frequently found in SSLD and MLH1 immunohistochemical staining may help to define dysplasia [37]. However, the grading system for SSLD has not been suggested yet. Therefore, we simply recommend the presence or absence of dysplasia, regardless of dysplasia subtype or grade, for the description of SSL as a pre-existing adenoma of CRC.

All TSAs are regarded as precancerous dysplastic lesions, although classification or grading systems for dysplasia in TSAs have not been established. Thus, we recommend the term TSA without any description of dysplasia as a pre-existing adenoma of CRC. TSA is morphologically characterized by broad-topped, sharply-invaginated luminal serration, tall columnar cells with abundant eosinophilic cytoplasm, pencillate nuclei, and ectopic crypt formation (Fig. 4D). TSAs can frequently be found as mixed lesions accompanying other serrated lesions or conventional adenomas [37,38].

In the case of a premalignant lesion consisting of two or more different histologic types of conventional adenomas and/or serrated lesions, the lesion can be referred to as a mixed adenoma.

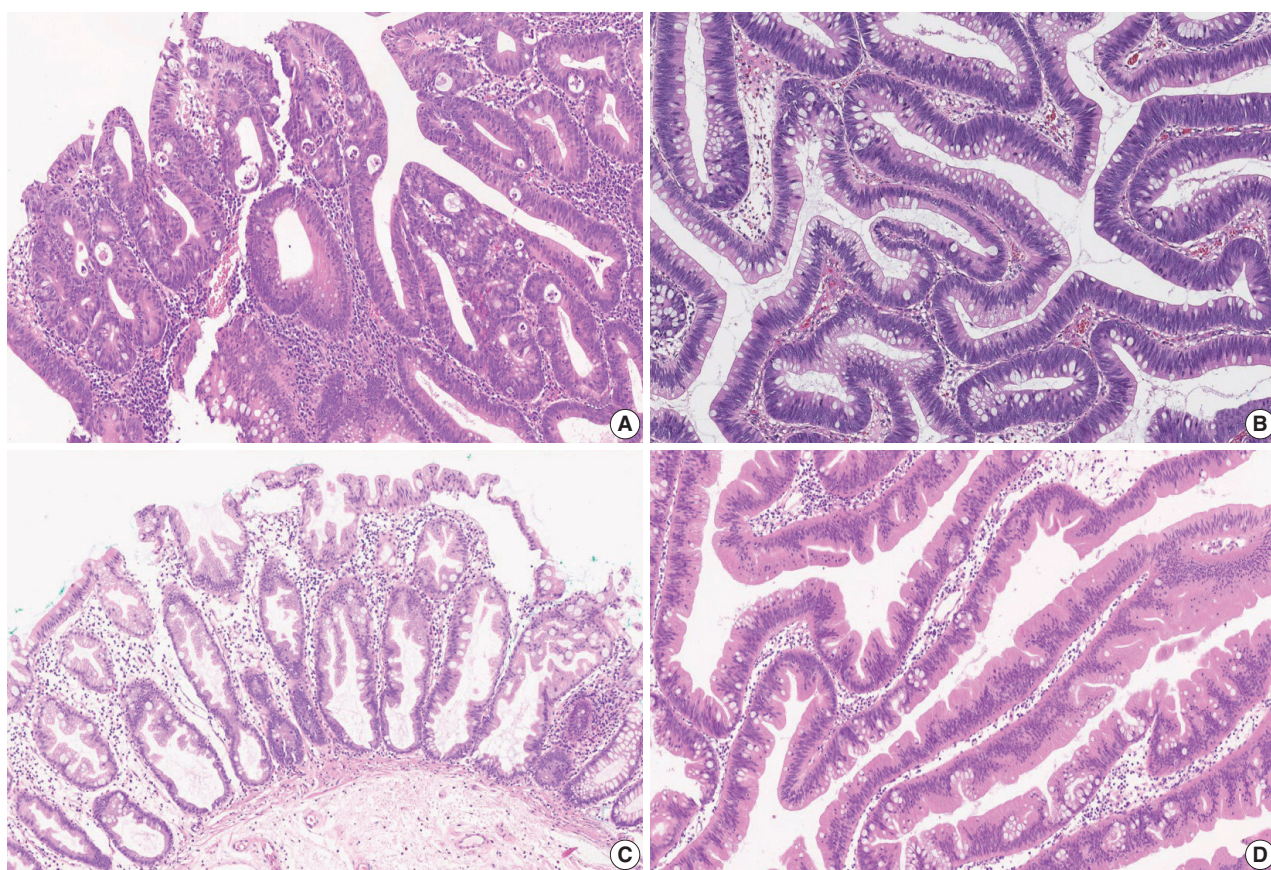


**Fig. 4.** Histologic features of premalignant lesions of the colorectum. (A) Tubular adenoma with high-grade dysplasia. Note the architectural complexity including cribriform pattern or back-to-back fusion of dysplastic glands. (B) Tubulovillous adenoma with low-grade dysplasia. Note the retained cellular polarity with pseudostratified, elongated nuclei. (C) Sessile serrated adenoma without dysplasia. Note the dilated base of crypts. (D) Traditional serrated adenoma. Note the deep-invaginated pattern of crypt serration with hyper eosinophilic cytoplasm and pencilated nuclei.

### Associated findings

Tumor perforation is associated with a poor outcome in CRC [39]. It is known that perforation of the uninvolved colon proximal to an obstructing tumor can cause peritonitis or sepsis, and is associated with poor prognosis. Distant metastasis is now divided into metastasis to one site or organ (pM1a), or metastasis to two or more sites or organs (pM1b), in the absence of peritoneal surface metastasis according to the AJCC 8th edition. Peritoneal surface metastasis is classified as pM1c [4].

### Separate lesions

When there are lesions other than colorectal cancer, such as separate adenomas, polyps, gastrointestinal stromal tumors, or inflammatory bowel disease, they can be denoted in this section.

## CONDITIONAL DATA ELEMENTS FOR RESECTED COLORECTUM

### Tumor budding

Tumor budding is a well-known independent adverse prognostic factor of CRC [40]. Tumor budding components in the pathologic report can be potentially helpful in the decision-making process for the management of patients with CRC. First, in patients presenting with endoscopically resected submucosal invasive CRC, the presence of tumor budding is positively correlated with increased risk of lymph node metastases [26,41,42]. Therefore, patients with tumor budding can be potential surgical candidates. Second, stage II CRC patients with high-grade tumor budding show worse disease-free survival than those with no or low-grade tumor budding. Therefore, high-grade tumor budding may be useful for screening patients who need adjuvant therapy [43]. Finally, the presence of tumor budding in pre-operative bi-

opsies can aid in the selection of high-risk rectal cancer patients for neoadjuvant therapy [44,45]. As mentioned above, in endoscopically resected pT1 CRC patients and stage II CRC patients, it is recommended to include tumor budding in the pathologic report.

The International Tumor Budding Consensus Conference (ITBCC) held in 2016 has recommended the following criteria for evaluation of tumor budding [46]. (1) Tumor budding is defined as a single tumor cell or a cell cluster containing  $\leq 4$  tumor cells. (2) Tumor budding should be assessed in the hotspot at the invasive tumor front (in a field measuring  $0.785 \text{ mm}^2$ , which corresponds to a  $20\times$  objective lens with an eyepiece having a field number that is 20 mm in diameter) chosen after a review of the available slides. (3) Tumor budding can be assessed on H&E slides. IHC for keratin can be helpful in evaluation of obscure cases showing a peritumoral inflammatory infiltrate on H&E-stained slides, which is difficult to distinguish from reactive stromal cells. In such cases, IHC enables better visualization of tumor budding and superior reproducibility and inter-observer agreement [47]. However, keratin also stains apoptotic bodies and cellular debris, which should not be misinterpreted as tumor budding [46,48].

We also recommend a 3-tier grading system for reporting of tumor budding. However, this grading system is not an absolute standard. Measuring and reporting the number of tumor bud-dings could be more beneficial to avoid any loss of information that may occur when applying a cut-off value in borderline cases. In rare histopathological subtypes, such as mucinous, signet-ring cells, micropapillary, and medullary carcinomas, the evaluation of tumor budding should be performed with caution [46]. Therefore, when tumor budding cannot be accurately assessed, it is recommended that the findings be reported as “cannot be assessed” with an explanatory note added to the report.

### Tumor border configuration

Regarding tumor border configuration, there is currently no recommendation in the AJCC 8th edition, nor in the CAP protocol for CRC, and only a brief mention in the WHO classification [3-5]. Although the assessment of tumor border configuration can be easily carried out using H&E slides, inter-observer reproducibility is lacking due to ambiguous definitions [49]. For these reasons, the tumor border configuration was excluded from this standardization report.

### Completeness of total mesorectal excision

Total mesorectal excision is a surgical technique that dissects within the areolar plane outside the visceral mesorectal fascia to

remove rectum [50]. A large number of non-randomized studies have shown that if total mesorectal excision is appropriately performed, then adequate resection margin is secured, and local recurrence rate is reduced. The surface of the fresh rectal specimen is examined circumferentially, and the completeness of the mesorectal excision is scored according to the worst area, as below [3,4,7].

- Complete: Mesorectum is totally resected. The surface of the specimen is smooth and there is no coning towards the distal margin (there is no surface defect greater than 0.5 cm in depth).
- Nearly complete: There is irregularity of the mesorectal surface. The surface defect is greater than 0.5 cm, but proper muscle layer is not exposed (except for levator ani muscles).
- Incomplete: Severe mesorectal defects down to the muscularis propria. Muscularis propria is exposed.

### Preoperative chemoradiotherapy

Preoperative chemoradiotherapy (CRT) followed by curative resection with TME has been established as a standard treatment for patients with locally advanced rectal cancer [51,52]. Tumor regression after preoperative CRT has an important role that can improve patient outcomes and the potential for achieving no residual tumor status [53-55]. Many studies have been performed to perceive a practical and applicable tumor regression grading (TRG) system [4,53-59]. The tumor regression after CRT was assessed only in the primary tumor and the nodal status was not included in the assessment of the TRG system [4]. The TRG system recommended in the previous edition of the “standardized pathology report for colorectal cancer” used a descriptive 5-tier system and can be easily translated into the Mandard and Dworak TRG scoring system [1]. However, even with a descriptive TRG system there is an inter-observer variation between pathologists, and this descriptive TRG system is not widely used and is often confused with other existing TRG systems. To overcome this, we suggest a new TRG system, which can be widely used in the pathologic practice, based on the AJCC 8th edition and CAP cancer protocol (Fig. 5) [3,4].

The number of blocks taken is dependent on the size of the residual tumor. If the tumor is grossly visible, a minimum of 4 paraffin blocks should be taken from the tumor, including samples from its closest point to the nearest margin. However, if the tumor is ill-defined and impossible to distinguish from fibrous stromal tissue or the tumor bed size is less than 2.0 cm, the entire embedding of the macroscopically identifiable tumor bed or entire scar area is recommended, orientated from proximal to distal in 0.4-cm levels. Careful examination of the residual tumor cells is essential and is mandatory for assessment of complete response

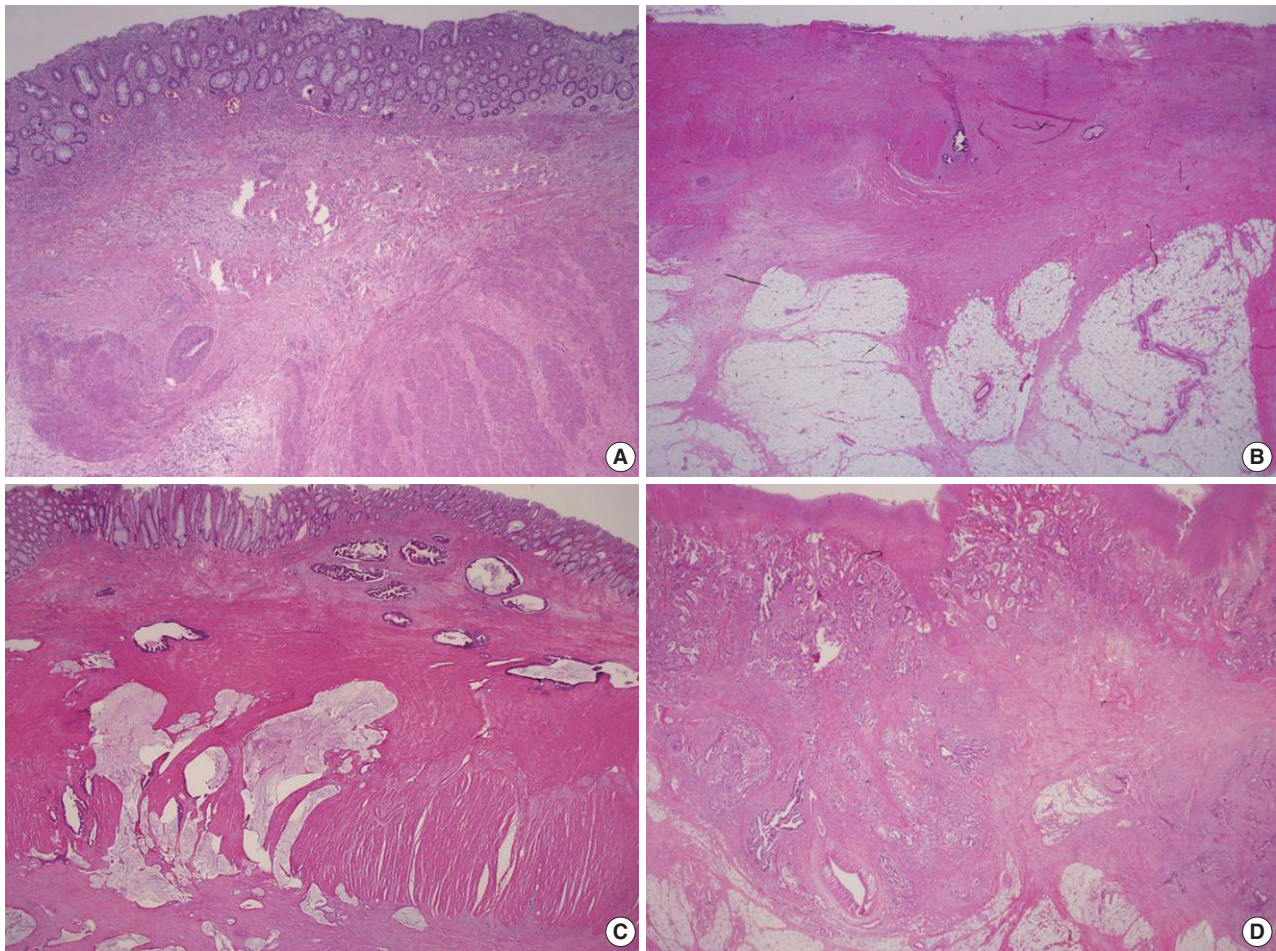


**Fig. 5.** Recommended tumor regression grading system. (A) Grade 0, complete response. No residual tumor cells are identified. (B) Grade 1, near complete response. The tumor bed contained abundant fibrosis with only a few or scattered tumor cells. (C) Grade 2, partial response. Residual tumor glands are easily identified in tumor bed. (D) Grade 3, poor or no response. The tumor cells do not demonstrate any response to chemoradiotherapy because abundant residual adenocarcinoma is present.

after CRT in CRC patients. Histologically, the tumor bed is characterized by abundant fibrotic stroma with a moderate number of mononuclear inflammatory cells or foamy macrophages. In these areas, there may be edema or mucinous or myxoid changes of the stroma or even areas of necrosis. The presence of mucin lakes without viable tumor cells (acellular mucin) should be defined as a pathologically complete response. If it is difficult to differentiate between giant cells or fibroblast and tumor cells, it may be helpful to perform serial H&E sections, mucin staining, or cytokeratin IHC in TRG grading.

#### EGFR immunohistochemistry

Expression of epidermal growth factor receptor (EGFR) by IHC has been reported in 25% to 90% of patients with CRC [60-64]. In almost all of the initial studies regarding the efficacy of targeted therapies with cetuximab or panitumumab in CRC

patients, evidence of EGFR expression by IHC was essential for the application of therapeutic agents [65]. However, subsequent studies have shown no correlation between the degree of EGFR expression and the therapeutic responses to these drugs [66-68]. Thus, immunohistochemical expression of EGFR is not considered a predictor of response to EGFR-targeted drugs, and a number of recent studies do not include EGFR expression in selection criteria for anti-EGFR targeted therapy. However, in Korea, EGFR IHC has been routinely performed on CRC tissues of patients with stage IV CRC who are candidates for EGFR-targeted therapy according to the reimbursement criteria proposed by the Health Insurance Review and Evaluation Center, which mandates patient selection based on EGFR testing prior to application of EGFR-targeted therapy. In conclusion, whether immunohistochemical expression of EGFR accurately predicts the patients who would benefit from EGFR-targeted drugs has not

been demonstrated until now.

### DNA mismatch repair immunohistochemistry

IHC for the detection of DNA mismatch repair (MMR) proteins in CRC samples is a simple and useful tool to determine MMR deficiency, which is caused by germline mutation in one of the MMR genes (*MLH1*, *MSH2*, *MSH6*, or *PMS2*) or promoter CpG island hypermethylation of the *MLH1* gene [69-71]. MMR deficiency results in a high level of microsatellite instability (MSI-H) that is characterized by genome-wide length alterations of DNA microsatellite repeat sequences [72]. Because *MLH1* dimerizes with *PMS2* in order to conduct DNA MMR function, when a mutation or promoter hypermethylation in *MLH1* occurs in CRC, IHC expression of both *MLH1* and *PMS2* is negative in the tumor [69,70]. Similarly, as *MSH2* dimerizes with *MSH6*, *MSH2*-mutated CRCs show negativity for both *MSH2* and *MSH6* [69,70]. However, when mutations in *PMS2* or *MSH6* occur, expression of only *PMS2* or *MSH6*, respectively, is lost, with the expression of *MLH1* and *MSH2* remaining intact [69,70].

Nuclear staining should be observed for the IHC detection of MMR positivity. MMR deficiency is determined when the nuclear expression of at least one of the MMR proteins is not observed in tumor cells (Fig. 6).

MMR IHC is a well-established histopathological screening tool for Lynch syndrome or sporadic MSI-H molecular subtype in CRCs [69-71]. Previous data and meta-analyses have shown that MMR deficiency (or MSI-H) in CRCs is significantly associated with both a better prognosis as well as resistance to 5-fluorouracil-based adjuvant chemotherapy [72-74]. Moreover, recent evidence has indicated that MMR deficiency (or MSI-H) is a significant predictor of a positive response to immunotherapy using immune checkpoint blockade in solid tumors [75,76]. Therefore, the pathologic reporting of MMR or microsatellite instability (MSI) status is strongly recommended for all surgically resected CRC cases.

### Immunoscore

Tumor-infiltrating lymphocytes (TILs) in tumor tissue has emerged as a strong prognostic factor in CRC. Many previous studies have consistently shown that TIL count is a strong prognostic factor with a high TIL count being significantly associated with a better prognosis in CRC [77]. Several investigations have reported that TIL count can be a strong predictor of patient prognosis in CRC regardless of both TNM staging and MSI [78,79]. The anti-tumor functions of TILs are conducted mainly by cytotoxic T cells. Thus, IHC for CD3<sup>+</sup> and CD8<sup>+</sup> T cells has been

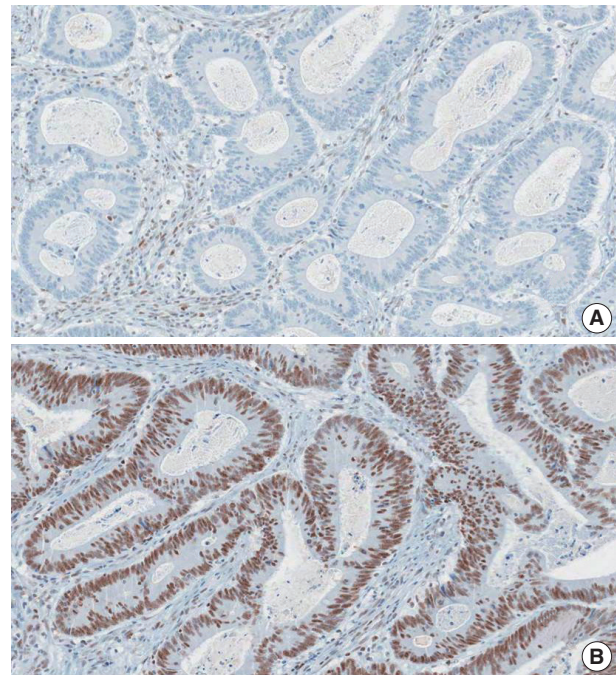


**Fig. 6.** A representative case of colorectal cancer with MMR deficiency (*MLH1* deficiency). (A) *MLH1* immunohistochemical staining showed negativity of nuclear expression in tumor cells. Note the retained nuclear expression in adjacent inflammatory cells. (B) *MSH2* immunohistochemical staining demonstrated positivity of nuclear expression in tumor cells.

used as one of the major methods for the evaluation of TILs in CRC [78,80].

Based on the accumulating data, a TIL-based methodology named “immunoscore” has been under development and validation since 2012 by an international consortium led by Dr. Jerome Galon (<http://www.immunoscore.org>) [80,81]. The steps for determining the immunoscore of a CRC are as follows: (1) selection of a representative tumor section, (2) IHC for CD3 and CD8 on the tumor section, (3) evaluation of CD3<sup>+</sup> and CD8<sup>+</sup> cell densities at two tumor areas—invasive margin (IM) and tumor center (TC), (4) dichotomous categorization (high vs. low) of each of the four CD3/CD8 variables (CD3<sup>+</sup> IM, CD3<sup>+</sup> TC, CD8<sup>+</sup> IM, and CD8<sup>+</sup> TC), (5) determination of the final immunoscore based on the four CD3/CD8 variables (e.g., no “high” variable indicates I0; one “high” variable indicates I1; two “high” variables indicate I2; three “high” variables indicate I3; four “high” variables indicate I4).

Although there is strong evidence for the prognostic significance of the immunoscore in CRC, there is still a lack of global consensus regarding the application of immunoscore in terms of indication, evaluation, and classification. One of the critical limitations of the current immunoscore system is the absence

of a standard cut-off value for the high versus low categorization of CD3<sup>+</sup> or CD8<sup>+</sup> cell density. It is expected that a consensus established from digitalized image-based, automated analyses will aid the establishment of a standardized immunoscore system.

### Microsatellite instability

MSI is a condition of genome-wide alterations in the number of repeat nucleotide(s) caused by a defective mismatch repair (dMMR) system in the context of germline mutations in mismatch repair genes, including *MLH1*, *MSH2*, *MSH6*, and *PMS2*, or *MLH1* promoter hypermethylation [72]. MSI testing is recommended for all CRC patients for the screening of Lynch syndrome in NCCN guidelines and guidelines from the American Society for Clinical Pathology (ASCP)/College of American Pathologists (CAP)/Association for Molecular Pathology (AMP)/American Society of Clinical Oncology (ASCO) [82]. Moreover, MSI-H is associated with better prognosis but poor therapeutic response to 5-fluorouracil-based cytotoxic chemotherapy [83,84]. Recently, MSI-H is considered as a predictive marker for PD-1 inhibitor-based cancer immunotherapy [75,85].

The gold standard method to evaluate MSI is the capillary gel electrophoresis, which compares the length in polymerase chain reaction (PCR) products of mono- or di-nucleotide repeats between cancer tissue and normal tissue. The Bethesda panel is composed of two mononucleotide repeat markers (BAT-25 and BAT-26) and three dinucleotide repeat markers (D5S346, D2S123, and D17S250), while the quasimonomorphic mononucleotides panel is composed of five mononucleotide repeat markers (NR-21, NR-24, NR-27 [or Mono-27], BAT-25, and BAT-26) [86,87]. Real-time PCR can be an alternative method for MSI evaluation in quasimonomorphic mononucleotides panel. Cancers classified as MSI-H should undergo immunohistochemistry of mismatch repair genes to screen for Lynch syndrome. If the *BRAF* V600E mutation is detected in MSI-H CRCs with *MLH1* loss, Lynch syndrome can be ruled out [88]. Because MSI corresponds to dMMR, immunohistochemistry of four mismatch repair proteins (*MLH1*, *MSH2*, *MSH6*, and *PMS2*) could be acceptable for an alternative method to capillary gel electrophoresis. The results of the MSI testing using the Bethesda panel are reported as MSI-H, MSI-low, and MSI-stable (MSS) if the tumor show instability in at least two, only one, and none of the 5 markers, respectively [87]. In determination of MSI using the quasimonomorphic mononucleotide panel, there is a controversy regarding the cut-off of MSI-H ( $\geq 3/5$  or  $\geq 2/5$ ) [89,90].

### *KRAS* and *NRAS* mutation analysis

The extended *RAS* mutation test is a molecular test for the detection of mutations in exons 2 to 4 of *KRAS* and *NRAS* genes [82,91]. It is widely known that EGFR blockers improve survival in patients with metastatic CRCs. However, mutations of exons 2 to 4 of *KRAS* and *NRAS* genes are associated with resistance to EGFR blockers. Thus, European Society for Medical Oncology (ESMO) guidelines for metastatic CRCs, NCCN guidelines, and ASCP/CAP/AMP/ASCO guidelines recommend extended *RAS* mutation tests in patients with metastatic CRCs [82,91-93]. Besides, a point mutation of *KRAS* exon 2 is associated with poor prognosis in CRCs [94-98]. Sanger sequencing, pyrosequencing, and real-time PCR-based methods can be used for extended *RAS* mutation testing. Next generation sequencing (NGS) panels for solid tumors should include *KRAS* and *NRAS* tests in South Korea. The presence or absence of nucleotide and amino acid changes in *KRAS* and *NRAS* exons 2-4 should be reported with appropriate nomenclature.

### *BRAF* mutation analysis

*BRAF* V600E mutations are observed in approximately two-thirds of MSI-H CRCs caused by *MLH1* promoter hypermethylation, however, it never occurs in Lynch syndrome [99]. Thus, if the MSI-H CRCs harbor the *BRAF* V600E mutation, we can exclude Lynch syndrome. Genetic tests for germline mutation of mismatch repair genes are not indicated in MSI-high CRCs with the *BRAF* V600E mutation [88].

Of the molecular subtypes generated by MSI and *BRAF/KRAS* mutations, MSS CRCs with *BRAF* V600E mutations were associated with the worst prognosis. However, the association between *BRAF* V600E mutations and worse prognosis is weakened by the presence of MSI-H, because MSI-H CRCs with *BRAF* V600E mutations showed no difference in survival compared with MSS CRCs with wild-type *KRAS/BRAF* [95-98]. Hence, MSI tests and *BRAF* mutation tests should be performed in CRC patients. Two retrospective studies showed that the *BRAF* V600E mutation is associated with shorter relapse-free survival and overall survival in metastatic CRC patients that underwent liver resection [98,100].

Some studies reported that the *BRAF* V600E mutation is associated with poor therapeutic response to EGFR blockers. However, it is still controversial whether the *BRAF* V600E mutation is an independent predictive marker for EGFR blockers [101,102]. 2017 National Comprehensive Cancer Network (NCCN) guidelines recommend *BRAF* V600E mutation testing for metastatic CRC patients; however, ASCP/CAP/AMP/

ASCO and ESMO guidelines for metastatic CRCs do not recommend *BRAF* V600E mutation testing for metastatic CRC [82,91].

Sanger sequencing, pyrosequencing, and real-time PCR-based methods can be used for *BRAF* mutation testing. NGS panels for solid tumors should include *BRAF* tests in South Korea. The presence or absence of nucleotide and amino acid changes in *BRAF* exon 15 should be reported. Appropriate nomenclature should be used.

### Supplementary Materials

The Data Supplement is available with this article at <https://doi.org/10.4132/jptm.2019.09.28>.

### ORCID

Baek-hui Kim: <https://orcid.org/0000-0001-6793-1991>  
 Joon Mee Kim: <https://orcid.org/0000-0003-1355-4187>  
 Gyeong Hoon Kang: <https://orcid.org/0000-0003-2380-6675>  
 Hee Jin Chang: <https://orcid.org/0000-0003-2263-2247>  
 Dong Wook Kang: <https://orcid.org/0000-0002-4300-3469>  
 Jung Ho Kim: <https://orcid.org/0000-0002-6031-3629>  
 Jeong Mo Bae: <https://orcid.org/0000-0003-0462-3072>  
 An Na Seo: <https://orcid.org/0000-0001-6412-3067>  
 Ho Sung Park: <https://orcid.org/0000-0002-4879-874X>  
 Yun Kyung Kang: <https://orcid.org/0000-0002-2075-4665>  
 Kyung-Hwa Lee: <https://orcid.org/0000-0002-3935-0361>  
 Mee Yon Cho: <https://orcid.org/0000-0002-7955-4211>  
 In-Gu Do: <https://orcid.org/0000-0001-7832-7116>  
 Hye Seung Lee: <https://orcid.org/0000-0002-1667-7986>  
 Hee Kyung Chang: <https://orcid.org/0000-0002-4843-5316>  
 Do Youn Park: <https://orcid.org/0000-0001-7641-1509>  
 Hyo Jeong Kang: <https://orcid.org/0000-0002-5285-8282>  
 Jin Hee Sohn: <https://orcid.org/0000-0002-4735-3853>  
 Mee Soo Chang: <https://orcid.org/0000-0002-0948-799X>  
 Eun Sun Jung: <https://orcid.org/0000-0002-8451-939X>  
 So-Young Jin: <https://orcid.org/0000-0002-9900-8322>  
 Eunsil Yu: <https://orcid.org/0000-0001-5474-9744>  
 Hye Seung Han: <https://orcid.org/0000-0002-3591-9995>  
 Youn Wha Kim: <https://orcid.org/0000-0002-8259-5620>

### Author Contributions

Conceptualization: BHK, JMK, GHK, HJC, DWK, JHK, JMB, ANS, HSP, YKK, KHL, MYC, IGD, HSL, HKC, JHS, MSC, ESJ, SYJ, EY, HSH.

Project administration: BHK, JMK, GHK, HJC, DYP.

Supervision: JMK, GHK, HJC, SYJ, ESJ, YWK, MSC, JHS, EY.

Writing—original draft preparation: HSP, ANS, JHK, IGD, YKK, MYC, JMK, DWK, JMB, BHK, HSL, KHL.

Writing—review & editing: BHK, JMK, GHK, HJC, DWK, JHK, JMB, ANS, HSP, YKK, KHL, MYC, IGD, HSL, HKC, DYP, HJK, JHS, MSC, ESJ, SYJ, EY, HSH, YWK.

### Conflicts of Interest

G.H.K., J.H.K., and H.S.L., contributing editors of the *Journal of Pathology and Translational Medicine*, were not involved in the editorial evaluation or decision to publish this article. All remaining authors have declared no conflicts of interest.

### Funding

No funding to declare.

## REFERENCES

1. Chang HJ, Park CK, Kim WH, et al. A standardized pathology report for colorectal cancer. *Korean J Pathol* 2006; 40: 193-203.
2. Ministry of Health and Welfare. Annual report of cancer statistics in Korea in 2015. Sejong: Ministry of Health and Welfare, 2017.
3. Kakar S, Shi C, Berho ME, et al. Protocol for the examination of specimens from patients with primary carcinoma of the colon and rectum, version 4.0.0.0. Illinois: College of American Pathologists, 2017.
4. Amin MB, Edge S, Greene F, et al. AJCC cancer staging system. 8th ed. New York: Springer, 2017.
5. WHO Classification of Tumours Editorial Board. WHO classification of tumours: digestive system tumours. 5th ed. Geneva: World Health Organization, 2019.
6. Fritz AG, Percy C, Jack A, et al. International classification of diseases for oncology (ICD-O). 3rd ed. 1st rev. Lyon: International Agency for Research on Cancer, 2013.
7. Langman G, Loughrey M, Shepherd N, Quirke P. Association of Coloproctology of Great Britain & Ireland (ACPGBI): guidelines for the management of cancer of the colon, rectum and anus (2017)-pathology standards and datasets. *Colorectal Dis* 2017; 19 Suppl 1: 74-81.
8. Nagtegaal I, Gaspar C, Marijnen C, Van De Velde C, Fodde R, Van Krieken H. Morphological changes in tumour type after radiotherapy are accompanied by changes in gene expression profile but not in clinical behaviour. *J Pathol* 2004; 204: 183-92.
9. Verdu M, Roman R, Calvo M, et al. Clinicopathological and molecular characterization of colorectal micropapillary carcinoma. *Mod*

- Pathol 2011; 24: 729-38.
10. Lee HJ, Eom DW, Kang GH, et al. Colorectal micropapillary carcinomas are associated with poor prognosis and enriched in markers of stem cells. *Mod Pathol* 2013; 26: 1123-31.
  11. Nassar H. Carcinomas with micropapillary morphology: clinical significance and current concepts. *Adv Anat Pathol* 2004; 11: 297-303.
  12. Xu F, Xu J, Lou Z, et al. Micropapillary component in colorectal carcinoma is associated with lymph node metastasis in T1 and T2 Stages and decreased survival time in TNM stages I and II. *Am J Surg Pathol* 2009; 33: 1287-92.
  13. Haupt B, Ro JY, Schwartz MR, Shen SS. Colorectal adenocarcinoma with micropapillary pattern and its association with lymph node metastasis. *Mod Pathol* 2007; 20: 729-33.
  14. Jakubowska K, Guzinska-Ustymowicz K, Pryczynicz A. Invasive micropapillary component and its clinico-histopathological significance in patients with colorectal cancer. *Oncol Lett* 2016; 12: 1154-8.
  15. Tuppurainen K, Makinen JM, Junttila O, et al. Morphology and microsatellite instability in sporadic serrated and non-serrated colorectal cancer. *J Pathol* 2005; 207: 285-94.
  16. Patai AV, Molnár B, Tulassay Z, Sipos F. Serrated pathway: alternative route to colorectal cancer. *World J Gastroenterol* 2013; 19: 607-15.
  17. Mäkinen MJ. Colorectal serrated adenocarcinoma. *Histopathology* 2007; 50: 131-50.
  18. Barresi V, Reggiani Bonetti L, Ieni A, Domati F, Tuccari G. Prognostic significance of grading based on the counting of poorly differentiated clusters in colorectal mucinous adenocarcinoma. *Hum Pathol* 2015; 46: 1722-9.
  19. Bosman FT, Carneiro F, Hruban RH, Theise ND. WHO classification of tumours of the digestive system. 4th ed. Lyon: International Agency for Research on Cancer, 2010.
  20. Kojima M, Shimazaki H, Iwaya K, et al. Intramucosal colorectal carcinoma with invasion of the lamina propria: a study by the Japanese Society for Cancer of the Colon and Rectum. *Hum Pathol* 2017; 66: 230-7.
  21. Panarelli NC, Schreiner AM, Brandt SM, Shepherd NA, Yantiss RK. Histologic features and cytologic techniques that aid pathologic stage assessment of colonic adenocarcinoma. *Am J Surg Pathol* 2013; 37: 1252-8.
  22. Uehara K, Nakanishi Y, Shimoda T, Taniguchi H, Akasu T, Moriya Y. Clinicopathological significance of microscopic abscess formation at the invasive margin of advanced low rectal cancer. *Br J Surg* 2007; 94: 239-43.
  23. Smith KD, Tan D, Das P, et al. Clinical significance of acellular mucin in rectal adenocarcinoma patients with a pathologic complete response to preoperative chemoradiation. *Ann Surg* 2010; 251: 261-4.
  24. Kang CM, Lim SB, Hong SM, et al. Prevalence and clinical significance of cellular and acellular mucin in patients with locally advanced mucinous rectal cancer who underwent preoperative chemoradiotherapy followed by radical surgery. *Colorectal Dis* 2016; 18: O10-6.
  25. Kitajima K, Fujimori T, Fujii S, et al. Correlations between lymph node metastasis and depth of submucosal invasion in submucosal invasive colorectal carcinoma: a Japanese collaborative study. *J Gastroenterol* 2004; 39: 534-43.
  26. Bosch SL, Teerenstra S, de Wilt JH, Cunningham C, Nagtegaal ID. Predicting lymph node metastasis in pT1 colorectal cancer: a systematic review of risk factors providing rationale for therapy decisions. *Endoscopy* 2013; 45: 827-34.
  27. Haggitt RC, Glotzbach RE, Soffer EE, Wruble LD. Prognostic factors in colorectal carcinomas arising in adenomas: implications for lesions removed by endoscopic polypectomy. *Gastroenterology* 1985; 89: 328-36.
  28. Kikuchi R, Takano M, Takagi K, et al. Management of early invasive colorectal cancer: risk of recurrence and clinical guidelines. *Dis Colon Rectum* 1995; 38: 1286-95.
  29. Watanabe T, Muro K, Ajioka Y, et al. Japanese Society for Cancer of the Colon and Rectum (JSCCR) guidelines 2016 for the treatment of colorectal cancer. *Int J Clin Oncol* 2018; 23: 1-34.
  30. Betge J, Pollheimer MJ, Lindtner RA, et al. Intramural and extramural vascular invasion in colorectal cancer: prognostic significance and quality of pathology reporting. *Cancer* 2012; 118: 628-38.
  31. Kim WH, Park CK, Kim YB, et al. A standardized pathology report for gastric cancer. *Korean J Pathol* 2005; 39: 106-13.
  32. Liebig C, Ayala G, Wilks J, et al. Perineural invasion is an independent predictor of outcome in colorectal cancer. *J Clin Oncol* 2009; 27: 5131-7.
  33. Liebig C, Ayala G, Wilks JA, Berger DH, Albo D. Perineural invasion in cancer: a review of the literature. *Cancer* 2009; 115: 3379-91.
  34. Gibson JA, Odze RD. Pathology of premalignant colorectal neoplasia. *Dig Endosc* 2016; 28: 312-23.
  35. Rex DK, Ahnen DJ, Baron JA, et al. Serrated lesions of the colorectum: review and recommendations from an expert panel. *Am J Gastroenterol* 2012; 107: 1315-29.
  36. Bateman AC, Shepherd NA. UK guidance for the pathological reporting of serrated lesions of the colorectum. *J Clin Pathol* 2015; 68: 585-91.
  37. Liu C, Walker NI, Leggett BA, Whitehall VL, Bettington ML, Rosty C. Sessile serrated adenomas with dysplasia: morphological patterns and correlations with MLH1 immunohistochemistry. *Mod*

- Pathol 2017; 30: 1728-38.
38. Chetty R, Hafezi-Bakhtiari S, Serra S, Colling R, Wang LM. Traditional serrated adenomas (TSAs) admixed with other serrated (so-called precursor) polyps and conventional adenomas: a frequent occurrence. *J Clin Pathol* 2015; 68: 270-3.
  39. Anwar MA, D'Souza F, Coulter R, Memon B, Khan IM, Memon MA. Outcome of acutely perforated colorectal cancers: experience of a single district general hospital. *Surg Oncol* 2006; 15: 91-6.
  40. Mitrovic B, Schaeffer DF, Riddell RH, Kirsch R. Tumor budding in colorectal carcinoma: time to take notice. *Mod Pathol* 2012; 25: 1315-25.
  41. Choi DH, Sohn DK, Chang HJ, Lim SB, Choi HS, Jeong SY. Indications for subsequent surgery after endoscopic resection of submucosally invasive colorectal carcinomas: a prospective cohort study. *Dis Colon Rectum* 2009; 52: 438-45.
  42. Ueno H, Mochizuki H, Hashiguchi Y, et al. Risk factors for an adverse outcome in early invasive colorectal carcinoma. *Gastroenterology* 2004; 127: 385-94.
  43. Wang LM, Kevans D, Mulcahy H, et al. Tumor budding is a strong and reproducible prognostic marker in T3N0 colorectal cancer. *Am J Surg Pathol* 2009; 33: 134-41.
  44. Giger OT, Comtesse SC, Lugli A, Zlobec I, Kurrer MO. Intra-tumoral budding in preoperative biopsy specimens predicts lymph node and distant metastasis in patients with colorectal cancer. *Mod Pathol* 2012; 25: 1048-53.
  45. Rogers AC, Gibbons D, Hanly AM, et al. Prognostic significance of tumor budding in rectal cancer biopsies before neoadjuvant therapy. *Mod Pathol* 2014; 27: 156-62.
  46. Lugli A, Kirsch R, Ajioka Y, et al. Recommendations for reporting tumor budding in colorectal cancer based on the International Tumor Budding Consensus Conference (ITBCC) 2016. *Mod Pathol* 2017; 30: 1299-311.
  47. Koelzer VH, Zlobec I, Berger MD, et al. Tumor budding in colorectal cancer revisited: results of a multicenter interobserver study. *Virchows Arch* 2015; 466: 485-93.
  48. Koelzer VH, Assarzadegan N, Dawson H, et al. Cytokeratin-based assessment of tumour budding in colorectal cancer: analysis in stage II patients and prospective diagnostic experience. *J Pathol Clin Res* 2017; 3: 171-8.
  49. Jass JR, Love SB, Northover JM. A new prognostic classification of rectal cancer. *Lancet* 1987; 1: 1303-6.
  50. Bosch SL, Nagtegaal ID. The importance of the pathologist's role in assessment of the quality of the mesorectum. *Curr Colorectal Cancer Rep* 2012; 8: 90-8.
  51. Aklilu M, Eng C. The current landscape of locally advanced rectal cancer. *Nat Rev Clin Oncol* 2011; 8: 649-59.
  52. Bibeau F, Rullier A, Jourdan MF, et al. Locally advanced rectal cancer management: which role for the pathologist in 2011? *Ann Pathol* 2011; 31: 433-41.
  53. Dhadda AS, Dickinson P, Zaitoun AM, Gandhi N, Bessell EM. Prognostic importance of Mandard tumour regression grade following pre-operative chemo/radiotherapy for locally advanced rectal cancer. *Eur J Cancer* 2011; 47: 1138-45.
  54. Mihaylova I, Parvanova V, Velikova C, Kurteva G, Ivanova D. Degree of tumor regression after preoperative chemo-radiotherapy in locally advanced rectal cancer-Preliminary results. *Rep Pract Oncol Radiother* 2011; 16: 237-42.
  55. Vallböhmer D, Bollschweiler E, Brabender J, et al. Evaluation of histological regression grading systems in the neoadjuvant therapy of rectal cancer: do they have prognostic impact? *Int J Colorectal Dis* 2012; 27: 1295-301.
  56. Kim SH, Chang HJ, Kim DY, et al. What is the ideal tumor regression grading system in rectal cancer patients after preoperative chemoradiotherapy? *Cancer Res Treat* 2016; 48: 998-1009.
  57. Mandard AM, Dalibard F, Mandard JC, et al. Pathologic assessment of tumor regression after preoperative chemoradiotherapy of esophageal carcinoma: clinicopathologic correlations. *Cancer* 1994; 73: 2680-6.
  58. Dworak O, Keilholz L, Hoffmann A. Pathological features of rectal cancer after preoperative radiochemotherapy. *Int J Colorectal Dis* 1997; 12: 19-23.
  59. Ryan R, Gibbons D, Hyland JM, et al. Pathological response following long-course neoadjuvant chemoradiotherapy for locally advanced rectal cancer. *Histopathology* 2005; 47: 141-6.
  60. Krasinskas AM. EGFR Signaling in Colorectal Carcinoma. *Patholog Res Int* 2011; 2011: 932932.
  61. Goldstein NS, Armin M. Epidermal growth factor receptor immunohistochemical reactivity in patients with American Joint Committee on Cancer Stage IV colon adenocarcinoma: implications for a standardized scoring system. *Cancer* 2001; 92: 1331-46.
  62. McKay JA, Murray LJ, Curran S, et al. Evaluation of the epidermal growth factor receptor (EGFR) in colorectal tumours and lymph node metastases. *Eur J Cancer* 2002; 38: 2258-64.
  63. Spano JP, Fagard R, Soria JC, Rixe O, Khayat D, Milano G. Epidermal growth factor receptor signaling in colorectal cancer: preclinical data and therapeutic perspectives. *Ann Oncol* 2005; 16: 189-94.
  64. Resnick MB, Routhier J, Konkin T, Sabo E, Pricolo VE. Epidermal growth factor receptor, c-MET, beta-catenin, and p53 expression as prognostic indicators in stage II colon cancer: a tissue microarray study. *Clin Cancer Res* 2004; 10: 3069-75.
  65. de Castro-Carpeno J, Belda-Iniesta C, Casado Saenz E, Hernandez Agudo E, Feliu Batlle J, Gonzalez Baron M. EGFR and colon cancer:

- a clinical view. *Clin Transl Oncol* 2008; 10: 6-13.
66. Saltz LB, Meropol NJ, Loehrer PJ Sr, Needle MN, Kopit J, Mayer RJ. Phase II trial of cetuximab in patients with refractory colorectal cancer that expresses the epidermal growth factor receptor. *J Clin Oncol* 2004; 22: 1201-8.
  67. Vallböhmer D, Zhang W, Gordon M, et al. Molecular determinants of cetuximab efficacy. *J Clin Oncol* 2005; 23: 3536-44.
  68. Ogino S, Meyerhardt JA, Cantor M, et al. Molecular alterations in tumors and response to combination chemotherapy with gefitinib for advanced colorectal cancer. *Clin Cancer Res* 2005; 11: 6650-6.
  69. Geiersbach KB, Samowitz WS. Microsatellite instability and colorectal cancer. *Arch Pathol Lab Med* 2011; 135: 1269-77.
  70. Pino MS, Chung DC. Microsatellite instability in the management of colorectal cancer. *Expert Rev Gastroenterol Hepatol* 2011; 5: 385-99.
  71. Samowitz WS. Evaluation of colorectal cancers for Lynch syndrome: practical molecular diagnostics for surgical pathologists. *Mod Pathol* 2015; 28 Suppl 1: S109-13.
  72. Boland CR, Goel A. Microsatellite instability in colorectal cancer. *Gastroenterology* 2010; 138: 2073-87.
  73. Guastadisegni C, Colafranceschi M, Ottini L, Dogliotti E. Microsatellite instability as a marker of prognosis and response to therapy: a meta-analysis of colorectal cancer survival data. *Eur J Cancer* 2010; 46: 2788-98.
  74. Pritchard CC, Grady WM. Colorectal cancer molecular biology moves into clinical practice. *Gut* 2011; 60: 116-29.
  75. Le DT, Uram JN, Wang H, et al. PD-1 blockade in tumors with mismatch-repair deficiency. *N Engl J Med* 2015; 372: 2509-20.
  76. Le DT, Durham JN, Smith KN, et al. Mismatch repair deficiency predicts response of solid tumors to PD-1 blockade. *Science* 2017; 357: 409-13.
  77. Roxburgh CS, McMillan DC. The role of the in situ local inflammatory response in predicting recurrence and survival in patients with primary operable colorectal cancer. *Cancer Treat Rev* 2012; 38: 451-66.
  78. Kirilovsky A, Marliot F, El Sissy C, Haicheur N, Galon J, Pages F. Rational bases for the use of the Immunoscore in routine clinical settings as a prognostic and predictive biomarker in cancer patients. *Int Immunol* 2016; 28: 373-82.
  79. Mlecnik B, Bindea G, Angell HK, et al. Integrative analyses of colorectal cancer show immunoscore is a stronger predictor of patient survival than microsatellite instability. *Immunity* 2016; 44: 698-711.
  80. Galon J, Mlecnik B, Bindea G, et al. Towards the introduction of the 'Immunoscore' in the classification of malignant tumours. *J Pathol* 2014; 232: 199-209.
  81. Galon J, Pagès F, Marincola FM, et al. Cancer classification using the Immunoscore: a worldwide task force. *J Transl Med* 2012; 10: 205.
  82. Sepulveda AR, Hamilton SR, Allegra CJ, et al. Molecular biomarkers for the evaluation of colorectal cancer: guideline from the American Society for Clinical Pathology, College of American Pathologists, Association for Molecular Pathology, and the American Society of Clinical Oncology. *J Clin Oncol* 2017; 35: 1453-86.
  83. Zaanani A, Shi Q, Taieb J, et al. Role of deficient DNA mismatch repair status in patients with stage III colon cancer treated with FOLFOX adjuvant chemotherapy: a pooled analysis from 2 randomized clinical trials. *JAMA Oncol* 2018; 4: 379-83.
  84. Sargent DJ, Marsoni S, Monges G, et al. Defective mismatch repair as a predictive marker for lack of efficacy of fluorouracil-based adjuvant therapy in colon cancer. *J Clin Oncol* 2010; 28: 3219-26.
  85. Overman MJ, McDermott R, Leach JL, et al. Nivolumab in patients with metastatic DNA mismatch repair-deficient or microsatellite instability-high colorectal cancer (CheckMate 142): an open-label, multicentre, phase 2 study. *Lancet Oncol* 2017; 18: 1182-91.
  86. Umar A, Boland CR, Terdiman JP, et al. Revised Bethesda Guidelines for hereditary nonpolyposis colorectal cancer (Lynch syndrome) and microsatellite instability. *J Natl Cancer Inst* 2004; 96: 261-8.
  87. Boland CR, Thibodeau SN, Hamilton SR, et al. A National Cancer Institute Workshop on Microsatellite Instability for cancer detection and familial predisposition: development of international criteria for the determination of microsatellite instability in colorectal cancer. *Cancer Res* 1998; 58: 5248-57.
  88. Adar T, Rodgers LH, Shannon KM, et al. A tailored approach to BRAF and MLH1 methylation testing in a universal screening program for Lynch syndrome. *Mod Pathol* 2017; 30: 440-7.
  89. Buhard O, Cattaneo F, Wong YF, et al. Multipopulation analysis of polymorphisms in five mononucleotide repeats used to determine the microsatellite instability status of human tumors. *J Clin Oncol* 2006; 24: 241-51.
  90. Goel A, Nagasaka T, Hamelin R, Boland CR. An optimized pentaplex PCR for detecting DNA mismatch repair-deficient colorectal cancers. *PLoS One* 2010; 5: e9393.
  91. Van Cutsem E, Cervantes A, Adam R, et al. ESMO consensus guidelines for the management of patients with metastatic colorectal cancer. *Ann Oncol* 2016; 27: 1386-422.
  92. Amado RG, Wolf M, Peeters M, et al. Wild-type KRAS is required for panitumumab efficacy in patients with metastatic colorectal cancer. *J Clin Oncol* 2008; 26: 1626-34.
  93. Douillard JY, Oliner KS, Siena S, et al. Panitumumab-FOLFOX4 treatment and RAS mutations in colorectal cancer. *N Engl J Med*

- 2013; 369: 1023-34.
94. Rui Y, Wang C, Zhou Z, Zhong X, Yu Y. K-Ras mutation and prognosis of colorectal cancer: a meta-analysis. *Hepatogastroenterology* 2015; 62: 19-24.
95. Phipps AI, Limburg PJ, Baron JA, et al. Association between molecular subtypes of colorectal cancer and patient survival. *Gastroenterology* 2015; 148: 77-87.
96. Sinicrope FA, Shi Q, Smyrk TC, et al. Molecular markers identify subtypes of stage III colon cancer associated with patient outcomes. *Gastroenterology* 2015; 148: 88-99.
97. Taieb J, Le Malicot K, Shi Q, et al. Prognostic value of *BRAF* and *KRAS* mutations in MSI and MSS stage III colon cancer. *J Natl Cancer Inst* 2017; 109: djw272.
98. Schirripa M, Bergamo F, Cremolini C, et al. *BRAF* and *RAS* mutations as prognostic factors in metastatic colorectal cancer patients undergoing liver resection. *Br J Cancer* 2015; 112: 1921-8.
99. Wang L, Cunningham JM, Winters JL, et al. *BRAF* mutations in colon cancer are not likely attributable to defective DNA mismatch repair. *Cancer Res* 2003; 63: 5209-12.
100. Loes IM, Immervoll H, Sorbye H, et al. Impact of *KRAS*, *BRAF*, *PIK3CA*, *TP53* status and intraindividual mutation heterogeneity on outcome after liver resection for colorectal cancer metastases. *Int J Cancer* 2016; 139: 647-56.
101. Di Nicolantonio F, Martini M, Molinari F, et al. Wild-type *BRAF* is required for response to panitumumab or cetuximab in metastatic colorectal cancer. *J Clin Oncol* 2008; 26: 5705-12.
102. Pietrantonio F, Petrelli F, Coinu A, et al. Predictive role of *BRAF* mutations in patients with advanced colorectal cancer receiving cetuximab and panitumumab: a meta-analysis. *Eur J Cancer* 2015; 51: 587-94.

# Tumor immune response and immunotherapy in gastric cancer

Yoonjin Kwak<sup>1,2</sup>, An Na Seo<sup>3</sup>, Hee Eun Lee<sup>4</sup>, Hye Seung Lee<sup>2,5</sup>

<sup>1</sup>Department of Pathology, Seoul National University Hospital, Seoul;

<sup>2</sup>Department of Pathology, Seoul National University College of Medicine, Seoul;

<sup>3</sup>Department of Pathology, School of Medicine, Kyungpook National University, Kyungpook National University Chilgok Hospital, Daegu, Korea;

<sup>4</sup>Division of Anatomic Pathology, Mayo Clinic, Rochester, MN, USA;

<sup>5</sup>Department of Pathology, Seoul National University Bundang Hospital, Seongnam, Korea

Remarkable developments in immuno-oncology have changed the landscape of gastric cancer (GC) treatment. Because immunotherapy intervenes with tumor immune response rather than directly targeting tumor cells, it is important to develop a greater understanding of tumor immunity. This review paper summarizes the tumor immune reaction and immune escape mechanisms while focusing on the role of T cells and their co-inhibitory signals, such as the immune checkpoint molecules programmed death-1 and programmed death-ligand 1 (PD-L1). This paper also describes past clinical trials of immunotherapy for patients with GC and details their clinical implications. Strong predictive markers are essential to improve response to immunotherapy. Microsatellite instability, Epstein-Barr virus, PD-L1 expression, and tumor mutational burden are now regarded as potent predictive markers for immunotherapy in patients with GC. Novel immunotherapy and combination therapy targeting new immune checkpoint molecules such as lymphocyte-activation gene 3, T cell immunoglobulin, and mucin domain containing-3, and indoleamine 2,3-dioxygenase have been suggested, and trials are ongoing to evaluate their safety and efficacy. Immunotherapy is an important treatment option for patients with GC and has great potential for improving patient outcome, and further research in immuno-oncology should be carried out.

**Key Words:** Stomach neoplasms; Immunotherapy; Programmed cell death-ligand 1; Microsatellite instability; Epstein-Barr virus; Tumor mutational burden; Tumor-infiltrating lymphocytes; Biomarker

**Received:** July 29, 2019 **Revised:** October 2, 2019 **Accepted:** October 8, 2019

**Corresponding Author:** Hye Seung Lee, MD, PhD, Department of Pathology, Seoul National University Bundang Hospital, Seoul National University College of Medicine, 82 Gumi-ro 173beon-gil, Bundang-gu, Seongnam 13620, Korea  
 Tel: +82-31-787-7714, Fax: +82-31-787-4012, E-mail: [hye2@snu.ac.kr](mailto:hye2@snu.ac.kr)

Recent studies have reported the promising results of immunotherapy in many solid tumors [1]. Unlike traditional cancer therapy, which targets the tumor directly, immunotherapy offers a different approach and is an alternative treatment option for patients with cancer. Because immunotherapy generally engages immune reactions to recognize and eliminate tumor cells, demand for understanding the tumor immune response has increased. Resulting from increased study, novel biomarkers associated with the tumor immune reaction have emerged. These biomarkers may allow innovative approaches in patient selection for immunotherapy and lead to advanced treatment response, expanding the potential impact of immunotherapy. After the advent of U.S. Food and Drug Administration (FDA)-approved anti-programmed cell death-1 (PD-1)/programmed death-ligand 1 (PD-L1) therapy agents, the importance of immunotherapy in gastric cancer (GC)

has continuously increased. In this review article, we recapitulate the general concept of immuno-oncology and discuss its clinical application while focusing on historical and current clinical trials.

## TUMOR IMMUNE MICROENVIRONMENT: GENERAL CONCEPTS AND PROGNOSTIC SIGNIFICANCE

### Tumor immune response

While the immune response to tumor cells is mainly caused by CD8-positive cytotoxic T cells, it is a multistep process (so-called cancer-immunity cycle) [2,3], including (1) tumor antigen production by tumor cells and processing of released tumor antigens by antigen presenting cells (APCs) such as dendritic cells (DCs), (2) tumor antigen presentation on the surface of

APCs through major histocompatibility complex (MHC) class I and MHC class II substances for recognition by T cells, (3) priming and activation of T cells in lymph nodes after recognition of tumor antigens, (4) migration of activated T cells to tumor through blood vessels, (5) infiltration of T cells into and around the tumor, (6) T cell recognition of antigen presenting tumor cells by binding between MHC class I substances on tumor cells and T cell receptors (TCRs) on the surface of T cells, and (7) killing of tumor cells recognized by T cells. The tumor cells destroyed by T cells release additional tumor antigens, increasing immune response. Some receptors and their ligands have been reported to promote or inhibit each step.

Because patients with tumors have enhanced immune reactions, many researchers have tried to identify tumor antigens that are expressed in tumor cells [4]. Proteins made from gene mutations can be recognized as tumor antigens. As normal cells become tumor cells, mutations are observed in various oncogenes and tumor suppressor genes (Fig. 1A). Furthermore, mutations can easily occur during the gene replication process of cell division due to the genetic instability of tumor cells [5]. Many proteins made from mutated genes are recognized as tumor antigens by immune cells regardless of their function. Neoantigens

produced by genetic mutations can induce strong tumor immune responses [6]. Viral proteins from oncogenic viruses, such as human papillomaviruses and Epstein-Barr virus (EBV), are also tumor antigens. In patients infected with the virus, immune cells recognize proteins produced by the virus as antigens, resulting in an immune response to remove the virus-infected cells. Thus, proteins produced from viral genes in tumor cells are important tumor antigens [7]. In addition, proteins that are not expressed in normal cells can be overexpressed in tumor cells. These proteins could be recognized by the immune system as non-self [8]. Some glycoproteins and glycolipids expressed on the cellular surface are overexpressed or modified in tumor cells, which can be recognized as tumor antigens. Oncofetal antigens, such as carcinoembryonic antigen, can also cause immune responses with weak intensity and may be used as diagnostic markers.

Cell-mediated immunity is the main response to tumors, and the inhibitory effect of cytotoxic T cells on tumor cells is well known [9]. Cytotoxic T cells express CD8 and CD3, and have TCRs that recognize tumor antigens presented by MHC class I molecules [10]. T cell proliferation and activation in tumor tissues requires stimulation, usually by two stimuli (Fig. 1B). The first stimulus is a tumor antigen presented on MHC molecules.

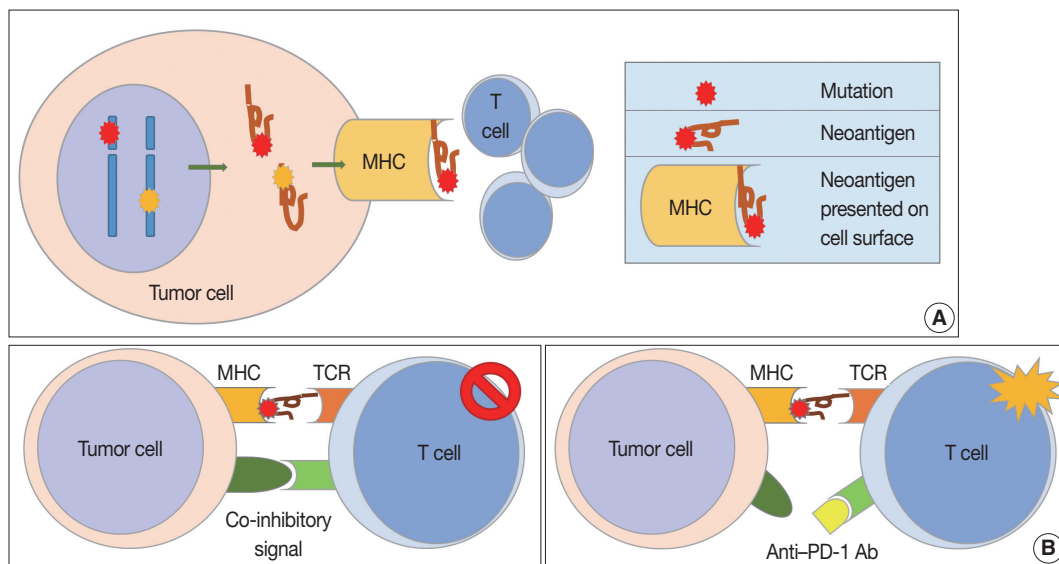


**Fig. 1.** Cell-mediated tumor immunity. (A) Altered proteins are produced following genetic mutation of tumor cells or viral genes in tumor cells. Neoantigens can arise from these altered tumor proteins and be presented on tumor cell surface via major histocompatibility complex. Newly formed antigens on tumor cell surfaces are recognized by the immune system, and the tumor immune reaction is initiated. (B) T cell responses are generated by two signals. The first signal is binding between neoantigen presented on major histocompatibility complex (MHC) molecule and T cell receptor (TCR). The second signal is co-inhibitory or co-stimulatory and determines whether T cells will be activated or not. Programmed cell death protein-1 (PD-1), lymphocyte-activation gene 3, and T cell immunoglobulin, and mucin domain containing-3 are well known co-inhibitory receptors that bind specific ligands, such as programmed death-ligand 1 (PD-L1) or PD-L2. Binding between co-inhibitory receptors and their ligands induces T cell inactivation. Blockade of these co-inhibitory signals is the basic strategy for cancer immunotherapy.

As described above, neoantigens from genetically mutated or viral genes are major tumor antigens that cause tumor antigen-specific T cell responses. Second, co-stimulatory molecules affect T cell proliferation and survival. T cells have co-stimulatory receptors that combine with expressed co-stimulatory ligands on the surface of tumor cells to promote T cell activation. CD28 and CD27 expression is observed in T cells, and CD134 and CD137 are mainly expressed in antigen-activated T cells [11,12]. Helper T cells are positive for CD4 and CD3 expression. The role of helper T cells in tumor immunity has yet to be fully elucidated, but their main role is to aid humoral immunity via B cell antibody secretion and to enhance the function of cytotoxic T cells [13]. Helper T cells are reported to have cytotoxic functions in some tumors expressing MHC class II. Regulatory T cells (Tregs) express CD4, FOXP3, and CD25 and regulate the immune response by suppressing the immune response to self-proteins and the tumor immune response [14]. Tregs inhibit the tumor immune response by producing high-affinity interleukin-2 (IL-2) receptor, cytotoxic T lymphocyte-associated protein 4 (CTLA-4), IL-10, and immunosuppressive cytokines such as transforming growth factor  $\beta$  (TGF- $\beta$ ).

### Mechanism of immune evasion in solid tumors

The immune surveillance system attempts to eliminate tumor cells in the early stages of cancer. However, tumor cells can inhibit the immune system or cause tumor cells themselves to avoid immune responses, a process called immunoeediting [15]. Tumor cells can adapt to avoid the immune response by various mechanisms. They can then reach an equilibrium state and escape from the tumor immune response [16].

In contrast to the co-stimulatory receptors described above, tumor cells produce several co-inhibitory receptors, including PD-1, CTLA-4, T cell immunoglobulin, and mucin domain containing-3 (TIM-3), lymphocyte-activation gene 3 (LAG-3), and indoleamine 2,3-dioxygenase (IDO). These receptors inhibit T cell activation by binding to their tumor cell ligands [11,12]. Tumor-infiltrating lymphocytes (TILs) release interferon  $\gamma$  (IFN- $\gamma$ ) and induce expression of PD-L1 (also known as B7-H1 or CD274) in surrounding tumor cells, stromal cells, and blood cells [17]. Overexpressed PD-L1 activates and binds to PD-1 co-inhibitory receptors on CD8-positive T cells, rendering them inactive. In addition to PD-L1, PD-L2 (also known as B7-DC or CD273) also binds to PD-1 with a weaker binding strength than PD-L1. CTLA-4 is overexpressed early in CD4-positive and CD8-positive T cells. CTLA-4 binds to CD80 (B7-1) and CD86 (B7-2) on APCs, preventing them from binding to the co-stimulatory

receptor CD28 and inhibiting TCRs by intracellular PP2A and SHP-2 signaling pathways [18]. CTLA-4 is continuously expressed in Tregs and supports the immunosuppressive function of Tregs [19]. LAG-3 expression is increased in activated T cells and natural killer cells, and its ligands are MHC class II, LSECtin, and galectin-3 [20,21]. LAG-3 inhibits T cell proliferation and cytokine production. TIM-3 binds to its ligands, including galectin-9, high mobility group box 1 (HMGB1), and carcinoembryonic antigen cell adhesion molecule 1, and plays a role in immune evasion of tumor cells by inactivating T cells [22].

MHC molecules are observed on the surface of all nucleated cells, and MHC class I molecules consist of a heavy chain (HLA-A, -B, and -C) and  $\beta$ -2-microglobulin ( $\beta$ 2M) [23]. MHC class I molecules play a major role in the cell-mediated immunity caused by cytotoxic T cells. Expression of MHC class I molecules is heterogeneously observed in patients with cancer. Downregulation or loss of MHC class I molecule expression has been reported and is regarded as the main mechanism of avoiding immune responses [24].  $\beta$ 2M gene mutation and alterations in *HLA* gene transcription and translation are thought to be major causes of decreased MHC class I expression [25].

Tumor cells produce and secrete immunosuppressive factors that inhibit the function of immune cells, such as IL-10, galectins, tumor necrosis factor, TGF- $\beta$ , prostaglandin E2, and vascular endothelial growth factor [26]. They not only inhibit the function of immune cells but also interfere with their differentiation and maturation. In addition, tumor cells can evade the immune response by modifying tumor antigens [26]. As a tumor grows, tumor cells with immunogenic tumor antigens are removed by the immune response. The immune response can no longer remove tumor cells that lack tumor antigens.

### Prognostic significance of tumor-infiltrating lymphocytes in gastric cancer

In recent years, TILs have been studied for their role as prognostic markers and potential therapeutic targets. Neoantigens presented on cancer cells can recruit TILs and trigger an immune reaction. CD8-positive cytotoxic T cells play a role as the effector cytotoxic T cells involved in direct killing of tumor cells [5]. Therefore, they are regarded as the anti-tumorigenic T cell population. Many previous studies reported that higher TIL density was associated with favorable prognosis in patients with cancer, including GC. Furthermore, previous studies consistently demonstrated that higher TIL densities, such as CD3- or CD8-positive cytotoxic T cells, were associated with better outcome in patients with GC [27,28]. These studies investigated TIL density by immunohisto-

chemistry (IHC) of CD3, CD4, CD8, and other markers (Table 1) [29–42]. An image analyzing software was used to quantify TIL density and ensure constant analysis, or TIL density was counted manually. Most studies dichotomized TIL density into a low and high group for statistical analysis. However, the detailed methods and cut-offs are diverse and not yet standardized. For example, analysis areas were selected in various ways and cut-off values for TIL density had a diverse range. TILs were counted in one representative area, two to six representative areas, or in both the center and at the invasive border. Some studies defined cutoffs as a median value, but others defined cutoffs as a mean, 25th percentile, or 60th percentile value calculated in their own cohort. Thus, the

cutoff number for CD8-positive cytotoxic T cells ranged from 21.6/mm<sup>2</sup> to 946.22/mm<sup>2</sup>. Although higher TIL density is repeatedly reported as a favorable prognostic biomarker, diagnostic methods are not standardized and there is no consensus regarding the cutoff for high TIL density. Therefore, further study and consensus are needed to clarify the diagnostic reliability and practical usefulness of TIL densities in patients with GC.

## CURRENT STATUS OF IMMUNOTHERAPY FOR GASTRIC CANCER

GC is the fourth most common cancer in the world and the

**Table 1.** Detailed methods of density of CD8-positive tumor-infiltrating lymphocytes in the previous studies

Study	Region	No.	Subsets	Outcomes	TMA	Study	Selected area	CD8 cutoff point	CD8 cutoff number (/mm <sup>2</sup> )
Lee et al. (2008) [29]	Korea	220	CD3/CD8/CD45RO	OS	Yes	Consecutive GC	Representative one area	Mean	435.73
Haas et al. (2009) [30]	Germany	52	CD3/CD8/CD20/Foxp3/Granzyme B/M	OS	Yes	Gastric cardia cancer	Six representative areas	Median	21.6 (epithelial) 212.7 (stromal)
Shen et al. (2010) [31]	China	133	CD4/CD8/Foxp3	OS	Yes	GC with R0 resection	Average of two centers and two invasive border	Median	946.22 (intratumoral) 744.40 (peritumoral)
Kim et al. (2011) [32]	Korea	180	CD3/CD4/CD8/Foxp3/Granzyme B	OS/RFS	No	Gastric cardia cancer	Mean of 5 HPFs (center areas)	Median	60.8/HPF (253.33)
Kim et al. (2014) [33]	Korea	99	CD8/Foxp3	OS	Yes	MSI-H advanced GC	Average of 3 representative areas	60th percentile	601.5 (median, 542.6)
Li e al. (2015) [34]	China	192	CD4/CD8	OS	No	Advanced GC	Representative one slide	26%–100% staining	Not available
Liu et al. (2015) [35]	China	166	CD3/CD4/CD8/Foxp3/CD57/M	OS	No	Surgical resection cases	Average of 5 noncontiguous and the densest random areas, in intratumoral and stromal area	Median	839.69 (intratumoral) 523.90 (stromal)
Hennequin et al. (2016) [36]	France	82	CD8/CD20/Foxp3/Tbet	RFS	No	Consecutive GC (including preop-chemotherapy)	Mean of 3 HPF in core and invasive margin	Median	Not available
Kim et al. (2016) [37]	Korea	243	CD3/CD4/CD8	DFS	Yes	Consecutive GC	Representative one core	Median	375.48
Giampieri et al. (2017) [38]	Italy	73	CD3	OS	No	Metastatic GC with 1st-line chemotherapy	Biopsy or resected specimens	More than 50%–60% stromal area covered by TILs	Not available
Kawazoe et al. (2017) [39]	Japan	383	CD3/CD4/CD8/Foxp3	OS	Yes	Advanced GC	Invasive area (two cores)	Median	384
Koh et al. (2017) [40]	Korea	392	CD3/CD4/CD8/Foxp3	OS	Yes	Stage II and III GC	Tumor center and invasive border	25th percentile	130.07 (center) 101.76 (border)
Pernot et al. (2019) [41]	France	67	CD8/Foxp3/CD57	OS	No	Locally advanced or metastatic GC	Mean of 3 representative HPFs	Median	31/HPF
Kim et al. (2019) [42]	Korea	297	CD3/CD8/Foxp3	OS	Yes	Early GC with submucosal invasion and advanced GC	Tumor center and invasive border	Median	Not available

TMA, tissue microarray; OS, overall survival; GC, gastric cancer; RFS, relapse-free survival; HPF, high power field; MSI-H, microsatellite instability-high; DFS, disease-free survival; TIL, tumor-infiltrating lymphocyte.

second-leading cause of cancer-associated death [43]. For localized GC, the only curative treatment modality is radical surgery with or without perioperative chemotherapy [44]. For unresectable or metastatic GC, systemic chemotherapy has been the mainstay of palliation. Over the last decade, two new agents, monoclonal antibodies targeting human epidermal growth factor receptor 2 (HER2; trastuzumab) and vascular endothelial growth factor receptor 2 (VEGFR-2; ramucirumab), have been approved by the FDA to treat GC in the palliative setting [44]. Briefly, first-line therapy includes a combination of platinum and fluoropyrimidine (5-fluorouracil or capecitabine) with trastuzumab added in HER2-positive tumors [44]. In the second-line setting, therapeutic options include docetaxel, paclitaxel, or irinotecan monotherapy or ramucirumab alone or in combination with paclitaxel [44]. In fact, nearly all patients with advanced GC experience disease progression following treatment [45]. There is currently no standard third-line therapy but options include apatinib, a small molecule multitargeted tyrosine kinase inhibitor with activity against VEGFR-2, and regorafenib, a multikinase inhibitor [44]. More recently, immune checkpoint inhibitors have emerged as among the most advanced therapeutic options available for patients with advanced GC [46].

Pembrolizumab is a selective, humanized, high-affinity IgG4 kappa monoclonal antibody that binds to PD-1, blocking its interaction with PD-L1 and 2 [45,47]. The FDA approved pembrolizumab in May 2017 for patients with unresectable or metastatic microsatellite instability-high (MSI-H) or mismatch repair deficient (dMMR) solid tumors that progressed even after prior treatment and who have no other optimal treatment choices [48]. The approval was based on promising results of five different clinical trials; the overall/objective response rate (ORR), defined as proportion of patients with a complete or partial response, was 39.6% among 149 patients with various tumor types (95% confidence interval [CI], 31.7% to 47.9%). A complete response was seen in 7% of patients [48]. The duration of response ranged from 1.6+ to 22.7+ months (+ indicates no progressive disease at last patient assessment) [48]. The phase 1b KEYNOTE-012 trial had ORR of 22% among 36 patients with PD-L1 positive recurrent or metastatic gastric or gastroesophageal (G/GEJ) adenocarcinomas, and all responses were partial [49]. The phase 2 KEYNOTE-059 trial enrolled 259 patients with locally advanced or metastatic G/GEJ adenocarcinoma to further assess the safety and efficacy of pembrolizumab [50]. The ORR was 11.6% (95% CI, 8.0% to 16.1%), with complete response in 2.3% of cases (95% CI, 0.9% to 5.0%), and the response duration ranged from 1.6+ to 17.3+ months. Among 55% of the

tumors with PD-L1 expression based on a combined positive score (CPS)  $\geq 1$  and that were either microsatellite stable or with undetermined microsatellite instability, the ORR was 13.3% (95% CI, 8.2 to 20.0), with complete response in 1.4% of cases. The duration of response was relatively long, ranging from 2.8+ to 19.4+ months. Based on these results, the FDA granted approval with acceleration for pembrolizumab to treat patients with recurrent, locally advanced or metastatic G/GEJ adenocarcinoma with disease progression on or after two or more standard systemic therapies and if tumors express PD-L1, as determined by an FDA-approved test (PD-L1 IHC 22C3 pharmDx test, Dako, Agilent, Santa Clara, CA, USA) [47]. In the phase 3 KEYNOTE-061 trial, pembrolizumab did not demonstrate significant improvement in overall survival (OS) compared to paclitaxel as second-line therapy for advanced G/GEJ cancer with PD-L1 CPS  $\geq 1$  [51]. However, pembrolizumab had a better safety profile than paclitaxel. The phase 3 KEYNOTE-062 trial enrolled 763 patients with PD-L1-positive, HER2-negative, advanced G/GEJ cancer; pembrolizumab used as a first-line therapy resulted in noninferior OS compared with standard chemotherapy [52]. Additionally, pembrolizumab showed significant improvement in OS among patients that had tumors with PD-L1 CPS  $\geq 10$ .

Nivolumab, a human IgG4 monoclonal antibody that inhibits PD-1, has been approved for monotherapy and combination therapy in metastatic melanoma, non-small cell lung cancer, and renal cell carcinoma [46]. The phase 1/2 CheckMate-032 trial showed ORR of 12% in the nivolumab alone group in patients with chemotherapy-refractory G/GEJ cancer [53]. The phase 3 ATTRACTION-2 trial demonstrated significantly longer OS in the nivolumab alone group vs placebo (5.26 months vs. 4.14 months) in patients with advanced G/GEJ cancer refractory to at least two previous chemotherapies [45]. As a consequence, nivolumab was approved to treat advanced GC as a third-line therapy in Japan [46]. In addition, interim results of the phase 2 ATTRACTION-4 trial showed that nivolumab combined with standard chemotherapy showed promising efficacy as a first-line therapy for unresectable advanced or recurrent HER2-negative G/GEJ cancer [54]. The ATTRACTION-4 trial has proceeded to part 2 (phase 3) to compare nivolumab plus standard chemotherapy versus placebo plus standard chemotherapy. Another phase 3 trial (CheckMate-649) is ongoing to evaluate the efficacy and safety of nivolumab combined with standard chemotherapy or ipilimumab (anti-CTLA-4) as a first-line therapy in patients with advanced G/GEJ cancer [55].

There are many other ongoing clinical trials to evaluate the

safety and efficacy of a variety of immune checkpoint inhibitors in patients with advanced G/GEJ cancer. These include tremelimumab (anti-CTLA-4) [56], avelumab (anti-PD-L1) [57,58],

durvalumab (anti-PD-L1) [56,59], and relatlimab (anti-LAG3) [60]. Most of the trials are currently ongoing. A completed trial (JAVELIN Gastric 300) showed that treatment of patients with

**Table 2.** Summary of clinical trials of immunotherapy in locally advanced, recurrent, or metastatic gastric/gastroesophageal junction cancer

Trials	Target	Phase	Treatment arms	Setting (line)	No. of patients	Results/primary endpoints
Pembrolizumab						
KEYNOTE-012 [49]	PD-1	1b	Pembrolizumab	Any	39 with positive PD-L1	ORR (%): 22 (95% CI, 10–39; all PR)
KEYNOTE-059 (cohort 1) [50]	PD-1	2	Pembrolizumab	≥3rd	259	ORR (%): 11.6 (95% CI, 8.0–16.1; CR in 2.3) Median response duration (mo): 8.4 (1.6 <sup>a</sup> to 17.3+) OS (mo): 5.6; PFS (mo): 2.0
KEYNOTE-061 [51]	PD-1	3	Pembrolizumab Paclitaxel	2nd	592 (395 with CPS ≥ 1)	OS (mo): 9.1 vs. 8.3 (HR, 0.82; 95% CI, 0.66–1.03) PFS (mo): 1.5 vs. 4.1 (HR, 1.27; 95% CI, 1.03–1.57) (both analyses in the subgroup of positive PD-L1)
KEYNOTE-062 [52]	PD-1	3	Pembrolizumab vs Pembrolizumab + cisplatin + 5-FU or capecitabine Placebo + cisplatin + 5-FU or capecitabine	1st	763 with CPS ≥ 1 (281 with CPS ≥ 10)	OS (mo): 10.6 vs. 12.5 vs. 11.1 (CPS ≥ 1) OS (mo): 17.4 vs. 12.3 vs. 10.8 (CPS ≥ 10) PFS (mo): 2.0 vs. 6.9 vs. 6.4 (CPS ≥ 1) PFS (mo): 2.9 vs. 5.7 vs. 6.1 (CPS ≥ 10)
Nivolumab (± ipilimumab)						
CheckMate-032 [53]	PD-1 CTLA-4	1/2	Nivolumab 3 mg/kg nivolumab 1 mg/kg + ipilimumab 3 mg/kg Nivolumab 3 mg/kg + ipilimumab 1 mg/kg	≥2nd	160	ORR (%): 12 vs. 24 vs. 8 (independent of PD-L1 status) 12-mo PFS rates (%): 8 vs. 17 vs. 10 12-mo OS rates (%): 39 vs. 35 vs. 24
ONO-4538-12, ATTRAC-TION-2 [46]	PD-1	3	Nivolumab alone placebo	≥3rd	493	OS (mo): 5.26 vs. 4.14 (HR, 0.63; 95% CI, 0.51–0.78) 12-mo OS rates (%): 26.2 vs. 10.9
ATTRACTION-4, part 1 [54]	PD-1	2	Nivolumab + oxaliplatin + capecitabine Nivolumab + oxaliplatin + S-1	1st	40	ORR (%): 76.5 vs. 57.1 PFS (mo): 10.6 vs. 9.7
ATTRACTION-4, part 2	PD-1	3	Nivolumab + oxaliplatin + S-1 or capecitabine Placebo + oxaliplatin + S-1 or capecitabine	1st	Approx. 650	Ongoing
CheckMate-649 [55]	PD-1 CTLA-4	3	Nivolumab + ipilimumab Nivolumab + oxaliplatin + 5-FU or capecitabine Oxaliplatin + 5-FU or capecitabine	1st	870	Ongoing
Others						
JAVELIN Gastric 100 [58]	PD-L1	3	Avelumab BSC after response or stability to oxaliplatin + fluoropyrimidine	Maintenance after 1st-line	499	Ongoing
JAVELIN Gastric 300 [57]	PD-L1	3	Avelumab Paclitaxel or irinotecan	3rd	371	OS (mo): 4.6 vs. 5.0 (HR, 1.1; 95% CI, 0.9–1.4) PFS (mo): 1.4 vs. 2.7 (HR, 1.73; 95% CI, 1.4–2.2) ORR (%): 2.2 vs. 4.3
NCT02340975 [59]	PD-L1 CTLA-4	1b/2	Durvalumab (anti-PD-L1) Tremelimumab (anti-CTLA-4) Durvalumab + tremelimumab	≥2nd	94 (phase 2; as of Sep 13, 2017)	Ongoing
NCT01968109 [60]	LAG-3 PD-1	1/2a	Relatlimab (anti-LAG3) vs. Relatlimab + nivolumab	Last	Advanced solid tumors	Ongoing

PD-1, programmed death-1; PD-L1, programmed death-ligand 1; ORR, objective response rate; CI, confidence interval; PR, partial response; CR, complete response; OS, overall survival; PFS, progression-free survival; CPS, Combined Positive Score for PD-L1; HR, hazard ratio; CI, confidence interval; 5-FU, 5-fluorouracil; CTLA-4, cytotoxic T lymphocyte-associated protein 4; LAG-3, lymphocyte-activation gene 3.

<sup>a</sup>+ indicates that patients had no progressive disease at their last assessment.

G/GEJ cancer with single-agent avelumab in the third-line setting did not demonstrate improved OS or progression-free survival (PFS) compared with standard chemotherapy [57]. The completed and ongoing immunotherapy clinical trials in locally advanced, recurrent, or metastatic G/GEJ cancers are summarized in Table 2.

## BIOMARKERS FOR IMMUNOTHERAPY IN GASTRIC CANCER PATIENTS

### IHC of PD-L1

PD-1 was first discovered in 1992 by Honjo and colleagues [61]. PD-1 is mainly expressed on activated cytotoxic T cells and other immune cells [51,62]. Within the tumor microenvironment, PD-L1 and PD-L2 can upregulate their expression in cancer cells [62]. In several previous studies and currently published genomic profiles, PD-L1 expression has been observed in more than 40% of GC; it is particularly specific for EBV-positive and MSI-H subtypes [37,63-65].

The PD-L1 IHC 22C3 pharmDx assay on the Autostainer Link 48 platform is the FDA-approved companion diagnostic assay to help identify recurrent or metastatic G/GEJ adenocarcinoma in patients who could be treated with pembrolizumab [49,50]. PD-L1 expression assessed by this assay can be quantified by the CPS method (Fig. 2), which is the number of PD-L1 staining cells (tumor cells, lymphocytes, and macrophages) divided by the total number of viable tumor cells, multiplied by 100. If the result of the calculation exceeds 100, the maximum score is regarded as CPS 100 [66]. A tumor with CPS $\geq$ 1 score is considered positive for PD-L1 expression. For adequate evaluation, at least 100 viable tumor cells are needed in a stained slide [66]. At 20 $\times$  magnification, partial or complete membrane staining of viable tumor cells and membrane and/or cytoplasmic staining of mononuclear inflammatory cells within tumor and peri-tumoral areas were evaluated, respectively [66]. Another interpretation of PD-L1 expression is the tumor proportion score (TPS), which is evaluation of membrane staining of PD-L1 expression on tumor cells. The Asian ATTRACTION-2 study, which determined the efficacy of nivolumab in advanced G/GEJ adenocarcinoma, retrospectively evaluated PD-L1 expression by PD-L1 IHC 28-8 pharmDx assay (Dako, Carpinteria, CA, USA); PD-L1 positivity was defined as TPS  $\geq$  1 [46]. Of note, the ATTRACTION-2 study showed that nivolumab had significant benefit in all patients, regardless of PD-L1 expression [46]. The PD-L1 IHC 28-8 pharmDx assay gained FDA approval as a complementary diagnostic test for nivolumab as second line treatment for advanced non-small cell lung cancer (NSCLC) [67].

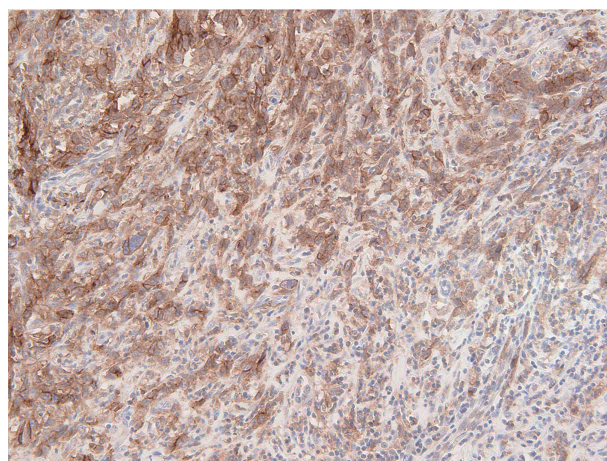


**Fig. 2.** Representative figure of PD-L1 22C3 PharmDx assay. Most tumor cells show membranous staining. Some immune cells adjacent to tumor cells also had immunoreactivity to programmed death-ligand 1.

### Microsatellite instability

MSI-H GC was proposed as a distinct subgroup of GCs by two large scale molecular studies, The Cancer Genome Atlas (TCGA) and the Asian Cancer Research Group classification [65,68,69]. The incidence of MSI-H GCs varies between countries and ethnicity, ranging from 5.6 to 22.7% [65,68,70-73]. MSI-H GCs are associated with antrum location, female gender, relatively older age, earlier stage, and Lauren intestinal type [72]. The presence of dMMR results in tumor cells accumulating frequent genetic mutations. With high mutational burden, tumor cells produce several neo-antigens that trigger T cell activation and recruitment. As the tumor immune reaction increases, expression of checkpoint molecules in tumor cells and immune cells is upregulated [69]. MSI-H GCs are significantly related to both high TILs and high expression of PD-L1 [74,75]. This has been confirmed by several previous genomic profiling studies [76]. On the basis of these hypotheses, recent studies have suggested that MSI-H status may be used as a biomarker for treatment selection with immune-checkpoint inhibitors [50,69]. In Korean patients with metastatic and/or recurrent GC, almost all patients with MSI-H GCs achieve a dramatic response with pembrolizumab alone [75].

Because accurate and reliable evaluation of MSI status is important for treatment decisions, more sensitive, more precise, and faster techniques are required [69]. Three representative methods are currently used to detect GCs with dMMR: polymerase chain reaction (PCR), IHC, and next-generation sequencing (NGS). First, PCR amplification with specific primers for microsatellite repeats is a conventional method using capillary gel

electrophoresis [77]. By comparing the allelic position of a microsatellite locus in tumor tissue and corresponding normal tissue, MSI can be determined by peak patterns with a shift [69,77]. The National Cancer Institute recommends the Bethesda Panel, which is composed of five microsatellite markers specific for two mononucleotide repeats (BAT25 and BAT26) and three dinucleotide repeats (D5S346, D2S123, and D17S250) [69,77,78]. Another MSI test is composed of a pentaplex panel of quasi-monomorphic mononucleotide markers (NR-27, NR-21, NR-24, BAT-25, and BAT-26) [77,79]. MSI-H is designated when a size shift is identified in at least two of five microsatellites loci [77]. Second, IHC is assessed by expression or total loss of mismatch repair (MMR) proteins (MLH1, MSH2, PMS2, and MSH6) [77]. Loss of expression in one or more MMR proteins is defined as dMMR. Compared with the PCR-based method, IHC has high sensitivity and specificity (more than 90%, respectively) [77,80], but a combination of both methods increases sensitivity. Although IHC allows the determination of which MMR gene is defective, GCs with MSI-H are mainly caused by epigenetic inactivation of MMR genes (hypermethylation of CpG island methylator pathway and hMLH1 silencing) [65,68,72,73]. Therefore, loss of MLH1 and PMS2 was predominantly found in sporadic GCs (~95.8%), unlike with Lynch syndrome [72]. Interestingly, BRAFV600E mutation has not been found in MSI-H GCs, unlike in MSI-H sporadic colorectal cancer [69,81]. Recently developed NGS-based methods cover a broader range of microsatellite loci. However, NGS has several disadvantages: (1) high investment costs per sample; (2) longer run time; and (3) exponential bioinformatics analysis [69,82].

### Epstein-Barr virus

EBV-positive GCs constitute a unique subgroup of GCs in the TCGA with several distinct clinicopathologic characteristics, including abundant TILs, male predominance, relatively young age, earlier stage, and favorable prognosis [65,72,73,76]. The incidence of EBV-positive GCs also varies with country and ethnicity, with a range of 2%–20.1% and a worldwide average of nearly 10% [65,72,73,77,83,84]. EBV-positive GCs display *CDKN2A* (p16INK4A) promoter hyper-methylation, and PD-L1/L2 expression was elevated in genomic profiling, in which IL-12-mediated signaling signatures induced robust presence of immune cells [65,85]. Nearly 50% of EBV-positive GCs showed high expression of PD-L1 [86]. In Korean patients with metastatic and/or recurrent GCs, the patients with EBV-positive GCs achieved dramatic response with pembrolizumab alone [75]. This study suggests that EBV-positive GCs may be good candi-

dates for pembrolizumab monotherapy [75]. Another open-label, multi-arm phase II trial (NCT02951091) is testing the efficacy of nivolumab in EBV-positive GCs as second-line treatment [87]. EBV-positive GCs are commonly accompanied by more extensive infiltration of CD8-positive cytotoxic T cells and IFN- $\gamma$ , which induce expression of IDO, a potent immune cell inhibitor [76,85]. The IFN- $\gamma$  driven gene signature, an additional proposed marker of sensitivity to anti-PD-1 treatment, was enriched in EBV-positive GCs [76]. EBV infection demonstrates four latency patterns depending on combinations of latent gene products during the EBV latency cycle: latency Ia, Ib, II, and III. EBV-positive GC demonstrates the latency I pattern, which is limited to EBV-encoded small RNAs (EBERs), BamHI-A rightward transcripts, and Epstein-Barr nuclear antigen 1 [87,88]. The presence of latent membrane protein (LMP) 2A can distinguish latency type Ia or Ib, and LMP2A is expressed in over 50% of EBV-positive GCs [87].

In situ hybridization (ISH) detection of EBER in tumor cells is considered the gold standard to identify the presence of EBV in tissue samples (Fig. 3) [77,89]. EBER ISH allows examination of paraffin sections from surgical excision and biopsy specimens or on cytology preparations [77]. This method uses light microscopy to demonstrate EBER transcripts concentrated in the nuclei of latently infected cells. Cells are considered EBV positive if brown or blue staining is detected in GC cell nuclei. Commercially available EBER probes are labeled with biotin, digoxigenin, or fluorescein (Ventana Medical Systems, Tucson, AZ, USA; Dako, Glostrup, Denmark; Enzo Diagnostics, Farmingdale, NY, USA; Kreatech Diagnostics, Amsterdam, The Neth-

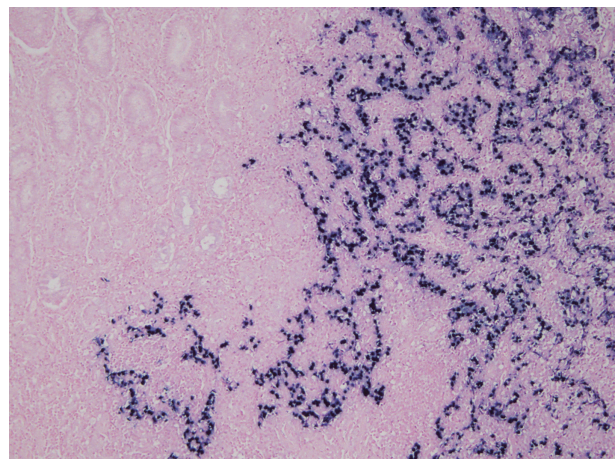


**Fig. 3.** Representative figure of Epstein-Barr virus (EBV) in situ hybridization. This case was diagnosed as gastric carcinoma with lymphoid stroma. EBV-positive cells highlight tumor cell clusters that form vague glandular structures.

erlands; Novocastra Laboratories Ltd., Newcastle, UK; Shandon Lipshaw, Pittsburgh, PA, USA; Innogenex, San Ramon, CA, USA) [77,90]. Other methods include PCR or serology comparing EBV nucleic acid positivity or sero-positivity in GC tissues versus non-tumor tissues or in blood of GC patients versus healthy controls [91]. Although IHC is easy and convenient, LMP-1 of representative EBV markers is undetectable in EBV-positive GCs [77].

### Tumor mutational burden

Tumor mutational burden (TMB), a new predictive biomarker for response to immunotherapy, is a quantitative measure of the total number of somatic nonsynonymous mutations per megabase of genome examined in the DNA of cancer cells [92]. Accumulating data have shown that TMB, or mutational load, is associated with good response to immunotherapy and improved survival [92-96]. Tumors with higher TMB are hypothesized to be more likely to express neoantigens that can be recognized by the immune system in response to immune checkpoint inhibitors [92,97]. The recent CheckMate 227 trial showed that PFS increased in patients with NSCLC treated with nivolumab plus ipilimumab as first-line chemotherapy in tumors with high ( $\geq 10$  mutations per megabase [Mb]) TMB, regardless of PD-L1 expression [96]. According to this trial, TMB is a promising biomarker for predicting immunotherapy and could lead the way for immuno-oncology entering the era of precision medicine [97]. Clinical trial NCT02915432, which investigated the safety and efficacy of toripalimab in Chinese advanced GC patients, demonstrated that patients with high TMB showed significant treatment response and OS benefit compared with patients with low TMB [98].

TMB can be measured by whole-exome sequencing (WES) or targeted sequencing panels using NGS [92]. Standardized and stabilized sample processing and methodology are crucial factors that influence the reproducibility of TMB measurements [92]. Initial TMB measurements were assessed by WES using tumor tissue and corresponding non-tumor tissue. Because most WES protocols require a minimum of 150–200 ng of genomic DNA, a limited amount of DNA in small biopsy samples is sometimes problematic [92]. The ability to detect somatic nucleic variants depends on allele frequency within a tumor as well as on sequencing depth [92]. Theoretically, at  $50 \times$  coverage, if an allele frequency of the specific variant is at least 15%, 95% of single nucleotide variants and short insertions and deletions can consistently be identified [92,99]. Unfortunately, WES has some disadvantages: (1) high cost; (2) extensive analysis; and (3) data manage-

ment [92]. Gene-targeted sequencing panels using NGS have advantages compared with WES: (1) lower sequencing cost; (2) deeper sequencing despite small amount of DNA; (3) higher sensitivity for mutation detection; and (4) shorter turnaround time [92]. Chalmers et al. [100] demonstrated that comprehensive genomic profiling with the FoundationOne assay targeting ~1.1 Mb of the coding genome can accurately evaluate TMB compared to WES and has high correlation. Some commercial gene panels are now available, such as the Ion Torrent OncoPrint Tumor Mutation Load Assay (Thermo Fisher Scientific, Waltham, MA, USA), which targets 1.7 Mb of the genome in 409 key cancer genes.

## BEYOND PD-1/PD-L1: NEW TARGETS OR COMBINATION THERAPY

While anti-PD-1/PD-L1 therapy has proved successful in GC, many patients do not respond to this treatment or develop resistance. To overcome this limitation of current immunotherapy, a number of ongoing studies are investigating new biomarkers and future strategies for GC treatment. Recently, new immune checkpoints such as LAG-3, TIM-3, and IDO have been suggested as therapeutic targets.

LAG-3 is a member of the immunoglobulin superfamily that acts as a co-inhibitory receptor expressed on exhausted TILs [101]. It may reduce T cell responses by interacting with MHC class II on antigen presenting cells. A previous study by Woo et al. [102] showed that LAG-3 expression is upregulated on TILs, inhibiting T cell immunity and reducing IFN- $\gamma$  production within the PD-1 upregulated tumor microenvironment. Co-expression of PD-1 and LAG-3 was demonstrated by in vivo study in a murine cancer model, and LAG-3/PD-1 expression was mostly restricted to TILs. This suggests that combination immunotherapy targeting LAG-3 and PD-1 could magnify tumor-specific responses and avoid non-specific autoimmune responses. Several trials assessing the efficacy of combination therapy of immune checkpoint inhibitors are currently ongoing [103]. The FRACTION-GC trial is investigating whether nivolumab in combination with anti-LAG-3 or anti-IDO inhibitor is more effective than nivolumab in combination with ipilimumab (anti-CTLA-4) in treating patients with advanced GC (NCT 02935634). Another trial starting soon will determine the effectiveness of anti-LAG-3 inhibitor+nivolumab alone or in combination with conventional chemotherapy in participants with G/GEJ adenocarcinoma that recurred or metastasized after prior therapy (NCT03704077).

TIM-3 is another co-inhibitory receptor expressed on T cells

that induces T cell anergy, apoptosis, and exhaustion through interaction with galectin-9 on immune cells [104]. Additionally, TIM-3 can competitively bind to HMGB1 protein, impairing HMGB1-mediated recruitment of nucleic acids into endosomes, an essential step for DNA sensing by the innate immune system [105]. Because of the T cell exhaustion function, TIM-3 has been suggested as an attractive immunotherapy target [106]. A previous study using murine cancer models showed that combined TIM-3/PD-1 blockade is more effective in controlling tumor growth compared to single blockade of TIM-3 or PD-1 [106]. Another in vivo study confirmed that dual blockade of TIM-3 and PD-1 improved the antitumor function of cancer CD8-positive T cells [106]. An ongoing Phase 1 trial is evaluating the safety of anti-TIM-3 inhibitor administered alone or in combination with anti-PD-L1 antibody in participants with advanced or relapsed solid tumors (NCT03099109).

IDO is a catabolic enzyme produced by Tregs and macrophages to convert tryptophan into kynurenine [107]. IDO-mediated tryptophan deficiency activates naïve T cells and causes them to differentiate into Tregs, causing immune tolerance. In addition, kynurenine converted from tryptophan by IDO also has an immunosuppressive role [108,109]. A study using a melanoma mouse model showed that combinations of CTLA-4 or PD-1/PD-L1 with IDO blockade restored both CD8-positive T cell proliferation and IL-2 production, suggesting the possibility of an IDO inhibitor as a therapeutic option [110]. IDO inhibitors are clinically developing for a variety of cancers, although some trials were stopped due to lack of efficacy [108].

Because of its central role in tumor immunity, HLA molecules could be biomarkers in future immunotherapy. In a previous study of malignant melanoma, down-regulation of the HLA I molecule was suggested as a potential mechanism of resistance to PD-1 blockade therapy [111]. For sophisticated patient selection, confirmation of HLA I molecule downregulation could become essential. A recent study by Chowell et al. [112] reported that zygosity at HLA loci or certain HLA alleles may influence immunotherapy survival. The authors suggested that greater diversity within the HLA I molecule would result in a larger repertoire of neoantigens for presentation. Through HLA genotype data of cancer patients, homozygosity in at least one HLA class I locus was significantly associated with poor prognosis for immunotherapy. Hence, patient HLA genotype might be utilized as a biomarker for immunotherapy discovery.

## CONCLUSION

Due to important contributions of past research and clinical trials, immunotherapy is now regarded as an important option for treating patients with advanced GC. The mechanism of the tumor immune reaction is complicated; however, understanding of immune responses to cancer cell is crucial for advanced patient selection. MSI and EBV status are regarded as significant prognostic markers in patients with GC. Along with PD-L1 IHC, MSI, and EBV status are now clinically utilized as predictive markers for immunotherapy. Several ongoing studies and clinical trials are validating the efficacy of novel immunotherapy targeting immune checkpoint molecules including LAG-3, TIM-3, and IDO. As demonstrated by previous clinical trials, immunotherapy will greatly improve survival of patients with GC in the future. Thus, research in immuno-oncology should continue, including studies investigating novel biomarkers and clinical trials.

## ORCID

Yoonjin Kwak: <https://orcid.org/0000-0001-5314-2465>

An Na Seo: <https://orcid.org/0000-0001-6412-3067>

Hee Eun Lee: <https://orcid.org/0000-0001-6335-7312>

Hye Seung Lee: <https://orcid.org/0000-0002-1667-7986>

## Author Contributions

Conceptualization: HSL.

Funding acquisition: HSL.

Investigation: YK, ANS, HEL, HSL.

Methodology: YK, ANS, HEL, HSL.

Supervision: HSL.

Writing—original draft: YK, ANS, HEL, HSL.

Writing—review & editing: YK, HSL.

## Conflicts of Interest

H.S.L., a contributing editor of the *Journal of Pathology and Translational Medicine*, was not involved in the editorial evaluation or decision to publish this article. All remaining authors have declared no conflicts of interest.

## Funding

This research was supported by a Basic Science Research Program through the National Research Foundation (NRF) funded by the Ministry of Education, Republic of Korea (NRF-2016 R1D1A1B03931744).

## REFERENCES

1. Kaufman HL, Atkins MB, Subedi P, et al. The promise of Immunology: implications for defining the value of cancer treatment. *J Immunother Cancer* 2019; 7: 129.
2. Chen DS, Mellman I. Oncology meets immunology: the cancer-immunity cycle. *Immunity* 2013; 39: 1-10.
3. Kim JM, Chen DS. Immune escape to PD-L1/PD-1 blockade: seven steps to success (or failure). *Ann Oncol* 2016; 27: 1492-504.
4. Melief CJ, van Hall T, Arens R, Ossendorp F, van der Burg SH. Therapeutic cancer vaccines. *J Clin Invest* 2015; 125: 3401-12.
5. Gajewski TF, Schreiber H, Fu YX. Innate and adaptive immune cells in the tumor microenvironment. *Nat Immunol* 2013; 14: 1014-22.
6. van der Burg SH, Arens R, Ossendorp F, van Hall T, Melief CJ. Vaccines for established cancer: overcoming the challenges posed by immune evasion. *Nat Rev Cancer* 2016; 16: 219-33.
7. Welters MJ, Kenter GG, Piersma SJ, et al. Induction of tumor-specific CD4+ and CD8+ T-cell immunity in cervical cancer patients by a human papillomavirus type 16 E6 and E7 long peptides vaccine. *Clin Cancer Res* 2008; 14: 178-87.
8. Coulie PG, Van den Eynde BJ, van der Bruggen P, Boon T. Tumour antigens recognized by T lymphocytes: at the core of cancer immunotherapy. *Nat Rev Cancer* 2014; 14: 135-46.
9. Dranoff G. Cytokines in cancer pathogenesis and cancer therapy. *Nat Rev Cancer* 2004; 4: 11-22.
10. Houghton AN, Guevara-Patiño JA. Immune recognition of self in immunity against cancer. *J Clin Invest* 2004; 114: 468-71.
11. Schwartz RH. T cell anergy. *Annu Rev Immunol* 2003; 21: 305-34.
12. Pardoll DM. The blockade of immune checkpoints in cancer immunotherapy. *Nat Rev Cancer* 2012; 12: 252-64.
13. Chen DS, Mellman I. Elements of cancer immunity and the cancer-immune set point. *Nature* 2017; 541: 321-30.
14. Tanaka A, Sakaguchi S. Regulatory T cells in cancer immunotherapy. *Cell Res* 2017; 27: 109-18.
15. Vesely MD, Kershaw MH, Schreiber RD, Smyth MJ. Natural innate and adaptive immunity to cancer. *Annu Rev Immunol* 2011; 29: 235-71.
16. Dunn GP, Old LJ, Schreiber RD. The three Es of cancer immunoevasion. *Annu Rev Immunol* 2004; 22: 329-60.
17. Taube JM, Anders RA, Young GD, et al. Colocalization of inflammatory response with B7-h1 expression in human melanocytic lesions supports an adaptive resistance mechanism of immune escape. *Sci Transl Med* 2012; 4: 127ra37.
18. Buchbinder EI, Desai A. CTLA-4 and PD-1 pathways: similarities, differences, and implications of their inhibition. *Am J Clin Oncol* 2016; 39: 98-106.
19. Schildberg FA, Klein SR, Freeman GJ, Sharpe AH. Coinhibitory pathways in the B7-CD28 ligand-receptor family. *Immunity* 2016; 44: 955-72.
20. Huard B, Prigent P, Tournier M, Bruniquel D, Triebel F. CD4/major histocompatibility complex class II interaction analyzed with CD4- and lymphocyte activation gene-3 (LAG-3)-Ig fusion proteins. *Eur J Immunol* 1995; 25: 2718-21.
21. Liu B, Wang M, Wang X, et al. Liver sinusoidal endothelial cell lectin inhibits CTL-dependent virus clearance in mouse models of viral hepatitis. *J Immunol* 2013; 190: 4185-95.
22. Anderson AC, Joller N, Kuchroo VK. Lag-3, Tim-3, and TIGIT: co-inhibitory receptors with specialized functions in immune regulation. *Immunity* 2016; 44: 989-1004.
23. Parham P, Ohta T. Population biology of antigen presentation by MHC class I molecules. *Science* 1996; 272: 67-74.
24. Garrido F, Algarra I. MHC antigens and tumor escape from immune surveillance. *Adv Cancer Res* 2001; 83: 117-58.
25. del Campo AB, Kyte JA, Carretero J, et al. Immune escape of cancer cells with beta2-microglobulin loss over the course of metastatic melanoma. *Int J Cancer* 2014; 134: 102-13.
26. Kumar V, Abbas A, Aster J. Robbins and Cotran pathologic basis of disease. 9th ed. Philadelphia: Elsevier, 2014.
27. Jiang W, Liu K, Guo Q, et al. Tumor-infiltrating immune cells and prognosis in gastric cancer: a systematic review and meta-analysis. *Oncotarget* 2017; 8: 62312-29.
28. Zheng X, Song X, Shao Y, et al. Prognostic role of tumor-infiltrating lymphocytes in gastric cancer: a meta-analysis. *Oncotarget* 2017; 8: 57386-98.
29. Lee HE, Chae SW, Lee YJ, et al. Prognostic implications of type and density of tumour-infiltrating lymphocytes in gastric cancer. *Br J Cancer* 2008; 99: 1704-11.
30. Haas M, Dimmler A, Hohenberger W, Grabenbauer GG, Niedobitek G, Distel LV. Stromal regulatory T-cells are associated with a favourable prognosis in gastric cancer of the cardia. *BMC Gastroenterol* 2009; 9: 65.
31. Shen Z, Zhou S, Wang Y, et al. Higher intratumoral infiltrated Foxp3+ Treg numbers and Foxp3+/CD8+ ratio are associated with adverse prognosis in resectable gastric cancer. *J Cancer Res Clin Oncol* 2010; 136: 1585-95.
32. Kim HI, Kim H, Cho HW, et al. The ratio of intra-tumoral regulatory T cells (Foxp3+)/helper T cells (CD4+) is a prognostic factor and associated with recurrence pattern in gastric cardia cancer. *J Surg Oncol* 2011; 104: 728-33.
33. Kim KJ, Lee KS, Cho HJ, et al. Prognostic implications of tumor-infiltrating FoxP3+ regulatory T cells and CD8+ cytotoxic T cells in microsatellite-unstable gastric cancers. *Hum Pathol* 2014; 45: 285-93.

34. Li K, Zhu Z, Luo J, et al. Impact of chemokine receptor CXCR3 on tumor-infiltrating lymphocyte recruitment associated with favorable prognosis in advanced gastric cancer. *Int J Clin Exp Pathol* 2015; 8: 14725-32.
35. Liu K, Yang K, Wu B, et al. Tumor-infiltrating immune cells are associated with prognosis of gastric cancer. *Medicine (Baltimore)* 2015; 94: e1631.
36. Hennequin A, Derangere V, Boidot R, et al. Tumor infiltration by Tbet+ effector T cells and CD20+ B cells is associated with survival in gastric cancer patients. *Oncoimmunology* 2016; 5: e1054598.
37. Kim JW, Nam KH, Ahn SH, et al. Prognostic implications of immunosuppressive protein expression in tumors as well as immune cell infiltration within the tumor microenvironment in gastric cancer. *Gastric Cancer* 2016; 19: 42-52.
38. Giampieri R, Maccaroni E, Mandolesi A, et al. Mismatch repair deficiency may affect clinical outcome through immune response activation in metastatic gastric cancer patients receiving first-line chemotherapy. *Gastric Cancer* 2017; 20: 156-63.
39. Kawazoe A, Kuwata T, Kuboki Y, et al. Clinicopathological features of programmed death ligand 1 expression with tumor-infiltrating lymphocyte, mismatch repair, and Epstein-Barr virus status in a large cohort of gastric cancer patients. *Gastric Cancer* 2017; 20: 407-15.
40. Koh J, Ock CY, Kim JW, et al. Clinicopathologic implications of immune classification by PD-L1 expression and CD8-positive tumor-infiltrating lymphocytes in stage II and III gastric cancer patients. *Oncotarget* 2017; 8: 26356-67.
41. Pernot S, Terme M, Radosevic-Robin N, et al. Infiltrating and peripheral immune cell analysis in advanced gastric cancer according to the Lauren classification and its prognostic significance. *Gastric Cancer* 2019 Jul 2 [Epub]. <https://doi.org/10.1007/s10120-019-00983-3>.
42. Kim JY, Kim WG, Kwon CH, Park DY. Differences in immune contextures among different molecular subtypes of gastric cancer and their prognostic impact. *Gastric Cancer* 2019; 22: 1164-75.
43. Torre LA, Bray F, Siegel RL, Ferlay J, Lortet-Tieulent J, Jemal A. Global cancer statistics, 2012. *CA Cancer J Clin* 2015; 65: 87-108.
44. Charalampakis N, Economopoulou P, Kotsantis I, et al. Medical management of gastric cancer: a 2017 update. *Cancer Med* 2018; 7: 123-33.
45. Kiyozumi Y, Iwatsuki M, Yamashita K, Koga Y, Yoshida N, Baba H. Update on targeted therapy and immune therapy for gastric cancer, 2018. *J Cancer Metastasis Treat* 2018; 4: 31.
46. Kang YK, Boku N, Satoh T, et al. Nivolumab in patients with advanced gastric or gastro-oesophageal junction cancer refractory to, or intolerant of, at least two previous chemotherapy regimens (ONO-4538-12, ATTRACTION-2): a randomised, double-blind, placebo-controlled, phase 3 trial. *Lancet* 2017; 390: 2461-71.
47. Fashoyin-Aje L, Donoghue M, Chen H, et al. FDA approval summary: pembrolizumab for recurrent locally advanced or metastatic gastric or gastroesophageal junction adenocarcinoma expressing PD-L1. *Oncologist* 2019; 24: 103-9.
48. Marcus L, Lemery SJ, Keegan P, Pazdur R. FDA approval summary: pembrolizumab for the treatment of microsatellite instability-high solid tumors. *Clin Cancer Res* 2019; 25: 3753-8.
49. Muro K, Chung HC, Shankaran V, et al. Pembrolizumab for patients with PD-L1-positive advanced gastric cancer (KEYNOTE-012): a multicentre, open-label, phase 1b trial. *Lancet Oncol* 2016; 17: 717-26.
50. Fuchs CS, Doi T, Jang RW, et al. Safety and efficacy of pembrolizumab monotherapy in patients with previously treated advanced gastric and gastroesophageal junction cancer: phase 2 clinical KEYNOTE-059 Trial. *JAMA Oncol* 2018; 4: e180013.
51. Shitara K, Özgüroğlu M, Bang YJ, et al. Pembrolizumab versus paclitaxel for previously treated, advanced gastric or gastro-oesophageal junction cancer (KEYNOTE-061): a randomised, open-label, controlled, phase 3 trial. *Lancet* 2018; 392: 123-33.
52. Tabernero J, Van Cutsem E, Bang YJ, et al. Pembrolizumab with or without chemotherapy versus chemotherapy for advanced gastric or gastroesophageal junction (G/GEJ) adenocarcinoma: the phase III KEYNOTE-062 study. *J Clin Oncol* 2019; 37: LBA4007.
53. Janjigian YY, Bendell J, Calvo E, et al. CheckMate-032 study: efficacy and safety of nivolumab and nivolumab plus ipilimumab in patients with metastatic esophagogastric cancer. *J Clin Oncol* 2018; 36: 2836-44.
54. Boku N, Ryu MH, Kato K, et al. Safety and efficacy of nivolumab in combination with S-1/capecitabine plus oxaliplatin in patients with previously untreated, unresectable, advanced, or recurrent gastric/gastroesophageal junction cancer: interim results of a randomized, phase II trial (ATTRACTION-4). *Ann Oncol* 2019; 30: 250-8.
55. Janjigian YY, Adenis A, Aucoin JS, et al. Checkmate 649: a randomized, multicenter, open-label, phase 3 study of nivolumab (Nivo) plus ipilimumab (Ipi) versus oxaliplatin plus fluoropyrimidine in patients (Pts) with previously untreated advanced or metastatic gastric (G) or gastroesophageal junction (GEJ) cancer. *J Clin Oncol* 2017; 35: TPS213.
56. Kelly RJ, Lee J, Bang YJ, et al. Safety and efficacy of durvalumab in combination with tremelimumab, durvalumab monotherapy, and tremelimumab monotherapy in patients with advanced gastric cancer. *J Clin Oncol* 2018; 36: 4031.
57. Bang YJ, Ruiz EY, Van Cutsem E, et al. Phase III, randomised trial of avelumab versus physician's choice of chemotherapy as third-line treatment of patients with advanced gastric or gastro-oesophageal junction cancer: primary analysis of JAVELIN Gastric 300.

- Ann Oncol 2018; 29: 2052-60.
58. Moehler M, Ryu MH, Dvorkin M, et al. Maintenance avelumab versus continuation of first-line chemotherapy in gastric cancer: JAVELIN Gastric 100 study design. *Future Oncol* 2019; 15: 567-77.
  59. A phase 1b/2 study of MEDI4736 with tremelimumab, MEDI4736 or tremelimumab monotherapy in gastric or GEJ adenocarcinoma. Bethesda: ClinicalTrials.gov, 2015 [cited 2019 Jul 21]. Available from: <https://clinicaltrials.gov/ct2/show/NCT02340975>.
  60. An investigational immuno-therapy study to assess the safety, tolerability and effectiveness of anti-LAG-3 with and without anti-PD-1 in the treatment of solid tumors [Internet]. Bethesda: ClinicalTrials.gov, 2013 [cited 2019 Jul 21]. Available from: <https://clinicaltrials.gov/ct2/show/NCT01968109>.
  61. Ishida Y, Agata Y, Shibahara K, Honjo T. Induced expression of PD-1, a novel member of the immunoglobulin gene superfamily, upon programmed cell death. *EMBO J* 1992; 11: 3887-95.
  62. Ribas A. Tumor immunotherapy directed at PD-1. *N Engl J Med* 2012; 366: 2517-9.
  63. Qing Y, Li Q, Ren T, et al. Upregulation of PD-L1 and APE1 is associated with tumorigenesis and poor prognosis of gastric cancer. *Drug Des Devel Ther* 2015; 9: 901-9.
  64. Wu C, Zhu Y, Jiang J, Zhao J, Zhang XG, Xu N. Immunohistochemical localization of programmed death-1 ligand-1 (PD-L1) in gastric carcinoma and its clinical significance. *Acta Histochem* 2006; 108: 19-24.
  65. Cancer Genome Atlas Research Network. Comprehensive molecular characterization of gastric adenocarcinoma. *Nature* 2014; 513: 202-9.
  66. Interpretation manual: gastric or gastroesophageal junction adenocarcinoma. PD-L1 IHC 22C3 pharmDx interpretation manual: gastric or gastroesophageal junction adenocarcinoma [Internet]. Santa Clara: DAKO Agilent Technologies, 2018 [cited 2019 Jul 21]. Available from: [https://www.agilent.com/cs/library/usermanuals/public/29219\\_pd-l1-ihc-22C3-pharmdx-gastric-interpretation-manual\\_us.pdf](https://www.agilent.com/cs/library/usermanuals/public/29219_pd-l1-ihc-22C3-pharmdx-gastric-interpretation-manual_us.pdf).
  67. Batenchuk C, Albitar M, Zerba K, et al. A real-world, comparative study of FDA-approved diagnostic assays PD-L1 IHC 28-8 and 22C3 in lung cancer and other malignancies. *J Clin Pathol* 2018; 71: 1078-83.
  68. Cristescu R, Lee J, Nebozhyn M, et al. Molecular analysis of gastric cancer identifies subtypes associated with distinct clinical outcomes. *Nat Med* 2015; 21: 449-56.
  69. Ratti M, Lampis A, Hahne JC, Passalacqua R, Valeri N. Microsatellite instability in gastric cancer: molecular bases, clinical perspectives, and new treatment approaches. *Cell Mol Life Sci* 2018; 75: 4151-62.
  70. Polom K, Marano L, Marrelli D, et al. Meta-analysis of microsatellite instability in relation to clinicopathological characteristics and overall survival in gastric cancer. *Br J Surg* 2018; 105: 159-67.
  71. Kim JY, Shin NR, Kim A, et al. Microsatellite instability status in gastric cancer: a reappraisal of its clinical significance and relationship with mucin phenotypes. *Korean J Pathol* 2013; 47: 28-35.
  72. Setia N, Agoston AT, Han HS, et al. A protein and mRNA expression-based classification of gastric cancer. *Mod Pathol* 2016; 29: 772-84.
  73. Ahn S, Lee SJ, Kim Y, et al. High-throughput protein and mRNA expression-based classification of gastric cancers can identify clinically distinct subtypes, concordant with recent molecular classifications. *Am J Surg Pathol* 2017; 41: 106-15.
  74. Cho J, Chang YH, Heo YJ, et al. Four distinct immune microenvironment subtypes in gastric adenocarcinoma with special reference to microsatellite instability. *ESMO Open* 2018; 3: e000326.
  75. Kim ST, Cristescu R, Bass AJ, et al. Comprehensive molecular characterization of clinical responses to PD-1 inhibition in metastatic gastric cancer. *Nat Med* 2018; 24: 1449-58.
  76. Lee J, Kim KM. Biomarkers for gastric cancer: molecular classification revisited. *Precis Future Med* 2017; 1: 59-68.
  77. Lee HS, Kim WH, Kwak Y, et al. Molecular testing for gastrointestinal cancer. *J Pathol Transl Med* 2017; 51: 103-21.
  78. Murphy KM, Zhang S, Geiger T, et al. Comparison of the microsatellite instability analysis system and the Bethesda panel for the determination of microsatellite instability in colorectal cancers. *J Mol Diagn* 2006; 8: 305-11.
  79. Campanella NC, Berardinelli GN, Scapulatempo-Neto C, et al. Optimization of a pentaplex panel for MSI analysis without control DNA in a Brazilian population: correlation with ancestry markers. *Eur J Hum Genet* 2014; 22: 875-80.
  80. Bae YS, Kim H, Noh SH, Kim H. Usefulness of immunohistochemistry for microsatellite instability screening in gastric cancer. *Gut Liver* 2015; 9: 629-35.
  81. Normanno N, Rachiglio AM, Lambiase M, et al. Heterogeneity of KRAS, NRAS, BRAF and PIK3CA mutations in metastatic colorectal cancer and potential effects on therapy in the CAPRI GOIM trial. *Ann Oncol* 2015; 26: 1710-4.
  82. Vanderwalde A, Spetzler D, Xiao N, Gatalica Z, Marshall J. Microsatellite instability status determined by next-generation sequencing and compared with PD-L1 and tumor mutational burden in 11,348 patients. *Cancer Med* 2018; 7: 746-56.
  83. Lee HS, Chang MS, Yang HK, Lee BL, Kim WH. Epstein-barr virus-positive gastric carcinoma has a distinct protein expression profile in comparison with epstein-barr virus-negative carcinoma. *Clin Cancer Res* 2004; 10: 1698-705.

84. Kang BW, Seo AN, Yoon S, et al. Prognostic value of tumor-infiltrating lymphocytes in Epstein-Barr virus-associated gastric cancer. *Ann Oncol* 2016; 27: 494-501.
85. Cho J, Kang MS, Kim KM. Epstein-Barr virus-associated gastric carcinoma and specific features of the accompanying immune response. *J Gastric Cancer* 2016; 16: 1-7.
86. Derks S, Liao X, Chiaravalli AM, et al. Abundant PD-L1 expression in Epstein-Barr virus-infected gastric cancers. *Oncotarget* 2016; 7: 32925-32.
87. Naseem M, Barzi A, Brezden-Masley C, et al. Outlooks on Epstein-Barr virus associated gastric cancer. *Cancer Treat Rev* 2018; 66: 15-22.
88. Yau TO, Tang CM, Yu J. Epigenetic dysregulation in Epstein-Barr virus-associated gastric carcinoma: disease and treatments. *World J Gastroenterol* 2014; 20: 6448-56.
89. Ambinder RF, Mann RB. Epstein-Barr-encoded RNA in situ hybridization: diagnostic applications. *Hum Pathol* 1994; 25: 602-5.
90. Gulley ML. Molecular diagnosis of Epstein-Barr virus-related diseases. *J Mol Diagn* 2001; 3: 1-10.
91. Chen XZ, Chen H, Castro FA, Hu JK, Brenner H. Epstein-Barr virus infection and gastric cancer: a systematic review. *Medicine (Baltimore)* 2015; 94: e792.
92. Melendez B, Van Campenhout C, Rorive S, Rummelink M, Salmon I, D'Haene N. Methods of measurement for tumor mutational burden in tumor tissue. *Transl Lung Cancer Res* 2018; 7: 661-7.
93. Van Allen EM, Wagle N, Stojanov P, et al. Whole-exome sequencing and clinical interpretation of formalin-fixed, paraffin-embedded tumor samples to guide precision cancer medicine. *Nat Med* 2014; 20: 682-8.
94. Rizvi NA, Hellmann MD, Snyder A, et al. Cancer immunology. Mutational landscape determines sensitivity to PD-1 blockade in non-small cell lung cancer. *Science* 2015; 348: 124-8.
95. Snyder A, Makarov V, Merghoub T, et al. Genetic basis for clinical response to CTLA-4 blockade in melanoma. *N Engl J Med* 2014; 371: 2189-99.
96. Hellmann MD, Ciuleanu TE, Pluzanski A, et al. Nivolumab plus Ipilimumab in lung cancer with a high tumor mutational burden. *N Engl J Med* 2018; 378: 2093-104.
97. Steuer CE, Ramalingam SS. Tumor mutation burden: leading immunotherapy to the era of precision medicine? *J Clin Oncol* 2018; 36: 631-2.
98. Wang F, Wei XL, Wang FH, et al. Safety, efficacy and tumor mutational burden as a biomarker of overall survival benefit in chemorefractory gastric cancer treated with toripalimab, a PD-1 antibody in phase Ib/II clinical trial NCT02915432. *Ann Oncol* 2019; 30: 1479-86.
99. Griffith M, Miller CA, Griffith OL, et al. Optimizing cancer genome sequencing and analysis. *Cell Syst* 2015; 1: 210-23.
100. Chalmers ZR, Connelly CF, Fabrizio D, et al. Analysis of 100,000 human cancer genomes reveals the landscape of tumor mutational burden. *Genome Med* 2017; 9: 34.
101. He Y, Rivard CJ, Rozeboom L, et al. Lymphocyte-activation gene-3, an important immune checkpoint in cancer. *Cancer Sci* 2016; 107: 1193-7.
102. Woo SR, Turnis ME, Goldberg MV, et al. Immune inhibitory molecules LAG-3 and PD-1 synergistically regulate T-cell function to promote tumoral immune escape. *Cancer Res* 2012; 72: 917-27.
103. Coutzac C, Pernot S, Chaput N, Zaanani A. Immunotherapy in advanced gastric cancer, is it the future? *Crit Rev Oncol Hematol* 2019; 133: 25-32.
104. Zhu C, Anderson AC, Schubart A, et al. The Tim-3 ligand galectin-9 negatively regulates T helper type 1 immunity. *Nat Immunol* 2005; 6: 1245-52.
105. Yanai H, Ban T, Wang Z, et al. HMGB proteins function as universal sentinels for nucleic-acid-mediated innate immune responses. *Nature* 2009; 462: 99-103.
106. Sakuishi K, Apetoh L, Sullivan JM, Blazar BR, Kuchroo VK, Anderson AC. Targeting Tim-3 and PD-1 pathways to reverse T cell exhaustion and restore anti-tumor immunity. *J Exp Med* 2010; 207: 2187-94.
107. Prendergast GC, Smith C, Thomas S, et al. Indoleamine 2,3-dioxygenase pathways of pathogenic inflammation and immune escape in cancer. *Cancer Immunol Immunother* 2014; 63: 721-35.
108. Hornyak L, Dobos N, Koncz G, et al. The Role of Indoleamine-2,3-Dioxygenase in Cancer Development, Diagnostics, and Therapy. *Front Immunol* 2018; 9: 151.
109. Terness P, Bauer TM, Röse L, et al. Inhibition of allogeneic T cell proliferation by indoleamine 2,3-dioxygenase-expressing dendritic cells: mediation of suppression by tryptophan metabolites. *J Exp Med* 2002; 196: 447-57.
110. Spranger S, Koblish HK, Horton B, Scherle PA, Newton R, Gajewski TF. Mechanism of tumor rejection with doublets of CTLA-4, PD-1/PD-L1, or IDO blockade involves restored IL-2 production and proliferation of CD8(+) T cells directly within the tumor microenvironment. *J Immunother Cancer* 2014; 2: 3.
111. Zaretsky JM, Garcia-Diaz A, Shin DS, et al. Mutations associated with acquired resistance to PD-1 blockade in melanoma. *N Engl J Med* 2016; 375: 819-29.
112. Chowell D, Morris LG, Grigg CM, et al. Patient HLA class I genotype influences cancer response to checkpoint blockade immunotherapy. *Science* 2018; 359: 582-7.

## HER2 status in breast cancer: changes in guidelines and complicating factors for interpretation

Soomin Ahn<sup>1</sup>, Ji Won Woo<sup>1,2</sup>, Kyoungyul Lee<sup>3</sup>, So Yeon Park<sup>1,2</sup>

<sup>1</sup>Department of Pathology, Seoul National University Bundang Hospital, Seongnam;

<sup>2</sup>Department of Pathology, Seoul National University College of Medicine, Seoul;

<sup>3</sup>Department of Pathology, Kangwon National University Hospital, Chuncheon, Korea

Human epidermal growth factor receptor 2 (HER2) protein overexpression and/or *HER2* gene amplification is found in about 20% of invasive breast cancers. It is a sole predictive marker for treatment benefits from HER2 targeted therapy and thus, HER2 testing is a routine practice for newly diagnosed breast cancer in pathology. Currently, HER2 immunohistochemistry (IHC) is used for a screening test, and in situ hybridization is used as a confirmation test for HER2 IHC equivocal cases. Since the American Society of Clinical Oncology (ASCO)/College of American Pathologists (CAP) guidelines on HER2 testing was first released in 2007, it has been updated to provide clear instructions for HER2 testing and accurate determination of HER2 status in breast cancer. During HER2 interpretation, some pitfalls such as intratumoral HER2 heterogeneity and increase in chromosome enumeration probe 17 signals may lead to inaccurate assessment of HER2 status. Moreover, HER2 status can be altered after neoadjuvant chemotherapy or during metastatic progression, due to biologic or methodologic issues. This review addresses recent updates of ASCO/CAP guidelines and factors complicating in the interpretation of HER2 status in breast cancers.

**Key Words:** Breast cancer; HER2; ASCO/CAP guidelines; HER2 heterogeneity; CEP17 copy number gain

**Received:** October 9, 2019 **Accepted:** November 3, 2019

**Corresponding Author:** So Yeon Park, MD, PhD, Department of Pathology, Seoul National University Bundang Hospital, 82 Gumi-ro 173beon-gil, Bundang-gu, Seongnam 13620, Korea

Tel: +82-31-787-7712, Fax: +82-31-787-4012, E-mail: sypmd@snu.ac.kr

Human epidermal growth factor receptor 2 (*HER2*) is a proto-oncogene that encodes epidermal growth factor receptor with tyrosine kinase activity, located on chromosome 17 at q21. In breast cancers, *HER2* gene is amplified in 15%–20% of invasive breast cancers and its amplification is closely linked to HER2 protein overexpression [1,2]. *HER2* amplification is a poor prognostic factor associated with a high rate of recurrence and mortality, and is a predictive factor for response to anthracycline-based chemotherapies in patients with breast cancer [1,2]. Most importantly, it is a sole predictive marker for treatment benefits from HER2-targeting agents such as trastuzumab, lapatinib, and pertuzumab. As HER2-targeted therapy is exclusively effective in HER2-overexpressed and/or *HER2*-amplified breast cancers, precise assessment of HER2 status is an essential step for treatment of breast cancer. In this review, we focused on changes in the American Society of Clinical Oncology (ASCO)/College of American Pathologists (CAP) guidelines on HER2

interpretation and some pitfalls in the interpretation of HER2 status in breast cancers.

### METHODS OF HER2 TESTING

Currently, immunohistochemistry (IHC), fluorescence in situ hybridization (FISH), and chromogenic in situ hybridization (CISH) including silver in situ hybridization (SISH) are regarded as standard methods for determination of HER2 status in breast cancer, and some of them have been approved by the U.S. Food and Drug Administration (FDA) for HER2 testing in breast cancer since 1998.

Although HER2 status can be directly tested by in situ hybridization (ISH), many laboratories have adopted IHC as a screening test, and FISH as a confirmation test for HER2 IHC equivocal cases, considering higher failure rate, longer procedure time and higher reagent cost of FISH, compared to that of IHC. Moreover,

high concordance has been found between HER2 protein over-expression by IHC and gene amplification by FISH [3-5]. Finally, the 2007 ASCO/CAP guidelines stated that HER2 status should be initially assessed by IHC using a semi-quantitative scoring system (Fig. 1), and confirmed by FISH in all IHC score 2+ equivocal cases [6].

Bright-field in situ hybridization such as CISH and SISH has advantage in that it allows histologic evaluation of tumors, utilizes ordinary microscope, leaves permanent signals for archival storage, and can be fully automated [7]. Moreover, it shows more than 95% concordance rate with FISH [8-11]. Thus, CISH and SISH are now admitted as an alternative to FISH.

### CHANGES IN GUIDELINES ON INTERPRETATION OF HER2 STATUS

For uniformity in accuracy and reproducibility of HER2 test-

ing in breast cancer, ASCO/CAP jointly released guidelines and recommendations for HER2 testing first in 2007, addressing a wide range of pre-analytic, analytic and post-analytic variables [6]. This guideline focused on limiting the false-positive results, adopting a higher cutoff of 30% for HER2 IHC positivity (3+), instead of 10% cutoff previously recommended by FDA (Table 1). For FISH analysis, *HER2* gene was regarded as amplified if *HER2*/chromosome enumeration probe 17 (CEP17) ratio > 2.2 for dual-probe assay (instead of the previously recommended ratio of 2.0) or *HER2* gene copy > 6 signals per cell for single-probe assay.

After then, the revised 2013 ASCO/CAP guideline focused on maximizing identification of patients who can benefit from HER2-targeted therapy and minimizing false-negative results [12]. The range of HER2 IHC equivocal cases (2+) was widened, and HER2 IHC 3+ was defined using 10% as cutoff value, not using 30% (Table 1). When using validated dual-probe

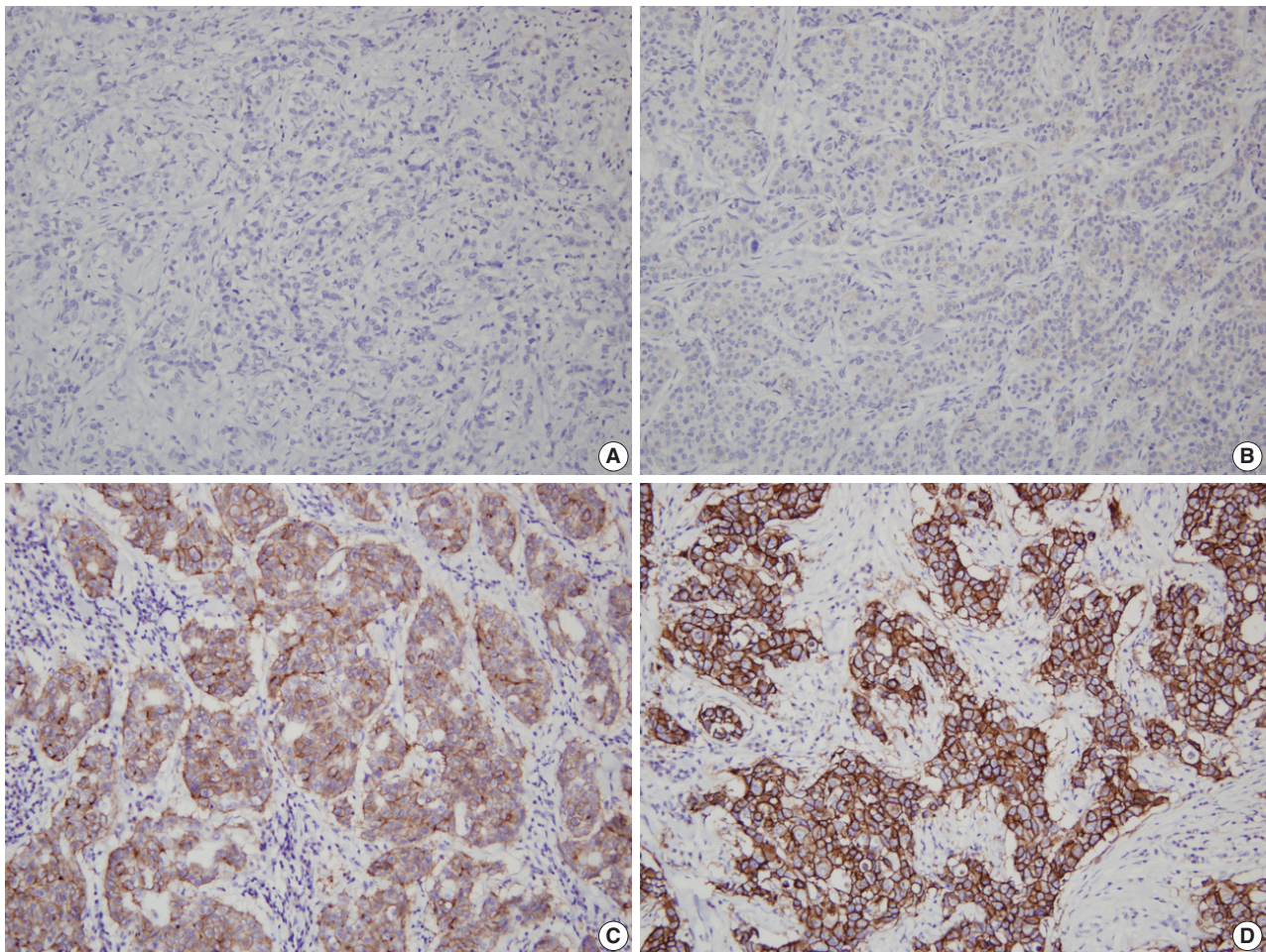


**Fig. 1.** Representative examples of human epidermal growth factor receptor 2 (HER2) immunohistochemistry (IHC) in breast cancer. (A) HER2 IHC negative (0). (B) HER2 IHC negative (1+). (C) HER2 IHC equivocal (2+). (D) HER2 IHC positive (3+).

**Table 1.** Changes in the ASCO/CAP guidelines: interpretation of HER2 immunohistochemistry

HER2 IHC status	2007 ASCO/CAP guidelines	2013 ASCO/CAP guidelines	2018 ASCO/CAP guidelines
Positive (3+)	Uniform intense membrane staining of >30% of invasive tumor cells	Circumferential membrane staining that is complete, intense, and in >10% of tumor cells	Circumferential membrane staining that is complete, intense, and in >10% of tumor cells
Equivocal (2+)	Complete membrane staining that is either non-uniform or weak in intensity but with obvious circumferential distribution in at least 10% of cells	Circumferential membrane staining that is incomplete and/or weak to moderate and within >10% of the invasive tumor cells Complete and circumferential membrane staining that is intense and within ≤10% of the invasive tumor cells	Weak to moderate complete membrane staining observed in >10% of tumor cells <sup>a</sup>
Negative (1+)	Weak incomplete membrane staining in any proportion of tumor cells Weak, complete membrane staining in <10% of tumor cells	Incomplete membrane staining that is faint or barely perceptible and within >10% of the invasive tumor cells	Incomplete membrane staining that is faint or barely perceptible and within >10% of the invasive tumor cells
Negative (0)	No staining	No staining observed Incomplete membrane staining that is faint or barely perceptible and within ≤10% of the invasive tumor cells	No staining observed Incomplete membrane staining that is faint or barely perceptible and within ≤10% of the invasive tumor cells

ASCO, American Society of Clinical Oncology; CAP, College of American Pathologists; HER2, human epidermal growth factor receptor 2; IHC, immunohistochemistry.

<sup>a</sup>Unusual staining patterns of HER2 by IHC can be encountered that are not covered by these definitions. As one example, some specific subtypes of breast cancers can show IHC staining that is moderate to intense but incomplete (basolateral or lateral) and can be found to be *HER2* amplified. Another example is circumferential membrane staining that is intense but in ≤10% tumor cells. Such cases can be considered equivocal (2+).

**Table 2.** Changes in the ASCO/CAP guidelines: interpretation of HER2 status using dual-probe in situ hybridization assay

HER2 ISH status	2007 ASCO/CAP guidelines	2013 ASCO/CAP guidelines	2018 ASCO/CAP guidelines
ISH positive	<i>HER2</i> /CEP17 ratio >2.2	<i>HER2</i> /CEP17 ratio ≥2.0 <i>HER2</i> /CEP17 ratio <2.0 and average <i>HER2</i> copy number ≥6.0	<i>HER2</i> /CEP17 ratio ≥2.0 and average <i>HER2</i> copy number ≥4.0 (group 1) <i>HER2</i> /CEP17 ratio ≥2.0 and average <i>HER2</i> copy number <4.0 (group 2) with concurrent IHC 3+ <i>HER2</i> /CEP17 ratio <2.0 and average <i>HER2</i> copy number ≥6.0 (group 3) with concurrent IHC 2+ <sup>a</sup> <i>HER2</i> /CEP17 ratio <2.0 and average <i>HER2</i> copy number ≥6.0 (group 3) with concurrent IHC 3+ <i>HER2</i> /CEP17 ratio <2.0 with average <i>HER2</i> copy number ≥4.0 and <6.0 (group 4) with concurrent IHC 3+ (no equivocal category)
ISH equivocal	<i>HER2</i> /CEP17 ratio of 1.8–2.2	<i>HER2</i> /CEP17 ratio <2.0 with average <i>HER2</i> copy number ≥4.0 and <6.0	
ISH negative	<i>HER2</i> /CEP17 ratio of <1.8	<i>HER2</i> /CEP17 ratio <2.0 with average <i>HER2</i> copy number <4.0	<i>HER2</i> /CEP17 ratio <2.0 with average <i>HER2</i> copy number <4.0 (group 5) <i>HER2</i> /CEP17 ratio ≥2.0 and average <i>HER2</i> copy number <4.0 (group 2) with concurrent IHC 2+ <sup>b</sup> <i>HER2</i> /CEP17 ratio <2.0 with average <i>HER2</i> copy number ≥4.0 and <6.0 (group 4) with concurrent IHC 2+ <sup>b</sup> Groups 2, 3, and 4 with concurrent IHC 0 or 1+

ASCO, American Society of Clinical Oncology; CAP, College of American Pathologists; HER2, human epidermal growth factor receptor 2; ISH, in situ hybridization; CEP17, chromosome enumeration probe 17; IHC, immunohistochemistry.

<sup>a</sup>An additional observer blinded to previous result recounts ISH. If the repeated ISH result is categorized to the same group, it is finally regarded as HER2 positive; <sup>b</sup>An additional observer blinded to previous result recounts ISH. If the repeated ISH result is designated to same ISH group, it is finally regarded as HER2 negative.

ISH assay, *HER2*/CEP17 ratio ≥2.0 or *HER2*/CEP17 ratio <2.0 and average *HER2* copy number ≥6.0 was regarded as ISH positive (Table 2). The 2007 and 2013 ASCO/CAP guidelines included ISH equivocal results, which had been a problem for clinical decision making.

Since the publication of the 2013 guideline, several laboratories and clinical investigators have reported on the practical im-

plications of the 2013 guidelines and increased frequencies of equivocal results [13]. The HER2 testing Expert Panel wished to clarify controversial issues in the 2013 guideline, and in that context the 2018 updated ASCO/CAP guidelines on HER2 testing was reported [13]. The updated guideline addressed five clinical questions. The first question was about the definition of HER2 IHC 2+, and it was revised as weak to moderate com-

plete membrane staining observed in >10% of tumor cells. The second question was about repeated HER2 test of initially negative case, and it was recommended that if the initial HER2 testing result in a core needle biopsy specimen is negative, a new HER2 test may (not “must”) be ordered on the excision specimen based on specific clinical criteria. These two clinical questions were addressed in a previous correspondence by the Expert Panel [14]. The remaining three questions were about less common ISH patterns, and the updated HER2 testing algorithm addressed the workup for these three clinical scenarios, occasionally found when using a dual-probe ISH assay. These scenarios were described as ISH group 2 (*HER2/CEP17* ratio  $\geq 2.0$ ; average *HER2* copy number  $< 4.0$  signals per cell), ISH group 3 (*HER2/CEP17* ratio  $< 2.0$ ; average *HER2* copy number  $\geq 6.0$  signals per cell), and ISH group 4 (*HER2/CEP17* ratio  $< 2.0$ ; average *HER2* copy number  $\geq 4.0$  and  $< 6.0$  signals per cell) [13]. The diagnostic approach includes more rigorous interpretation criteria for ISH and requires concomitant IHC review for dual-probe ISH groups 2 to 4 to achieve the most accurate determination of HER2 status based on combined interpretation of the ISH and IHC assay [13]. It was recommended that laboratories using single-probe ISH assays include concomitant IHC review as part of the interpretation of all ISH assay results [13]. By this approach, the HER2 status was designated to positive or negative with no equivocal category.

Although complicated, HER2 status is basically determined by IHC results in the dual-probe ISH groups 2 to 4. While cases with HER2 IHC 3+ are regarded as HER2 positive, those with HER2 IHC 0 or 1+ are regarded as HER2 negative. In cases with HER2 IHC 2+, an additional observer blinded to previous result recounts ISH. As for ISH groups 2 and 4, if the repeated ISH result is designated to the same ISH group, it is finally regarded as HER2 negative. On the contrary, as for ISH group 3, if the repeated ISH result is categorized to the same group, it is finally regarded as HER2 positive. If the repeated ISH shows other ISH result, the results should be adjudicated per internal procedures to determine final category. The changes on HER2 interpretation in the updated 2018 ASCO/CAP guidelines in comparison with previous 2007 and 2013 guidelines are summarized in Tables 1 and 2.

Recent studies on implementation of the updated 2018 ASCO/CAP guidelines have shown significant increases of HER2 negative rates through reclassification of ISH equivocal cases by the 2013 guidelines [15-17]. The updated guidelines seem to provide much clearer instructions for HER2 status designation by using concomitant IHC review in ISH groups 2, 3 and 4, and

eliminating ISH equivocal category [15].

## COMPLICATING FACTORS FOR HER2 INTERPRETATION

### Intratumoral HER2 heterogeneity

HER2 status has been thought to be fairly homogeneous within a tumor. However, intratumoral heterogeneity of *HER2* gene amplification, that is, intratumoral HER2 heterogeneity, is found in a subset of breast cancers. It has important clinical implications, in that it can contribute to inaccurate assessment of HER2 status and affect treatment responses to HER2-targeted therapy [18]. In previous studies, our group has shown that intratumoral HER2 heterogeneity is more common in breast cancer with equivocal *HER2* protein expression and low-grade *HER2* gene amplification [19,20]. Intratumoral HER2 heterogeneity was associated with poor clinical outcome in patients with HER2-positive primary breast cancer [19]. Moreover, it was related to poor response to trastuzumab and decreased survival in patients with HER2-positive metastatic breast cancer [20]. In a subsequent study, Lee et al. [21] reported that cases with HER2 regional heterogeneity showed a decreased disease-free survival rate compared to those without heterogeneity in the hormone receptor-positive subgroup of breast cancer patients treated with adjuvant trastuzumab. In a neoadjuvant setting, intratumoral HER2 heterogeneity was also found to be associated with incomplete response to anti-HER2 chemotherapy [22].

The CAP addressed this issue and published a separate recommendation in 2009 and defined *HER2* genetic heterogeneity as the presence of tumor cells with *HER2/CEP17* signal ratios greater than 2.2 in 5% to 50% of the tumor cells tested [23]. However, this recommendation has some problems, in that it was based on expert opinion rather than evidence, and artificial heterogeneity caused by technical issues could be regarded as *HER2* genetic heterogeneity. Finally, the 2013 ASCO/CAP guidelines added a recommendation about HER2 heterogeneity for HER2 ISH interpretation, stating that if there is a second population of cells with increased HER2 signals/cell and this cell population is more than 10% of tumor cells on the slide, a separate counting of at least 20 non-overlapping cells must also be performed within this cell population and reported [12].

HER2 heterogeneity can be found as distinct clusters of amplified cells among non-amplified cells or appear as intermixed amplified and non-amplified cells (Fig. 2). Basically, it is important to scan all fields when observing ISH slide and to match it with HER2 IHC slide to detect areas with HER2 heterogeneity.

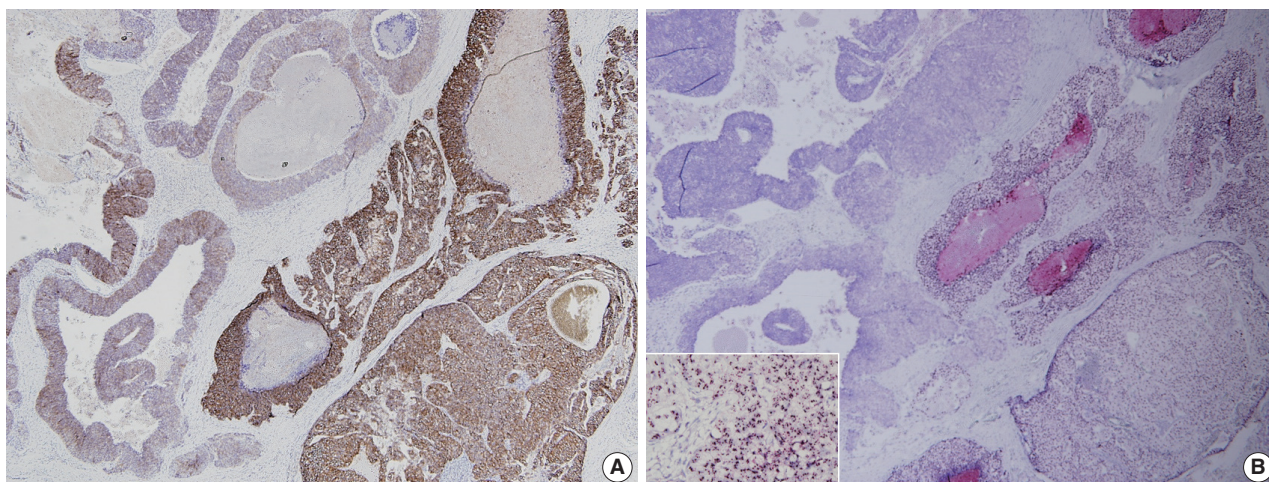


**Fig. 2.** A representative breast cancer with intratumoral human epidermal growth factor receptor 2 (HER2) heterogeneity. (A) HER2 immunohistochemistry shows heterogeneous expression with strong, complete membranous expression on the right, and weak to moderate, incomplete membranous expression on the left. (B) HER2 silver in situ hybridization reveals high-level amplification on the right and no amplification on the left (inset, area of high-level amplification).

**Table 3.** Assessment of HER2 heterogeneity in breast cancer

#### Suggestions

The pathologist should scan entire HER2 ISH slide before counting.

Review of HER2 IHC slide is helpful to find areas with potential *HER2* amplification

From this point of view, CISH or SISH has an advantage to evaluate HER2 heterogeneity, because it can be easily matched with HER2 IHC slide under light microscope.

If there is a subpopulation of tumor cells with *HER2* amplification comprising >10% of tumor cells on the slide, a separate counting should be performed within the subpopulation.

The *HER2*/CEP17 ratios or *HER2* gene copy number should be calculated for both amplified and non-amplified areas separately.

If possible, it is recommended that in situ hybridization report includes proportion of amplified cells within a tumor.

HER2, human epidermal growth factor receptor 2; ISH, in situ hybridization; IHC, immunohistochemistry; CISH, chromogenic in situ hybridization; SISH, silver in situ hybridization; CEP17, chromosome enumeration probe 17.

From this point of view, CISH or SISH has an advantage in evaluating HER2 heterogeneity, because it can be easily matched with HER2 IHC slide under light microscope. The *HER2*/CEP17 ratios or *HER2* copy number should be calculated separately for amplified and non-amplified areas. Suggestions for how to assess intratumoral HER2 heterogeneity are summarized in Table 3 [24,25].

#### CEP17 copy number gain

CEP17 copy number gain is a genetic change commonly observed during dual-probe HER2 ISH for breast cancer, with reported frequency of 3% to 46% in breast cancers [26]. In our study using 945 cases of invasive breast cancer, CEP17 copy number gain was observed in 29.9% when using the definition of CEP17 copy number gain as mean CEP17  $\geq 2.6$ , and was found in 19.7% with the definition of CEP17 copy number gain as CEP17  $\geq 3.0$  [27]. This had been thought to result from increasing numbers of whole chromosome 17, which is referred to as

polysomy 17. However, subsequent studies have revealed that true polysomy 17 is a rare phenomenon in breast cancers, and CEP17 copy number gain results from amplification or copy number gain in the centromeric or pericentromeric region [28-32].

Although it is still controversial, CEP17 copy number gain has been found to be associated with increased HER2 protein expression [27,33-35]. However, CEP17 copy number gain without *HER2* gene amplification was not associated with benefit from HER2-targeted therapy in breast cancers [36,37]. Moreover, CEP17 copy number gain in breast cancers has been reported to be associated with adverse clinicopathological features [27,38-40] and response to anthracycline-based therapy in breast cancer [41,42]. However, as for its prognostic significance, there have been conflicting results [43-46]. Recently, our group has shown that CEP17 copy number gain is an independent poor prognostic factor in patients with luminal/HER2-negative breast cancers, suggesting that CEP17 copy number gain may reflect chromosomal instability in breast cancer [27].

CEP17 copy number gain may affect the interpretation of HER2 ISH, and lead to an underestimation of HER2 status. Therefore, the 2013 ASCO/CAP guideline recommended to repeat HER2 testing using an alternative probe for CEP17 or for another gene in chromosome 17 not expected to co-amplify with *HER2* for the ISH equivocal cases (now ISH group 4 in the updated 2018 ASCO/CAP guideline) [12,26]. However, following studies have shown that with alternative probes, HER2 ISH equivocal cases were upgraded to HER2 ISH positive status in a significant proportion, and clinicopathologic features of those upgraded cases were not compatible with those of *HER2*-amplified breast cancers, suggesting that use of alternative probe is not reliable in clinical practice [32,47]. The updated 2018 ASCO/CAP guidelines do not recommend the use of alternative probe as standard practice due to limited evidence on its analytical and clinical validity [13].

#### Changes in HER2 status after neoadjuvant chemotherapy

Neoadjuvant chemotherapy (NAC) is currently considered as standard treatment for locally advanced breast cancer [48]. Alteration of biomarker status after NAC is occasionally found in breast cancer [49,50]. Hormone receptor status changed more often than HER2 status, and as for hormone receptors, positive to negative conversion was more common than negative to positive conversion [51,52]. The frequency of HER2 change after NAC is reported in up to 15%, and both positive to negative conversion and negative to positive conversion were found with no preponderance [52-66]. Previous studies on HER2 change after NAC are summarized in Table 4. In our study, HER2 status

was altered after NAC in 3.4% with positive to negative conversion in 0.9% and negative to positive conversion in 2.5% [52]. Most cases with negative to positive conversion of HER2 status after NAC showed low level of *HER2* amplification, and the *HER2*/CEP17 ratio ranged from 2.2 to 4.4 (data not shown in a previous study) [52]. Cockburn et al. [61] also reported the mean *HER2*/CEP17 ratio in resection specimens with HER2 positive conversion was 3.7. Although there are no guidelines about whether treatment should be modified based on altered biomarker status after NAC, the change of HER2 status may have an impact on the therapeutic management in certain patients. Accordingly, re-evaluation of biomarkers including HER2 after NAC is recommended for proper management.

The mechanism of HER2 conversion after NAC is not well understood. This can be partly explained by the selection of HER2-positive or HER2-negative clones after NAC, tumor heterogeneity, and pre-analytical and analytical pitfalls, Guarneri et al. [67] evaluated HER2 status change on 107 HER2-positive patients treated with NAC with or without anti-HER2 agents. They reported that patients with tumors undergoing HER2 negative conversion following treatment had significantly reduced disease-free survival compared to patients with maintained HER2 positivity [67]. However, the prognostic significance of HER2 status change is still unclear.

Finally, caution is needed in interpretation of HER2 ISH after NAC in distinguishing between a true *HER2* amplification and increase of *HER2* copy number by chromosome 17 polysomy [68]. Increase in *HER2* copy number could not be attributed to true *HER2* amplifications, but instead could reflect polyploidi-

**Table 4.** Summary of the previous studies on HER2 status alteration after neoadjuvant chemotherapy

Year	Author	Total No. of cases	Method	Frequency of HER2 alteration, n (%)		
				Total	+ to -	- to +
2018	De La Cruz et al. [53]	54	IHC/FISH	2/54 (3.7)	1/54 (1.9)	1/54 (1.9)
2018	Ahn et al. [52]	442	IHC/SISH	15/442 (3.4)	4/442 (0.9)	11/442 (2.5)
2017	Xian et al. [54]	77	IHC/FISH	6/77 (7.8)	5/77 (6.5)	1/77 (1.3)
2017	Reddy et al. [55]	140	IHC/FISH	8/97 (8.2)	5/97 (5.2)	3/97 (3.1)
2016	Gahlaut et al. [56]	133	IHC/FISH	8/133 (6.0)	5/133 (3.8)	3/133 (2.3)
2016	Lim et al. [57]	290	IHC/FISH	17/290 (5.9)	17/290 (5.9)	0/290 (0)
2016	Zhou et al. [58]	107	IHC/FISH	5/107 (4.7)	3/107 (2.8)	2/107 (1.9)
2015	Jin et al. [59]	423	IHC/FISH	40/423 (9.5)	27/423 (6.4)	13/423 (3.1)
2013	Yang et al. [60]	113	IHC	17/113 (15.0)	9/113 (8.0)	8/113 (7.1)
2013	Cockburn et al. [61]	133	IHC/FISH	16/133 (12.0)	9/133 (6.8)	7/133 (5.3)
2013	Lee et al. [62]	120	IHC/FISH	11/107 (10.3)	6/107 (5.6)	5/107 (4.7)
2009	Hirata et al. [63]	368	IHC/FISH	35/368 (9.5)	22/368 (6.0)	13/368 (3.5)
2008	Kasami et al. [64]	173	IHC/FISH	0/173 (0)	0/173 (0)	0/173 (0)
2006	Neubauer et al. [65]	87	IHC	13/87 (14.9)	11/87 (12.6)	2/87 (2.3)
2003	Faneyte et al. [66]	50	IHC	3/50 (6.0)	2/50 (4.0)	1/50 (2.0)

HER2, human epidermal growth factor receptor 2; IHC, immunohistochemistry; FISH, fluorescence in situ hybridization; SISH, silver in situ hybridization.

**Table 5.** Summary of the previous studies on HER2 status alteration during metastatic progression

Year	Author	Total No. of cases	Method	Site	Frequency of HER2 alteration, n (%)		
					Total	+ to -	- to +
2019	Woo et al. [79]	152	IHC/SISH	All	12/152 (7.9)	9/152 (5.9)	3/152 (2.0)
2014	de Duenas et al. [70]	165	IHC/FISH	All	5/165 (3.0)	0/165 (0.0)	5/165 (3.0)
2013	Curtit et al. [71]	219	IHC/FISH	All	8/219 (3.7)	6/219 (2.7)	2/219 (0.9)
2013	Nakamura et al. [72]	156	IHC/FISH	All	13/156 (8.3)	5/156 (3.2)	8/156 (5.1)
2013	Aurilio et al. [73]	86	IHC/FISH	Bone	6/86 (7.0)	2/86 (2.3)	4/86 (4.7)
2012	Duchnowska et al. [74]	119	IHC/FISH	Brain	17/119 (14.3)	7/119 (5.9)	10/119 (8.4)
2012	Jensen et al. [75]	114	IHC/FISH	All	10/114 (8.8)	2/114 (1.8)	8/114 (7.0)
2011	Bogina et al. [76]	136	IHC/SISH	All	1/136 (0.7)	0/136 (0.0)	1/136 (0.7)
2011	Chang et al. [77]	56	IHC/FISH	All	7/56 (12.5)	2/56 (3.6)	5/56 (8.9)
2010	Hoefnagel et al. [78]	233	IHC/SISH	All	12/233 (5.2)	6/233 (2.6)	6/233 (2.6)

HER2, human epidermal growth factor receptor 2; IHC, immunohistochemistry; SISH, silver in situ hybridization; FISH, fluorescence in situ hybridization.

zation after chemotherapy, which presumably affects all chromosomes [68]. Careful evaluation using dual-probe ISH with concomitant IHC review is recommended.

#### Change in HER2 status with metastatic progression

Change in receptor status during metastatic progression, a phenomenon called “receptor conversion” occurs not only in hormonal receptors, but also in HER2. The reported frequency of HER2 conversion varies a lot between studies, but it is usually observed less often than hormone receptor conversion. Schrijver et al. [69] reported in their meta-analysis that pooled frequency of HER2 positive to negative conversion was 21.3%, and that of negative to positive conversion was 9.5%. Previous studies on HER2 change during metastatic progression are summarized in Table 5 [70-79]. In our study, HER2 receptor status changed in 12 out of 152 cases (7.9%) during metastatic progression: nine cases (5.9%) were negative conversion, and three cases (2.0%) were positive conversion [79].

Similar to HER2 status alteration after NAC, little is known about the true mechanism of HER2 status conversion during metastatic progression. It would be reasonable to postulate intratumoral heterogeneity and selection pressure from treatment play a role in HER2 status conversion. In our study, cases with positive to negative conversion showed significantly lower level of HER2 protein expression and heterogeneous *HER2* gene amplification, compared to consistently positive cases [79]. From this observation, it can be inferred that tumors with HER2 heterogeneity have a propensity to show different status in metastatic sites, because HER2-targeted therapy drives susceptible clones to fade away.

HER2 conversion is not a common event, but it is important to discover it because of its relation with treatment. There are some studies which reported response to trastuzumab treatment

in patients who gained HER2 positivity in metastatic lesions [77,80]. For this reason, it is now widely recommended to re-evaluate receptor status including HER2 in metastatic lesions, if possible [13,81].

## CONCLUSION

The ASCO/CAP guidelines on HER2 interpretation in breast cancer, which were released first in 2007 and subsequently updated in 2013 and 2018, have been changing to provide much clearer instructions for HER2 status designation. The updated 2018 ASCO/CAP guideline focused on three dual-probe ISH groups (groups 2, 3, and 4) with less common ISH patterns, and recommended concomitant IHC review for these ISH groups to achieve the most accurate determination of HER2 status. Finally, in the updated 2018 ASCO/CAP guideline, HER2 status, as determined by ISH, is categorized to positive or negative with no equivocal results.

There are some complicating factors for HER2 interpretation including HER2 heterogeneity, CEP17 copy number gain, and HER2 status alteration after NAC or during metastatic progression. It is important to scan the entire ISH slide and to match it with HER2 IHC to detect HER2 heterogeneity. Separate counting should be performed in both amplified and non-amplified areas. CEP17 copy number gain may lead to an underestimation of HER2 status, but the use of alternative probe is not recommended in the updated 2018 ASCO/CAP guidelines due to the limited evidence on its analytical and clinical validity. HER2 conversion is occasionally found after NAC or during metastasis progression. The change of HER2 status may have an impact on the therapeutic decision and response to treatment. Accordingly, re-evaluation of HER2 status should be performed in post-NAC specimens and metastatic lesions.

## ORCID

Soomin Ahn: <https://orcid.org/0000-0002-1979-4010>  
 Ji Won Woo: <https://orcid.org/0000-0003-1659-7123>  
 Kyoungyul Lee: <https://orcid.org/0000-0002-9444-394X>  
 So Yeon Park: <https://orcid.org/0000-0002-0299-7268>

## Author Contributions

Project administration: SA.  
 Supervision: SYP.  
 Writing—original draft: SA, JWW, KL, SYP.  
 Writing—review & editing: SYP.

## Conflicts of Interest

S.Y.P. is the editor-in-chief of the *Journal of Pathology and Translational Medicine* and was not involved in the editorial evaluation or decision to publish this article. All remaining authors declare that they have no potential conflicts of interest.

## Funding

No funding to declare.

## REFERENCES

- Slamon DJ, Clark GM, Wong SG, Levin WJ, Ullrich A, McGuire WL. Human breast cancer: correlation of relapse and survival with amplification of the HER-2/neu oncogene. *Science* 1987; 235: 177-82.
- Tandon AK, Clark GM, Chamness GC, Ullrich A, McGuire WL. HER-2/neu oncogene protein and prognosis in breast cancer. *J Clin Oncol* 1989; 7: 1120-8.
- Couturier J, Vincent-Salomon A, Nicolas A, et al. Strong correlation between results of fluorescent in situ hybridization and immunohistochemistry for the assessment of the *ERBB2* (HER-2/neu) gene status in breast carcinoma. *Mod Pathol* 2000; 13: 1238-43.
- Lebeau A, Deimling D, Kaltz C, et al. Her-2/neu analysis in archival tissue samples of human breast cancer: comparison of immunohistochemistry and fluorescence in situ hybridization. *J Clin Oncol* 2001; 19: 354-63.
- Yaziji H, Goldstein LC, Barry TS, et al. HER-2 testing in breast cancer using parallel tissue-based methods. *JAMA* 2004; 291: 1972-7.
- Wolff AC, Hammond ME, Schwartz JN, et al. American Society of Clinical Oncology/College of American Pathologists guideline recommendations for human epidermal growth factor receptor 2 testing in breast cancer. *J Clin Oncol* 2007; 25: 118-45.
- Tanner M, Gancberg D, Di Leo A, et al. Chromogenic in situ hybridization: a practical alternative for fluorescence in situ hybridization to detect HER-2/neu oncogene amplification in archival breast cancer samples. *Am J Pathol* 2000; 157: 1467-72.
- Dandachi N, Dietze O, Hauser-Kronberger C. Chromogenic in situ hybridization: a novel approach to a practical and sensitive method for the detection of HER2 oncogene in archival human breast carcinoma. *Lab Invest* 2002; 82: 1007-14.
- Gong Y, Gilcrease M, Sneige N. Reliability of chromogenic in situ hybridization for detecting *HER-2* gene status in breast cancer: comparison with fluorescence in situ hybridization and assessment of interobserver reproducibility. *Mod Pathol* 2005; 18: 1015-21.
- Dietel M, Ellis IO, Hofler H, et al. Comparison of automated silver enhanced in situ hybridisation (SISH) and fluorescence ISH (FISH) for the validation of *HER2* gene status in breast carcinoma according to the guidelines of the American Society of Clinical Oncology and the College of American Pathologists. *Virchows Arch* 2007; 451: 19-25.
- Koh YW, Lee HJ, Lee JW, Kang J, Gong G. Dual-color silver-enhanced in situ hybridization for assessing *HER2* gene amplification in breast cancer. *Mod Pathol* 2011; 24: 794-800.
- Wolff AC, Hammond ME, Hicks DG, et al. Recommendations for human epidermal growth factor receptor 2 testing in breast cancer: American Society of Clinical Oncology/College of American Pathologists clinical practice guideline update. *J Clin Oncol* 2013; 31: 3997-4013.
- Wolff AC, Hammond ME, Allison KH, et al. Human epidermal growth factor receptor 2 testing in breast cancer: American Society of Clinical Oncology/College of American Pathologists clinical practice guideline focused update. *J Clin Oncol* 2018; 36: 2105-22.
- Wolff AC, Hammond ME, Hicks DG, et al. Reply to E.A. Rakha et al. *J Clin Oncol* 2015; 33: 1302-4.
- Liu ZH, Wang K, Lin DY, et al. Impact of the updated 2018 ASCO/CAP guidelines on HER2 FISH testing in invasive breast cancer: a retrospective study of HER2 FISH results of 2233 cases. *Breast Cancer Res Treat* 2019; 175: 51-7.
- Gordian-Arroyo AM, Zynger DL, Tozbikian GH. Impact of the 2018 ASCO/CAP HER2 Guideline Focused Update. *Am J Clin Pathol* 2019; 152: 17-26.
- Xu B, Shen J, Guo W, Zhao W, Zhuang Y, Wang L. Impact of the 2018 ASCO/CAP HER2 guidelines update for HER2 testing by FISH in breast cancer. *Pathol Res Pract* 2019; 215: 251-5.
- Moeder CB, Giltnane JM, Harigopal M, et al. Quantitative justification of the change from 10% to 30% for human epidermal growth factor receptor 2 scoring in the American Society of Clinical Oncology/College of American Pathologists guidelines: tumor heterogeneity in breast cancer and its implications for tissue microarray based assessment of outcome. *J Clin Oncol* 2007; 25: 5418-25.
- Seol H, Lee HJ, Choi Y, et al. Intratumoral heterogeneity of *HER2*

- gene amplification in breast cancer: its clinicopathological significance. *Mod Pathol* 2012; 25: 938-48.
20. Lee HJ, Seo AN, Kim EJ, et al. HER2 heterogeneity affects trastuzumab responses and survival in patients with HER2-positive metastatic breast cancer. *Am J Clin Pathol* 2014; 142: 755-66.
  21. Lee HJ, Kim JY, Park SY, et al. Clinicopathologic significance of the intratumoral heterogeneity of *HER2* gene amplification in HER2-positive breast cancer patients treated with adjuvant trastuzumab. *Am J Clin Pathol* 2015; 144: 570-8.
  22. Hou Y, Nitta H, Wei L, et al. HER2 intratumoral heterogeneity is independently associated with incomplete response to anti-HER2 neoadjuvant chemotherapy in HER2-positive breast carcinoma. *Breast Cancer Res Treat* 2017; 166: 447-57.
  23. Vance GH, Barry TS, Bloom KJ, et al. Genetic heterogeneity in HER2 testing in breast cancer: panel summary and guidelines. *Arch Pathol Lab Med* 2009; 133: 611-2.
  24. Walker RA, Bartlett JM, Dowsett M, et al. HER2 testing in the UK: further update to recommendations. *J Clin Pathol* 2008; 61: 818-24.
  25. Starczynski J, Atkey N, Connelly Y, et al. *HER2* gene amplification in breast cancer: a rogues' gallery of challenging diagnostic cases: UKNEQAS interpretation guidelines and research recommendations. *Am J Clin Pathol* 2012; 137: 595-605.
  26. Hanna WM, Ruschoff J, Bilous M, et al. HER2 in situ hybridization in breast cancer: clinical implications of polysomy 17 and genetic heterogeneity. *Mod Pathol* 2014; 27: 4-18.
  27. Lee K, Jang MH, Chung YR, et al. Prognostic significance of centromere 17 copy number gain in breast cancer depends on breast cancer subtype. *Hum Pathol* 2017; 61: 111-20.
  28. Gunn S, Yeh IT, Lytvak I, et al. Clinical array-based karyotyping of breast cancer with equivocal HER2 status resolves gene copy number and reveals chromosome 17 complexity. *BMC Cancer* 2010; 10: 396.
  29. Yeh IT, Martin MA, Robetorye RS, et al. Clinical validation of an array CGH test for HER2 status in breast cancer reveals that polysomy 17 is a rare event. *Mod Pathol* 2009; 22: 1169-75.
  30. Moelans CB, de Weger RA, van Diest PJ. Absence of chromosome 17 polysomy in breast cancer: analysis by CEP17 chromogenic in situ hybridization and multiplex ligation-dependent probe amplification. *Breast Cancer Res Treat* 2010; 120: 1-7.
  31. Marchio C, Lambros MB, Gugliotta P, et al. Does chromosome 17 centromere copy number predict polysomy in breast cancer? A fluorescence in situ hybridization and microarray-based CGH analysis. *J Pathol* 2009; 219: 16-24.
  32. Jang MH, Kim EJ, Kim HJ, Chung YR, Park SY. Assessment of HER2 status in invasive breast cancers with increased centromere 17 copy number. *Breast Cancer Res Treat* 2015; 153: 67-77.
  33. Ma Y, Lespagnard L, Durbecq V, et al. Polysomy 17 in HER-2/neu status elaboration in breast cancer: effect on daily practice. *Clin Cancer Res* 2005; 11: 4393-9.
  34. Merola R, Mottolese M, Orlandi G, et al. Analysis of aneusomy level and *HER-2* gene copy number and their effect on amplification rate in breast cancer specimens read as 2+ in immunohistochemical analysis. *Eur J Cancer* 2006; 42: 1501-6.
  35. Hyun CL, Lee HE, Kim KS, et al. The effect of chromosome 17 polysomy on HER-2/neu status in breast cancer. *J Clin Pathol* 2008; 61: 317-21.
  36. Downey L, Livingston RB, Koehler M, et al. Chromosome 17 polysomy without human epidermal growth factor receptor 2 amplification does not predict response to lapatinib plus paclitaxel compared with paclitaxel in metastatic breast cancer. *Clin Cancer Res* 2010; 16: 1281-8.
  37. Perez EA, Reinholz MM, Hillman DW, et al. HER2 and chromosome 17 effect on patient outcome in the N9831 adjuvant trastuzumab trial. *J Clin Oncol* 2010; 28: 4307-15.
  38. Orsaria M, Khelifa S, Buza N, Kamath A, Hui P. Chromosome 17 polysomy: correlation with histological parameters and HER2NEU gene amplification. *J Clin Pathol* 2013; 66: 1070-5.
  39. Krishnamurti U, Hammers JL, Atem FD, Storto PD, Silverman JF. Poor prognostic significance of unamplified chromosome 17 polysomy in invasive breast carcinoma. *Mod Pathol* 2009; 22: 1044-8.
  40. Vanden Bempt I, Van Loo P, Drijkoningen M, et al. Polysomy 17 in breast cancer: clinicopathologic significance and impact on HER-2 testing. *J Clin Oncol* 2008; 26: 4869-74.
  41. Bartlett JM, Munro AF, Dunn JA, et al. Predictive markers of anthracycline benefit: a prospectively planned analysis of the UK National Epirubicin Adjuvant Trial (NEAT/BR9601). *Lancet Oncol* 2010; 11: 266-74.
  42. Tibau A, Lopez-Vilaro L, Perez-Olabarria M, et al. Chromosome 17 centromere duplication and responsiveness to anthracycline-based neoadjuvant chemotherapy in breast cancer. *Neoplasia* 2014; 16: 861-7.
  43. Kim A, Shin HC, Bae YK, et al. Multiplication of chromosome 17 centromere is associated with prognosis in patients with invasive breast cancers exhibiting normal HER2 and TOP2A status. *J Breast Cancer* 2012; 15: 24-33.
  44. Nielsen KV, Ejlertsen B, Moller S, et al. Lack of independent prognostic and predictive value of centromere 17 copy number changes in breast cancer patients with known HER2 and TOP2A status. *Mol Oncol* 2012; 6: 88-97.
  45. Zaczek A, Markiewicz A, Supernat A, et al. Prognostic value of TOP2A gene amplification and chromosome 17 polysomy in early breast cancer. *Pathol Oncol Res* 2012; 18: 885-94.
  46. Fountzilias G, Dafni U, Bobos M, et al. Evaluation of the prognostic

- role of centromere 17 gain and HER2/topoisomerase II alpha gene status and protein expression in patients with breast cancer treated with anthracycline-containing adjuvant chemotherapy: pooled analysis of two Hellenic Cooperative Oncology Group (HeCOG) phase III trials. *BMC Cancer* 2013; 13: 163.
47. Sneige N, Hess KR, Multani AS, Gong Y, Ibrahim NK. Prognostic significance of equivocal human epidermal growth factor receptor 2 results and clinical utility of alternative chromosome 17 genes in patients with invasive breast cancer: a cohort study. *Cancer* 2017; 123: 1115-23.
  48. Thompson AM, Moulder-Thompson SL. Neoadjuvant treatment of breast cancer. *Ann Oncol* 2012; 23 Suppl 10: x231-6.
  49. Lee SH, Chung MA, Quddus MR, Steinhoff MM, Cady B. The effect of neoadjuvant chemotherapy on estrogen and progesterone receptor expression and hormone receptor status in breast cancer. *Am J Surg* 2003; 186: 348-50.
  50. Makris A, Powles TJ, Allred DC, et al. Quantitative changes in cytological molecular markers during primary medical treatment of breast cancer: a pilot study. *Breast Cancer Res Treat* 1999; 53: 51-9.
  51. Zhang N, Moran MS, Huo Q, Haffty BG, Yang Q. The hormonal receptor status in breast cancer can be altered by neoadjuvant chemotherapy: a meta-analysis. *Cancer Invest* 2011; 29: 594-8.
  52. Ahn S, Kim HJ, Kim M, et al. Negative conversion of progesterone receptor status after primary systemic therapy is associated with poor clinical outcome in patients with breast cancer. *Cancer Res Treat* 2018; 50: 1418-32.
  53. De La Cruz LM, Harhay MO, Zhang P, Ugras S. Impact of neoadjuvant chemotherapy on breast cancer subtype: does subtype change and, if so, how?: IHC profile and neoadjuvant chemotherapy. *Ann Surg Oncol* 2018; 25: 3535-40.
  54. Xian Z, Quinones AK, Tozbikian G, Zynger DL. Breast cancer biomarkers before and after neoadjuvant chemotherapy: does repeat testing impact therapeutic management? *Hum Pathol* 2017; 62: 215-21.
  55. Reddy OL, Apple SK. Breast cancer biomarker changes after neoadjuvant chemotherapy: a single institution experience and literature review. *Clin Oncol* 2017; 2: 1245.
  56. Gahlaut R, Bennett A, Fatayer H, et al. Effect of neoadjuvant chemotherapy on breast cancer phenotype, ER/PR and HER2 expression: implications for the practising oncologist. *Eur J Cancer* 2016; 60: 40-8.
  57. Lim SK, Lee MH, Park IH, et al. Impact of molecular subtype conversion of breast cancers after neoadjuvant chemotherapy on clinical outcome. *Cancer Res Treat* 2016; 48: 133-41.
  58. Zhou X, Zhang J, Yun H, et al. Alterations of biomarker profiles after neoadjuvant chemotherapy in breast cancer: tumor heterogeneity should be taken into consideration. *Oncotarget* 2015; 6: 36894-902.
  59. Jin X, Jiang YZ, Chen S, Yu KD, Shao ZM, Di GH. Prognostic value of receptor conversion after neoadjuvant chemotherapy in breast cancer patients: a prospective observational study. *Oncotarget* 2015; 6: 9600-11.
  60. Yang YF, Liao YY, Li LQ, Xie SR, Xie YF, Peng NF. Changes in ER, PR and HER2 receptors status after neoadjuvant chemotherapy in breast cancer. *Pathol Res Pract* 2013; 209: 797-802.
  61. Cockburn A, Yan J, Rahardja D, et al. Modulatory effect of neoadjuvant chemotherapy on biomarkers expression; assessment by digital image analysis and relationship to residual cancer burden in patients with invasive breast cancer. *Hum Pathol* 2014; 45: 249-58.
  62. Lee HC, Ko H, Seol H, et al. Expression of immunohistochemical markers before and after neoadjuvant chemotherapy in breast carcinoma, and their use as predictors of response. *J Breast Cancer* 2013; 16: 395-403.
  63. Hirata T, Shimizu C, Yonemori K, et al. Change in the hormone receptor status following administration of neoadjuvant chemotherapy and its impact on the long-term outcome in patients with primary breast cancer. *Br J Cancer* 2009; 101: 1529-36.
  64. Kasami M, Uematsu T, Honda M, et al. Comparison of estrogen receptor, progesterone receptor and Her-2 status in breast cancer pre- and post-neoadjuvant chemotherapy. *Breast* 2008; 17: 523-7.
  65. Neubauer H, Gall C, Vogel U, et al. Changes in tumour biological markers during primary systemic chemotherapy (PST). *Anticancer Res* 2008; 28: 1797-804.
  66. Faneyte IF, Schrama JG, Peterse JL, Remijnse PL, Rodenhuis S, van de Vijver MJ. Breast cancer response to neoadjuvant chemotherapy: predictive markers and relation with outcome. *Br J Cancer* 2003; 88: 406-12.
  67. Guarneri V, Dieci MV, Barbieri E, et al. Loss of HER2 positivity and prognosis after neoadjuvant therapy in HER2-positive breast cancer patients. *Ann Oncol* 2013; 24: 2990-4.
  68. Valent A, Penault-Llorca F, Cayre A, Kroemer G. Change in *HER2* (*ERBB2*) gene status after taxane-based chemotherapy for breast cancer: polyploidization can lead to diagnostic pitfalls with potential impact for clinical management. *Cancer Genet* 2013; 206: 37-41.
  69. Schrijver W, Suijkerbuijk KP, van Gils CH, van der Wall E, Moelans CB, van Diest PJ. Receptor conversion in distant breast cancer metastases: a systematic review and meta-analysis. *J Natl Cancer Inst* 2018; 110: 568-80.
  70. de Duenas EM, Hernandez AL, Zotano AG, et al. Prospective evaluation of the conversion rate in the receptor status between primary breast cancer and metastasis: results from the GEICAM 2009-03 ConvertHER study. *Breast Cancer Res Treat* 2014; 143: 507-15.
  71. Curtit E, Nerich V, Mansi L, et al. Discordances in estrogen recep-

- tor status, progesterone receptor status, and HER2 status between primary breast cancer and metastasis. *Oncologist* 2013; 18: 667-74.
72. Nakamura R, Yamamoto N, Onai Y, Watanabe Y, Kawana H, Miyazaki M. Importance of confirming HER2 overexpression of recurrence lesion in breast cancer patients. *Breast Cancer* 2013; 20: 336-41.
73. Aurilio G, Monfardini L, Rizzo S, et al. Discordant hormone receptor and human epidermal growth factor receptor 2 status in bone metastases compared to primary breast cancer. *Acta Oncol* 2013; 52: 1649-56.
74. Duchnowska R, Dziadziuszko R, Trojanowski T, et al. Conversion of epidermal growth factor receptor 2 and hormone receptor expression in breast cancer metastases to the brain. *Breast Cancer Res* 2012; 14: R119.
75. Jensen JD, Knoop A, Ewertz M, Laenkholm AV. ER, HER2, and TOP2A expression in primary tumor, synchronous axillary nodes, and asynchronous metastases in breast cancer. *Breast Cancer Res Treat* 2012; 132: 511-21.
76. Bogina G, Bortesi L, Marconi M, et al. Comparison of hormonal receptor and HER-2 status between breast primary tumours and relapsing tumours: clinical implications of progesterone receptor loss. *Virchows Arch* 2011; 459: 1-10.
77. Chang HJ, Han SW, Oh DY, et al. Discordant human epidermal growth factor receptor 2 and hormone receptor status in primary and metastatic breast cancer and response to trastuzumab. *Jpn J Clin Oncol* 2011; 41: 593-9.
78. Hoefnagel LD, van de Vijver MJ, van Slooten HJ, et al. Receptor conversion in distant breast cancer metastases. *Breast Cancer Res* 2010; 12: R75.
79. Woo JW, Chung YR, Ahn S, et al. Changes in biomarker status in metastatic breast cancer and their prognostic value. *J Breast Cancer* 2019; 22: 439-52.
80. Fabi A, Di Benedetto A, Metro G, et al. HER2 protein and gene variation between primary and metastatic breast cancer: significance and impact on patient care. *Clin Cancer Res* 2011; 17: 2055-64.
81. Van Poznak C, Harris LN, Somerfield MR. Use of biomarkers to guide decisions on systemic therapy for women with metastatic breast cancer: American Society of Clinical Oncology clinical practice guideline. *J Oncol Pract* 2015; 11: 514-6.

## Molecular characteristics of meningiomas

Young Suk Lee, Youn Soo Lee

Department of Hospital Pathology, College of Medicine, The Catholic University of Korea, Seoul, Korea

Meningioma is the most common primary intracranial tumor in adults. The grading of meningioma is based on World Health Organization criteria, which rely on histopathological features alone. This grading system is unable to conclusively predict the clinical behavior of these tumors (i.e., recurrence or prognosis in benign or atypical grades). Advances in molecular techniques over the last decade that include genomic and epigenomic data associated with meningiomas have been used to identify genetic biomarkers that can predict tumor behavior. This review summarizes the molecular characteristics of meningioma using genetic and epigenetic biomarkers. Molecular alterations that can predict meningioma behavior may be integrated into the upcoming World Health Organization grading system.

**Key Words:** Meningioma; Molecular diagnosis; Pathological diagnosis

**Received:** August 30, 2019 **Revised:** October 22, 2019 **Accepted:** November 5, 2019

**Corresponding Author:** Youn Soo Lee, MD, PhD, Department of Hospital Pathology, College of Medicine, The Catholic University of Korea, 222 Banpo-daero, Seocho-gu, Seoul 06591, Korea

Tel: +82-2-2258-1626, Fax: +82-2-2258-1628, E-mail: lys9908@catholic.ac.kr

Meningioma is the most common primary neoplasm of the central nervous system (CNS) in adults [1]. It accounts for one-third (37.1%) of all primary intracranial tumors [1,2] with an incidence rate of 8.33/100,000 person/yr in the United States [2]. Meningiomas primarily occur in the elderly population and are more frequent in the 6th to 7th decades, but are exceedingly rare in childhood (0.4%–4.1% of all pediatric neoplasms) [3]. In adults, females are affected by meningioma more frequently, with a female-to-male ratio [2] of 2.27:1, whereas in childhood it occurs equally [3,4].

The majority of meningiomas (79.8%) are intracranial tumors, and 4.2% of meningiomas have spinal locations [2]. Meningothelial arachnoid cells are the precursors of meningiomas [5] and have different origins in embryogenesis according to their location [5]. The meninges of the brain convexity and skull base are developed from the neural crest and mesodermal structure, respectively [5,6]. This difference affects not only the histologic features but also the recurrent somatic mutations [5,6].

Older age and genetic susceptibility are known risk factors for meningiomas [7], and one important established cause is ionizing radiation [7,8]. As well as with high-dose radiation, therapeutic exposure to low-dose radiation (1–2 Gy), especially in childhood, has been linked to higher meningioma risk [9]. Radiation-

induced meningiomas tend to present with multiple tumors and have aggressive clinicopathological features [8,9]. Other possible risk factors may include head trauma, gonadal steroid hormones, smoking, and some viral infections [7,10–13]. Several findings, such as a higher incidence in females and the expression of progesterone receptor in 76% of benign meningiomas, suggest an endocrine influence on the pathogenesis of meningiomas [13,14].

According to the World Health Organization (WHO) classification, most meningiomas (80%) are grade I, which have benign histology and indolent behavior [15]. Whereas the remaining tumors (20%) are a higher grade (grade II and III) with atypical to malignant histology and demonstrate more aggressive course [2,6].

To date, surgery is the mainstay of treatment and 70%–80% of meningiomas can be cured by surgical resection [6]. The most reliable prognostic factors of meningiomas are histologic grade (WHO grade) and the extent of resection (Simpson grade) [6, 16,17]. After complete resection, the 5-year recurrence rates of WHO grade I, II, and III tumors are 5%–10%, 50%, and 80%, respectively [18].

Meningiomas in surgically challenging locations such as the skull base, meningiomas with higher histologic grade and aggres-

sive behavior, and meningiomas that recur despite radical resection, all require another treatment strategy [6]. Radiation therapy has been used as an adjuvant modality, but systemic therapy has demonstrated limited benefits [6].

In the last decade, our understanding of the molecular profile of meningiomas has improved. Identification of genetic and epigenetic alterations in meningiomas enable the clarification of their biologic behavior and prognostic stratification. Comprehensive information on molecular features provides the opportunity of refining the classification of meningiomas that can predict tumor behavior and provide a framework for precision targeted therapy.

We review the relevant genetic and epigenetic data in meningiomas and highlight associations with clinical features.

## HISTOPATHOLOGICAL CLASSIFICATION OF MENINGIOMAS

The revised 2016 WHO classification of the CNS categorizes meningiomas into 15 different variants [19]. The heterogeneity of their histopathological features is the most interesting characteristic of meningiomas. The 15 variants are classified into three histologic grades (Fig. 1). The WHO grade I (benign) includes nine variants, and the most frequent are meningothehal, fibrous, and transitional variants. Psammomatous, angiomatous, microcystic, secretory, lymphoplasmacyte-rich, and metaplastic variants are also included in grade I [19]. The WHO grade II and III both include three variants [19]. Atypical, chor-

doid, and clear cell variants are included in grade II, whereas anaplastic, papillary, and rhabdoid variants are included in grade III [19]. Each variant is diagnosed according to their characteristic histologic morphology. However, many meningiomas show mixed histology in the same tumor, so are diagnosed by the dominant histology. Atypical and anaplastic meningiomas have a set of morphological criteria. Atypical meningiomas are diagnosed either by the presence of 4–19 mitoses per 10 high-power fields (HPF) or by evidence of brain invasion, or by showing at least three of five of the following features: high cellularity, small cells with high nuclear-to-cytoplasmic ratio, sheeting (uninterrupted patternless or sheet-like growth), prominent nucleoli, and spontaneous necrosis [19]. Anaplastic meningiomas are diagnosed either by markedly elevated mitotic activity ( $\geq 20$  mitoses per 10 HPF) or by overtly malignant morphology such as carcinomatous, sarcomatous, and melanomatous cytology [19].

Although the current histologic grade is valuable in the prognostication of meningiomas, there is still considerable unreliability in predicting clinical behavior and the risk of recurrence and, moreover, determining clinical management. Recently, the revised 2016 WHO classification of the CNS consents to integrated diagnosis, incorporating molecular findings in the diagnosis of some brain tumors, such as gliomas, but not yet meningiomas [20]. The integration of essential molecular profiles in current diagnosis may refine the pathologic classification of meningiomas.

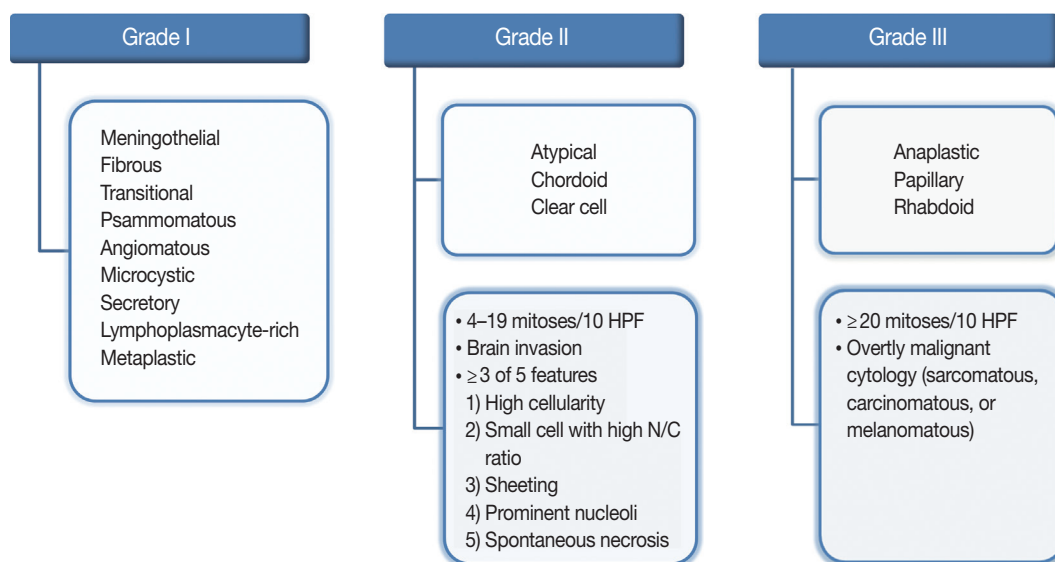


**Fig. 1.** Overview of the 2016 World Health Organization classification system for grading meningiomas. HPF, high-power fields; N/C, nuclear/cytoplasmic.

## GENETIC ALTERATIONS IN MENINGIOMAS

In the 1970s, the loss of chromosome 22 was first established by a fluorescence technique as a recurrent genetic alteration in meningiomas [21]. Several rare familial syndromes predisposing individuals to meningioma were identified, including neurofibromatosis type 2 (NF2) [22]. In the 1990s, the mutation of the neurofibromin 2 (NF2) gene on chromosome 22 was identified as a major driver, with an incidence of 40%–60% in sporadic meningiomas [23]. Since then, efforts to discover other candidate genes of NF2 wild-type meningiomas have continued, but no critical genetic driver was found until 2013. Powered by the whole-genome sequencing technique, a number of recurrent genetic drivers have been uncovered, such as tumor necrosis factor receptor-associated factor 7 (TRAF7), Kruppel-like factor 4 (KLF4), v-Akt murine thymoma viral oncogene homolog 1 (AKT1), and smoothened frizzled class receptor (SMO) [24,25]. In 2016, the mutation of the phosphatidylinositol-4,5-bisphosphate 3-kinase catalytic subunit alpha (PIK3CA) gene was also identified as a repetitive driver in some meningiomas (Fig. 2) [26].

We first review the genetic status of meningiomas in terms of cytogenetic alterations, followed by germline mutations along with familial syndrome, and then somatic mutations.

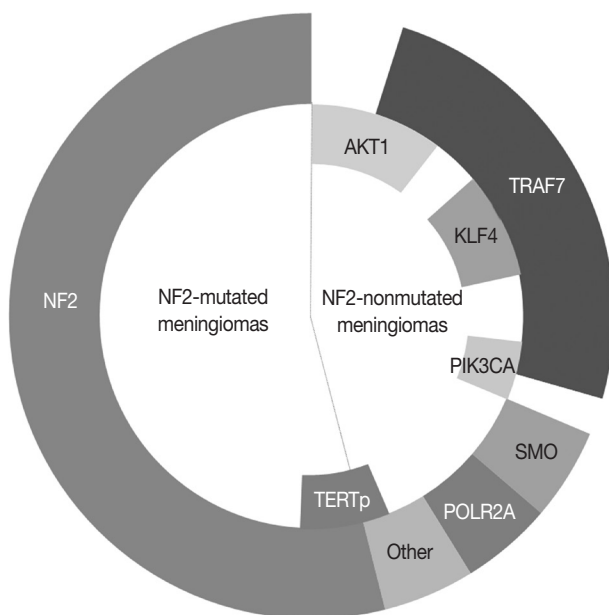


**Fig. 2.** The most common genetic alterations found in meningiomas.

## CYTOGENETIC PROGRESSION OF MENINGIOMAS

Cytogenetic studies provide insight into the genetic status of tumors and launch studies for candidate driver genes because a deletion or duplication in a large fraction of chromosome affects a number of genes within these regions. In meningiomas, the loss of chromosome 22 was found early in the cytogenetic era [21] and brought about the identification of NF2 (located on chromosome 22q) as a powerful driver gene [27].

The loss of chromosome 22q is the most common cytogenetic alteration in meningiomas, found in 60%–70% of all meningiomas [28]. The frequency of this alteration increases with tumor grade, with an incidence of 50% and 75%–85%, in benign and atypical or anaplastic meningiomas, respectively [29]. Except for this loss of 22q, benign meningiomas are typically stable at the cytogenetic level [29]. Unusually, angiomatous meningioma harbors multiple polysomies including chromosome 5, 13, and 20, but do not manifest aggressive behavior [30].

In general, the cytogenetic alterations accumulate with increasing tumor grades, therefore atypical and anaplastic meningiomas show complex cytogenetic profiles (Fig. 3) [29,31]. The losses of chromosome 1p, 14q, and 9p are major additional alterations found in higher-grade meningiomas, and the losses of chromosome 6q, 10, and 18q or the gain of 1q, 9q, 12q, 15q, 17q, and 20q are also noted [28,29,32]. The loss of 1p is the second most frequent alteration and related with a higher recurrence rate [33]. The candidate genes on this chromosomal arm include TP73, CDKN2C, RAD54, EPB41, GADD45A, and ALPL [34–37]. Similarly, the loss of 14q is common in higher-grade tumors, resulting in the inactivation of genes located there, such as NDRG family member 2 (NDRG2) and maternally expressed gene 3 (MEG3), and are associated with poor prognosis [38,39]. Codeletion of 1p and 14q is also reported with early recurrence and progression of tumors, suggesting an independent prognostic factor for the WHO grade [40].

The loss of chromosome 9p is strongly associated with malignant progression to anaplastic meningioma, predicting short survival and a worse prognosis [29,33]. This chromosomal arm harbors several important genes regulating cell cycle and apoptosis, such as cyclin-dependent kinase inhibitor 2A (CDKN2A) and cyclin-dependent kinase inhibitor 2B (CDKN2B) [41]. The amplification of 17q is also found in anaplastic meningioma [42]. Interestingly, recurrent and progressive meningiomas exhibit a more frequent loss of 1p, 14q, and 22q than de novo higher-grade tumors.



**Fig. 3.** Cytogenetic changes during initiation and progression of meningiomas.

**Table 1.** Familial syndromes associated with meningiomas

Familial syndrome	Affected gene	Chromosome locus
Neurofibromatosis type 2	<i>NF2</i>	22q12
Familial schwannomatosis	<i>SMARCB1</i>	22q11.23
Multiple spinal meningiomas	<i>SMARCE1</i>	17q21.2
BAP1 tumor predisposition syndrome	<i>BAP1</i>	3p21.1
Gorlin syndrome	<i>PTCH1</i>	9q22.3
(nevoid basal cell carcinoma syndrome)	<i>SUFU</i>	10q24.32
Familial multiple meningiomas	<i>SUFU</i>	10q24.32
Rubinstein-Taybi syndrome	<i>CREBBP</i>	16p13.3
von Hippel-Lindau syndrome	<i>VHL</i>	3p25-26
Cowden disease	<i>PTEN</i>	10q23.31
Li-Fraumeni syndrome	<i>TP53/CHEK2</i>	17p13.1/22q12.1
Gardner syndrome	<i>APC</i>	5q21-22
Multiple endocrine neoplasia type 1	<i>MEN</i>	11q13
Werner syndrome	<i>LMNA</i>	1q21.1

## GERMLINE ALTERATIONS AND FAMILIAL SYNDROMES PREDISPOSING MENINGIOMAS

Although the majority of meningiomas arise sporadically, several rare familial syndromes (Table 1) increase the risk of meningioma development [22,43]. Understanding these syndromes will help the management of patients with familial history, as well as give the basis for further clarification of meningioma tumorigenesis.

### Neurofibromatosis type 2

NF2 is the most well-known familial syndrome, which is caused by the germline mutation of the *NF2* gene on 22q12.2 and characterized by the development of multiple benign tumors in the nervous system, such as vestibular schwannoma and meningioma [44]. Over 50% of individuals in this syndrome manifest at least one meningioma in their lifetime, with a mean age of 30 years [22,45]. The type of mutation corresponds to the risk and severity of meningioma, a truncating mutation by frameshift or nonsense is correlated with a larger tumor burden and an early onset of meningioma rather than a nontruncating mutation

by missense or splice-site [45]. Most of the meningiomas in an NF2 disorder background present a fibrous or transitional phenotype and are generally more aggressive than sporadic tumors [43,46].

### Familial syndromes associated with the SWI/SNF complex: *SMARCB1* and *SMARCE1*

The switch/sucrose nonfermentable (SWI/SNF) chromatin remodeling complex regulates gene expression by nucleosome restructuring and is composed of 10–15 subunits: the ATPase subunits (*SMARCA2* or *SMARCA4*), the conserved core subunits (*SMARCB1*, *SMARCC1*, and *SMARCC2*) and additional complex-specific variant subunits (e.g., *SMARCE1*) [43]. Genetic aberrations in these subunits are associated with a variety of tumors, and the germline mutations of *SMARCB1* and *SMARCE1* are found in familial syndrome with risk of meningiomas [47,48]. Germline mutation of the *SMARCB1* gene on 22q11.23 causes several hereditary conditions, such as rhabdoid tumor predisposition syndrome (e.g., atypical teratoid/rhabdoid tumor [AT/RT] in CNS) [49], schwannomatosis [50], and Coffin-Siris syndrome [51]. Among these conditions, about 5% of individuals with schwannomatosis develop meningiomas [52], and the remaining two conditions have no significant relation to meningiomas. This is because the type and location of the mutations within the same gene are significantly different from each other, which has an influence on the phenotype of each condition [53]. Schwannomatosis harbors a nontruncating mutation at the beginning or end of the *SMARCB1* gene that presents as a benign tumor predisposition syndrome, whereas AT/RT is a highly aggressive malignant tumor in pediatrics and associated with a truncating mutation in the central exons or whole gene [52,53]. Although Coffin-Siris syndrome associated with a nontruncating mutation in exon 8 or 9 is a developmental disorder without the risk of tumors, a point mutation (p.Arg377His) in the *SMARCB1* gene was reported as a recurrent somatic mutation in one study [51,54]. *SMARCB1* is closely located (6 Mb apart) to *NF2* on

chromosome 22, and co-mutation of these two genes has been described during the tumorigenesis of meningiomas [47]. Germline mutation of *SMARCE1* gene on 17q21.2 was identified in families with multiple spinal meningiomas, and later this mutation was also found in individuals with intracranial meningiomas [48,55]. Almost all *SMARCE1* mutations are truncating with loss of function mutations and present a specific clear cell morphology [55].

### BAP1 tumor predisposition syndrome

Germline mutation of the BRCA1-associated protein 1 (*BAP1*) gene on 3p21.1 is a genetic cause of BAP1 tumor predisposition syndrome (BAP1-TPDS), which is susceptible to various neoplasms, including uveal and cutaneous melanomas, pleural and peritoneal mesotheliomas, renal cell carcinoma, and mesothelioma [56]. Affected individuals initially present with multiple skin-colored or light red dome-shaped papules, so-called *BAP1*-inactivated nevi/melanocytoma of the skin and develop meningiomas by the time they reach 50 years [57]. Meningiomas in BAP1-TPDS tend to have high-grade rhabdoid morphology and aggressive clinical behavior [56]. *BAP1* encodes a ubiquitin carboxyl-terminal hydrolase 1, which is involved in the regulation of transcription factor chromatin modification as a part of the polycomb repressive complex (PRC), and response to DNA damage by interacting with an important tumor suppressor, BRCA1 [56]. Currently, a BAP1 antibody is available for immunohistochemistry (IHC) and the loss of BAP1 expression on IHC is well correlated with the *BAP1* mutation [56].

### Gorlin syndrome (Nevoid basal cell carcinoma syndrome): PTCH1 and SUFU

Several genes in the sonic hedgehog (SHH) signaling pathway are relevant to nevoid basal cell carcinoma syndrome (NBCCS), also known as Gorlin syndrome, affecting multiple organ systems by nontumorous or tumorous conditions [44]. Together with diverse craniofacial and skeletal abnormalities, multiple basal cell carcinomas and medulloblastomas are presented [44]. The SHH pathway plays a critical role in embryonic development, and then it is strictly regulated in adult tissue [58]. Aberrant SHH signaling is reported in various solid cancers [58]. Germline mutations of the human homolog of the *Drosophila* patched gene (*PTCH1*) on 9p22.32 and suppressor of fusion (*SUFU*) gene on 10q24.32 increase the risk of meningiomas in this syndrome [59,60]. Normally, the PTCH1 protein maintains this pathway in an inactivated state by retaining SMO. The inactivating germline mutation of *PTCH1* in NBCCS leads to aberrant

activation of the SHH pathway, which is responsible for meningioma development [61]. Another germline mutation of the downstream factor, *SUFU*, is also infrequently found in NBCCS with pediatric medulloblastoma. A missense mutation of *SUFU* (p.Arg123Cys) can be found, although rarely, in families with hereditary multiple meningiomas [61].

### Other familial syndromes

Other familial syndromes associated with meningiomas include Rubinstein-Taybi syndrome, von Hippel-Lindau syndrome, Cowden disease, Li-Fraumeni syndrome, Gardner syndrome, Multiple endocrine neoplasia type 1, and Werner syndrome (Table 1) [44].

## SOMATIC MUTATIONS IN MENINGIOMAS

### *NF2*-mutated meningiomas

Genetic alterations of the *NF2* gene on 22q12.2 are found in up to 60% of sporadic meningiomas and identified not only in benign but also in higher-grade tumors, suggesting an initial role of tumorigenesis in meningiomas [28,62]. Around 60% of meningiomas with monosomy 22 also harbor the second allelic mutation in the remaining *NF2* gene, compatible with the two-hit hypothesis of the tumor suppressor gene [28,63]. Truncated or nontruncated proteins are made from the *NF2* mutation [64]. The protein Merlin, encoded by the *NF2* gene, is a member of the protein 4.1 family and keeps the original cell shape by linking membrane proteins to the cytoskeleton [64]. Therefore, *NF2* mutant meningiomas tend to exhibit more of a mesenchymal phenotype, such as fibrous or transitional rather than meningothelial histology [28]. The cells with impaired intercellular adhesion due to defected merlin, lose the inhibitory function on contact-mediated cellular proliferation [64]. Merlin is also involved in several signaling pathways, including Hippo, Notch, and mammalian target of the rapamycin (mTOR), so the loss of this protein results in the dysregulation of cell proliferation, growth, and motility [28,65]. The finding that *NF2*-mutated meningiomas harbor more genetic alterations than the *NF2*-nonmutated tumor, even within the same benign grade, gives the impression that chromosomal instability is increased with the presence of the *NF2* mutation [66].

### *NF2*-nonmutated meningiomas

About 40% of sporadic meningiomas occur in context with no *NF2* mutation, that is, these tumors are driven by other genetic alterations [6]. In the last decade, next-generation sequencing

**Table 2.** Genes associated with meningiomas

Gene	Full name	Locus	Product	Function
<i>NF2</i>	Neurofibromin 2	22q12.2	Merlin	Tumor suppressor Maintain cell shape by linkage cell membrane proteins to cytoskeleton
<i>TRAF7</i>	TNF receptor-associated factor 7	16p13.3	TNF receptor-associated factor 7	E3 ubiquitin ligase Interaction with MAPK pathway
<i>KLF4</i>	Kruppel-like factor 4	9p31	Kruppel-like factor 4	Transcription factor Induction of pluripotency
<i>AKT1</i>	v-Akt murine thymoma viral oncogene homolog 1	14q32.33	AKT1 kinase (serine/threonine protein kinase)	Oncogene Regulate cell growth and division, control apoptosis
<i>SMO</i>	Smoothed, frizzled class receptor	7p32.1	Smoothed, G protein-coupled receptor	Activation of hedgehog pathway Cell growth, proliferation
<i>PIK3CA</i>	Phosphatidylinositol-4,5-bisphosphate 3-kinase catalytic subunit alpha	3q26.32	Catalytic subunit of kinase, PI3K	Activation of PI3K/AKT pathway
<i>POLR2A</i>	RNA polymerase II subunit A	17p13.1	RNA polymerase II subunit A	Formation of preinitiation complex for transcription
<i>FAK</i>	Focal adhesion kinase	8q24.3	Protein tyrosine kinase2	Cytoplasmic tyrosine kinase Cellular proliferation and motility
<i>BAP1</i>	BRCA1-associated protein 1	3p21.1	Ubiquitin carboxyl-terminal hydrolase 1	Deubiquitinase, tumor suppressor Control cell growth, division and cell death
<i>SMARCB1</i>	SWI/SNF related, matrix associated, actin dependent regulator of chromatin, subfamily b, member 1	22q11.23	Subunit of SWI/SNF complex	Tumor suppressor Regulate gene activity by chromatin remodeling
<i>SMARCE1</i>	SWI/SNF related, matrix associated, actin dependent regulator of chromatin, subfamily e, member 1	17q21.2	Subunit of SWI/SNF complex	Tumor suppressor Regulate gene activity by chromatin remodeling
<i>BRAF V600E</i>	B-Raf proto-oncogene	7q34	Serine/threonine kinase	Oncogene Involved in MAPK pathway
<i>NOTCH2</i>	Notch receptor 2	1p12	Notch2 (notch receptor family)	Transmembrane receptor Involved in Notch signaling pathway
<i>CHEK2</i>	Checkpoint kinase2	22q12.1	Checkpoint kinase 2 (CHK2)	Tumor suppressor Regulate cell division
<i>PTEN</i>	Phosphatase and tensin homolog	10q23.31	Phosphatidylinositol-3,4,5-triphosphate 3-phosphatase	Tumor suppressor Negative regulation of mTOR pathway
<i>CDKN2A</i>	Cyclin-dependent kinase inhibitor 2A	9p21.3	p16(INK4A) p14(ARF)	Tumor suppressor Cell cycle progression (G1/S phase)
<i>CDKN2B</i>	Cyclin-dependent kinase inhibitor 2B	9p21.3	p15(INK4B)	Tumor suppressor Cell cycle progression (G1/S phase)
<i>DMD</i>	Dystrophin	Xp21.1	Dystrophin	Cytoskeletal construction, cell proliferation and motility
<i>TERTp</i>	Telomerase reverse transcriptase	5p15.33	Telomerase reverse transcriptase	Maintain telomere end

has elucidated a number of recurrent genetic alterations in *NF2*-nonmutated meningiomas, typically including *TRAF7*, *KLF4*, *AKT1*, *SMO*, *PIK3CA*, and RNA polymerase II subunit A (*POLR2A*) [22,24,25]. These somatic mutations are usually found in grade I meningiomas and mostly do not coexist with *NF2* mutations or monosomy 22 [22]. *TRAF7* mutations present alone or co-occur with *KLF4*, *AKT1*, or *PIK3CA* mutations, whereas *SMO* and *POLR2A* mutations are usually mutually exclusive (Fig. 2) [22,67]. In addition, the somatic mutation of the telomerase reverse transcriptase (*TERT*) promoter is revealed as a notable factor in the prognosis of meningiomas [22]. Here we detail the relevant somatic mutations one by one (Table 2).

#### *TRAF7* mutations

The somatic mutation of the *TRAF7* gene on 16p13.3 is the

most frequent genetic aberration observed in meningiomas without an *NF2* mutation and found in 15%–25% of sporadic meningiomas [24]. After the TRAF family was first identified as a signal adaptor of the tumor necrosis factor (TNF)-receptor superfamily, diverse receptor families engaging TRAFs for adaptor molecules have been found [68]. In addition, most TRAFs play a role as E3 ubiquitin ligase, activate downstream signaling pathways, and lead to the activation of mitogen-activated protein kinase (MAPK), nuclear factor- $\kappa$ B, and interferon-regulatory factor [68,69]. TRAF proteins transport various stimuli into the cell and engage in multiple physiologic processes, such as embryonal development, regulation of immunity, and stress response with tissue homeostasis [68]. The role of TRAF proteins in the pathogenesis of multiple diseases has been established, and aberrant *TRAF7*, the last member of the family, was identified as an

important genetic driver of meningiomas [6]. *TRAF7* mutations are mainly confined to exons 13–20, encoding seven WD40 repeats and approximating the domain through which TRAF7 interacts with other factors [24]. *TRAF7* mutated meningiomas usually show meningeothelial and benign histology, but also present with higher-grade tumors [24]. *TRAF7* mutations frequently co-occur with other somatic mutations, including *KLF4*, *AKT1*, and *PIK3CA* mutations, but are mutually exclusive to *NF2* or *SMO* mutations. Depending on what it is a coexisting mutation, it will affect the prognosis of *TRAF7* mutant meningioma [24,70]. Interestingly, almost all secretory meningiomas carry mutations in both *TRAF7* and *KLF4* genes [70].

#### *KLF4* mutations

The *KLF4* gene on 9q31 encodes a transcription factor belonging to a large Kruppel-like factor family, which is involved in many physiologic processes including proliferation, apoptosis, development, and pluripotency [71]. It promotes the reprogramming of differentiated adult cells to pluripotent stem cells, which might give a chance to driving tumors [71]. The only recurrent mutation of *KLF4* is a missense mutation at codon 409, which is present in the DNA-binding domain [72]. The substitution of lysine to glutamate (p.Lys409Gln) in that site affects the interaction with DNA target sequence and gene expression [72]. About one-fourth of *NF2*-nonmutated meningiomas harbor a *KLF4* mutation, corresponding to 9%–12% of all meningiomas [24]. *KLF4* mutations occur frequently with *TRAF7* mutation and exclusively with *NF2* and *AKT1* mutations [24,70]. Nearly all secretory meningiomas have *KLF4* and *TRAF7* co-mutations [70]. Secretory meningiomas have cytokeratin-positive globules, which is related with the regulatory role of *KLF4* to cytokeratin 4 and 19 [72].

#### *AKT1* mutations

*AKT1* on 14q32.33 encodes the AKT1 kinase (serine/threonine-protein kinase), which regulates cell proliferation, growth, and survival by phosphorylation of downstream factors in the phosphatidylinositol 3-kinase (PI3K)/AKT/mTOR signaling pathway [25,73]. The somatic mutation at codon 17 (p.Glu17Lys) causes an overactive AKT1 protein and constitutive activation of this pathway and is then related to uncontrolled cell proliferation [73]. The *AKT1* mutation is found in 7%–12% of grade I meningiomas and is rare in grade II or III [24]. More than half of the *AKT1* mutated tumors also harbor mutations in *TRAF7* but not in *NF2*, *KLF4*, and *SMO* [24,25]. The *AKT1*-mutant meningiomas present predominantly meningeothelial histology,

anterior skull base location, and reduced time to recurrence [74]. Moreover, a somatic mutation in *AKT1* (p.Glu17Lys) is also found in Proteus syndrome, a rare disorder characterized by overgrowth of the bones, skin, and other tissues, and some of these develop meningiomas [75].

#### *SMO* mutations

As with the *AKT1* mutation, the *SMO* mutation results in uncontrolled activation of the SHH signaling pathway, which then leads to the initiation and growth of meningioma [24,25,60]. The *SMO* gene on 7q32.1 has two mutation hotspots, more frequently p.Leu412Phe and p.Trp535Leu mutations occur [76]. *SMO* mutations are found in 1%–5% of *NF2*-nonmutated meningiomas and are mutually exclusive to *TRAF7* [24,25]. Meningiomas with *SMO* mutation show meningeothelial and grade I histology, and are mainly located in the medial anterior skull base near the midline [24,25,77]. A p.Leu412Phe mutation especially reported in olfactory groove meningioma is associated with larger tumor volume and high risk of recurrence [76].

#### *PIK3CA* mutations

PI3K is a member of the PI3K/AKT/mTOR signaling pathway, encoded by the *PIK3CA* gene [26] on 3q26.32. On mutation, PI3K constitutively phosphorylates downstream factor, AKT, and leads to oncogenic activation of this pathway [26]. *PIK3CA* mutation is found in 4%–7% of meningiomas, in exclusive fashion with *NF2*, *AKT1*, and *SMO*, but often coexists with the *TRAF7* mutation [26]. The *PIK3CA* mutant meningiomas mostly present meningeothelial or transitional histology of WHO grade I and locate at the skull base [26,78]. Out of several identified *PIK3CA* mutation hotspots, p.His1047Arg and p.Glu545Lys are rarely found in WHO grade II or III, suggesting their association with poor prognosis [78].

#### *POLR2A* mutations

The *POLR2A* gene on 17p13.1 encodes DNA-directed RNA polymerase II subunit A, which is the largest subunit of RNA polymerase II and crucial for the formation of the preinitiation complex [79]. Mutations of the *POLR2A* gene, mainly p.Gly403Lys or p.Leu438\_His439del at exon 7, can affect gene transcription [79]. The *POLR2A* mutation is found in 6% of meningiomas, exclusively from other mutations [79]. *POLR2A* mutated meningiomas present meningeothelial histology and arise from the tuberculum sellae of the skull base [79]. They are almost all WHO grade I and have a low risk of recurrence [79].

### FAK mutations

The focal adhesion kinase (*FAK*) gene on 8q24.3 encodes a cytoplasmic protein tyrosine kinase, which regulates several cell mechanisms involved in cell growth, proliferation, survival, and motility [80,81]. *FAK* overexpression has been found in several advanced solid cancers and is a potential therapeutic target [80]. Poulidakos et al. [80] reported a relationship between merlin and the *FAK* pathway in cancer; merlin negatively regulates the phosphorylation of *FAK* and inhibits the activity of *FAK* [81]. Upregulation of *FAK* is found in some meningiomas and related to a higher grade [82].

### BAP1 mutations

As mentioned previously, *BAP1* mutations were first reported in a distinct subset of rhabdoid meningiomas as a germline mutation in *BAP1-TPDS* [57,83]. Some *BAP1* mutant meningiomas have no germline mutation, indicating that the somatic mutation of *BAP1* also occurs [56]. But the difference in the clinical features between germline and somatic mutations is still unknown, in contrast to other *BAP1*-associated tumors [56]. Germline mutation is more commonly found in *BAP1*-mutant meningioma [56]. *BAP1* mutation is also related to early tumor recurrence [56]. A wide span of *BAP1* gene alterations are detected by *BAP1* IHC, which may be a useful surrogate marker for the loss of the *BAP1* protein, and is important to the risk stratification of meningiomas showing a rhabdoid morphology [56,57,84].

### SMARCB1 and SMARCE1 mutations

As with the *BAP1* gene, the somatic mutations of *SMARCB1* and *SMARCE1* are also found in a few sporadic meningiomas without an inherited background [54]. Generally, these mutations of subunits in the SWI/SNF complex are more frequently found in higher-grade meningiomas and so present poor prognosis [85]. Again, the loss of *SMARCE1* expression in IHC is a specific marker for the diagnosis of clear cell meningiomas. Spinal or cranial clear cell meningiomas present moderately aggressive features with a high risk of recurrence [55,86].

### BRAF V600E mutations

Somatic mutations of the B-Raf proto-oncogene (*BRAF*) gene are found in several tumors, including malignant melanoma and papillary thyroid carcinoma [87]. *BRAF* is located on 7q34 and encodes a serine/threonine kinase of the MAPK pathway, which tightly regulates cell growth and division [87]. The point mutation at codon 600 produces constitutively activated *BRAF* kinase, that leads to the activation of the downstream pathway and un-

controlled cell proliferation [87]. Two cases of *BRAF* V600E mutant rhabdoid meningiomas have been reported and one of them, presenting an aggressive clinical course, was improved with *BRAF* inhibitor (dabrafenib) [88-90]. No other histologic variants of the *BRAF* V600E mutation were found [88].

### NOTCH2 mutations

The Notch receptor 2 (*NOTCH2*) gene on 1p12 encodes a transmembrane protein of the Notch receptor family, which is involved in Notch signaling pathway and has a role in the developmental process [91]. In meningiomas, the overexpression of activated Notch 2 is thought to be associated with tetraploidy and chromosomal instability, but an accurate mechanism has not yet been found [91].

### CHEK2 mutations

The mutation of the checkpoint kinase 2 (*CHEK2*) gene on 22q12.1 is associated with chromosomal instability in meningiomas [92]. *CHEK2* encodes checkpoint kinase 2, which is activated when DNA is damaged. Consequently, it is involved in cell cycle arrest, DNA damage repair, or apoptosis, interacting with other proteins, such as tumor protein 53 (p53). Therefore, the loss of function in this protein leads to the development of tumors [92]. The codeletion of the *NF2* gene on the same chromosomal band 22q12 is frequently reported and it is associated with a more aggressive behavior [92].

### PTEN mutations

Somatic mutation of the phosphatase and tensin homolog (*PTEN*) gene on 10q23.31 is one of the most common genetic alterations in numerous tumors, including prostate cancer, endometrial cancer, and gliomas [93,94]. *PTEN* encodes a phosphatidylinositol-3,4,5-triphosphate 3-phosphatase, which negatively regulates the PI3K/AKT/mTOR pathway [94]. A loss of function mutation in *PTEN* is responsible for the progression to higher-grade meningiomas [95].

### CDKN2A and CDKN2B mutations

The *CDKN2A* gene on 9p21.3 encodes the tumor suppressor proteins, p16(INK4A) and p14(ARF) [35]. The p16(INK4A) protein binds to cyclin-dependent kinase 4 (CDK4) and cyclin-dependent kinase 6 (CDK6), preventing cell cycle progression and cell division. The p14(ARF) protein also controls cell cycle progression in the G1 phase, protecting the p53 protein from degradation [35]. The *CDKN2B* gene on 9p21.3 encodes the tumor suppressor, p15(INK4B), which also binds CDK4 or

CDK6, preventing cell cycle progression [35]. Mutation or deletion of the chromosomal band harboring *CDKN2A* and *CDKN2B* is frequently found in a wide range of tumors [35]. In meningioma, these alterations are usually related to anaplastic histology and poor outcome [41].

#### *DMD mutations*

Recently, the dystrophin (*DMD*) gene on Xp21.2–p21.1 has been suggested as a potential prognostic gene and is originally known for its germline mutation in Duchenne muscular dystrophy [96]. *DMD* encodes dystrophin, a large protein regulating cytoskeletal construction, cell proliferation, and motility [96]. In addition to a typical myogenic function, a role as an oncogenic gene in tumors originating from the neural crest and mesoderm is indicated [96]. An inactivating mutation of *DMD* is identified in progressive and higher-grade meningiomas and responsible for poor prognosis [96]. The location on the X chromosome partly supports the fact that aggressive meningiomas are common in males, in contrast to the female predominance of benign tumors [96]. *DMD* mutation is a mutually independent prognostic factor with *TERT* promoter alteration [96].

#### *TERT promoter mutations*

The *TERT* gene on 5p15.33 encodes a catalytic subunit of the telomerase complex, maintaining telomeres by adding small DNA repeats (TTAGGG) to the end of the chromosome [97]. In most somatic cells, expression of the telomerase complex is repressed, so the telomere is continuously shortened and finally leads to apoptosis [97]. The somatic mutation of the promoter region of the *TERT* gene, at hotspot C228T or C250T, increases the number of transcription factor binding sites [98]. This upregulates the expression of *TERT* and results in the constant survival of tumor cells [97]. In several cancers, such as glioma, melanoma, and bladder cancer, the presence of a *TERT* promoter mutation is usually associated with aggressive behavior and poor survival [99]. Similarly, in meningiomas, the *TERT* promoter mutation definitely affects the prognosis [100]. The *TERT* promoter mutation is more frequently identified in higher grades, 1.7%, 5.7%, and 20% in WHO grade I, II, and III, respectively, and related with the time to progression [100,101]. The median time to progression is 10.1 months versus 179 months in individuals with or without the *TERT* promoter mutation [100]. In addition, this mutation is mainly found in secondary atypical meningioma progressed from benign tumor rather than de novo atypical meningioma, therefore if it is identified in grade I meningioma, it implicates a high recurrence rate and malignant

transformation [100,101].

## EPIGENETIC ALTERATIONS IN MENINGIOMAS

Abnormal gene expression is crucial for cancer development and is induced primarily by genetic alterations [7]. However, epigenetic alterations that regulate gene expression without changing the DNA sequence are also responsible for the development of cancer [7]. Recently, evidence that epigenetic alterations have a pivotal role in the tumorigenesis and progression of meningiomas has accumulated [7,102]. In addition, it has been suggested that the status of global DNA methylation more accurately reflects tumor behavior and predicts tumor recurrence compared with WHO and Simpson grades [103–105]. Here we summarize the epigenetic alterations of meningiomas, including aberrant DNA methylation, aberration of chromatin remodeling, and abnormal expression of microRNAs (Table 3).

#### Aberrant DNA methylation

DNA methylation in CpG islands is a well-known epigenetic regulation of gene transcription [106]. Both focal DNA hypermethylation and global DNA methylation profiles have an effect on tumorigenesis [107]. The reliable single genes that are silenced by focal DNA hypermethylation without inactivating mutations in meningiomas include tissue inhibitor of metalloproteinase 3 (*TIMP3*), tumor protein p73 (*TP73*), *MEG3*, glutathione S-transferase Pi 1 (*GSTP1*), homeobox (*HOX*) family, WNK lysine deficient kinase 2 (*WNK2*), and MAL proteolipid protein 2 (*MAL2*). Hypermethylation of *TIMP3* gene on the 22q12.3, inhibits matrix metalloproteinases and results in downregulation of transcription and is associated with higher grades and aggressive behavior [106,108]. Nearly all *TIMP3*-hypermethylated meningiomas have an allelic loss of 22q [108,109]. Another tumor suppressor gene inactivated by epigenetic hypermethylation is *TP73* on 1p36.32, which is found in higher grades, frequently with allelic loss of 1p, and associated with malignant transformation [110]. *MEG3* on 14q32.2 encodes an imprinted long noncoding RNA, suppressing tumor cell growth and interacting with the tumor suppressor p53 [111]. *MEG3* RNA is considerably expressed in normal arachnoid cells, whereas it is not expressed in meningioma as a consequence of deletion or hypermethylation [39]. The silencing of the *MEG3* gene via promoter methylation is more commonly found in higher grades [39]. Hypermethylation of the *GSTP1* gene on 11q13.2 is also more frequently found in higher grades [106]. Concordant hypermethylation of *HOX* genes on 7p15.2, such as *HOXA5*,

**Table 3.** Epigenetic changes in meningiomas

Affected gene	Product	Physiologic function	Possible role in meningioma
Focal DNA methylation			
<i>TIMP3</i>	Metalloproteinase inhibitor 3	Inhibit MMP9 activity, tumor suppressor	Higher grade
<i>TP73</i>	p73	Cell cycle and growth regulation, tumor suppressor	Tumorigenesis
<i>MEG3</i>	Noncoding RNA	Cell cycle, p53 activation, tumor suppressor	Malignant transformation Tumorigenesis
<i>GSTP1</i>	Glutathione S transferase 1	Carcinogen detoxification, tumor suppressor	Higher grade
<i>HOXA5, 6, 9, 11</i>	Homeobox A gene cluster	Organ development and cell signaling	Tumorigenesis Higher grade, progression
<i>WNK2</i>	Serine-threonine kinase	Negatively regulation of EGFR signaling	Tumorigenesis Higher grade, progression
<i>MAL2</i>	Mal proteolipid protein2	Potential role in apoptosis	Higher grade Malignant transformation
Histone modification			
<i>H3K27</i>	Histone H3	Trimethylated H3K27 (H3K27m3): gene silencing	Tumorigenesis Worse outcome
<i>HIST1HIC</i>	Histone H1.2	Maintenance of methylation pattern Tumor suppressor	Recurrence
<i>KDM5C</i>	Lysine demethylase 5C	Chromatin structuring	Grade I, III
<i>KDM6A</i>	Lysine demethylase 5C	Chromatin structuring	Grade I
Chromatin remodeler			
<i>SMARCB1</i>	Subunit of SWI/SNF complex	Chromatin structuring	Higher grade
<i>SMARCE1</i>	Subunit of SWI/SNF complex	Chromatin structuring	Higher grade
microRNA			
miR-21	MicroRNA		Tumorigenesis, progression
miR-190a	MicroRNA	Antiapoptosis	Recurrence
miR-335	MicroRNA	Proliferation, RB1 signaling	Progression
miR-29c-3p	MicroRNA	Proliferation	Recurrence
miR-219-5p	MicroRNA	Proliferation, apoptosis	Recurrence
miR-145	MicroRNA	Collagen regulation Apoptosis, migration	Higher grade
miR-200a	MicroRNA	E-cadherin regulation Wnt/ $\beta$ -catenin signaling	Tumorigenesis Multifunctional
miR-224	MircoRNA		Progression

*HOXA6*, *HOXA9*, and *HOXA11*, induces silencing and down-regulation of target tumor suppressors [112]. The *WNK2* gene on 9q22.31 has an inhibitory function on the epidermal growth factor receptor (EGFR) signaling pathway, and the aberrant hypermethylation of this gene results in tumor cell proliferation by relieving inhibition [7,113]. The *MAL2* gene on 8q24.12 encodes a transmembrane protein required for the intracellular transport of macromolecules and transcytosis [114]. Hypermethylation of its promoter region and consequent gene silencing are found in higher grade meningiomas [102,114].

Powered by the development of molecular techniques, genome-wide methylation profiles are actively investigated in cancer biology. Emerging evidence indicates that global DNA methylation profiles may more precisely predict tumor recurrence and behaviors, and are more useful for the molecular classification of meningiomas [15]. In 2017, the first pivotal study was published by Olar et al. [103] As a result of profiling 140 cases of menin-

giomas, they recognized two distinct methylation subgroups of meningiomas, naming the prognostically favorable (MM-FAV) and unfavorable (MM-UNFAV) subgroups [103]. They defined a baseline meningioma methylation classifier, which is composed of 238 probes corresponding to hypermethylated CpG loci located on 157 gene lesions [103]. MM-FAV and MM-UNFAV groups show 98 CpG loci for 52 genes and 105 CpG loci for 105 genes, respectively [103]. After further optimization adapting existing prognostic factors, such as WHO and Simpson grades, they derived a 64 CpG loci of meningioma methylation predictor from 238 probes [103]. Each group shows a notably different risk of recurrence [103]. In the same year, Sahm et al. [104] identified two major epigenetic groups, group A and group B, by profiling genome-wide DNA methylation patterns from 497 cases of meningiomas. They further classified the groups into six subgroups, designated into methylation classes (MC), which are associated with distinct patterns of histology, cytogenetic alteration,

and mutation [104]. Group A is subdivided into four MC, MC benign 1, 2, 3, and MC intermediate A [104]. Group B is subdivided into two MC, MC intermediate B and MC malignant [104]. They demonstrate that the MCs are well correlated with histologic variant, cytogenetic alteration, and major mutations, and propose that a DNA methylation-based classification system can give a more accurate prognostication of clinical outcomes, such as progression-free survival [104]. Interestingly, they analyzed the potential of this system within the same WHO grade. WHO grade I with MC intermediate had a worse clinical outcome than the average outcome of WHO grade I [104]. Likewise, WHO grade II with MC benign showed a better clinical course than the average of WHO grade II [104]. Accordingly, this system may more accurately define individuals with a higher risk of progression in WHO grade I tumor and individuals with lower risk of progression in WHO grade II, and therefore assist in the precise decision making [104]. More recently, Nassiri et al. [105] announced a DNA methylation-based model for predicting the risk of early 5-year recurrence of meningiomas. They then combined the validated methylome predictor with existing prognostic factors (WHO and Simpson grades) and developed a nomogram calculating a 5-year meningioma recurrence score [105]. It is expected that the meningioma recurrence score will provide information about more personalized clinical outcomes and guidelines for clinical decision making [105].

### Aberration of chromatin remodeling

Chromatin remodeling is an important epigenetic regulation of gene expression. It governs the accessibility of the target gene DNA by changing the chromatin structure and exposing or hiding the target region [115]. It is mainly carried out by covalent modification of histone and ATP-dependent regulation of chromatin remodelers [115,116]. Aberration of this chromatin remodeling results in loss of transcriptional regulation of downstream genes and can cause the growth and progression of tumors [115,116]. Deregulation of histone modification and mutations in the members of remodeling complexes are reported in meningiomas [107].

### Histone modification

The abnormal modification of histones is reported in many diseases including cancers, although the detailed mechanisms are unclear [117]. Histone proteins not only condense chromatin to form nucleosomes but also participate in the regulation of gene expression through posttranslational modification by methylation, acetylation, phosphorylation, and ubiquitination [118]. It

is suggested that modified histones can recruit other proteins, then open or close the chromatin [118]. Among histone members (H2A, H2B, H3, and H4), trimethylation of lysine 27 of histone H3 (H3K27me<sub>3</sub>) has an important role in the target gene silencing and tumorigenesis of several cancers [115]. Katz et al. [119] reported that meningiomas with the loss of H3K27me<sub>3</sub> present more rapid progression and are well correlated with a previously designated DNA-methylation based classification scheme. They suggest that IHC for trimethylation of H3K27 might be useful for the assessment of prognosis particularly in WHO grade II [119]. On the other hand, molecular profiling studies reported mutations of genes associated with histones [120]. An overexpression of the histone cluster H1 family member C (*HIST1H1c*) gene on 6p22.2 is more frequently found in recurrent meningiomas [120]. It encodes histone H1.2 protein, which interacts with linker DNA and condenses chromatin structure more tightly [120]. It is believed that the H1.2 protein may be engaged in epigenetic regulation of target gene expression by preserving the specific patterns of DNA methylation [120]. In addition, loss of function mutations of *KDM5C* (on Xp11.22) and *KDM6A* (on Xp11.3), encoding histone lysine-specific demethylases, affect the function of histones and are also involved in epigenetic regulation in meningiomas [118].

### SWI/SNF chromatin remodeler

For the precise expression of genes at the correct time, transcription machinery recruits chromatin remodelers into the chromatin region, where they reconstruct and reposition nucleosome using energy from ATP to obtain a nucleosome-free region for gene expression [115]. The SWI/SNF complex (also known as the BAF complex) is well-known as a chromatin remodeler, and genetic alterations involving various subunits constituting this multimeric complex are found in up to 20% of human neoplasms [121]. It is believed that inactivating mutations of SWI/SNF subunits cause the redistribution of the complex from promoter and enhancer (involved in differentiation) to super-enhancer (involved in self-renewal, proliferation, and survival) and this imbalance results in tumorigenesis [121]. As previously mentioned, mutations of two core subunits of the SWI/SNF complex, *SMARCB1* and *SMARCE1*, are identified in meningiomas [107,121]. In addition, PRC2, which antagonizes the SWI/SNF complex, is upregulated in high-grade meningioma, therefore loss of function mutations in the SWI/SNF complex plays a critical role in the epigenetic regulation of chromatin in meningioma pathogenesis [122].

## MicroRNA expression

MicroRNAs (miRNAs) are important epigenetic mechanisms, which are involved in various physiologic and pathologic processes [123]. MiRNAs are small noncoding RNAs of about 22 nucleotides [107] and regulate the translation of target mRNA by inducing cleavage or degradation of the target mRNA strand and therefore inhibiting translation into proteins [124]. Recently, the role of miRNAs in cancer biology has been actively investigated and considerable genes encoding miRNAs are found in mutational hotspots of tumors or at fragile chromosomal sites [124,125]. Dysregulated miRNA may have either oncogenic or tumor-suppressing functions [124]. Although the miRNA profile of meningiomas has not been so actively studied, an accumulation of evidence implicates the role of miRNAs in the initiation, progression, and recurrence of meningiomas [123]. For example, downregulation of miR-200a and upregulation of  $\beta$ -catenin are found in meningiomas [7,118]. Because miR-200a targets the mRNA of  $\beta$ -catenin, abnormal low expression of miR-200a causes the overexpression of  $\beta$ -catenin and consequently activates the Wnt signaling pathway in meningiomas [118]. Low levels of miR-200a are also associated with the downregulation of E-cadherin via repression of transcription factors, ZEB1 and SIP1 [118]. Accordingly, miR-200a may act as a multifunctional tumor suppressor and the downregulation of miR-200a may promote the development of meningiomas [118,126]. Another study to find candidate miRNA in higher-grade tumors, reported that the downregulation of miRNA-145 is found in higher-grade meningiomas, which is indirectly associated with the overexpression of the *COL5A1* gene (encoding collagen type V alpha) and migratory or invasive potential of meningioma cells [118,127]. In addition, a higher expression of miR-21 is found in WHO grade II or III meningioma than in WHO grade I [7,107]. Upregulation of miR-190a and downregulation of miR-29c-3p and miR-219-5p are associated with a significantly high rate of recurrence [7,123]. Overexpression of miR-335 is found in meningiomas and has an effect on tumor cell proliferation, which is associated with the retinoblastoma protein (RB) signaling pathway [7]. MiR-224 is related to the malignant progression of meningiomas and may indicate the prognosis for overall or recurrence free survival [107].

## ABERRANT SIGNALING PATHWAYS IN MENINGIOMAS

Most of the genetic alterations impact one or more signaling pathway associated with tumorigenesis and the progression of

meningiomas (Fig. 4) [128]. The understanding of aberrant signaling pathways and relevant molecules could provide the basis for the development of corresponding target agents.

## mTOR pathway

The aberrant activation of the mTOR pathway has been known to be frequently associated with various human cancers [129]. The key molecule of this pathway, mTOR is a serine/threonine kinase, that constitutes two distinct complexes, mTOR complex 1 (mTORC1) and mTOR complex 2 (mTORC2) [130,131]. Several upstream signaling molecules have an influence on the mTOR signaling pathway, which regulates cell growth, proliferation, survival, and metabolism [131]. Merlin is related to the inhibition of cell proliferation through several pathways, and it is believed that merlin negatively regulates mTORC1 and positively regulates mTORC2 [132]. Consequently, loss of merlin by *NF2* mutation causes aberrant overexpression of mTOR and results in the development of meningioma [132]. Another upstream signaling pathway related to mTOR is the PI3K/AKT pathway [129,131]. PI3K phosphorylates and activates AKT, which is an activator of mTORC1 and a substrate for mTORC2 [130]. So activating mutations of *PIK3CA* and *AKT* lead to the aberrant activation of the downstream oncogenic mTOR pathway and are found in up to 10% of meningiomas. In addition, PTEN negatively regulates PI3K function, therefore loss of PTEN is also connected to aberrant mTOR activation [130].

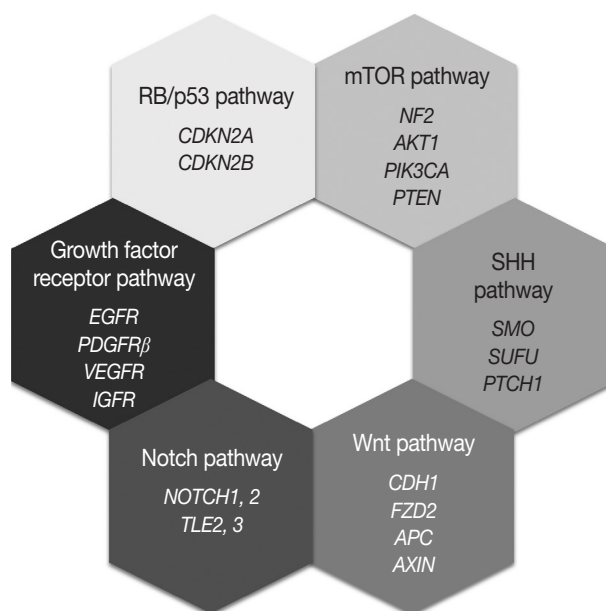


**Fig. 4.** Molecular signaling pathways associated with meningiomas.

Genetic alterations corresponding to the signaling molecules, merlin (NF2), PI3K, AKT, and PTEN, are all identified in a subset of meningiomas [107].

### SHH pathway

The SHH signaling pathway is essential for embryonic development [133]. In adults, it is involved and strictly regulated in several key cellular processes, including cell growth, proliferation, stem cell homeostasis, and angiogenesis [107,133]. The SHH ligand binds to the transmembrane receptor, PTCH1, and allows it to relieve its inhibition of SMO [134]. Freely released and activated SMO promotes the translocation of GLI transcription factors in the nucleus and results in the activation of the target gene [128,133]. Genetic alterations of *PTCH1* and *SMO* cause abnormal activation of this pathway and are associated with meningioma tumorigenesis [134]. *SUFU* is known as a negative regulator of the SHH pathway, and its germline mutation is also reported in meningiomas [107].

### Wnt pathway

The loss of E-cadherin expression is found in about 30% of meningiomas and is more frequently found in clinically aggressive and invasive meningiomas [135]. In addition, overexpression and translocation of  $\beta$ -catenin into the nucleus is also found in higher-grade meningiomas [135]. These suggest that Wnt signaling pathway has an important role in the tumorigenesis and progression of meningiomas. One of the receptors of this pathway, frizzled class receptor 2 (FZD2), is highly expressed in meningiomas, which is associated with the activation of the Wnt pathway, overexpression and translocation of cytosolic  $\beta$ -catenin, and the resultant upregulation of oncogenic proteins, such as c-myc and cyclin D1 [107,128,136]. Genetic aberration of genes encoding key molecules of the Wnt pathway, such as adenomatous polyposis coli (*APC*), E-cadherin (*CDH1*), and axis inhibition protein (*AXIN*), are also reported in meningiomas [107,128].

### Notch pathway

The Notch signaling pathway is highly conserved and plays an important role in embryonic development by proliferative signaling transduction through four transmembrane receptors, Notch1–4 [137]. When the jagged ligand binds to a Notch receptor, the cleaved intracellular portion of the Notch receptor is translocated into the nucleus and promotes the expression of a transcription factor, hairy and enhancer of split 1 (HES1) [128,135]. HES1 overexpression is found in all grades of meningiomas and is as-

sociated with the upregulation of jagged ligand, Notch1, and Notch2 [135]. In contrast, two corepressors modulating HES1 activity, transducin-like enhancer of split 2 (TLE2) and TLE3, are notably upregulated in higher-grade meningiomas [128,135]. As described above, dysregulation of this pathway is associated with tetraploidy and chromosomal instability [137].

### Growth factor receptor pathway

Growth factor receptors associated with tumor growth, angiogenesis, and tumor cell migration are implicated for meningioma tumorigenesis, including EGFR, platelet-derived growth factor receptor  $\beta$  (PDGFR $\beta$ ), vascular endothelial growth factor receptor, and insulin-like growth factor receptor [128,137]. EGFR and PDGFR usually transduce the mitogenic signal via the MAPK signaling pathway, which is reported to be aberrantly activated in meningiomas [135].

### RB and p53 pathway

The RB protein regulates the cell cycle progression at the G1/S phase checkpoint by inhibiting the E2F transcription factor [128]. When the mitogenic signal combines cyclin D with either CDK4 or CDK6, it causes phosphorylation of RB and releases the active E2F transcriptional factor, leading to expression of genes associated with the transition from G1 to S phase [128]. The p53 pathway functions as a negative regulator of the RB pathway, so induces the arrest of the cell cycle, repair of damaged DNA, and apoptosis [128,135]. p16(INK4a) and p15 (INK4b) prevent cell cycle progression by inhibiting the CDK4/cyclinD complex, and p14(ARF) connects the two RB and p53 pathways [135]. In fact, genetic alterations of genes encoding these proteins are found in higher-grade meningiomas [128].

## CLINICOPATHOLOGICAL FEATURES ASSOCIATED WITH GENETIC ALTERATION IN MENINGIOMAS

The difference in the embryonic origins of the meninges according to site is associated with the frequent histology, location, and recurrent mutations of meningiomas [138]. Meninges of the skull base originate from mesoderm, whereas meninges of the convexity originate from the neural crest [5]. Meningothelial variants are more frequently found in the skull base, whereas fibrous meningiomas mainly develop in the convexity [5,6]. Moreover, genetic alterations of the *NF2* gene are preferentially found in the convexity and most other genetic alterations except *NF2* are mainly found in skull base tumors (Table 4). The tumor site

**Table 4.** Clinicopathological features related to genetic alteration in meningiomas

Gene	Frequency (%)	Grade	Variant	Location	Prognosis
<i>NF2</i>	40–60	I, II, III	Fibrous Transitional	Convexity Posterior skull base	Poor for deletion
<i>TRAF7</i>	15–25	I>II, III	Meningothelial Secretory	Skull base	Dependent on coexisting mutation
<i>KLF4</i>	9–12	I	Secretory	Skull base	Low risk of malignant progression
<i>AKT1</i>	7–12	I	Meningothelial	Anterior skull base	Early tumor recurrence
<i>SMO</i>	1–5	I	Meningothelial	Medial anterior skull base Olfactory groove	Larger tumor volume Higher recurrence rate
<i>PIK3CA</i>	3–4	I>II, III	Meningothelial Transitional	Skull base	Rarely high grade, poor for Glu545Lys and His1047Arg
<i>POLR2A</i>	6	I	Meningothelial	Skull base (tuberculum sellae)	Low risk of recurrence and malignant progression
<i>TERT</i>	6	I<II, III	Atypical anaplastic (secondary)	Convexity skull base	High grade, poor
<i>SMARCB1</i>	5	I<II, III		Falx cerebri	High grade, poor
<i>SMARCE1</i>	3–4	II	Clear cell	Spinal	High risk of recurrence High grade, poor
<i>BAP1</i>	<1	III	Rhabdoid	Convexity	Poor

may also be related to the histologic grade, as the proportion of grade II and III tumors are much higher at the convexity than at the skull base, where grade I meningiomas are more common [6].

*AKT1*-mutant meningiomas tend to present meningothelial histology and anterior skull base localization, which are associated with early tumor recurrence [74]. *SMO*-mutant meningiomas also prefer the meningothelial variant at the anterior skull base and olfactory groove region, which tend to have larger tumor volume and higher recurrence rate [76]. Nearly all secretory meningiomas harbor *KLF4* mutations with or without *TRAF7* mutations but *TRAF7* mutations are also recurrent in other histologic variants, mainly the meningothelial variant [70]. *POLR2A*-mutant meningiomas are mainly located at the tuberculum sellae of the skull base and present meningothelial histology [79]. *PIK3CA*-mutant meningiomas are also located at the skull base and present meningothelial or transitional histology [26,78]. Two types of *PIK3CA* mutations, p.His1047Arg and p.Glu545Lys, are more frequently found in higher-grade tumors, which may be associated with poor prognosis [78]. Interestingly, mutation of *SMARCE1* is linked to clear cell histology in spinal cord meningiomas [55]. As previously stated, mutations of the *TERT* promoter obviously has an influence on the prognosis of meningiomas, which is definitely associated with malignant histological progression and time to progression [100]. *BAP1* mutations specific for rhabdoid meningioma [56], *TP53* mutations, loss of *CDKN2A* and *CDKN2B*, and epigenetic inactivation of *TIMP3* are all implicated in higher-grade histology and poor clinical outcome [41,106,108]. The deletion of 1p is also associated with the progression of meningiomas [33]. In contrast, genetic alterations of *TRAF7*, *SMO*, *KLF4*, *POLR2A*, and *PIK3CA* (except the above two types) are believed to be associated with a

relatively low risk of malignant progression and recurrence.

## CONCLUSION

The WHO grade and extent of resection are still the most important prognostic factors for meningioma. However, WHO classification does not always predict tumor recurrence or transformation to a higher grade. The molecular characteristics of meningiomas offer profound implications for pathologic classification and allow for the molecular subtyping of meningioma. Furthermore, the discovery of genetic and epigenetic biomarkers of meningioma may assist in the individualized management of precision medicine.

## ORCID

Young Suk Lee: <https://orcid.org/0000-0003-4794-639X>

Youn Soo Lee: <https://orcid.org/0000-0002-1653-6315>

## Author Contributions

Conceptualization: Youn Soo Lee, Young Suk Lee.

Data curation: Youn Soo Lee, Young Suk Lee.

Investigation: Youn Soo Lee, Young Suk Lee.

Methodology: Youn Soo Lee.

Supervision: Youn Soo Lee.

Writing—original draft: Youn Soo Lee, Young Suk Lee.

Writing—review & editing: Youn Soo Lee, Young Suk Lee.

## Conflicts of Interest

The authors declare that they have no potential conflicts of interest.

## Funding

No funding to declare.

## REFERENCES

1. Wiemels J, Wrensch M, Claus EB. Epidemiology and etiology of meningioma. *J Neurooncol* 2010; 99: 307-14.
2. Ostrom QT, Gittleman H, Truitt G, Boscia A, Kruchko C, Barnholtz-Sloan JS. CBTRUS statistical report: primary brain and other central nervous system tumors diagnosed in the United States in 2011-2015. *Neuro Oncol* 2018; 20: iv1-86.
3. Tufan K, Dogulu F, Kurt G, Emmez H, Ceviker N, Baykaner MK. Intracranial meningiomas of childhood and adolescence. *Pediatr Neurosurg* 2005; 41: 1-7.
4. Kotecha RS, Pascoe EM, Rushing EJ, et al. Meningiomas in children and adolescents: a meta-analysis of individual patient data. *Lancet Oncol* 2011; 12: 1229-39.
5. Kalamarides M, Stemmer-Rachamimov AO, Niwa-Kawakita M, et al. Identification of a progenitor cell of origin capable of generating diverse meningioma histological subtypes. *Oncogene* 2011; 30: 2333-44.
6. Preusser M, Brastianos PK, Mawrin C. Advances in meningioma genetics: novel therapeutic opportunities. *Nat Rev Neurol* 2018; 14: 106-15.
7. Galani V, Lampri E, Varouksi A, Alexiou G, Mitselou A, Kyritsis AP. Genetic and epigenetic alterations in meningiomas. *Clin Neurol Neurosurg* 2017; 158: 119-25.
8. Sadetzki S, Flint-Richter P, Ben-Tal T, Nass D. Radiation-induced meningioma: a descriptive study of 253 cases. *J Neurosurg* 2002; 97: 1078-82.
9. Phillips LE, Frankenfeld CL, Drangsholt M, Koepsell TD, van Belle G, Longstreth WT, Jr. Intracranial meningioma and ionizing radiation in medical and occupational settings. *Neurology* 2005; 64: 350-2.
10. Schneider B, Pülhorn H, Röhrig B, Rainov NG. Predisposing conditions and risk factors for development of symptomatic meningioma in adults. *Cancer Detect Prev* 2005; 29: 440-7.
11. Flint-Richter P, Mandelzweig L, Oberman B, Sadetzki S. Possible interaction between ionizing radiation, smoking, and gender in the causation of meningioma. *Neuro Oncol* 2011; 13: 345-52.
12. Phillips LE, Koepsell TD, van Belle G, Kukull WA, Gehrels JA, Longstreth WT Jr. History of head trauma and risk of intracranial meningioma: population-based case-control study. *Neurology* 2002; 58: 1849-52.
13. Huisman TW, Tanghe HJ, Koper JW, et al. Progesterone, oestradiol, somatostatin and epidermal growth factor receptors on human meningiomas and their CT characteristics. *European Journal of Cancer and Clinical Oncology* 1991; 27: 1453-7.
14. Sioka C, Kyritsis AP. Chemotherapy, hormonal therapy, and immunotherapy for recurrent meningiomas. *J Neurooncol* 2009; 92: 1-6.
15. Suppiah S, Nassiri F, Bi WL, et al. Molecular and translational advances in meningiomas. *Neuro Oncol* 2019; 21: i4-17.
16. Simpson D. The recurrence of intracranial meningiomas after surgical treatment. *J Neurol Neurosurg Psychiatry* 1957; 20: 22-39.
17. Gousias K, Schramm J, Simon M. The Simpson grading revisited: aggressive surgery and its place in modern meningioma management. *J Neurosurg* 2016; 125: 551-60.
18. Yuzawa S, Nishihara H, Tanaka S. Genetic landscape of meningioma. *Brain Tumor Pathol* 2016; 33: 237-47.
19. Louis DN, Ohgaki H, Wiestler OD, Cavenee WK. WHO classification of tumours of the central nervous system. Revised 4th ed. Lyon: International Agency for Research on Cancer, 2016.
20. Louis DN, Perry A, Reifenberger G, et al. The 2016 World Health Organization classification of tumors of the central nervous system: a summary. *Acta Neuropathol* 2016; 131: 803-20.
21. Zankl H, Zang KD. Cytological and cytogenetical studies on brain tumors. 4. Identification of the missing G chromosome in human meningiomas as no. 22 by fluorescence technique. *Humangenetik* 1972; 14: 167-9.
22. Proctor DT, Ramachandran S, Lama S, Sutherland GR. Towards molecular classification of meningioma: evolving treatment and diagnostic paradigms. *World Neurosurg* 2018; 119: 366-73.
23. Rutledge MH, Sarrazin J, Rangaratnam S, et al. Evidence for the complete inactivation of the NF2 gene in the majority of sporadic meningiomas. *Nat Genet* 1994; 6: 180-4.
24. Clark VE, Erson-Omay EZ, Serin A, et al. Genomic analysis of non-NF2 meningiomas reveals mutations in *TRAF7*, *KLF4*, *AKT1*, and *SMO*. *Science* 2013; 339: 1077-80.
25. Brastianos PK, Horowitz PM, Santagata S, et al. Genomic sequencing of meningiomas identifies oncogenic *SMO* and *AKT1* mutations. *Nat Genet* 2013; 45: 285-9.
26. Abedalthagafi M, Bi WL, Aizer AA, et al. Oncogenic *PI3K* mutations are as common as *AKT1* and *SMO* mutations in meningioma. *Neuro Oncol* 2016; 18: 649-55.
27. Seizinger BR, de la Monte S, Atkins L, Gusella JF, Martuza RL. Molecular genetic approach to human meningioma: loss of genes on chromosome 22. *Proc Natl Acad Sci U S A* 1987; 84: 5419-23.
28. Mawrin C, Perry A. Pathological classification and molecular genetics of meningiomas. *J Neurooncol* 2010; 99: 379-91.
29. Weber RG, Boström J, Wolter M, et al. Analysis of genomic alterations in benign, atypical, and anaplastic meningiomas: toward a

- genetic model of meningioma progression. *Proc Natl Acad Sci U S A* 1997; 94: 14719-24.
30. Abedalthagafi MS, Merrill PH, Bi WL, et al. Angiomatous meningiomas have a distinct genetic profile with multiple chromosomal polysomies including polysomy of chromosome 5. *Oncotarget* 2014; 5: 10596-606.
  31. Aizer AA, Abedalthagafi M, Bi WL, et al. A prognostic cytogenetic scoring system to guide the adjuvant management of patients with atypical meningioma. *Neuro Oncol* 2016; 18: 269-74.
  32. Cai DX, Banerjee R, Scheithauer BW, Lohse CM, Kleinschmidt-Demasters BK, Perry A. Chromosome 1p and 14q FISH analysis in clinicopathologic subsets of meningioma: diagnostic and prognostic implications. *J Neuropathol Exp Neurol* 2001; 60: 628-36.
  33. Lamszus K. Meningioma pathology, genetics, and biology. *J Neuropathol Exp Neurol* 2004; 63: 275-86.
  34. Lomas J, Bello MJ, Arjona D, et al. Analysis of p73 gene in meningiomas with deletion at 1p. *Cancer Genet Cytogenet* 2001; 129: 88-91.
  35. Bostrom J, Meyer-Puttitz B, Wolter M, et al. Alterations of the tumor suppressor genes *CDKN2A* (p16(INK4a)), *p14*(ARF), *CDKN2B* (p15(INK4b)), and *CDKN2C* (p18(INK4c)) in atypical and anaplastic meningiomas. *Am J Pathol* 2001; 159: 661-9.
  36. Mendiola M, Bello MJ, Alonso J, et al. Search for mutations of the hRAD54 gene in sporadic meningiomas with deletion at 1p32. *Mol Carcinog* 1999; 24: 300-4.
  37. Piaskowski S, Rieske P, Szybka M, et al. *GADD45A* and *EPB41* as tumor suppressor genes in meningioma pathogenesis. *Cancer Genet Cytogenet* 2005; 162: 63-7.
  38. Lusi EA, Watson MA, Chicoine MR, et al. Integrative genomic analysis identifies *NDRG2* as a candidate tumor suppressor gene frequently inactivated in clinically aggressive meningioma. *Cancer Res* 2005; 65: 7121-6.
  39. Zhang X, Gejman R, Mahta A, et al. Maternally expressed gene 3, an imprinted noncoding RNA gene, is associated with meningioma pathogenesis and progression. *Cancer Res* 2010; 70: 2350-8.
  40. Och W, Szmuda T, Sikorska B, et al. Recurrence-associated chromosomal anomalies in meningiomas: Single-institution study and a systematic review with meta-analysis. *Neurol Neurochir Pol* 2016; 50: 439-48.
  41. Perry A, Banerjee R, Lohse CM, Kleinschmidt-DeMasters BK, Scheithauer BW. A role for chromosome 9p21 deletions in the malignant progression of meningiomas and the prognosis of anaplastic meningiomas. *Brain Pathol* 2002; 12: 183-90.
  42. Buschges R, Ichimura K, Weber RG, Reifenberger G, Collins VP. Allelic gain and amplification on the long arm of chromosome 17 in anaplastic meningiomas. *Brain Pathol* 2002; 12: 145-53.
  43. Smith MJ. Germline and somatic mutations in meningiomas. *Cancer Genet* 2015; 208: 107-14.
  44. Kerr K, Qualmann K, Esquenazi Y, Hagan J, Kim DH. Familial syndromes involving meningiomas provide mechanistic insight into sporadic disease. *Neurosurgery* 2018; 83: 1107-18.
  45. Smith MJ, Higgs JE, Bowers NL, et al. Cranial meningiomas in 411 neurofibromatosis type 2 (NF2) patients with proven gene mutations: clear positional effect of mutations, but absence of female severity effect on age at onset. *J Med Genet* 2011; 48: 261-5.
  46. Antinheimo J, Haapasalo H, Haltia M, et al. Proliferation potential and histological features in neurofibromatosis 2-associated and sporadic meningiomas. *J Neurosurg* 1997; 87: 610-4.
  47. Christiaans I, Kenter SB, Brink HC, et al. Germline *SMARCB1* mutation and somatic *NF2* mutations in familial multiple meningiomas. *J Med Genet* 2011; 48: 93-7.
  48. Smith MJ, O'Sullivan J, Bhaskar SS, et al. Loss-of-function mutations in *SMARCE1* cause an inherited disorder of multiple spinal meningiomas. *Nat Genet* 2013; 45: 295-8.
  49. Biegel JA, Zhou JY, Rorke LB, Stenstrom C, Wainwright LM, Fogelgren B. Germ-line and acquired mutations of *INI1* in atypical teratoid and rhabdoid tumors. *Cancer Res* 1999; 59: 74-9.
  50. Hulsebos TJ, Plomp AS, Wolterman RA, Robanus-Maandag EC, Baas F, Wesseling P. Germline mutation of *INI1/SMARCB1* in familial schwannomatosis. *Am J Hum Genet* 2007; 80: 805-10.
  51. Tsurusaki Y, Okamoto N, Ohashi H, et al. Mutations affecting components of the SWI/SNF complex cause Coffin-Siris syndrome. *Nat Genet* 2012; 44: 376-8.
  52. Smith MJ, Wallace AJ, Bowers NL, et al. Frequency of *SMARCB1* mutations in familial and sporadic schwannomatosis. *Neurogenetics* 2012; 13: 141-5.
  53. Smith MJ, Wallace AJ, Bowers NL, Eaton H, Evans DG. *SMARCB1* mutations in schwannomatosis and genotype correlations with rhabdoid tumors. *Cancer Genet* 2014; 207: 373-8.
  54. Schmitz U, Mueller W, Weber M, Sevenet N, Delattre O, von Deimling A. *INI1* mutations in meningiomas at a potential hotspot in exon 9. *Br J Cancer* 2001; 84: 199-201.
  55. Smith MJ, Wallace AJ, Bennett C, et al. Germline *SMARCE1* mutations predispose to both spinal and cranial clear cell meningiomas. *J Pathol* 2014; 234: 436-40.
  56. Shankar GM, Abedalthagafi M, Vaubel RA, et al. Germline and somatic *BAP1* mutations in high-grade rhabdoid meningiomas. *Neuro Oncol* 2017; 19: 535-45.
  57. Haugh AM, Njauw CN, Bublely JA, et al. Genotypic and phenotypic features of BAP1 cancer syndrome: a report of 8 new families and review of cases in the literature. *JAMA Dermatol* 2017; 153: 999-1006.

58. Wicking C, Smyth I, Bale A. The hedgehog signalling pathway in tumorigenesis and development. *Oncogene* 1999; 18: 7844-51.
59. Smith MJ, Beetz C, Williams SG, et al. Germline mutations in *SUFU* cause Gorlin syndrome-associated childhood medulloblastoma and redefine the risk associated with *PTCH1* mutations. *J Clin Oncol* 2014; 32: 4155-61.
60. Ng JM, Curran T. The Hedgehog's tale: developing strategies for targeting cancer. *Nat Rev Cancer* 2011; 11: 493-501.
61. Aavikko M, Li SP, Saarinen S, et al. Loss of *SUFU* function in familial multiple meningioma. *Am J Hum Genet* 2012; 91: 520-6.
62. Choy W, Kim W, Nagasawa D, et al. The molecular genetics and tumor pathogenesis of meningiomas and the future directions of meningioma treatments. *Neurosurg Focus* 2011; 30: E6.
63. Nunes F, Shen Y, Niida Y, et al. Inactivation patterns of *NF2* and *DAL-1/4.1B (EPB41L3)* in sporadic meningioma. *Cancer Genet Cytogenet* 2005; 162: 135-9.
64. Pečina-Šlaus N. Merlin, the *NF2* gene product. *Pathol Oncol Res* 2013; 19: 365-73.
65. Lallemand D, Manent J, Couvelard A, et al. Merlin regulates transmembrane receptor accumulation and signaling at the plasma membrane in primary mouse Schwann cells and in human schwannomas. *Oncogene* 2009; 28: 854-65.
66. Goutagny S, Yang HW, Zucman-Rossi J, et al. Genomic profiling reveals alternative genetic pathways of meningioma malignant progression dependent on the underlying *NF2* status. *Clin Cancer Res* 2010; 16: 4155-64.
67. Zotti T, Scudiero I, Vito P, Stilo R. The emerging role of *TRAF7* in tumor development. *J Cell Physiol* 2017; 232: 1233-8.
68. Bouwmeester T, Bauch A, Ruffner H, et al. A physical and functional map of the human *TNF-alpha/NF-kappa B* signal transduction pathway. *Nat Cell Biol* 2004; 6: 97-105.
69. Xu LG, Li LY, Shu HB. *TRAF7* potentiates *MEKK3*-induced *AP1* and *CHOP* activation and induces apoptosis. *J Biol Chem* 2004; 279: 17278-82.
70. Reuss DE, Piro RM, Jones DT, et al. Secretory meningiomas are defined by combined *KLF4 K409Q* and *TRAF7* mutations. *Acta Neuropathol* 2013; 125: 351-8.
71. Tetreault MP, Yang Y, Katz JP. Kruppel-like factors in cancer. *Nat Rev Cancer* 2013; 13: 701-13.
72. Brembeck FH, Rustgi AK. The tissue-dependent keratin 19 gene transcription is regulated by *GKLF/KLF4* and *Sp1*. *J Biol Chem* 2000; 275: 28230-9.
73. Carpten JD, Faber AL, Horn C, et al. A transforming mutation in the pleckstrin homology domain of *AKT1* in cancer. *Nature* 2007; 448: 439-44.
74. Yesiloz U, Kirches E, Hartmann C, et al. Frequent *AKT1E17K* mutations in skull base meningiomas are associated with *mTOR* and *ERK1/2* activation and reduced time to tumor recurrence. *Neuro Oncol* 2017; 19: 1088-96.
75. Keppler-Noreuil KM, Baker EH, Sapp JC, Lindhurst MJ, Biesecker LG. Somatic *AKT1* mutations cause meningiomas colocalizing with a characteristic pattern of cranial hyperostosis. *Am J Med Genet A* 2016; 170: 2605-10.
76. Boetto J, Bielle F, Sanson M, Peyre M, Kalamarides M. *SMO* mutation status defines a distinct and frequent molecular subgroup in olfactory groove meningiomas. *Neuro Oncol* 2017; 19: 345-51.
77. Strickland MR, Gill CM, Nayyar N, et al. Targeted sequencing of *SMO* and *AKT1* in anterior skull base meningiomas. *J Neurosurg* 2017; 127: 438-44.
78. Zadeh G, Karimi S, Aldape KD. *PIK3CA* mutations in meningioma. *Neuro Oncol* 2016; 18: 603-4.
79. Clark VE, Harmanci AS, Bai H, et al. Recurrent somatic mutations in *POLR2A* define a distinct subset of meningiomas. *Nat Genet* 2016; 48: 1253-9.
80. Poulidakos PI, Xiao GH, Gallagher R, Jablonski S, Jhanwar SC, Testa JR. Re-expression of the tumor suppressor *NF2/merlin* inhibits invasiveness in mesothelioma cells and negatively regulates *FAK*. *Oncogene* 2006; 25: 5960-8.
81. Sulzmaier FJ, Jean C, Schlaepfer DD. *FAK* in cancer: mechanistic findings and clinical applications. *Nat Rev Cancer* 2014; 14: 598-610.
82. Wang X, Gong Y, Wang D, et al. Analysis of gene expression profiling in meningioma: deregulated signaling pathways associated with meningioma and *EGFL6* overexpression in benign meningioma tissue and serum. *PLoS One* 2012; 7: e52707.
83. Murali R, Wiesner T, Scolyer RA. Tumours associated with *BAP1* mutations. *Pathology* 2013; 45: 116-26.
84. Shankar GM, Santagata S. *BAP1* mutations in high-grade meningioma: implications for patient care. *Neuro Oncol* 2017; 19: 1447-56.
85. Harmanci AS, Youngblood MW, Clark VE, et al. Integrated genomic analyses of de novo pathways underlying atypical meningiomas. *Nat Commun* 2017; 8: 14433.
86. Evans LT, Van Hoff J, Hickey WE, et al. *SMARCE1* mutations in pediatric clear cell meningioma: case report. *J Neurosurg Pediatr* 2015; 16: 296-300.
87. Loo E, Khalili P, Beuhler K, Siddiqi I, Vasef MA. *BRAF V600E* mutation across multiple tumor types: correlation between DNA-based sequencing and mutation-specific immunohistochemistry. *Appl Immunohistochem Mol Morphol* 2018; 26: 709-13.
88. Bujko M, Kober P, Tysarowski A, et al. *EGFR*, *PIK3CA*, *KRAS* and *BRAF* mutations in meningiomas. *Oncol Lett* 2014; 7: 2019-22.
89. Mordechai O, Postovsky S, Vlodavsky E, et al. Metastatic rhab-

- doid meningioma with *BRAF* V600E mutation and good response to personalized therapy: case report and review of the literature. *Pediatr Hematol Oncol* 2015; 32: 207-11.
90. Behling F, Barrantes-Freer A, Skardelly M, et al. Frequency of *BRAF* V600E mutations in 969 central nervous system neoplasms. *Diagn Pathol* 2016; 11: 55.
  91. Baia GS, Stifani S, Kimura ET, McDermott MW, Pieper RO, Lal A. Notch activation is associated with tetraploidy and enhanced chromosomal instability in meningiomas. *Neoplasia* 2008; 10: 604-12.
  92. Yang HW, Kim TM, Song SS, et al. Alternative splicing of *CHEK2* and codeletion with *NF2* promote chromosomal instability in meningioma. *Neoplasia* 2012; 14: 20-8.
  93. Lino MM, Merlo A. PI3Kinase signaling in glioblastoma. *J Neurooncol* 2011; 103: 417-27.
  94. Basu S, Totty NF, Irwin MS, Sudol M, Downward J. Akt phosphorylates the Yes-associated protein, YAP, to induce interaction with 14-3-3 and attenuation of p73-mediated apoptosis. *Mol Cell* 2003; 11: 11-23.
  95. Peters N, Wellenreuther R, Rollbrocker B, et al. Analysis of the *PTEN* gene in human meningiomas. *Neuropathol Appl Neurobiol* 1998; 24: 3-8.
  96. Juratli TA, McCabe D, Nayyar N, et al. DMD genomic deletions characterize a subset of progressive/higher-grade meningiomas with poor outcome. *Acta Neuropathol* 2018; 136: 779-92.
  97. Koelsche C, Sahm F, Capper D, et al. Distribution of *TERT* promoter mutations in pediatric and adult tumors of the nervous system. *Acta Neuropathol* 2013; 126: 907-15.
  98. Gao K, Li G, Qu Y, et al. *TERT* promoter mutations and long telomere length predict poor survival and radiotherapy resistance in gliomas. *Oncotarget* 2016; 7: 8712-25.
  99. Simon M, Park TW, Leuenroth S, Hans VH, Loning T, Schramm J. Telomerase activity and expression of the telomerase catalytic subunit, hTERT, in meningioma progression. *J Neurosurg* 2000; 92: 832-40.
  100. Sahm F, Schrimpf D, Olar A, et al. *TERT* promoter mutations and risk of recurrence in meningioma. *J Natl Cancer Inst* 2016; 108: djv377.
  101. Goutagny S, Nault JC, Mallet M, Henin D, Rossi JZ, Kalamarides M. High incidence of activating *TERT* promoter mutations in meningiomas undergoing malignant progression. *Brain Pathol* 2014; 24: 184-9.
  102. He S, Pham MH, Pease M, et al. A review of epigenetic and gene expression alterations associated with intracranial meningiomas. *Neurosurg Focus* 2013; 35: E5.
  103. Olar A, Wani KM, Wilson CD, et al. Global epigenetic profiling identifies methylation subgroups associated with recurrence-free survival in meningioma. *Acta Neuropathol* 2017; 133: 431-44.
  104. Sahm F, Schrimpf D, Stichel D, et al. DNA methylation-based classification and grading system for meningioma: a multicentre, retrospective analysis. *Lancet Oncol* 2017; 18: 682-94.
  105. Nassiri F, Mamatjan Y, Suppiah S, et al. DNA methylation profiling to predict recurrence risk in meningioma: development and validation of a nomogram to optimize clinical management. *Neuro Oncol* 2019 Jun 3 [Epub]. <https://doi.org/10.1093/neuonc/noz061>.
  106. Liu Y, Pang JC, Dong S, Mao B, Poon WS, Ng HK. Aberrant CpG island hypermethylation profile is associated with atypical and anaplastic meningiomas. *Hum Pathol* 2005; 36: 416-25.
  107. Pereira BJ, Oba-Shinjo SM, de Almeida AN, Marie SK. Molecular alterations in meningiomas: Literature review. *Clin Neurol Neurosurg* 2019; 176: 89-96.
  108. Barski D, Wolter M, Reifenberger G, Riemenschneider MJ. Hypermethylation and transcriptional downregulation of the *TIMP3* gene is associated with allelic loss on 22q12.3 and malignancy in meningiomas. *Brain Pathol* 2010; 20: 623-31.
  109. Bello MJ, Amiñoso C, Lopez-Marin I, et al. DNA methylation of multiple promoter-associated CpG islands in meningiomas: relationship with the allelic status at 1p and 22q. *Acta Neuropathol* 2004; 108: 413-21.
  110. Nakane Y, Natsume A, Wakabayashi T, et al. Malignant transformation-related genes in meningiomas: allelic loss on 1p36 and methylation status of p73 and *RASSF1A*. *J Neurosurg* 2007; 107: 398-404.
  111. Zhou Y, Zhong Y, Wang Y, et al. Activation of p53 by MEG3 non-coding RNA. *J Biol Chem* 2007; 282: 24731-42.
  112. Kishida Y, Natsume A, Kondo Y, et al. Epigenetic subclassification of meningiomas based on genome-wide DNA methylation analyses. *Carcinogenesis* 2012; 33: 436-41.
  113. Jun P, Hong C, Lal A, et al. Epigenetic silencing of the kinase tumor suppressor *WNK2* is tumor-type and tumor-grade specific. *Neuro Oncol* 2009; 11: 414-22.
  114. Gao F, Shi L, Russin J, et al. DNA methylation in the malignant transformation of meningiomas. *PLoS One* 2013; 8: e54114.
  115. Nair SS, Kumar R. Chromatin remodeling in cancer: a gateway to regulate gene transcription. *Mol Oncol* 2012; 6: 611-9.
  116. Kumar R, Li DQ, Muller S, Knapp S. Epigenomic regulation of oncogenesis by chromatin remodeling. *Oncogene* 2016; 35: 4423-36.
  117. Feinberg AP, Koldobskiy MA, Göndör A. Epigenetic modulators, modifiers and mediators in cancer aetiology and progression. *Nat Rev Genet* 2016; 17: 284-99.
  118. Murányi B, Bognár L, Klekner Á, Hortobágyi T. Epigenetics of meningiomas. *Biomed Res Int* 2015; 2015: 532451.

119. Katz LM, Hielscher T, Liechty B, et al. Loss of histone H3K27me3 identifies a subset of meningiomas with increased risk of recurrence. *Acta Neuropathol* 2018; 135: 955-63.
120. Pérez-Magán E, Rodríguez de Lope A, Ribalta T, et al. Differential expression profiling analyses identifies downregulation of 1p, 6q, and 14q genes and overexpression of 6p histone cluster 1 genes as markers of recurrence in meningiomas. *Neuro Oncol* 2010; 12: 1278-90.
121. Lu C, Allis CD. SWI/SNF complex in cancer. *Nat Genet* 2017; 49: 178-9.
122. Collord G, Tarpey P, Kurbatova N, et al. An integrated genomic analysis of anaplastic meningioma identifies prognostic molecular signatures. *Sci Rep* 2018; 8: 13537.
123. Zhi F, Zhou G, Wang S, et al. A microRNA expression signature predicts meningioma recurrence. *Int J Cancer* 2013; 132: 128-36.
124. Lee YS, Dutta A. MicroRNAs in cancer. *Annu Rev Pathol* 2009; 4: 199-227.
125. Calin GA, Sevignani C, Dumitru CD, et al. Human microRNA genes are frequently located at fragile sites and genomic regions involved in cancers. *Proc Natl Acad Sci U S A* 2004; 101: 2999-3004.
126. Venza M, Visalli M, Beninati C, et al. Involvement of epimutations in meningioma. *Brain Tumor Pathol* 2015; 32: 163-8.
127. Kliese N, Gobrecht P, Pachow D, et al. miRNA-145 is downregulated in atypical and anaplastic meningiomas and negatively regulates motility and proliferation of meningioma cells. *Oncogene* 2013; 32: 4712-20.
128. Domingues P, González-Tablas M, Otero Á, et al. Genetic/molecular alterations of meningiomas and the signaling pathways targeted. *Oncotarget* 2015; 6: 10671-88.
129. Porta C, Paglino C, Mosca A. Targeting PI3K/Akt/mTOR signaling in cancer. *Front Oncol* 2014; 4: 64.
130. Sato T, Sekido Y. NF2/Merlin inactivation and potential therapeutic targets in mesothelioma. *Int J Mol Sci* 2018; 19: E988.
131. Saxton RA, Sabatini DM. mTOR signaling in growth, metabolism, and disease. *Cell* 2017; 168: 960-76.
132. Beltrami S, Kim R, Gordon J. Neurofibromatosis type 2 protein, NF2: an unconventional cell cycle regulator. *Anticancer Res* 2013; 33: 1-11.
133. Rimkus TK, Carpenter RL, Qasem S, Chan M, Lo HW. Targeting the sonic Hedgehog signaling pathway: review of smoothed and GLI inhibitors. *Cancers (Basel)* 2016; 8: E22.
134. Nigim F, Wakimoto H, Kasper EM, Ackermans L, Temel Y. Emerging medical treatments for meningioma in the molecular era. *Biomedicines* 2018; 6: E86.
135. Miller R Jr, DeCandio ML, Dixon-Mah Y, et al. Molecular targets and treatment of meningioma. *J Neurol Neurosurg* 2014; 1: 1000101.
136. Nelson WJ, Nusse R. Convergence of Wnt, beta-catenin, and cadherin pathways. *Science* 2004; 303: 1483-7.
137. Ragel BT, Jensen RL. Aberrant signaling pathways in meningiomas. *J Neurooncol* 2010; 99: 315-24.
138. Kros J, de Greve K, van Tilborg A, et al. NF2 status of meningiomas is associated with tumour localization and histology. *J Pathol* 2001; 194: 367-72.

# 2019 Practice guidelines for thyroid core needle biopsy: a report of the Clinical Practice Guidelines Development Committee of the Korean Thyroid Association

Chan Kwon Jung<sup>1,2</sup>, Jung Hwan Baek<sup>3</sup>, Dong Gyu Na<sup>4</sup>, Young Lyun Oh<sup>5</sup>, Ka Hee Yi<sup>6</sup>, Ho-Cheol Kang<sup>7</sup>,  
 Clinical Practice Guidelines Development Committee of the Korean Thyroid Association

<sup>1</sup>Department of Hospital Pathology, College of Medicine, The Catholic University of Korea, Seoul;

<sup>2</sup>Cancer Research Institute, College of Medicine, The Catholic University of Korea, Seoul;

<sup>3</sup>Department of Radiology and Research Institute of Radiology, Asan Medical Center, University of Ulsan College of Medicine, Seoul;

<sup>4</sup>Department of Radiology, Gangneung Asan Hospital, University of Ulsan College of Medicine, Gangneung;

<sup>5</sup>Department of Pathology and Translational Genomics, Samsung Medical Center, Sungkyunkwan University School of Medicine, Seoul;

<sup>6</sup>Department of Internal Medicine, Seoul Metropolitan Government Seoul National University Boramae Medical Center, Seoul;

<sup>7</sup>Department of Internal Medicine, Chonnam National University Hwasun Hospital, Chonnam National University Medical School, Hwasun, Korea

Ultrasound-guided core needle biopsy (CNB) has been increasingly used for the pre-operative diagnosis of thyroid nodules. Since the Korean Society of the Thyroid Radiology published the 'Consensus Statement and Recommendations for Thyroid CNB' in 2017 and the Korean Endocrine Pathology Thyroid CNB Study Group published 'Pathology Reporting of Thyroid Core Needle Biopsy' in 2015, advances have occurred rapidly not only in the management guidelines for thyroid nodules but also in the diagnostic terminology and classification schemes. The Clinical Practice Guidelines Development Committee of the Korean Thyroid Association (KTA) reviewed publications on thyroid CNB from 1995 to September 2019 and updated the recommendations and statements for the diagnosis and management of thyroid nodules using CNB. Recommendations for the resolution of clinical controversies regarding the use of CNB were based on expert opinion. These practical guidelines include recommendations and statements regarding indications for CNB, patient preparation, CNB technique, biopsy-related complications, biopsy specimen preparation and processing, and pathology interpretation and reporting of thyroid CNB.

**Key Words:** Thyroid gland; Thyroid nodule; Thyroid neoplasms; Biopsy, Fine-Needle; Core needle biopsy

**Received:** November 21, 2019 **Accepted:** December 4, 2019

**Corresponding Author:** Chan Kwon Jung, MD, PhD, Department of Pathology, Seoul St. Mary's Hospital, College of Medicine, The Catholic University of Korea, 222 Banpo-daero, Seocho-gu, Seoul 06591, Korea

Tel: +82-2-2258-1622, Fax: +82-2-2258-1627, E-mail: ckjung@catholic.ac.kr

**Corresponding Author:** Jung Hwan Baek, MD, PhD, Department of Radiology and Research Institute of Radiology, Asan Medical Center, University of Ulsan College of Medicine, 88 Olympic-ro 43-gil, Songpa-gu, Seoul 05505, Korea

Tel: +82-2-3010-4348, Fax: +82-2-476-0090, E-mail: radbaek@naver.com

Ultrasound (US)-guided fine-needle aspiration (FNA) is a cost-effective and safe tool for the assessment of thyroid nodules and has been used as a standard diagnostic modality for the management of thyroid nodules [1,2]. In the 1980s, FNA became the standard diagnostic tool for thyroid nodules, replacing large-needle biopsy because of its high diagnostic accuracy and low complication rate [3]. The main clinical role of FNA is to rule out malignant tumors requiring surgery. The use of FNA has reduced the number of unnecessary surgeries in patients with thyroid nodules. Although FNA is associated with high diagnos-

tic accuracy and safety, it has several limitations due to a substantial rate (approximately 22.4%) of inconclusive results including non-diagnostic or atypia of undetermined significance (AUS)/follicular lesion of undetermined significance (FLUS) [4]. The non-diagnostic rate in initial FNA is about 10% and an even higher rate of up to 50% in repeat FNA [5,6]. The rate of AUS/FLUS is about 10%–20% with higher rates of inconclusive results in repeat FNA [7-10]. FNA also shows a relatively low diagnostic accuracy for follicular lesions [11,12]. These limitations associated with FNA lead to repeated FNA or unnecessary

surgeries. Therefore, additional diagnostic tools for thyroid nodules are desirable to overcome the limitations of FNA for thyroid nodule assessment.

Advances in core needle biopsy (CNB) have led to the use of spring-activated single- or double-action needles in thyroid nodule diagnosis. In addition, widespread use of high-resolution US enables accurate diagnosis and minimization of complications associated with CNB in head and neck lesions [13]. CNB is safe, well-tolerated, and associated with a low incidence of complications when performed by an expert [1,14]. Several large-scale studies [15,16] and a systematic review and meta-analysis [17] validated the low rates of major and minor complications and absence of procedure-related deaths.

CNB has the potential to overcome the limitations of FNA by obtaining a large tissue sample, which reduces non-diagnostic results due to paucity of follicular cells and provides further information related to histological architecture underlying the capsule. Previous studies [18-21] reported that CNB yielded a lower rate of inconclusive results, including non-diagnostic or AUS/FLUS results compared with repeated FNA in the assessment of nodules with prior inconclusive results. Recently, several studies also reported the potential role of CNB as a first-line diagnostic tool for the management of thyroid nodules [22-25].

Together with thyroid FNA and CNB, a multidisciplinary approach for patients with a thyroid nodule is essential to improve the quality of life and achieve a better outcome. Standardized guidelines are needed to ensure the optimal management of patients with thyroid nodules. The terminology for reporting thyroid FNA cytology worldwide is based on the Bethesda System for Reporting Thyroid Cytopathology (TBSRTC), which was introduced in 2007. The second edition of TBSRTC was released in 2017 [26]. The Korean Society of Thyroid Radiology (KSThR) published 'Core needle biopsy of thyroid nodules: consensus statement and recommendations' in 2013 [27]. The Korean Endocrine Pathology Thyroid CNB Study Group published an initial proposal of 'Pathology Reporting of Thyroid Core Needle Biopsy' in 2015 [28]. In 2017, the KSThR published 'Core Needle Biopsy of the Thyroid: 2016 Consensus Statement and Recommendations from the Korean Society of Thyroid Radiology' [14]. The fourth edition of the World Health Organization (WHO) classification of endocrine tumors was released in 2017 [29]. The 2017 revisions of TBSRTC and the WHO classification in thyroid cytology and histopathology encompass molecular diagnostics and new diagnostic entities of borderline thyroid tumors such as noninvasive follicular thyroid neoplasm with papillary-like nuclear features (NIFTP).

Along with recent advances in the diagnostic classification and management guidelines of thyroid nodules, the Practice Guideline Committee of the Korean Thyroid Association (KTA) organized a taskforce for the development of practical guidelines of CNB for the diagnosis and management of thyroid nodules. This guideline includes the indications, patient preparation, biopsy technique, complications, specimen preparation, and pathology reporting.

## METHODS

A search of the PubMed, MEDLINE, and EMBASE databases was performed to retrieve publications on thyroid CNB from 1995 to September 2019 using the following keywords: (thyroid nodule OR thyroid cancer OR thyroid carcinoma OR thyroid malignancy OR thyroid neoplasm OR thyroid diagnosis) and (core needle biopsy OR core-needle biopsy OR core biopsy OR gun biopsy OR CNB). Since clinical controversies related to issues exist in many of the areas, the recommendations regarding some of the issues are based on expert opinion. This limitation needs to be overcome in the near future when new elements of evidence are accumulated. Because there is little high-level evidence, recommendations regarding some of the issues are based on expert opinion. This limitation needs to be addressed in the future based on further studies. The goal of this guideline is to provide the best scientific evidence available and a consensus expert opinion regarding the clinical use of CNB in thyroid nodules.

## INDICATIONS FOR CORE NEEDLE BIOPSY

The indications for CNB have yet to be clearly defined. Most thyroid guidelines recommend FNA as a first-line biopsy for thyroid nodule assessment; therefore, CNB is regarded as a complementary tool [14,30-32]. Recently, KSThR published the CNB Guideline in 2017 [14]. KSThR suggested several indications and the possible use of CNB for thyroid nodules with non-diagnostic or indeterminate FNA results. The National Cancer Institute (NCI) suggested that CNB under US guidance utilizing modern needles may be advantageous in cases rendered "unsatisfactory" by FNA [32]. In addition, the American Association of Clinical Endocrinologists (AACE)/American College of Endocrinology (ACE)/Associazione Medici Endocrinologi (AME), British Thyroid Association (BTA), and KSThR suggested the use of CNB for malignant thyroid tumors such as lymphoma, anaplastic cancer, medullary cancer, and metastasis [14,30,33]. However, the American Thyroid Association (ATA)

did not recommend the use of CNB for thyroid tumors [31].

A meta-analysis showed that the non-diagnostic and inconclusive rates of CNB were 5.5% (95% confidence interval [CI], 2.2% to 8.7%) and 8.0% (95% CI, 4.4% to 11.5%), respectively, whereas the non-diagnostic and inconclusive rates of FNA were 22.6% (95% CI, 12.2% to 33.0%) and 40.2% (95% CI, 25.1% to 55.3%), respectively [34-36]. In another meta-analysis focusing on initially non-diagnostic FNA results, the non-diagnostic rate (6.4%; 95% CI, 3.3% to 16.1%) of follow-up CNB was significantly lower than that of repeated FNA (36.5%; 95% CI, 29.9% to 43.1%) [35,36]. In large cohort CNB studies, the false-negative rate of CNB ranged from 1% to 3% [35,37-39]. Recently, several studies suggested the initial use of CNB, but it is still disputed [23,37,38,40].

Based on current evidence, CNB has been suggested as the next diagnostic method for previously non-diagnostic FNA results [18,19,41,42], previous AUS/FLUS [18,43-45], and clinically suspected rare thyroid malignancies [13,46-49].

## PREPARING PATIENTS FOR CORE NEEDLE BIOPSY

First, informed consent should be obtained and should include the information needed for the CNB procedure and possible complications [14]. The side effects associated with the use of drugs (i.e. bleeding tendency with drugs such as warfarin, heparin, aspirin, or clopidogrel bisulfate) should be evaluated, however, a screening blood test for coagulation is usually unnecessary. The KSThR guideline recommends withdrawal of aspirin and clopidogrel bisulfate for 7–10 days, warfarin for 3–5 days, and heparin for 4–6 hours before CNB [14]. Initiation of aspirin and clopidogrel bisulfate after CNB is recommended from the next day followed by warfarin at night, and heparin 2 hours later [14,50]. Considering the clinical significance of anticoagulant therapy, the withdrawal of anticoagulant should be carefully discussed with the prescribing physician. Warfarin can be transiently changed to shorter-acting heparin [14,50]. Fasting is usually not recommended for CNB in most patients [14].

## PLANNING THE CORE NEEDLE BIOPSY PROCEDURE

Before the procedure, the nodule characteristics, size, location, and vascularity should be evaluated on gray-scale US and color Doppler US. Careful monitoring of vascularity with color Doppler US can minimize bleeding during CNB [14]. The CNB approach

route is decided based on the information obtained from the pre-procedural US. Among the four approach routes available including transisthmic, lateral, longitudinal, and oblique [14], the trans-isthmic approach is considered the most suitable. The nodule size and location are important factors in deciding the size of specimen notch [14,18,39]. To improve the safety and diagnostic accuracy, CNB should be performed by experienced operators under US guidance [14].

## PREPARATION OF CORE BIOPSY EQUIPMENT

Before 2000, large-bore needles (14-gauge) had been used for large-needle biopsy [14,51]. Recent CNB devices are characterized by small bore (usually 18–21 gauge) and spring activation [14,18,51-53].

The KSThR recommends appropriate CNB needle conditions for thyroid nodules [14]. First, a short needle length (less than 10 cm) is recommended since thyroid gland is a superficial organ. Second, needle bore determines the thickness of the specimen. The thinner the needle, the less damage to normal tissue but the lower is the amount of tissue obtained [14]. Some studies report the use of 16–22 gauge needles [18,41,53-55]. Although the use of 18–21 gauge needles is universal for thyroid nodules, 18-gauge needles have been mainly used in Korea [14,18,43,56-58]. Finally, the stylet length or the penetration length can be selected according to the nodule size. Thickness of core needle is another issue. Ahn et al. [59] reported that CNB with an 18-gauge needle is more effective for the diagnosis of thyroid nodules than CNB with a 20-gauge needle. However, there is insufficient evidence supporting the relationship between needle thickness and complication rate or diagnostic accuracy.

CNB needles are composed of two needles, the stylet and the cutting cannula [14,18,52]. The stylet (inner needle) carries an approximately 2-mm-long tip with a sharp slope to penetrate tissue and a specimen notch to hold the sampled tissue. The cutting cannula (outer needle) is the outer component for cutting the tissue [14].

Core biopsy devices are divided into automated and semi-automated types according to the mechanism of action [14]. The automated needle is known as the double-action device because both inner and outer needles are activated by spring action. This type of needle fires the inner needle by the action of a spring that can more easily penetrate hard fibrotic or calcified tissue. However, it may be more prone to tissue or vessel damage. The semi-automated needle is known as a single-action needle because the spring activates only once: the inner needle is manually ad-

vanced, followed by the spring-activated outer cutting needle. The semi-automated needle is relatively safe, since operators manually push the inner needle into the tissue [14]. The amount of tissue obtained depends on the needle thickness and the length of the specimen notch [35,60].

## SAMPLING TECHNIQUES FOR CORE NEEDLE BIOPSY

Two options for needle guidance are available during US-guided CNB: a free-hand and a needle device under US guidance [29]. The KSThR Guideline recommends the free-hand technique (especially for experts) because it allows greater freedom for the operators in selecting the puncture point and adjusting the route during the procedure [14].

Patients lie down in a supine position under local anesthesia along the approach route. After vessel mapping using color Doppler US, a snapping wrist movement is favored for rapid and effective needle passage through the skin and thyroid capsule [14]. The entire length of the needle must be monitored during the procedure. Complete vessel mapping along the approach route (from the skin to the nodule) is crucial to avoid vessel injury and ensure safety of the procedure [14].

The number of core specimens is debatable. Hahn et al. [61] suggested at least two core specimens including a nodular tissue and a capsule for nodules with previous inconclusive cytology. The length of the core specimen is also important in that a large length decreases the biopsy number [38,62]. Suh et al. [38] performed less than two core biopsies; however, inconclusive results were not high in their factor analysis. Multiple biopsies can trigger further complications, which should be considered during CNB procedures [38].

Most importantly, the entire length of the needle and needle tip should be ensured during the CNB procedure [14,63]. The needle tip must be within thyroid capsule without large vessels along the imagined firing route. Further, the stylet can be fired followed by the cutting cannula (Fig. 1). When a successful method is used, the location of the specimen notch can be adjusted after stylet firing to select the most appropriate sampling site. Many studies suggest that the nodule tissue, nodule-parenchyma border (and/or visible capsule), and normal thyroid parenchyma should be obtained [14,54,60,64,65]. Nodules found in a dangerous location should be carefully evaluated. A single-action needle is safer because it enables fine adjustment of the specimen notch [14].

Occasionally, thyroid nodules exhibit severe fibrosis and/or

hard calcifications. To successfully obtain samples from such hard nodules, using a double-action core needle is useful [14,66-69]. A guiding (coaxial) needle is useful for multiple CNB. In this technique, the biopsy needle is inserted through the lumen of the guiding needle, which is located from the skin close to the nodule surface. After CNB, the tissue sample can be visually assessed to determine if additional CNB is required [14,18,39,42,66]. After visual assessment, the harvested tissue should be immediately fixed in formalin. One to two biopsies are adequate for histological diagnosis. Manual compression should be performed immediately after the biopsy for 20 to 30 minutes [14].

## BIOPSY-RELATED COMPLICATIONS

The KSThR or NCI guidelines suggest that CNB is safe, well-tolerated, and associated with a low incidence of complications when performed by experienced operators [14,18,32,41]. The reported complication rate is up to 4.1%, with the major complication rate up to 1.9% [16,43,53,55,58,70]. Various CNB complications were reported [14], including hematoma [18,39,41,53,70], voice change [43,55], infection [70,71], hemoptysis [41], edema [18,39,42], vasovagal reaction [70], and dysphagia [70]. A large single-center study (6,687 thyroid nodules of 6,169 patients) reported few major and minor complications (4/6,169 [0.06%] and 49/6,169 [0.79%], respectively) and no procedure-related death or sequelae [15]. A systematic review showed that the major complications including permanent voice changes, hematomas requiring hospital admission and a pseudoaneurysm, and minor complications were reported in six (0.04%) and 175 (1.18%) out of a total of 14,818 patients in 39 thyroid CNB studies from January 1994 to December 2016, respectively [17].

To avoid complications, CNB should be performed by an expert [14] with knowledge of anatomy, anatomic variations, and potential complications [72].

CNB is generally associated with pain and discomfort. US-guidance and the use of 18–21 gauge thin needles (commonly 18-gauge) can reduce the level of pain and the rate of complications [14]. Several studies compared FNA and CNB in terms of pain and tolerability and concluded that they were similar in both procedures [73-75]. A recent study reported that the overall satisfaction scores at 2 weeks after the procedure did not differ significantly between patients who underwent FNA and CNB [75].

Hematoma induced by vascular injury is the most common complication in thyroid CNB with a reported incidence of up to 3.9% [14,15,76], which is similar to that of FNA (1%–6.4%) [77]. Parenchymal edema induced by small vessel injury is fre-

quently associated with hematoma and pain [18,39,42,66]. These vascular injuries are mostly managed with simple compression without the need for medication in most cases [14,18,39]. A few cases of hematoma have been reported after CNB as a major

complication [53,78]. To prevent these complications, manual compression should be performed immediately after the biopsy for 20 to 30 minutes to prevent the risk of delayed hematoma [18,42].

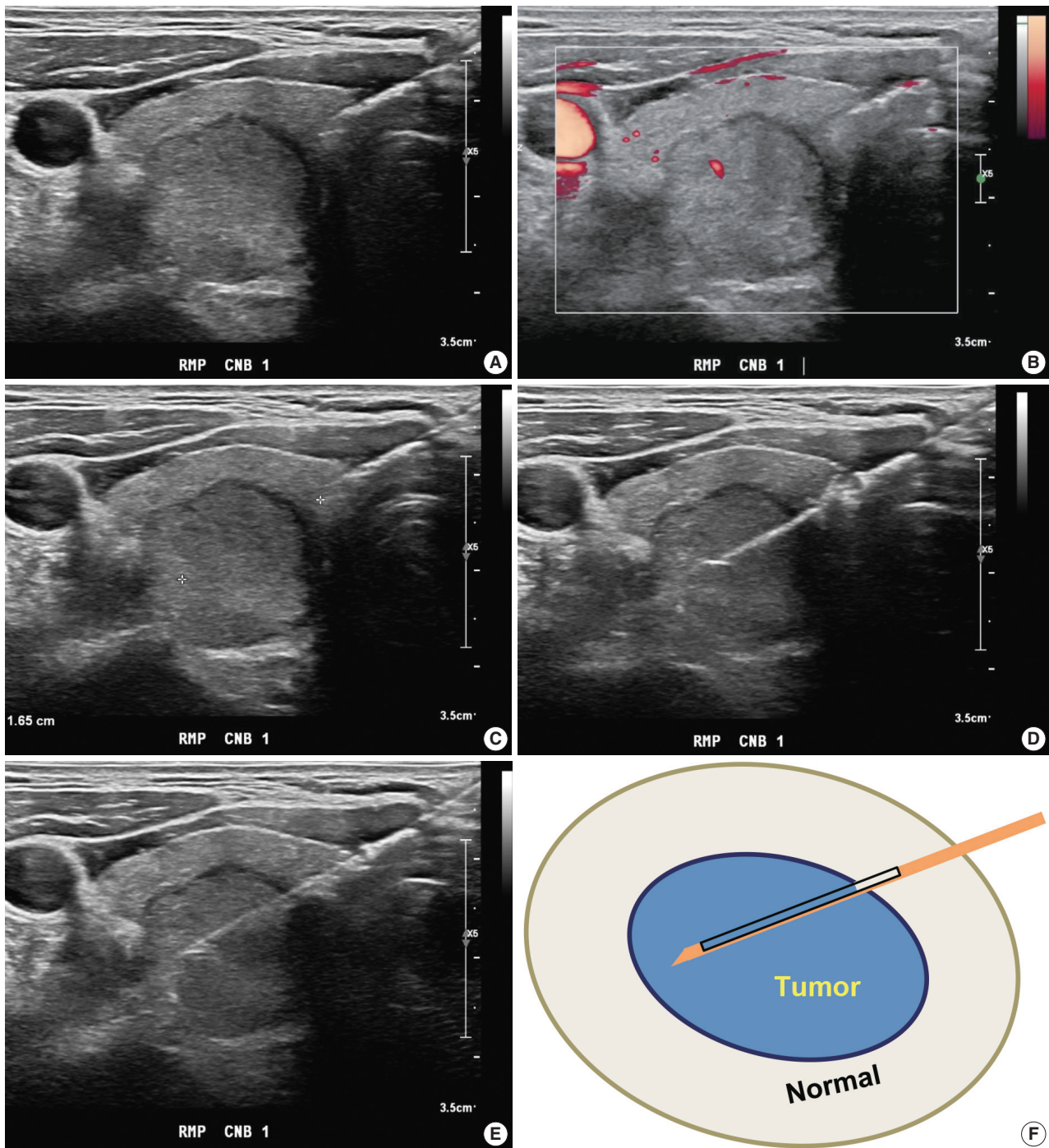


**Fig. 1.** Core needle biopsy of right thyroid nodule. (A) Core needle approach is made through isthmus. (B) Vessels are evaluated with Doppler ultrasound advanced along the direction of the needle. (C) Measurement of distance of fire. (D, E) Firing the stylet first followed by cutting cannula. (F) Schematic illustration of core needle biopsy showing the biopsy site. A cylindrical core of tissue includes tumor and adjacent non-tumor tissue.

Voice change, caused by direct injury or indirect injury due to bleeding or edema to the recurrent laryngeal nerve, is a rare but serious complication after thyroid CNB [37]. A systematic review showed that the overall incidence of permanent and transient voice change after thyroid CNB was 0.0013% (2/14,818) and 0.034% (5/14,818), respectively [17]. The highest incidence (1.9%, 1/54) of voice change was observed in a small study [43]. Recurrent laryngeal nerve palsy associated with hemorrhage/edema is usually transient [14,79]. A trans-isthmic approach under US monitoring is important to prevent direct injury to the recurrent laryngeal nerve [14,72]. A lateral-to-medial approach is dangerous to trachea, esophagus or recurrent laryngeal nerve [16].

Abscess formation is a very rare complication after CNB due to the rich vascular supply and lymphatic drainage, and high iodine content in the thyroid [14,71]. Therefore, the application of prophylactic antibiotics is not recommended before or after CNB.

In the case of a nodule located at the posteromedial margin of the thyroid, CNB is indicated after excluding a pharyngo-esophageal or esophageal diverticulum [14,72,80]. Direct injury to the trachea induces cough or hemoptysis [41]. Tinnitus, a rare complication, has been attributed to injury of the perithyroidal vertebral artery and vein followed by an arteriovenous fistula [81]. Tumor seeding after CNB has not been reported but is a possible rare complication [82]. For safe and effective CNB procedure, operators should be familiar with the broad spectrum of complications and preventive methods [14].

## **PATHOLOGY REQUEST FORM**

The request form for CNB should include the following information: identification of the patient sample: patient's name, date of birth, unit number or medical record number; name of the requesting clinician and the clinician who performed the procedure; side and site of the lesion; number of biopsy cores; US imaging findings; and relevant clinical history.

## **PREPARATION AND PROCESSING OF CORE NEEDLE BIOPSY SPECIMENS**

Proper tissue processing and histological staining procedures are essential for subsequent pathologic diagnosis. Biopsy specimens are fragile and should be handled with caution. As soon as the biopsy tissues are removed from the thyroid gland, biopsy cores should be wrapped in saline- or fixative-moistened gauze or filter paper to prevent specimen loss and tissue folding, and rap-

idly fixed with 10% neutral buffered formalin (NBF) (which is equivalent to 4% formaldehyde) to inhibit autolysis and putrefaction. Squeezing of biopsy specimen must be avoided to prevent cell rupture and loss of cell identity when examined microscopically. If a fixative cannot be added in a timely manner, the specimen should be wrapped in a moist saline gauze and refrigerated until the specimen is treated with an appropriate fixative. The ratio of formalin solution to tissue should be at least 10:1 with 10 mL of the fixative for every gram of tissue [83,84]. In clinical practice, the adequate volume of 10% NBF should be 15–20 times the specimen volume. The fixation time depends on sample size. Adequate fixation time with 10% NBF usually requires a minimum of 5 hours of exposure for small biopsy specimen [84]. However, practices may vary between laboratories. Incomplete or poor tissue fixation can lead to poor and unsatisfactory results. All specimens must be placed in a leak-proof container.

Sections obtained from formalin-fixed paraffin-embedded tissue blocks can be used for routine hematoxylin and eosin staining or ancillary tests such as special stain, immunohistochemistry, and molecular tests.

## **PATHOLOGY REPORTING FOR THYROID CORE NEEDLE BIOPSY**

The first edition of 'Pathology Reporting of Thyroid Core Needle Biopsy' published in 2015 by the Korean Endocrine Pathology CNB Study Group has been widely used by Korean pathologists [28]. A recent study performed in China showed that the pathology reporting system of thyroid CNB is objective, operable and valuable for the pathologic diagnosis of thyroid nodules clinically [85].

The thyroid CNB pathology must be correlated with clinical and US imaging findings. The biopsy results should be reviewed in conjunction with matching surgical pathology after surgery.

A categorical reporting system for CNB ensures effective communication between pathologists and clinicians, with less likelihood of misinterpretation of pathology results. The six original general categories have been retained in the 2019 revision.

To communicate with clarity, the pathology report of thyroid CNB begins with a general diagnostic category. The six general diagnostic categories are shown in Table 1. Subcategorization is often informative especially in diagnostic categories III and IV. A brief microscopic description of the biopsy specimen can be informative, but should not be used alone to report the diagnosis. The standardized terms for the diagnostic categories should be

**Table 1.** Diagnostic categories of thyroid core needle biopsy

---

I. Nondiagnostic or unsatisfactory
Non-tumor adjacent thyroid tissue only
Extrathyroid tissue only (e.g., skeletal muscle, mature adipose tissue)
Acellular specimen (e.g., acellular fibrotic tissue, acellular hyalinized tissue, cystic fluid only)
Blood clot only
Other
II. Benign lesion
Benign follicular nodule
Hashimoto's thyroiditis
Subacute granulomatous thyroiditis
Nonthyroidal lesion (e.g., parathyroid lesions, benign neurogenic tumors, benign lymph node)
Other
III. Indeterminate lesion
IIIa. Indeterminate follicular lesion with nuclear atypia
IIIb. Indeterminate follicular lesion with architectural atypia
IIIc. Indeterminate follicular lesion with nuclear and architectural atypia
IIId. Indeterminate follicular lesion with Hürthle cell changes
IIIe. Indeterminate lesion, not otherwise specified
IV. Follicular neoplasm
IVa. Follicular neoplasm, conventional type
IVb. Follicular neoplasm with nuclear atypia
IVc. Hürthle cell neoplasm
IVd. Follicular neoplasm, not otherwise specified
V. Suspicious for malignancy
Suspicious for papillary thyroid carcinoma, medullary thyroid carcinoma, poorly differentiated thyroid carcinoma, metastatic carcinoma, lymphoma, etc.
VI. Malignant
Papillary thyroid carcinoma, poorly differentiated thyroid carcinoma, anaplastic thyroid carcinoma, medullary thyroid carcinoma, lymphoma, metastatic carcinoma, etc
Comments:
1. The core needle biopsy provides an accurate diagnosis in most cases; however, it may miss some cancers or sometimes may be inconclusive.
2. Definitive therapeutic surgery (i.e., a total thyroidectomy) should not be undertaken as a result of a category III, IV, or V core needle biopsy diagnosis.
3. The management of a thyroid lesion must be based on a multidisciplinary approach.
4. In the category IIIc or IVb, some nuclear features raise the possibility of a noninvasive follicular thyroid neoplasm with papillary-like nuclear features or an invasive follicular variant of papillary thyroid carcinoma; definitive distinction among these entities is not possible on biopsy material.

---

used. The numerical code alone should not be used without the term of diagnostic category. The risk of malignancy and recommendations associated with each general category are not required but can be provided based on their own CNB-histology correlation or published studies.

### I. Non-diagnostic or unsatisfactory

This category is used when the volume of biopsy specimen and the number of follicular cells is inadequate or unsatisfactory to obtain appropriate diagnosis or when the specimen is not representative of US imaging findings of the lesion. The adequacy of the specimen may depend on the inherent nature of the thyroid lesion as well as the experience and technique of the technician conducting the biopsy. This diagnosis is subjective as there is no consensus on the minimum number or amount of follicular components required for satisfactory biopsy specimen. Therefore, the report should explain why the sample is non-diagnostic or unsatisfactory. For example, the sample may be non-tumor tissue adjacent to thyroid (Fig. 2A), extrathyroid tissue alone (e.g., skeletal muscle and mature adipose tissues) as shown in Fig.

2B, an acellular specimen (Fig. 2C, D), or a blood clot. It may show other non-diagnostic or unsatisfactory findings. However, any CNB specimen containing atypical cells should not be considered non-diagnostic or unsatisfactory.

Non-tumor adjacent thyroid tissue or extrathyroid tissue only implies that the thyroid lesion has not been sampled. For some benign follicular lesions with normofollicular structures (Fig. 2A), it may be difficult to assess specimen adequacy because follicular cells of the thyroid nodule show similar histological features with the adjacent thyroid tissue. It is important to determine the transition between the follicular lesion and the surrounding normal parenchyma and compare the pathologic findings with its US imaging results.

### II. Benign

This category includes all benign thyroidal and nonthyroidal diseases. A CNB specimen can be classified, based on the specific lesion diagnosis, under the benign category. For example, the sample may be a benign follicular nodule, Hashimoto's thyroiditis, subacute granulomatous thyroiditis, a nonthyroidal lesion

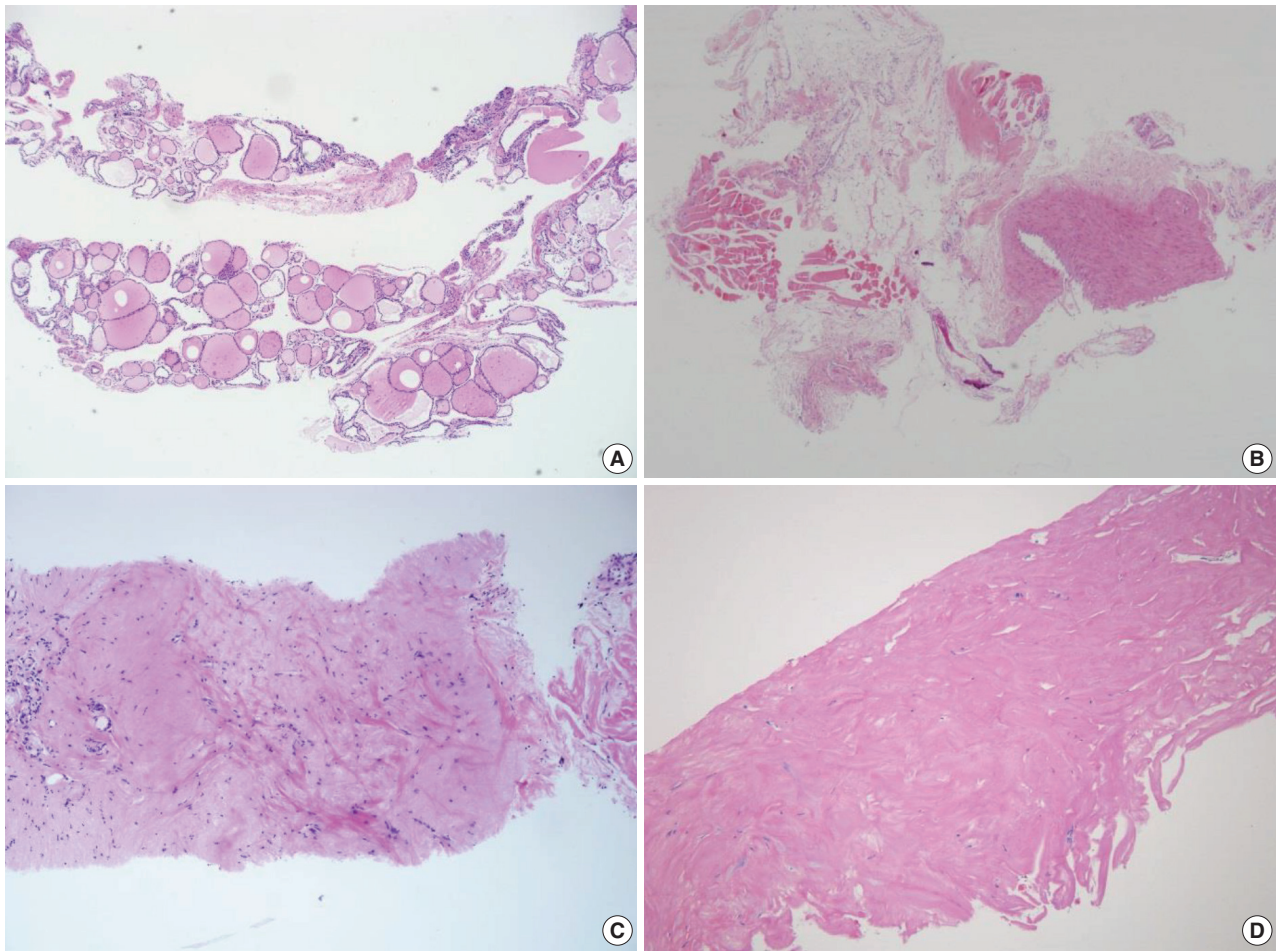


**Fig. 2.** Examples of non-diagnostic specimens (category I) in thyroid core needle biopsy. The examples include non-tumor adjacent thyroid tissue only (A), extrathyroidal soft tissue only (B), and acellular sclerotic nodules (C, D).

(e.g., a parathyroid lesion, benign neurogenic tumors, benign lymph node), or other benign lesions.

A benign follicular nodule encompasses nodular hyperplasia (adenomatoid nodule), colloid nodule, a nodule associated with Graves' disease, nodular Hashimoto's thyroiditis, and a subset of follicular adenoma. CNB specimens of these lesions show a benign-appearing normofollicular or macrofollicular structure and do not contain a well-defined fibrous capsule (Fig. 3A, B).

Most degenerating nodules are benign but they often show suspicious US findings and non-diagnostic or indeterminate cytologic results [69]. CNB of degenerating nodule according to the progression stage shows hemorrhagic materials in early phase, stromal fibrosis, and hyalinization infiltrated with chronic inflammatory cells after regression of hemorrhage in the middle phase, and paucicellular densely hyalinized stroma in late phase [69]. In a CNB specimen of degenerating nodule, the lesion can be diagnosed as a benign degenerating nodule if there are no atypical

cells in the fibrous hyalinized and/or hemorrhagic background with scarce follicular cells (Fig. 3C, D) [69]. The atypia status can be determined by comparing the histologic features of follicular cells in both the central and peripheral regions included in the CNB specimen. Benign Hürthle cell lesions often occur in patients with Hashimoto's thyroiditis and may resemble their neoplastic counterparts. The presence of lymphoid aggregates within the Hürthle cell lesion favors a diagnosis of benign (category II) over indeterminate Hürthle cell lesion (category III) or Hürthle cell neoplasm (category IVc) (Fig. 3E, F).

### III. Indeterminate lesion

Cytological atypia and histological growth patterns in this category are of uncertain significance and insufficient to be classified under other diagnostic categories. The diagnostic category III "indeterminate lesion" corresponds to "AUS" or "FLUS" in TBSRTC. Most Korean pathologists prefer the term "indeter-

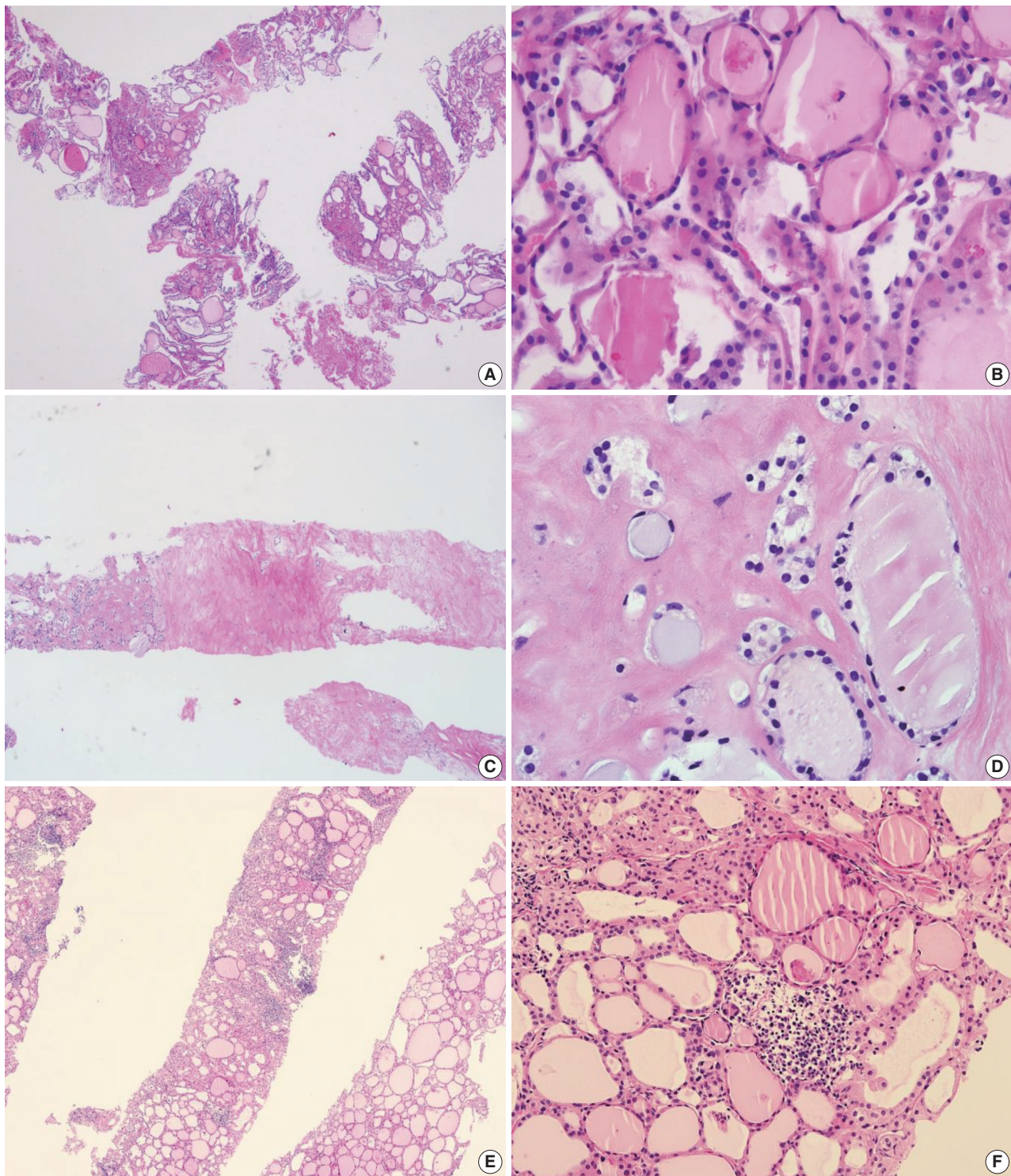


**Fig. 3.** Examples of benign nodules (category II) in thyroid core needle biopsy. (A) The biopsy specimen shows follicular proliferative lesion without a distinct tumor capsule. (B) The high-power view of Fig. 3A shows benign-appearing follicular cells. This lesion can be interpreted as a benign follicular nodule. (C) The specimen is densely hyalinized and paucicellular. (D) The high-power view of Fig. 3C reveals benign-appearing follicular cells in the hyalinized stroma, suggesting a benign follicular nodule. (E) The specimen shows a Hürthle cell proliferative lesion. (F) The high-power view of Fig. 3E reveals Hürthle cell proliferation and lymphoid aggregates. This lesion should be interpreted as a benign Hürthle cell proliferative lesion rather than Hürthle cell neoplasm.

minate lesion” for category III in the histopathological diagnosis of CNB specimens while some pathologists prefer the term “AUS” [28,65]. Regardless of the terminology used, it is important for the pathologists to use only a single term, either indeterminate lesion, AUS, or FLUS.

The diagnosis of category III is appropriate when a follicular proliferative lesion shows focal nuclear atypia such as nuclear enlargement with pale chromatin, irregular nuclear membrane, and nuclear grooves in a background of predominantly benign-appearing follicles. A microfollicular proliferative lesion separated by a fibrous capsule from the surrounding normal parenchyma suggests a diagnosis of follicular neoplasm (see category IV). If a fibrous capsule or adjacent nonlesional tissue is not identified in a CNB specimen that shows a predominantly microfollicular or trabecular growth pattern, it is reasonable to classify the lesion under diagnostic category III because it is uncertain whether the nodule has a fibrous capsule. A multidisciplinary approach to a thyroid nodule can improve the preoperative diagnostic accuracy of FNA and CNB specimens [9]. Macrofollicular lesions are usually diagnosed as benign on FNA specimens. When US images show a dominant solitary nodule and the CNB specimen microscopically reveals a follicular proliferative lesion with a definite fibrous capsule, then the CNB specimen is diagnosed under category IV “follicular neoplasm,” even in case of a macrofollicular lesion.

Category III should be subclassified according to nuclear atypia, histologic growth patterns, cell type, and other histological features because the subclassification suggests different histological features and a risk of malignancy in the thyroid nodules [65]. A subcategory of nuclear atypia indicates that papillary thyroid carcinoma must be ruled out whereas architectural atypia cannot exclude follicular neoplasm. The following common scenarios may be encountered in case of follicular proliferative lesions.

#### *IIIa. Indeterminate follicular lesion with nuclear atypia*

Examples in this category include follicular proliferative lesions with focal nuclear atypia (Fig. 4A, B), follicular proliferative lesions with equivocal or questionable nuclear atypia, and atypical follicular cells embedded in a fibrotic or hyalinized stroma. This subcategory increases the risk of papillary carcinoma; however, the diagnosis does not reveal the characteristic histological features.

#### *IIIb. Indeterminate follicular lesion with architectural atypia*

Examples in this category include microfollicular proliferative

lesions lacking a fibrous capsule or the adjacent nontumor tissue in the specimen; solid or trabecular follicular lesions lacking a fibrous capsule or adjacent nontumor tissue in the specimen (Fig. 4C, D). This subcategory exhibits no nuclear atypia. Some pathologists prefer category III “indeterminate follicular lesion” for a macrofollicular proliferative lesion with a definite fibrous capsule because a macrofollicular pattern is a characteristic of benign thyroid diseases.

#### *IIIc. Indeterminate follicular lesion with nuclear and architectural atypia*

In this category, follicular proliferative lesions show both nuclear and architectural atypia, but lack a fibrous capsule or the adjacent nontumor tissue in the specimen (Fig. 4E, F). Nuclear atypia is mild but lacking typical nuclear features of papillary carcinoma. Architectural atypia suggests microfollicular, solid, or trabecular proliferation. NIFTP is more frequently found in this subcategory [12].

#### *IIId. Indeterminate follicular lesion with Hürthle cell changes*

Follicular proliferative lesion is comprised exclusively of Hürthle cells, but the specimen lacks a fibrous capsule or the adjacent nontumor tissue (Fig. 5A, B). When Hürthle cell lesion is admixed with lymphoid aggregates, the CNB specimen should be diagnosed as benign Hürthle cell proliferative lesion (Fig. 3E, F).

#### *IIIe. Indeterminate lesion, not otherwise specified*

This category includes follicular proliferative lesions with psammoma bodies but lacking nuclear features of papillary carcinoma; rare cases not explicitly described elsewhere in category III. Pseudo-psammomatous calcifications found in follicular lumens occur in Hürthle cell neoplasms and differ from true psammoma bodies found in papillary carcinoma (Fig. 5C, D).

### **IV. Follicular neoplasm**

In CNB and FNA, the term “follicular neoplasm” is used to encompass neoplastic lesions with a follicular proliferative pattern (e.g., cellular nodular hyperplasia, follicular adenoma, NIFTP, follicular carcinoma, follicular variant of papillary carcinoma, follicular variant of medullary carcinoma) [26,86,87]. In TB-SRTC, the terms “follicular neoplasm” and “suspicious for a follicular neoplasm” were equally acceptable but were not intended to separately denote two different interpretations. Only a single terminology is recommended for use in this category. The histological diagnosis of “follicular neoplasm” in a CNB specimen is based on the presence of a fibrous capsule and microscopic fea-

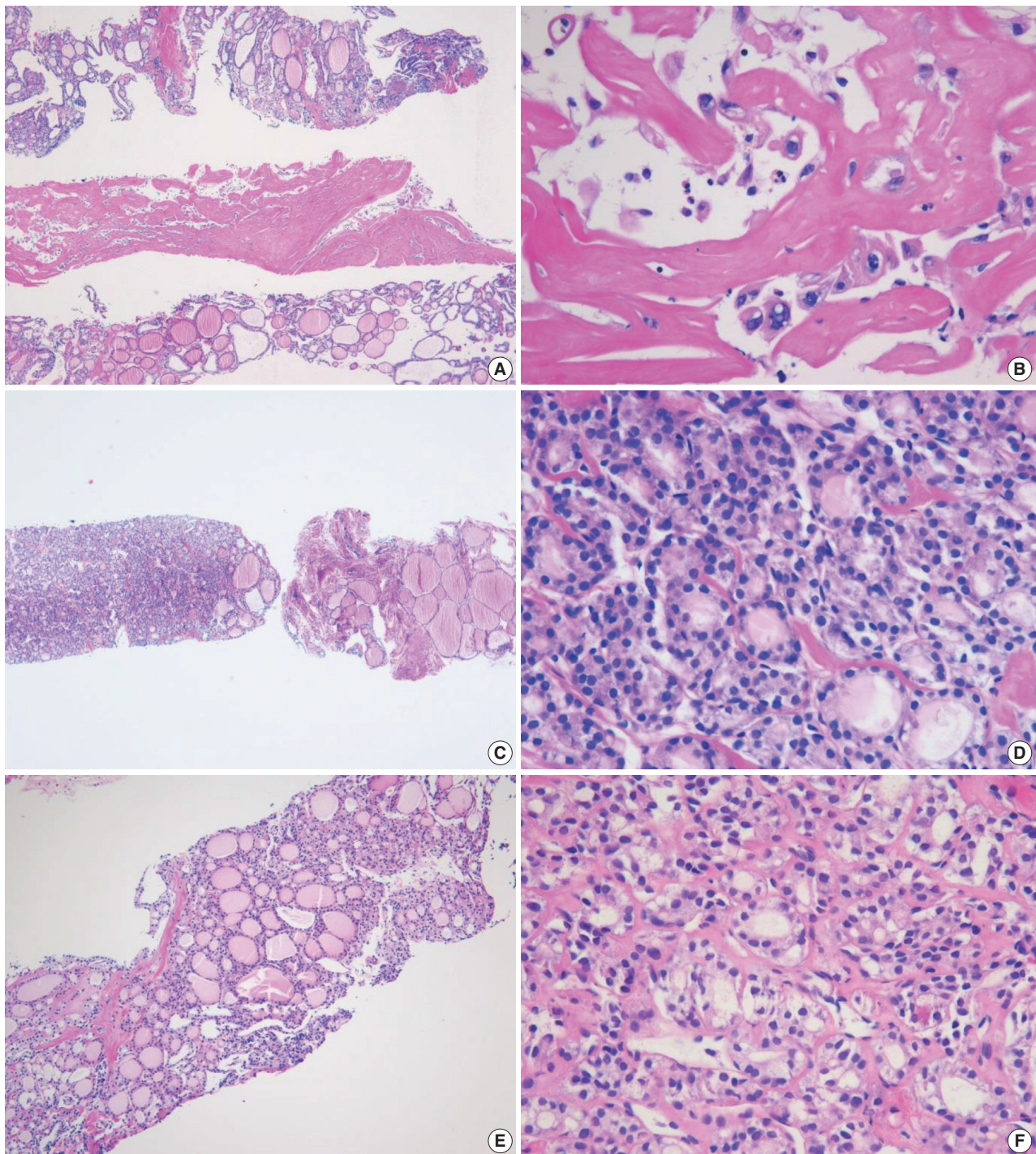


**Fig. 4.** Examples of indeterminate follicular lesion (category III) in thyroid core needle biopsy. (A) The middle one in the three biopsy cores shows densely hyalinized stroma. (B) The high-power view of Fig. 4A reveals atypical cells with nuclear atypia embedded in the hyalinized stroma. This lesion can be interpreted as indeterminate follicular lesion with nuclear atypia (category IIIa). (C) The specimen shows microfollicular proliferation and adjacent thyroid parenchyma. The lesion does not contain a fibrous capsule that is required to establish a diagnosis of follicular neoplasm. (D) The high-power view of Fig. 4C reveals microfollicular growth and absence of nuclear atypia. This lesion can be interpreted as indeterminate follicular lesion with architectural atypia (category IIIb). (E) The specimen shows microfollicular proliferation lacking a fibrous capsule and adjacent thyroid parenchyma in the specimen. (F) The high-power view of Fig. 4E reveals microfollicular growth, thin fibrous bands, and mild nuclear atypia, suggesting indeterminate follicular lesion with nuclear and architectural atypia (category IIIc).

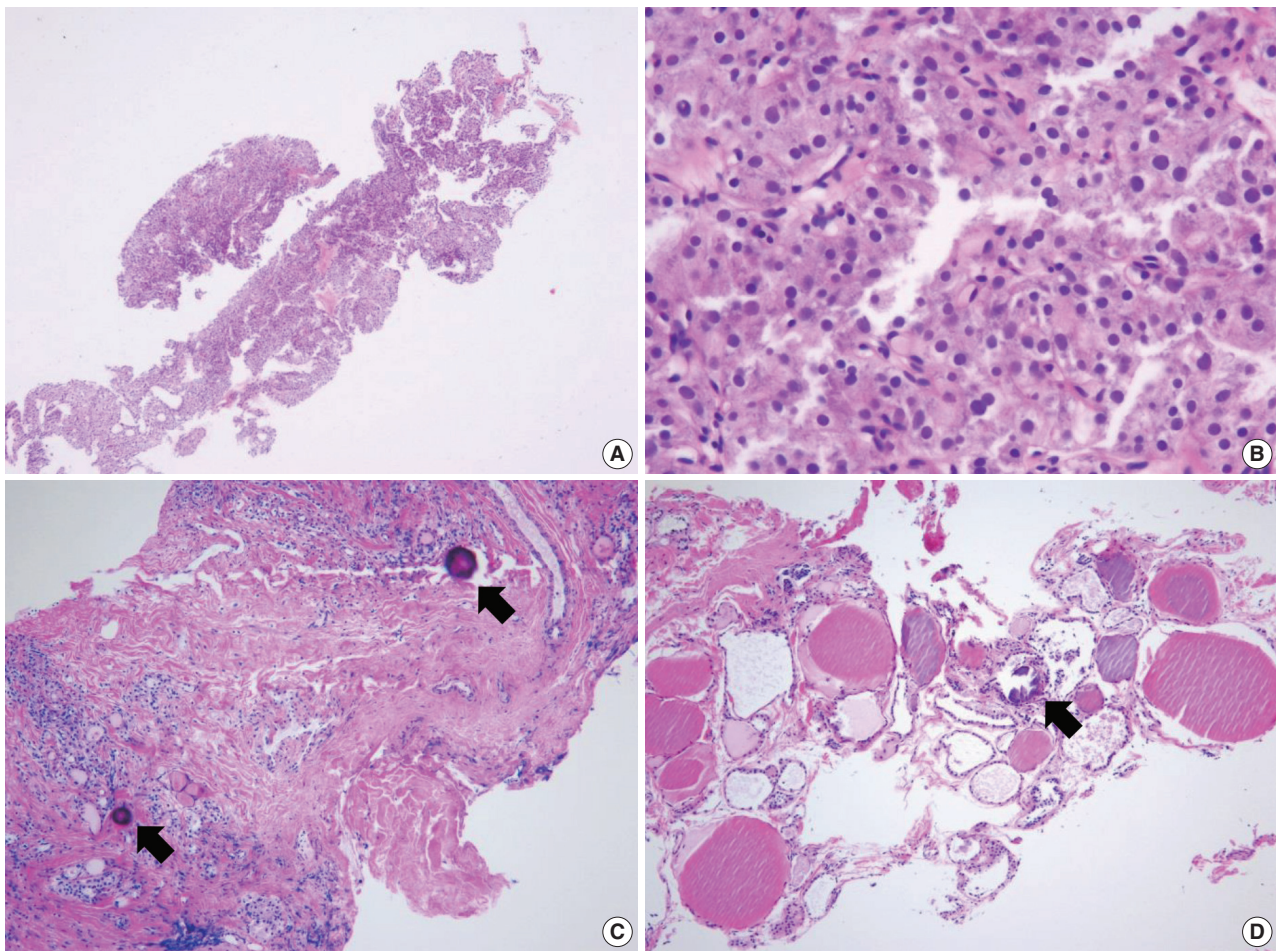


**Fig. 5.** (A) Specimen showing Hürthle cell proliferative lesion lacking a fibrous capsule or adjacent nonlesional thyroid tissue. (B) The high-power view of Fig. 5A reveals trabecular growth of Hürthle cells without nuclear atypia, suggesting indeterminate follicular lesion with Hürthle cell changes (category III<sub>d</sub>). Psammoma bodies (arrow) are found in a background of Hashimoto's thyroiditis (C) and normal thyroid tissue (D). These specimens lack nuclear features of papillary carcinoma and can be interpreted as indeterminate lesion, not otherwise specified (category III<sub>e</sub>).

tures that differ from the adjacent thyroid parenchyma (Fig. 6). In this category, follicular cells do not show typical nuclear features associated with papillary carcinoma. Papillary structure is often seen in hyperfunctioning follicular adenoma and follicular adenoma associated with papillary hyperplasia. The distinction is based on preserved cell polarity and lack of typical nuclear features of papillary carcinoma.

It is important to identify a well-formed fibrous capsule for the diagnosis of follicular neoplasm in the CNB specimen. Fibrous capsule is composed of fibrous connective tissue, which separates tumor cells from the adjacent thyroid tissue. However, it may be difficult to distinguish histologically between fibrous tumor capsule and intralesional fibrous band in small CNB samples (Fig. 7). Correlation between US and pathological findings can be used to differentiate fibrous tumor capsule from intralesional fibrosis. The location of the specimen notch in the US images

represents the contents of tissue sample.

The FNA diagnosis for follicular neoplasm is primarily based on the microfollicular or trabecular architecture and the lack of colloid. In a CNB specimen, the growth patterns of a follicular neoplasm can be microfollicular, normofollicular, solid, or trabecular when the tumor fibrous capsule is identified in the sample. A CNB cannot discriminate between a follicular carcinoma and a follicular adenoma because the diagnosis of these neoplasms requires examination of the entire tumor capsule. Neoplastic follicular and Hürthle cells show architectural and cytologic features that differ from the adjacent nontumor thyroid tissue (Figs. 6–8). Hürthle cell neoplasm is classified under a clinically and genetically distinct tumor category according to the 2017 WHO Classification of Tumors of Endocrine Organs [29]. Thyroid CNB is used as a screening test similar to thyroid FNA for the detection of neoplastic nodule that requires lobectomy for a defini-

tive histological diagnosis of surgical specimens. It is recommended that the category IV should be subclassified into four subgroups according to nuclear atypia, histologic growth patterns,

and cell type. The subclassification reflects differences in histology and the risk of malignancy in the thyroid nodules [88].

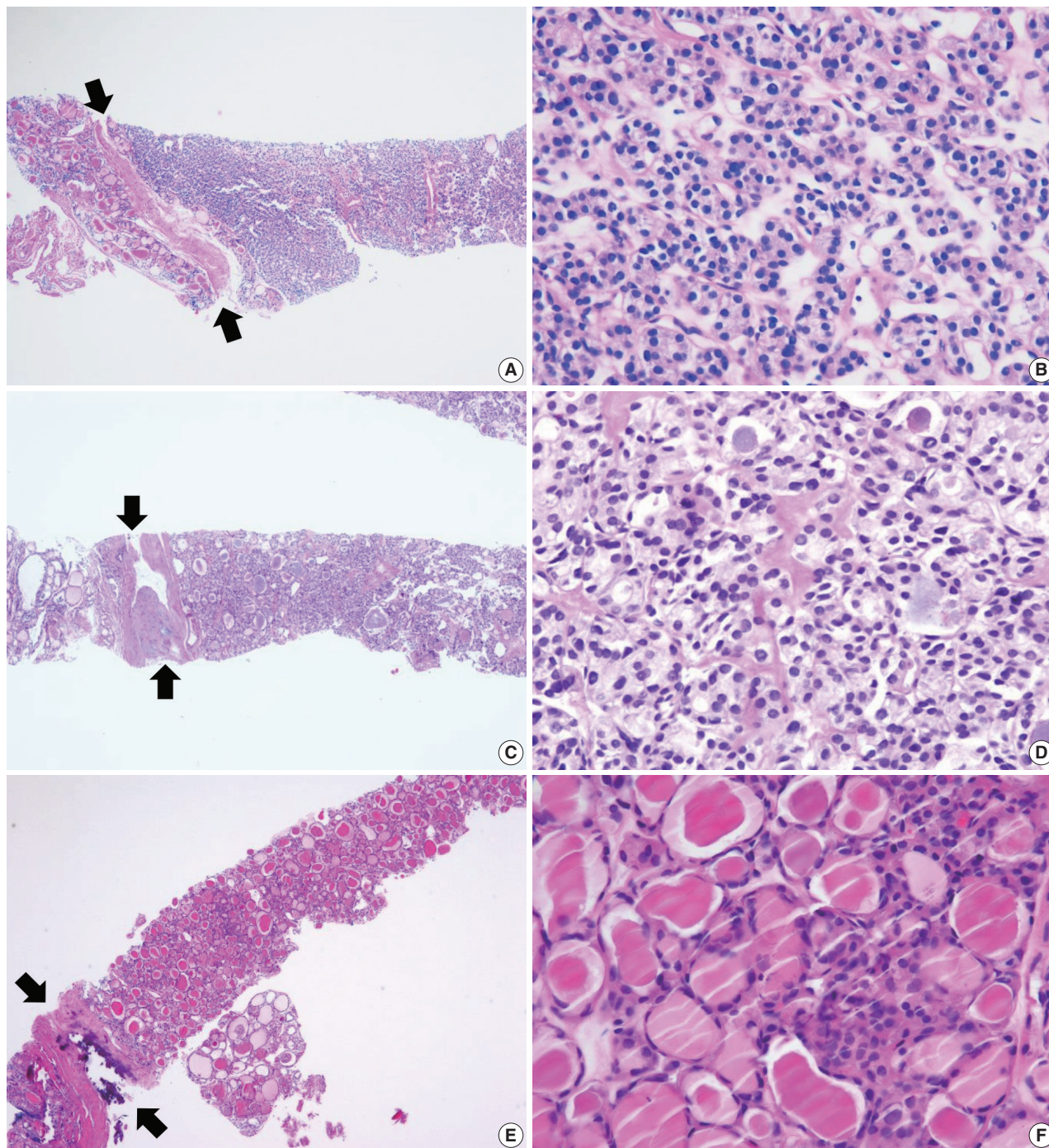


**Fig. 6.** Examples of follicular neoplasm (category IV) in thyroid core needle biopsy. (A) The low-power view shows a follicular proliferative lesion with a fibrous capsule (arrows). (B) The high-power view of Fig. 6A reveals microfollicular growth pattern and no nuclear atypia. This lesion can be interpreted as follicular neoplasm, conventional type (category IVa). (C) The specimen shows a follicular proliferative lesion with a thick fibrous capsule (arrows). (D) The high-power view of Fig. 6B reveals microfollicular growth pattern and follicular cells with nuclear atypia, suggesting follicular neoplasm with nuclear atypia (category IVb). (E, F) Another example of follicular neoplasm with nuclear atypia (category IVb), in which, the lesion shows a fibrous capsule (arrows) nuclear atypia in focal areas (F).

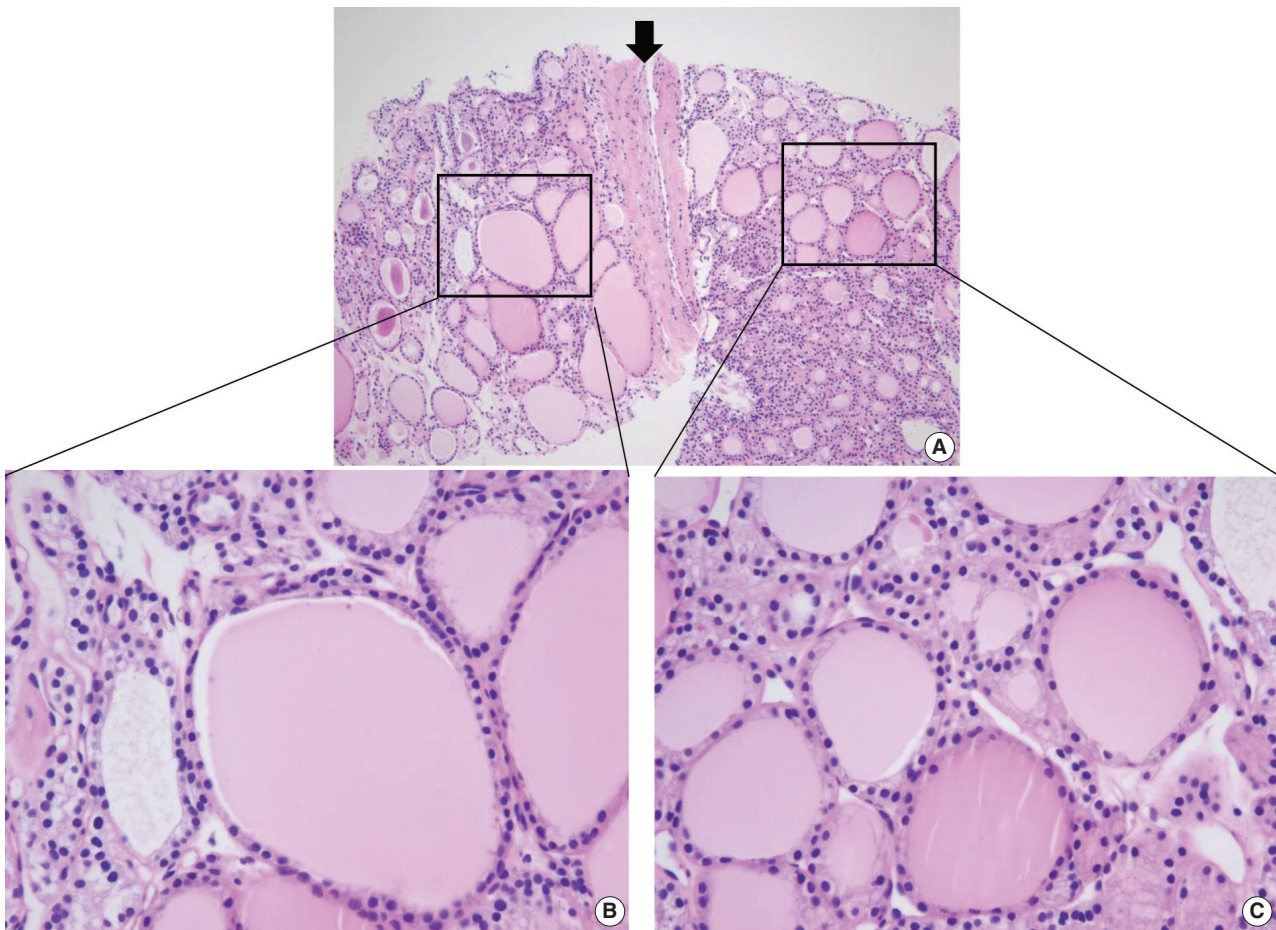


**Fig. 7.** Differential diagnosis of benign follicular nodule with a fibrous capsule (arrow) and follicular neoplasm (A). The specimen is composed of follicular proliferative lesion (right side), fibrous capsule (arrow), and adjacent normal thyroid parenchyma (left side). The morphology of follicular cell population within the nodule (C) is identical to that of the adjacent thyroid parenchyma (B). The specimen should be interpreted as benign follicular nodule based on differences in growth pattern of the follicular neoplasm compared with the surrounding thyroid parenchyma.

#### *Iva. Follicular neoplasm, conventional type*

This category includes the following types of neoplasm: a microfollicular proliferative lesion with a fibrous capsule (Fig. 6A, B); a mixed microfollicular and normofollicular proliferative lesion with a fibrous capsule; a solid or trabecular follicular lesion with a fibrous capsule; a follicular proliferative lesion showing papillary structure and fibrous capsule but lacking nuclear features of papillary carcinoma.

#### *Ivb. Follicular neoplasm with nuclear atypia*

Focal nuclear atypia in follicular neoplasm raises the possibility of NIFTP and follicular variants of papillary carcinoma (Fig. 6C, D) [57,88-90]. Before the NIFPT era, this subcategory frequently turned out to be a follicular variant of papillary carcinoma after surgery [89,90].

#### *Ivc. Hürthle cell neoplasm*

A Hürthle cell proliferative lesion with a fibrous capsule should be diagnosed in this category (Fig. 8). Hürthle cells exhibiting characteristic nuclear features of papillary carcinoma are papillary carcinoma cells, and therefore should not be diagnosed as Hürthle cell neoplasms. Hashimoto's thyroiditis often presents as a solitary nodule or as a dominant thyroid nodule. CNB sampling from a nodule of Hashimoto thyroiditis shows Hürthle cell proliferation in microfollicles, macrofollicles, or trabecula, which may contain a fibrous capsule surrounding the lesion that could be misinterpreted as Hürthle cell neoplasms (Fig. 3E, F). Careful search for lymphocyte and plasma cell infiltration is essential to distinguish such cases from Hürthle cell neoplasm. The Hürthle cell proliferative lesion admixed with lymphocytes and plasma cells should be diagnosed as benign Hürthle cell proliferative lesion rather than Hürthle cell neoplasm or indeterminate follicular

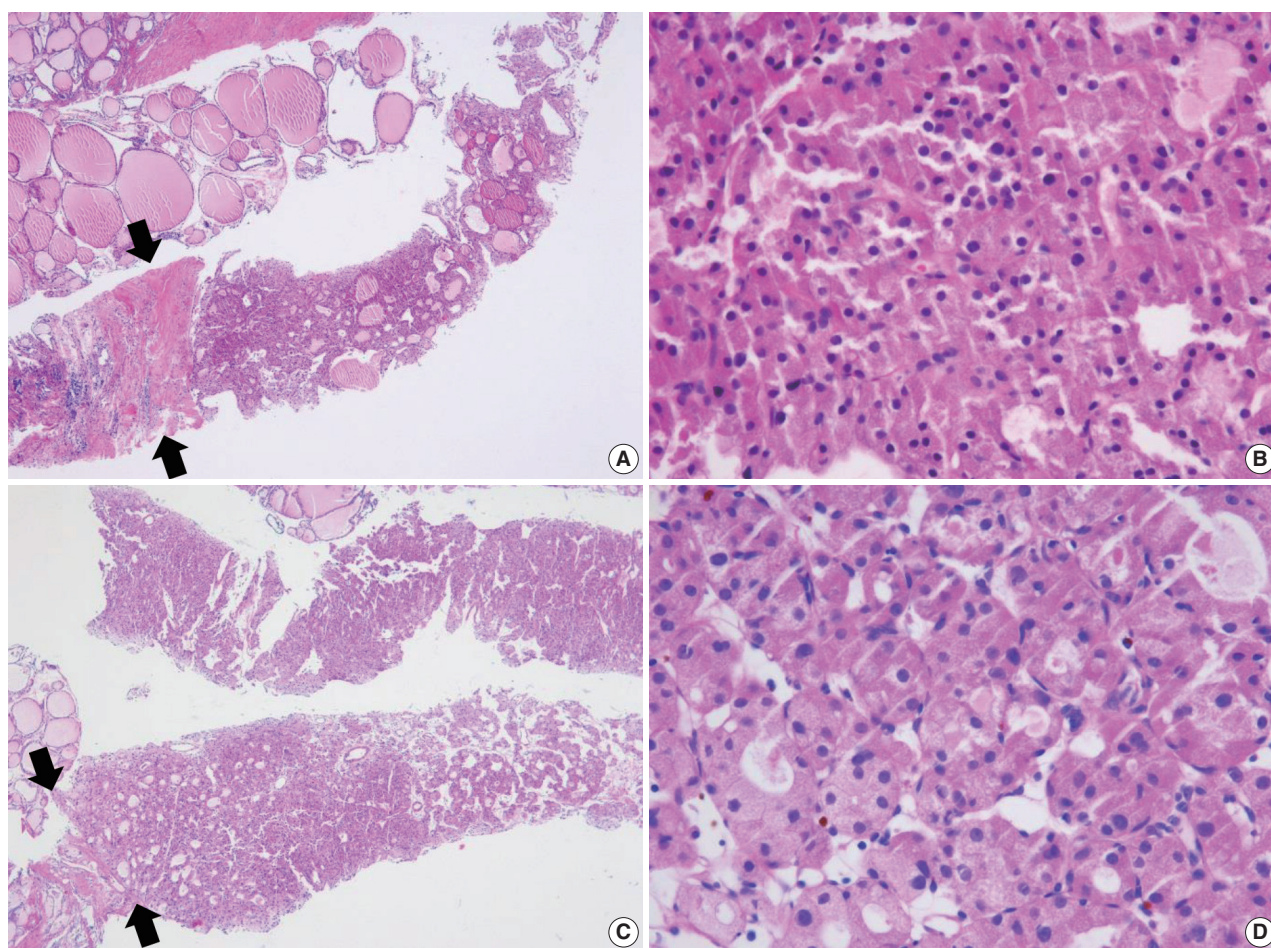


**Fig. 8.** Thyroid core needle biopsy showing Hürthle cell neoplasm (category IVc). The images in the left (A, C) and right (B, D) columns show low-power findings and corresponding high-power views, respectively. The tumor capsule (arrows) can be thick (A) or thin (C).

lesion with Hürthle cell changes.

#### *IVd. Follicular neoplasm, not otherwise specified*

This category includes rare cases not explicitly described elsewhere in category IV.

#### **V. Suspicious for malignancy**

The diagnosis of “suspicious for malignancy” is established when histological features are strongly suspicious for malignancy but are insufficient or equivocal for a definitive diagnosis of malignancy. In this category, a lesion may be suspicious for papillary thyroid carcinoma (Fig. 9), medullary thyroid carcinoma, poorly differentiated thyroid carcinoma, metastatic carcinoma, lymphoma, or show other suspicious findings. The diagnostic uncertainty in this category is generally caused by suboptimal sampling or low cellularity.

Follicular variants of papillary carcinoma and NIFTP share histologic features of follicular growth and nuclear features of

papillary carcinoma, and cannot be discriminated by FNA alone. The diagnosis of papillary carcinoma by FNA requires either intranuclear pseudoinclusions, papillae, or psammoma bodies. In a CNB specimen, both areas of tumor and nontumor can be histologically evaluated. When a follicular proliferative lesion with nuclear features of papillary carcinoma shows capsular invasion in CNB specimens, the findings should be interpreted as papillary carcinoma. In the absence of capsular invasion, it should be interpreted as follicular neoplasm with nuclear atypia. However, when a fibrous capsule or adjacent nonlesional tissue is not identified in the CNB specimen that shows a predominantly follicular growth pattern and nuclear features of papillary carcinoma, the findings are best interpreted as suspicious for papillary carcinoma.

Ancillary immunohistochemical or molecular studies facilitate the diagnosis of CNB specimens with suspected malignancy. An immunostaining panel consisting of galectin-3, HBME1, cytokeratin 19, or CD56 facilitates the diagnosis of lesions suspi-

cious for papillary thyroid carcinoma (Fig. 9) [91-93]. A combination of at least two immunostaining markers is recommended to improve the diagnostic accuracy [92]. The *BRAF* V600E

mutations detected via molecular test or immunohistochemistry for BRAF VE1 antibody strongly suggest a diagnosis of papillary carcinoma (Fig. 9) [91]. A diagnosis of medullary thyroid carci-

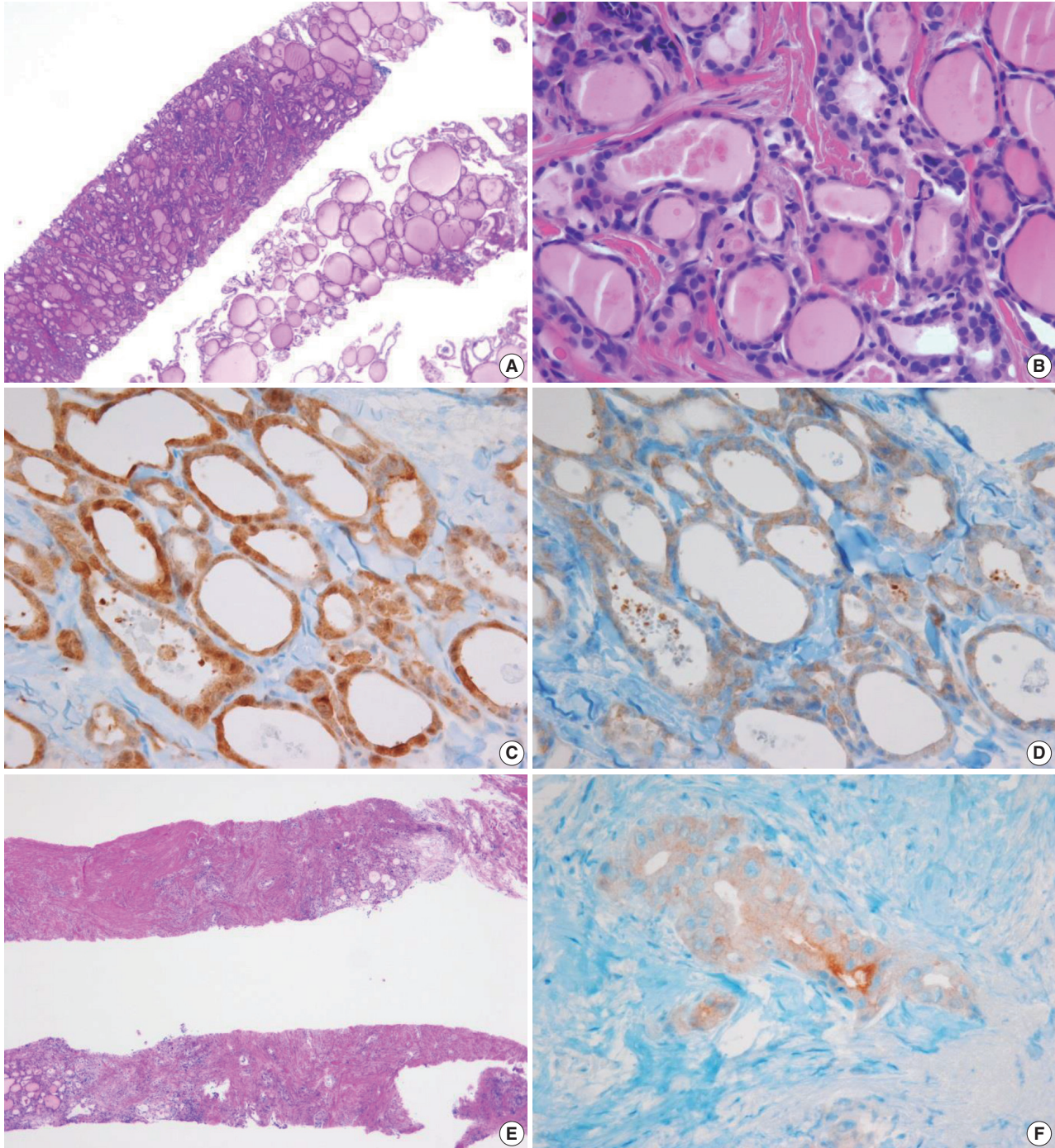


**Fig. 9.** (A) The specimen shows a follicular proliferative lesion with an ill-defined border showing a different morphology compared with adjacent normal thyroid tissue. (B) The high-power view in Fig. 9A reveals atypical follicular cells with nuclear atypia and fibrous bands. These morphological features can be interpreted as suspicious for papillary carcinoma (category V). In this case, immunohistochemical stains for galectin-3 (C) and BRAF VE1 (D, F) facilitate the diagnosis of papillary carcinoma. (E) A paucicellular, hyalinized follicular lesion exhibits morphological features pathognomonic for papillary carcinoma. The diagnosis of the lesion can be established as papillary carcinoma when atypical follicular cells in the specimen are positive for BRAF VE1 immunostaining (F).

noma can be confirmed with positive immunostaining for calcitonin on the CNB specimen. A diagnosis of lymphoma is established using immunophenotyping studies on a CNB specimen that is suspicious for lymphoma [56].

## VI. Malignant

Most thyroid malignancies, except for follicular carcinoma/Hürthle cell carcinoma, exhibit typical histological features and are easily diagnosed as a malignancy on a CNB specimen. The

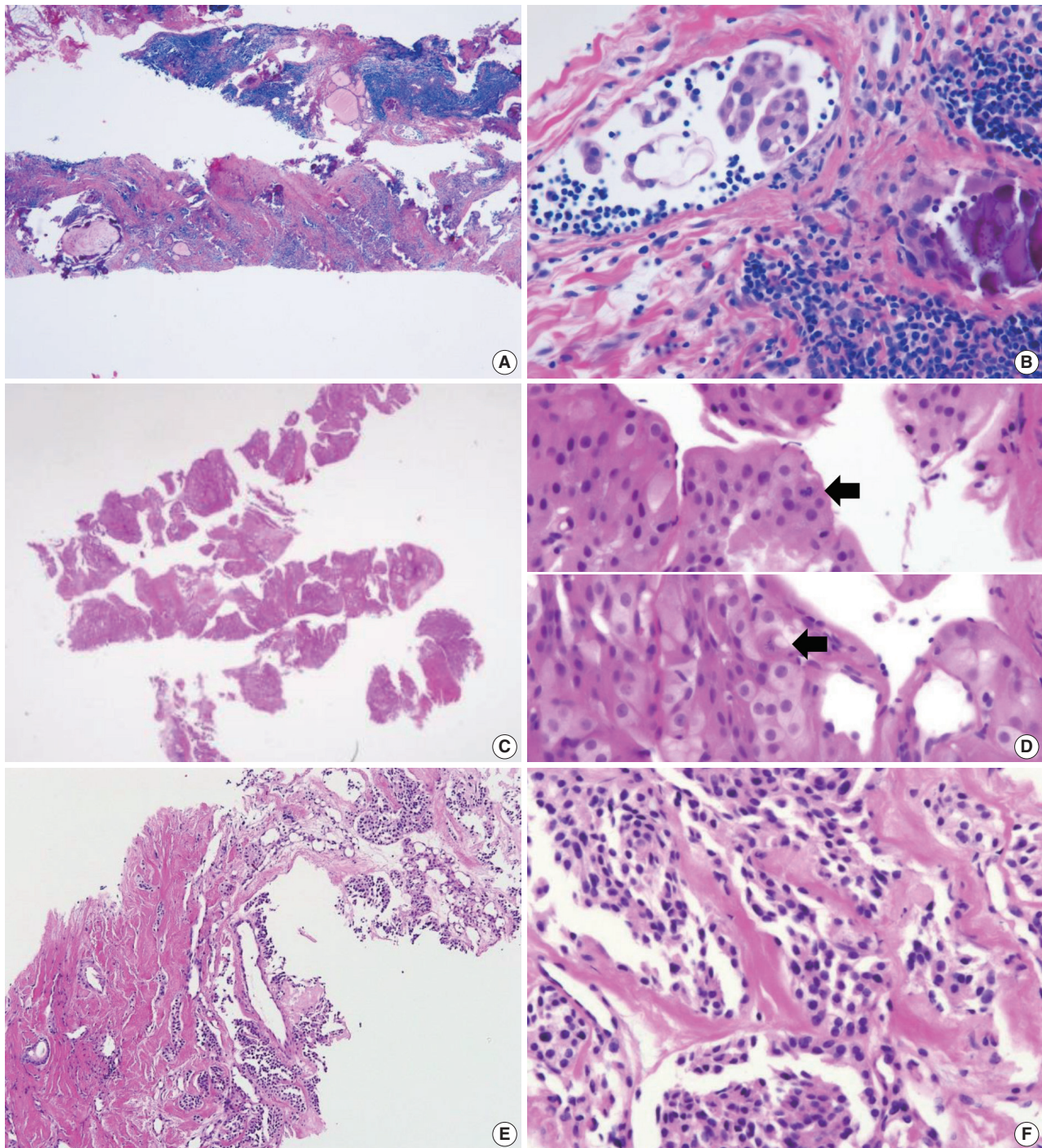


**Fig. 10.** Core needle biopsies of malignant thyroid tumors (category VI). (A, B) Diffuse sclerosing variant of papillary carcinoma. (C, D) Poorly differentiated carcinoma shows solid, trabecular, and insular growth patterns and mitosis (arrows) under high-power field. Medullary carcinoma shows typical histologic features under low-power field (E) and high-power field (F). Nuclei of tumor cells are round to oval and carry coarsely granular chromatin. The cytoplasm is finely granular eosinophilic to amphophilic.

category of thyroid malignancies includes the following diagnoses: papillary thyroid carcinoma (Fig. 10A, B), poorly differentiated carcinoma (Fig. 10C, D), medullary thyroid carcinoma (Fig. 10E, F), anaplastic thyroid carcinoma (Fig. 11A–C), lymphoma (Fig. 11D–F), and metastatic carcinoma.

### COMMON PITFALLS IN THE INTERPRETATION OF CORE NEEDLE BIOPSY

The follicular cells in a CNB specimen appear smaller and show darker chromatin than is typical in a surgical specimen (Fig.

12A, B). Therefore, the nuclear features of papillary carcinoma are less prominent in a CNB specimen (Fig. 12C, D).

Nuclear artifacts that mimic intranuclear cytoplasmic pseudoinclusions in papillary carcinoma may also be present in benign follicular cells (Fig. 12E). The artifactual vacuoles or bubbles are irregular in shape and appear pale on staining, whereas intranuclear pseudoinclusions in papillary carcinoma are round and sharply delineated by the rim of the nuclear membrane, and exhibit cytoplasmic staining quality (Fig. 12F).

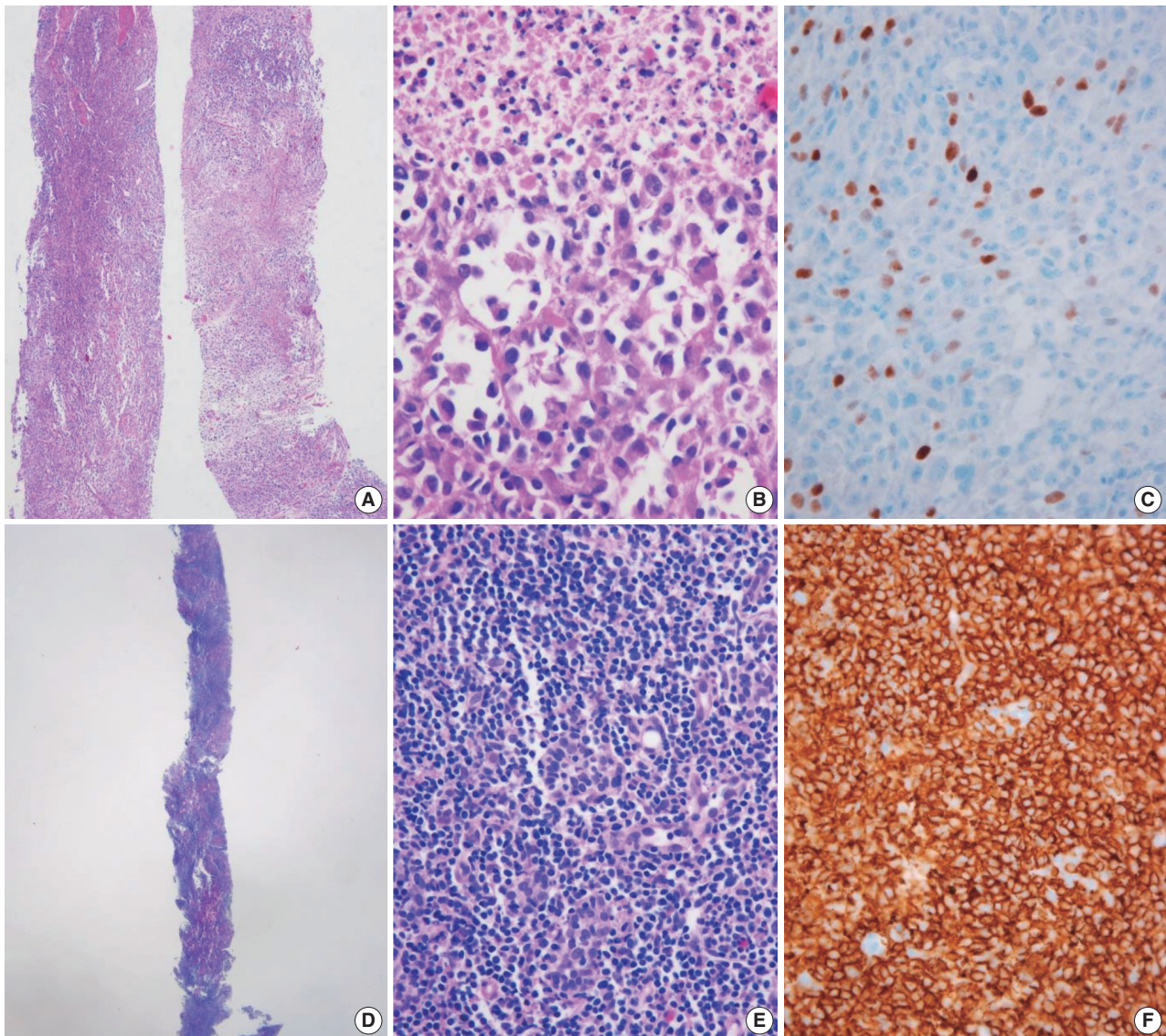


**Fig. 11.** Core needle biopsies of malignant thyroid tumors (category VI). (A) Anaplastic thyroid carcinoma shows diffuse growth infiltration, with no papillary or follicular structure. (B) The tumor cells show marked nuclear pleomorphism and necrosis. (C) PAX8 immunostaining is focally positive in this anaplastic thyroid carcinoma. (D) In extranodal marginal zone lymphoma of mucosa-associated tissue, the lymphoma cells infiltrate follicles and destroy normal parenchyma. (E) Lymphoepithelial lesions are shown. (F) Tumor cells are diffusely positive for CD20.

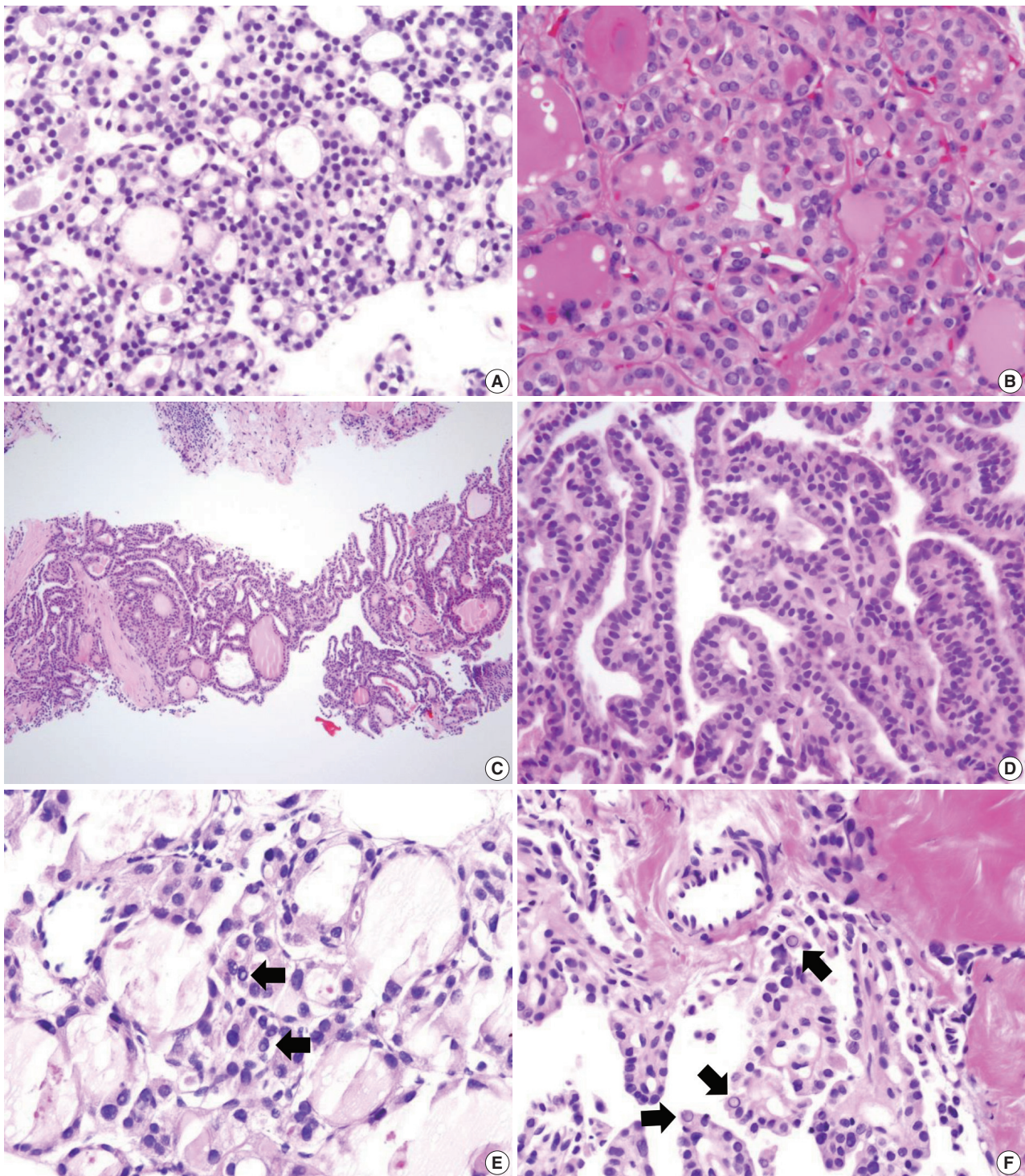


**Fig. 12.** Diagnostic pitfalls in thyroid core needle biopsy. Follicular cells are smaller and darker in core needle biopsy (A) compared with the resected specimen (B) in the same thyroid nodule. (C) The core needle biopsy shows histologic features of papillary carcinoma. (D) The high-power view of Fig. 12C shows nuclear overlapping and crowding. Nuclear chromatin is finely dispersed but nuclear clearance is not as prominent as in papillary carcinoma derived from routine formalin-fixed sections of the resected specimen. (E) Nuclear pseudoinclusion-like nuclear bubbles or vacuoles (arrows) are often seen in the core needle biopsy specimen of benign follicular nodule. These structures show empty appearance and lack a thick nuclear membrane rim. (F) Core needle biopsy of papillary carcinoma shows intranuclear pseudoinclusions (arrows) exhibiting the characteristic cytoplasmic staining and are sharply demarcated by a nuclear membrane.

## CONCLUSION

US-guided CNB represents an alternative procedure to overcome the challenges associated with FNA for the diagnosis of thyroid nodules. The main goal of thyroid CNB is to obtain a large amount of thyroid lesion with minimal morbidity, and to triage patients with thyroid disease who need surgical management. These practical guidelines serve as a clinical guide for successful thyroid CNB and provide a standardized system for pathology reporting of CNB specimens.

## ORCID

Chan Kwon Jung: <https://orcid.org/0000-0001-6843-3708>  
 Jung Hwan Baek: <https://orcid.org/0000-0003-0480-4754>  
 Dong Gyu Na: <https://orcid.org/0000-0001-6422-1652>  
 Young Lyun Oh: <https://orcid.org/0000-0002-9127-4642>  
 Ka Hee Yi: <https://orcid.org/0000-0002-1999-9841>  
 Ho-Cheol Kang: <https://orcid.org/0000-0002-0448-1345>

## Author Contributions

Conceptualization: CKJ, JHB.  
 Data curation: CKJ, JHB, DGN.  
 Formal analysis: CKJ, JHB, DGN.  
 Funding acquisition: CKJ.  
 Investigation: CKJ, JHB, DGN, YLO, HCK.  
 Methodology: CKJ, JHB, DGN, KHY, YLO, HCK.  
 Project administration: CKJ.  
 Resources: CKJ, JHB, DGN, KHY, YLO, HCK.  
 Supervision: CKJ, JHB.  
 Validation: CKJ, JHB, DGN, KHY, YLO, HCK.  
 Visualization: CKJ, JHB, DGN, KHY, YLO, HCK.  
 Writing—original draft: CKJ, JHB, DGN.  
 Writing—review & editing: CKJ, JHB, DGN, KHY, YLO, HCK.

## Conflicts of Interest

C.K.J. is the editor-in-chief of *Journal of Pathology and Translational Medicine*. He serves on the Board of Directors of the KTA and the Korean Society of Pathologists. J.H.B. is the president of the KSThR. D.G.N. serves on the KTA and KSThR Board of Directors. K.H.Y. served as a Director General of the KTA Board of Directors during 2017–2019. H.C.K. serves as a Director of Clinical Practice Guidelines Development Committee of the Korean Thyroid Association.

## Funding

These practical guidelines were supported by KTA without support from any commercial sources. This project was also partially supported by a grant (2017R1D1A1B03029597) from the Basic Science Research Program through the National Research Foundation of Korea.

## Acknowledgments

The authors would like to thank the members of KTA, KSThR, and the Endocrine Pathology Study Group of the Korean Society of Pathologists for their valuable expertise and suggestions throughout this study. This document was approved by the Clinical Practice Guidelines Development Committee of the KTA in October 2019. The following professional organizations reviewed and endorsed the final document: KSThR, Korean Endocrine Pathology Study Group, and Korean Endocrine Society.

## REFERENCES

- Pitman MB, Abele J, Ali SZ, et al. Techniques for thyroid FNA: a synopsis of the National Cancer Institute Thyroid Fine-Needle Aspiration State of the Science Conference. *Diagn Cytopathol* 2008; 36: 407-24.
- Ha EJ, Lim HK, Yoon JH, et al. Primary imaging test and appropriate biopsy methods for thyroid nodules: guidelines by Korean Society of Radiology and National Evidence-Based Healthcare Collaborating Agency. *Korean J Radiol* 2018; 19: 623-31.
- Ashcraft MW, Van Herle AJ. Management of thyroid nodules. II: Scanning techniques, thyroid suppressive therapy, and fine needle aspiration. *Head Neck Surg* 1981; 3: 297-322.
- Bongiovanni M, Spitale A, Faquin WC, Mazzucchelli L, Baloch ZW. The Bethesda System for Reporting Thyroid Cytopathology: a meta-analysis. *Acta Cytol* 2012; 56: 333-9.
- Alexander EK, Heering JP, Benson CB, et al. Assessment of nondiagnostic ultrasound-guided fine needle aspirations of thyroid nodules. *J Clin Endocrinol Metab* 2002; 87: 4924-7.
- Orija IB, Pineyro M, Biscotti C, Reddy SS, Hamrahian AH. Value of repeating a nondiagnostic thyroid fine-needle aspiration biopsy. *Endocr Pract* 2007; 13: 735-42.
- Nayar R, Ivanovic M. The indeterminate thyroid fine-needle aspiration: experience from an academic center using terminology similar to that proposed in the 2007 National Cancer Institute Thyroid Fine Needle Aspiration State of the Science Conference. *Cancer* 2009; 117: 195-202.
- Yang J, Schnadig V, Logrono R, Wasserman PG. Fine-needle aspiration of thyroid nodules: a study of 4703 patients with histologic

- and clinical correlations. *Cancer* 2007; 111: 306-15.
9. Yassa L, Cibas ES, Benson CB, et al. Long-term assessment of a multidisciplinary approach to thyroid nodule diagnostic evaluation. *Cancer* 2007; 111: 508-16.
  10. Bongiovanni M, Krane JF, Cibas ES, Faquin WC. The atypical thyroid fine-needle aspiration: past, present, and future. *Cancer Cytopathol* 2012; 120: 73-86.
  11. Deveci MS, Deveci G, LiVolsi VA, Baloch ZW. Fine-needle aspiration of follicular lesions of the thyroid: diagnosis and follow-up. *Cytojournal* 2006; 3: 9.
  12. Yoo C, Choi HJ, Im S, et al. Fine needle aspiration cytology of thyroid follicular neoplasm: cytohistologic correlation and accuracy. *Korean J Pathol* 2013; 47: 61-6.
  13. Novoa E, Gurtler N, Arnoux A, Kraft M. Role of ultrasound-guided core-needle biopsy in the assessment of head and neck lesions: a meta-analysis and systematic review of the literature. *Head Neck* 2012; 34: 1497-503.
  14. Na DG, Baek JH, Jung SL, et al. Core needle biopsy of the thyroid: 2016 consensus statement and recommendations from Korean Society of Thyroid Radiology. *Korean J Radiol* 2017; 18: 217-37.
  15. Ha EJ, Baek JH, Lee JH, et al. Complications following US-guided core-needle biopsy for thyroid lesions: a retrospective study of 6,169 consecutive patients with 6,687 thyroid nodules. *Eur Radiol* 2017; 27: 1186-94.
  16. Paja M, Del Cura JL, Zabala R, Korta I, Ugalde A, Lopez JI. Core-needle biopsy in thyroid nodules: performance, accuracy, and complications. *Eur Radiol* 2019; 29: 4889-96.
  17. Ha EJ, Suh CH, Baek JH. Complications following ultrasound-guided core needle biopsy of thyroid nodules: a systematic review and meta-analysis. *Eur Radiol* 2018; 28: 3848-60.
  18. Na DG, Kim JH, Sung JY, et al. Core-needle biopsy is more useful than repeat fine-needle aspiration in thyroid nodules read as non-diagnostic or atypia of undetermined significance by the Bethesda system for reporting thyroid cytopathology. *Thyroid* 2012; 22: 468-75.
  19. Samir AE, Vij A, Seale MK, et al. Ultrasound-guided percutaneous thyroid nodule core biopsy: clinical utility in patients with prior nondiagnostic fine-needle aspirate. *Thyroid* 2012; 22: 461-7.
  20. Cao H, Kao RH, Hsieh MC. Comparison of core-needle biopsy and fine-needle aspiration in screening for thyroid malignancy: a systematic review and meta-analysis. *Curr Med Res Opin* 2016; 32: 1291-301.
  21. Pyo JS, Sohn JH, Kang G. Core needle biopsy is a more conclusive follow-up method than repeat fine needle aspiration for thyroid nodules with initially inconclusive results: a systematic review and meta-analysis. *J Pathol Transl Med* 2016; 50: 217-24.
  22. Trimboli P, Nasrollah N, Guidobaldi L, et al. The use of core needle biopsy as first-line in diagnosis of thyroid nodules reduces false negative and inconclusive data reported by fine-needle aspiration. *World J Surg Oncol* 2014; 12: 61.
  23. Suh CH, Baek JH, Choi YJ, et al. Efficacy and safety of core-needle biopsy in initially detected thyroid nodules via propensity score analysis. *Sci Rep* 2017; 7: 8242.
  24. Kim HC, Kim YJ, Han HY, et al. First-line use of core needle biopsy for high-yield preliminary diagnosis of thyroid nodules. *AJNR Am J Neuroradiol* 2017; 38: 357-63.
  25. Hong MJ, Na DG, Kim SJ, Kim DS. Role of core needle biopsy as a first-line diagnostic tool for thyroid nodules: a retrospective cohort study. *Ultrasonography* 2018; 37: 244-53.
  26. Cibas ES, Ali SZ. The 2017 Bethesda System for Reporting Thyroid Cytopathology. *Thyroid* 2017; 27: 1341-6.
  27. Baek JH, Na DG, Lee JH, et al. Core needle biopsy of thyroid nodules: consensus statement and recommendations. *J Korean Soc Ultrasound Med* 2013; 32: 95-102.
  28. Jung CK, Min HS, Park HJ, et al. Pathology reporting of thyroid core needle biopsy: a proposal of the Korean Endocrine Pathology Thyroid Core Needle Biopsy Study Group. *J Pathol Transl Med* 2015; 49: 288-99.
  29. Lloyd RV, Osamura RY, Klöppel G, Rosai J. WHO classification of tumours of endocrine organs. 4th ed. Lyon: IARC Press, 2017; 66-103.
  30. Gharib H, Papini E, Garber JR, et al. American Association of Clinical Endocrinologists, American College of Endocrinology, and Associazione Medici Endocrinologi medical guidelines for clinical practice for the diagnosis and management of thyroid nodules: 2016 update. *Endocr Pract* 2016; 22: 622-39.
  31. Haugen BR, Alexander EK, Bible KC, et al. 2015 American Thyroid Association management guidelines for adult patients with thyroid nodules and differentiated thyroid cancer: The American Thyroid Association Guidelines Task Force on Thyroid Nodules and Differentiated Thyroid Cancer. *Thyroid* 2016; 26: 1-133.
  32. Baloch ZW, Cibas ES, Clark DP, et al. The National Cancer Institute Thyroid fine needle aspiration state of the science conference: a summation. *Cytojournal* 2008; 5: 6.
  33. Perros P, Boelaert K, Colley S, et al. Guidelines for the management of thyroid cancer. *Clin Endocrinol (Oxf)* 2014; 81 Suppl 1: 1-122.
  34. Yim Y, Baek JH. Core needle biopsy in the management of thyroid nodules with an indeterminate fine-needle aspiration report. *Gland Surg* 2019; 8(Suppl 2): S77-S85.
  35. Jung CK, Baek JH. Recent advances in core needle biopsy for thyroid nodules. *Endocrinol Metab (Seoul)* 2017; 32: 407-12.
  36. Suh CH, Baek JH, Kim KW, et al. The role of core-needle biopsy for thyroid nodules with initially nondiagnostic fine-needle aspiration

- results: a systematic review and meta-analysis. *Endocr Pract* 2016; 22: 679-88.
37. Paja M, del Cura JL, Zabala R, et al. Ultrasound-guided core-needle biopsy in thyroid nodules: a study of 676 consecutive cases with surgical correlation. *Eur Radiol* 2016; 26: 1-8.
  38. Suh CH, Baek JH, Lee JH, et al. The role of core-needle biopsy as a first-line diagnostic tool for initially detected thyroid nodules. *Thyroid* 2016; 26: 395-403.
  39. Sung JY, Na DG, Kim KS, et al. Diagnostic accuracy of fine-needle aspiration versus core-needle biopsy for the diagnosis of thyroid malignancy in a clinical cohort. *Eur Radiol* 2012; 22: 1564-72.
  40. Chung SR, Suh CH, Baek JH, Choi YJ, Lee JH. The role of core needle biopsy in the diagnosis of initially detected thyroid nodules: a systematic review and meta-analysis. *Eur Radiol* 2018; 28: 4909-18.
  41. Screaton NJ, Berman LH, Grant JW. US-guided core-needle biopsy of the thyroid gland. *Radiology* 2003; 226: 827-32.
  42. Yeon JS, Baek JH, Lim HK, et al. Thyroid nodules with initially nondiagnostic cytologic results: the role of core-needle biopsy. *Radiology* 2013; 268: 274-80.
  43. Park KT, Ahn SH, Mo JH, et al. Role of core needle biopsy and ultrasonographic finding in management of indeterminate thyroid nodules. *Head Neck* 2011; 33: 160-5.
  44. Lee KH, Shin JH, Oh YL, Hahn SY. Atypia of undetermined significance in thyroid fine-needle aspiration cytology: prediction of malignancy by US and comparison of methods for further management. *Ann Surg Oncol* 2014; 21: 2326-31.
  45. Na DG, Min HS, Lee H, Won JK, Seo HB, Kim JH. Role of core needle biopsy in the management of atypia/follicular lesion of undetermined significance thyroid nodules: comparison with repeat fine-needle aspiration in subcategory nodules. *Eur Thyroid J* 2015; 4: 189-96.
  46. Buxey K, Serpell J. Importance of core biopsy in the diagnosis of thyroid lymphoma. *ANZ J Surg* 2012; 82: 90.
  47. Kwak JY, Kim EK, Ko KH, et al. Primary thyroid lymphoma: role of ultrasound-guided needle biopsy. *J Ultrasound Med* 2007; 26: 1761-5.
  48. Nam M, Shin JH, Han BK, et al. Thyroid lymphoma: correlation of radiologic and pathologic features. *J Ultrasound Med* 2012; 31: 589-94.
  49. Ha EJ, Baek JH, Na DG, et al. The role of core needle biopsy and its impact on surgical management in patients with medullary thyroid cancer: clinical experience at 3 medical institutions. *AJNR Am J Neuroradiol* 2015; 36: 1512-7.
  50. Kwok A, Faigel DO. Management of anticoagulation before and after gastrointestinal endoscopy. *Am J Gastroenterol* 2009; 104: 3085-97.
  51. Baek JH. Current status of core needle biopsy of the thyroid. *Ultrasonography* 2017; 36: 83-5.
  52. Del Cura JL, Zabala R, Corta I. US-guided interventional procedures: what a radiologist needs to know. *Radiologia* 2010; 52: 198-207.
  53. Harvey JN, Parker D, De P, Shrimali RK, Otter M. Sonographically guided core biopsy in the assessment of thyroid nodules. *J Clin Ultrasound* 2005; 33: 57-62.
  54. Nasrollah N, Trimboli P, Guidobaldi L, et al. Thin core biopsy should help to discriminate thyroid nodules cytologically classified as indeterminate: a new sampling technique. *Endocrine* 2013; 43: 659-65.
  55. Zhang M, Zhang Y, Fu S, Lv F, Tang J. Thyroid nodules with suspicious ultrasound findings: the role of ultrasound-guided core needle biopsy. *Clin Imaging* 2014; 38: 434-8.
  56. Hahn SY, Shin JH, Han BK, Ko EY, Ko ES. Ultrasonography-guided core needle biopsy for the thyroid nodule: does the procedure hold any benefit for the diagnosis when fine-needle aspiration cytology analysis shows inconclusive results? *Br J Radiol* 2013; 86: 20130007.
  57. Min HS, Kim JH, Ryoo I, Jung SL, Jung CK. The role of core needle biopsy in the preoperative diagnosis of follicular neoplasm of the thyroid. *APMIS* 2014; 122: 993-1000.
  58. Yoon RG, Baek JH, Lee JH, et al. Diagnosis of thyroid follicular neoplasm: fine-needle aspiration versus core-needle biopsy. *Thyroid* 2014; 24: 1612-7.
  59. Ahn HS, Seo M, Ha SM, Kim HS. Comparison of the diagnostic efficacy of ultrasound-guided core needle biopsy with 18- versus 20-gauge needles for thyroid nodules. *J Ultrasound Med* 2018; 37: 2565-74.
  60. Lopez JI, Zabala R, Del Cura JL. Histological diagnosis of thyroid disease using ultrasound-guided core biopsies. *Eur Thyroid J* 2013; 2: 29-36.
  61. Hahn SY, Shin JH, Oh YL. What is the ideal core number for ultrasonography-guided thyroid biopsy of cytologically inconclusive nodules? *AJNR Am J Neuroradiol* 2017; 38: 777-81.
  62. Park HS, Baek JH, Gyu ND. Regarding "what is the ideal core number for ultrasonography-guided thyroid biopsy of cytologically inconclusive nodules?". *AJNR Am J Neuroradiol* 2017; 38: E53-4.
  63. Chung SR, Baek JH, Choi YJ, et al. The role of core needle biopsy for the evaluation of thyroid nodules with suspicious ultrasound features. *Korean J Radiol* 2019; 20: 158-65.
  64. Hong MJ, Sung JY, Baek JH, et al. Safety and efficacy of radiofrequency ablation for nonfunctioning benign thyroid nodules in children and adolescents in 14 patients over a 10-year period. *J Vasc Interv Radiol* 2019; 30: 900-6.
  65. Chung SR, Baek JH, Lee JH, et al. Risk of malignancy according to the sub-classification of atypia of undetermined significance and suspicious follicular neoplasm categories in thyroid core needle

- biopsies. *Endocr Pathol* 2019; 30: 146-54.
66. Ha EJ, Baek JH, Lee JH, et al. Core needle biopsy can minimise the non-diagnostic results and need for diagnostic surgery in patients with calcified thyroid nodules. *Eur Radiol* 2014; 24: 1403-9.
  67. Yi KS, Kim JH, Na DG, et al. Usefulness of core needle biopsy for thyroid nodules with macrocalcifications: comparison with fine-needle aspiration. *Thyroid* 2015; 25: 657-64.
  68. Na DG, Kim DS, Kim SJ, Ryoo JW, Jung SL. Thyroid nodules with isolated macrocalcification: malignancy risk and diagnostic efficacy of fine-needle aspiration and core needle biopsy. *Ultrasonography* 2016; 35: 212-9.
  69. Ren J, Baek JH, Chung SR, Choi YJ, Jung CK, Lee JH. Degenerating thyroid nodules: ultrasound diagnosis, clinical significance, and management. *Korean J Radiol* 2019; 20: 947-55.
  70. Khoo TK, Baker CH, Hallanger-Johnson J, et al. Comparison of ultrasound-guided fine-needle aspiration biopsy with core-needle biopsy in the evaluation of thyroid nodules. *Endocr Pract* 2008; 14: 426-31.
  71. Quinn SF, Nelson HA, Demlow TA. Thyroid biopsies: fine-needle aspiration biopsy versus spring-activated core biopsy needle in 102 patients. *J Vasc Interv Radiol* 1994; 5: 619-23.
  72. Ha EJ, Baek JH, Lee JH. Ultrasonography-based thyroidal and perithyroidal anatomy and its clinical significance. *Korean J Radiol* 2015; 16: 749-66.
  73. Nasrollah N, Trimboli P, Rossi F, et al. Patient's comfort with and tolerability of thyroid core needle biopsy. *Endocrine* 2014; 45: 79-83.
  74. Jeong EJ, Chung SR, Baek JH, Choi YJ, Kim JK, Lee JH. A comparison of ultrasound-guided fine needle aspiration versus core needle biopsy for thyroid nodules: pain, tolerability, and complications. *Endocrinol Metab (Seoul)* 2018; 33: 114-20.
  75. Kim HJ, Kim YK, Moon JH, Choi JY, Choi SI. Thyroid core needle biopsy: patients' pain and satisfaction compared to fine needle aspiration. *Endocrine* 2019; 65: 365-70.
  76. Karstrup S, Balslev E, Juul N, Eskildsen PC, Baumbach L. US-guided fine needle aspiration versus coarse needle biopsy of thyroid nodules. *Eur J Ultrasound* 2001; 13: 1-5.
  77. Polyzos SA, Anastasilakis AD. Clinical complications following thyroid fine-needle biopsy: a systematic review. *Clin Endocrinol (Oxf)* 2009; 71: 157-65.
  78. Kakiuchi Y, Idota N, Nakamura M, Ikegaya H. A fatal case of cervical hemorrhage after fine needle aspiration and core needle biopsy of the thyroid gland. *Am J Forensic Med Pathol* 2015; 36: 207-9.
  79. Tomoda C, Takamura Y, Ito Y, Miya A, Miyauchi A. Transient vocal cord paralysis after fine-needle aspiration biopsy of thyroid tumor. *Thyroid* 2006; 16: 697-9.
  80. Choi SH, Kim EK, Kim SJ, Kwak JY. Thyroid ultrasonography: pitfalls and techniques. *Korean J Radiol* 2014; 15: 267-76.
  81. Bergeron M, Beaudoin D. Simple core-needle biopsy for thyroid nodule, complicated tinnitus. *Eur Thyroid J* 2014; 3: 130-3.
  82. Shah KS, Ethunandan M. Tumour seeding after fine-needle aspiration and core biopsy of the head and neck: a systematic review. *Br J Oral Maxillofac Surg* 2016; 54: 260-5.
  83. Thavarajah R, Mudimbaimannar VK, Elizabeth J, Rao UK, Ranganathan K. Chemical and physical basics of routine formaldehyde fixation. *J Oral Maxillofac Pathol* 2012; 16: 400-5.
  84. Hewitt SM, Lewis FA, Cao Y, et al. Tissue handling and specimen preparation in surgical pathology: issues concerning the recovery of nucleic acids from formalin-fixed, paraffin-embedded tissue. *Arch Pathol Lab Med* 2008; 132: 1929-35.
  85. Xiong Y, Yan L, Nong L, Zheng Y, Li T. Pathological diagnosis of thyroid nodules based on core needle biopsies: comparative study between core needle biopsies and resected specimens in 578 cases. *Diagn Pathol* 2019; 14: 10.
  86. Cibas ES, Ali SZ; NCI Thyroid FNA State of the Science Conference. The Bethesda System For Reporting Thyroid Cytopathology. *Am J Clin Pathol* 2009; 132: 658-65.
  87. Ali SZ. Thyroid cytopathology: Bethesda and beyond. *Acta Cytol* 2011; 55: 4-12.
  88. Na HY, Woo JW, Moon JH, et al. Preoperative diagnostic categories of noninvasive follicular thyroid neoplasm with papillary-like nuclear features in thyroid core needle biopsy and its impact on risk of malignancy. *Endocr Pathol* 2019; 30: 329-39.
  89. Bae JS, Choi SK, Jeon S, et al. Impact of *NRAS* mutations on the diagnosis of follicular neoplasm of the thyroid. *Int J Endocrinol* 2014; 2014: 289834.
  90. Ustun B, Chhieng D, Van Dyke A, et al. Risk stratification in follicular neoplasm: a cytological assessment using the modified Bethesda classification. *Cancer Cytopathol* 2014; 122: 536-45.
  91. Crescenzi A, Guidobaldi L, Nasrollah N, et al. Immunohistochemistry for *BRAF(V600E)* antibody VE1 performed in core needle biopsy samples identifies mutated papillary thyroid cancers. *Horm Metab Res* 2014; 46: 370-4.
  92. Alshenawy HA. Utility of immunohistochemical markers in diagnosis of follicular cell derived thyroid lesions. *Pathol Oncol Res* 2014; 20: 819-28.
  93. El Demellawy D, Nasr AL, Babay S, Alowami S. Diagnostic utility of CD56 immunohistochemistry in papillary carcinoma of the thyroid. *Pathol Res Pract* 2009; 205: 303-9.

# Analysis of the molecular subtypes of preoperative core needle biopsy and surgical specimens in invasive breast cancer

Ye Sul Jeong<sup>1</sup>, Jun Kang<sup>1</sup>, Jieun Lee<sup>2,3</sup>, Tae-Kyung Yoo<sup>4</sup>, Sung Hun Kim<sup>5</sup>, Ahwon Lee<sup>1,3</sup>

<sup>1</sup>Department of Hospital Pathology, <sup>2</sup>Division of Medical Oncology, Department of Internal Medicine, Seoul St. Mary's Hospital, College of Medicine, The Catholic University of Korea, Seoul;

<sup>3</sup>Cancer Research Institute, The Catholic University of Korea, Seoul;

Departments of <sup>4</sup>Surgery and <sup>5</sup>Radiology, Seoul St. Mary's Hospital, College of Medicine, The Catholic University of Korea, Seoul, Korea

**Background:** Accurate molecular classification of breast core needle biopsy (CNB) tissue is important for determining neoadjuvant systemic therapies for invasive breast cancer. The researchers aimed to evaluate the concordance rate (CR) of molecular subtypes between CNBs and surgical specimens. **Methods:** This study was conducted with invasive breast cancer patients who underwent surgery after CNB at Seoul St. Mary's Hospital between December 2014 and December 2017. Estrogen receptor (ER), progesterone receptor (PR), human epidermal growth factor receptor 2 (HER2), and Ki67 were analyzed using immunohistochemistry. ER and PR were evaluated by Allred score (0–8). HER2 was graded from 0 to +3, and all 2+ cases were reflex tested with silver in situ hybridization. The labeling index of Ki67 was counted by either manual scoring or digital image analysis. Molecular subtypes were classified using the above surrogate markers. **Results:** In total, 629 patients were evaluated. The CRs of ER, PR, HER2, and Ki67 were 96.5% (kappa, 0.883;  $p < .001$ ), 93.0% (kappa, 0.824;  $p < .001$ ), 99.7% (kappa, 0.988;  $p < .001$ ), and 78.7% (kappa, 0.577;  $p < .001$ ), respectively. Digital image analysis of Ki67 in CNB showed better concordance with Ki67 in surgical specimens (CR, 82.3%; kappa, 0.639 for digital image analysis vs. CR, 76.2%; kappa, 0.534 for manual counting). The CRs of luminal A, luminal B, HER2, and triple negative types were 89.0%, 70.0%, 82.9%, and 77.2%, respectively. **Conclusions:** CNB was reasonably accurate for determining ER, PR, HER2, Ki67, and molecular subtypes. Using digital image analysis for Ki67 in CNB produced more accurate molecular classifications.

**Key Words:** Breast neoplasms; Core needle biopsy; Receptors, estrogen; Receptors, progesterone; Human epidermal growth factor receptor 2; Immunohistochemistry

Received: August 1, 2019 Revised: September 25, 2019 Accepted: October 14, 2019

Corresponding Author: Ahwon Lee, MD, PhD, Department of Hospital Pathology, Seoul St. Mary's Hospital, College of Medicine, The Catholic University of Korea, 222 Banpo-daero, Seocho-gu, Seoul 06591, Korea

Tel: +82-2-2258-1621, Fax: +82-2-2258-1627, E-mail: klee@catholic.ac.kr

Breast cancer is a heterogeneous disease that is classified into four molecular subtypes: luminal A, luminal B, human epidermal growth factor receptor 2 (HER2) positive, and triple negative. Proper disease subtyping is important for predicting response to systemic therapy and prognosis. Immunohistochemistry for estrogen receptor (ER), progesterone receptor (PR), HER2, and Ki67 can be used to approximate molecular subtype classifications [1-3].

Endocrine therapy, cytotoxic therapy, and anti-HER2 therapy are used in the adjuvant setting for breast cancer, and molecular subtyping is used to decide which therapies are appropriate [3]. Neoadjuvant therapy is important in advanced breast cancer as it can reduce tumor size, facilitating breast conserving surgery,

and decrease distant micrometastasis. Neoadjuvant therapy may also facilitate axillary preservation [4-7]. After receiving neoadjuvant therapy, some patients achieve pathologic complete response (pCR), at which point, core needle biopsy (CNB) tissue is the only specimen for obtaining information about prognostic markers that could impact therapeutic plans. Although some patients still have tumor burden after neoadjuvant therapy, CNB might be the only specimen available in which to evaluate histological markers because neoadjuvant therapy can alter histological grade, expression of hormonal receptors, HER2 status, and Ki67. Consequently, assessing the concordance rate (CR) of marker status between CNB and surgical specimen is crucial [8,9]. It has been reported that CRs of biomarker status between CNB and surgi-

cal specimen were high but variable: 79%–100% [10]. However, differences in Ki67 status according to manual or digital image analysis and the impact on subsequent molecular subtyping have not been adequately investigated. The aim of this study was to evaluate and analyze CRs of hormone receptors, HER2, Ki67, and molecular subtypes in invasive breast cancer patients between CNB and surgical specimens.

## MATERIALS AND METHODS

### Patient population and tissue samples

This study retroactively analyzed clinical data from cancer patients who underwent surgery after diagnosis by CNB at Seoul St. Mary's Hospital. Clinicopathologic data of age; histologic type; grade; operation method; pTNM stage; immunohistochemical staining results of ER, PR, HER2, and Ki67; and whether digital image analysis was used to analyze results of Ki67 staining and silver in situ hybridization (SISH) for HER2 were obtained through medical records and pathologic reports. CNBs were mostly performed by ultrasound guidance with 14-gauge needles; 4–5 pieces were received for mass forming lesions and > 7 pieces for microcalcifications. Especially when microcalcification was noted, an ultrasound-guided or stereotactic mamotome biopsy with 11-gauge needles was performed, and at least 12 pieces of core tissue were obtained for pathologic examination. All specimens were routinely processed and diagnosed according to national and international guidelines. Briefly, CNB specimens were fixed in 10% neutral formalin for 8–11 hours, embedded in paraffin, and sectioned at 4- $\mu$ m thickness; hematoxylin and eosin (H&E) staining was subsequently performed. Surgical specimens were cut into 0.5–1-cm-thick sections after the operation and fixed in 10% neutral formalin for 8–24 hours; H&E staining was subsequently performed. Patients who were diagnosed with ductal carcinoma in situ, microinvasive breast cancer, or had received preoperative systemic therapy were excluded.

### Evaluation of ER, PR, HER2, and Ki67

Immunohistochemistry (IHC) for ER, PR, HER2, and Ki67 was performed following the instructions of the pathology laboratory manual. Briefly, ER, PR, HER2, and Ki67 IHC staining was performed on an automated Ventana BenchmarkXT slide stainer (Ventana, Tucson, AZ, USA), using primary antibodies against ER (prediluted, SP1, Ventana), PR (prediluted, 1E2, Ventana), HER2 (prediluted, 4B5, Ventana), and Ki67 (prediluted, MIB-1, Ventana). The HER2 SISH assay was performed with INFORM HER2 DNA probes (Ventana) on the Ventana

BenchMarkXT automated slide stainer according to the manufacturer's protocols.

The Allred scoring system was used to interpret ER and PR staining [11]. The proportion of positive-stained tumor cells (the proportion score) was rated as follows: 0, no cells stained positive; 1, 0%–1% positive; 2, 1%–10% positive; 3, 10%–33% positive; 4, 33%–66% positive; and 5, 66%–100% positive. Intensity was scored on the basis of average staining intensity: 0, negative; 1, weak; 2, intermediate; and 3, strong. The sum of the proportion and intensity scores is referred to as the Allred score, and scores > 2 are defined as positive [11]. HER2 status was scored from 0–3+ by IHC, where 0 was defined as no staining or membrane staining that was incomplete, faint, or barely perceptible in  $\leq$ 10% of invasive tumor cells; 1+ was defined as > 10% invasive tumor cells with incomplete membrane staining that was faint or barely perceptible; 2+ was defined as > 10% invasive tumor cells with complete weak to moderate membrane staining (considered equivocal); and 3+ was defined as > 10% invasive tumor cells with complete, intense membrane staining (positive according to American Society of Clinical Oncology [ASCO]/College of American Pathologists [CAP] guidelines) [12,13]. Cases of scores 0 and 1+ were considered negative, while those 2+ were further evaluated by reflex HER2 SISH to confirm HER2 gene amplification.

Ki67 was evaluated according to the percentage of positively-stained invasive tumor cells of any intensity by pathologists manually or using an automated digital image analysis system. The “eyeballed” estimation method, which is approximate counting throughout the immunostained slide, was used for manual counting [14]. For Ki67 digital image analysis, slides were scanned by an iScan Coreo slide scanner with a 20 $\times$  objective (Ventana), and invasive tumor components were analyzed using Virtuoso software (Ventana). At least three high-power fields (400 $\times$ ) including hot spots where the highest Ki67 staining area and two average intensity areas of Ki67 staining were selected. More than 1,000 tumor cells were counted according to the International Ki67 in Breast Cancer Working Group [15]. In the case of CNB with a heterogeneous Ki67 staining pattern, researchers attempted to select all tumor cells to evaluate Ki67 expression. Cases in which less than 500 tumor cells were present in CNB were excluded from digital image analysis. Digital image analysis of Ki67 was performed in 41% (260/629) of CNBs and all but 14 surgical specimens. The cutoff value for Ki67 was 20%.

### Molecular subtype classifications

Molecular subtypes were classified as follows: luminal A: ER-

and/or PR-positive, HER2-negative, Ki67  $\leq$  20%; luminal B: ER- and/or PR-positive, HER2-negative, Ki67 > 20% or ER- and/or PR-positive, HER2-positive, any Ki67; HER2-positive: ER- and PR-negative, HER2-positive; and triple-negative (basal-like): ER-, PR-, and HER2-negative. Subsequently, luminal B was further divided as luminal B–HER2–negative (ER- and/or PR-positive, HER2-negative, Ki67 > 20%) and luminal B–HER2–positive (ER- and/or PR-positive, HER2-positive, any Ki67) [2,3].

### Statistical analysis

CRs of receptor status and molecular subtypes between CNB and surgical specimens were calculated as percentage and Kappa value. K-values < 0.20 were correlated with poor agreement, 0.21–0.40 fair agreement, 0.41–0.60 moderate agreement, 0.61–0.80 good agreement, and 0.81–1.00 very good agreement. p-values were calculated using the chi-square test or Fisher exact test, and p-values of < 0.05 were considered significant. Statistical analyses were performed using IBM SPSS Statistics software ver. 24.0 for Windows (IBM Corp., Armonk, NY, USA). Sankey diagrams depicting changes in Allred scores were computed in SankeyMATIC (<http://sankeymatic.com>).

### Ethics statement

The protocol of the study was approved by the Institutional Review Board of The Catholic Medical Center, which waived the requirement for informed consent (approval KC19RE-SI0333).

## RESULTS

### Patient characteristics

In total, 629 patients were included in the study. The median age was 53 (range, 23 to 89 years). All patients received either breast conserving surgery (70.4%) or mastectomy (29.6%). The most common pathological tumor type was invasive carcinoma of no special type (80.1%) (Tables 1, 2).

### Concordance of ER, PR, HER2, and Ki67

The CRs of surgical specimens with CNBs for ER and PR were 96.5% (kappa, 0.883;  $p < .001$ ) and 93.0% (kappa, 0.824;  $p < .001$ ), respectively (Table 3). The concordance of PR was slightly lower than that of ER. Changes in Allred score for ER and PR are shown in Figs. 1 and 2. The CR of surgical specimens with CNBs for hormone receptor status was 95.1%, with very good agreement (kappa, 0.824;  $p < .001$ ). The CR of HER2

**Table 1.** Patient and tumor characteristics

Variable	No. (%)
Age (yr), median (range)	53 (23–89)
$\leq$ 50	279 (44.4)
> 50	350 (55.6)
Surgery type	
Breast conserving surgery	443 (70.4)
Mastectomy	186 (29.6)
Pathological type	
Invasive carcinoma of no special type	504 (80.1)
Invasive lobular carcinoma	45 (7.2)
Mucinous carcinoma	24 (3.8)
Carcinoma with medullary feature	13 (2.1)
Metaplastic carcinoma	8 (1.3)
Minor pathological type	35 (5.6)
Histologic grade (Nottingham histologic grading)	
Grade 1	143 (22.7)
Grade 2	286 (45.5)
Grade 3	200 (31.8)
Pathologic T category	
pT1	374 (59.5)
pT2	242 (38.5)
pT3	11 (1.7)
pT4	2 (0.3)
Pathologic N category	
pNX	7 (1.1)
pN0	429 (68.2)
pN1	140 (22.3)
pN2	28 (4.5)
pN3	25 (4.0)

**Table 2.** Minor pathological type from Table 1

Pathological type	No. (%)
Mixed invasive ductal and mucinous carcinoma	7 (1.1)
Invasive micropapillary carcinoma	6 (1.0)
Mixed invasive ductal and micropapillary carcinoma	6 (1.0)
Carcinoma with apocrine differentiation	4 (0.6)
Tubular carcinoma	4 (0.6)
Mixed invasive ductal and lobular carcinoma	3 (0.5)
Invasive cribriform carcinoma	2 (0.3)
Medullary carcinoma	1 (0.2)
Invasive papillary carcinoma	1 (0.2)
Mixed invasive ductal and apocrine carcinoma	1 (0.2)

IHC was 81.4%, with moderate agreement (kappa, 0.591;  $p < .001$ ). After reflex HER2 SISH, the CR of HER2 status was 99.7% (kappa, 0.988;  $p < .001$ ). The CR for Ki67 was 78.7% (kappa, 0.577;  $p < .001$ , moderate agreement), which was lower than for hormone receptors and HER2 due to higher Ki67 expression in surgical specimens (Table 3).

We next analyzed whether the Ki67 counting method (automated digital image analysis system or manual scoring) affected the CR for Ki67. Among the 629 cases, 260 CNBs were analyzed

**Table 3.** Concordance between CNB and surgical specimen for ER, PR, HER2, and Ki67 results

Surgical specimen	CNB			Total (%)	Concordance rate	Kappa <sup>a</sup>	p-value
	Neg	Pos	Equi				
Hormone receptor							
Neg	90	24		114 (18.1)	95.1	0.824	<.001
Pos	7	508		515 (81.9)			
Total	97 (15.4)	532 (84.6)		629			
ER							
Neg	104	16		120 (19.1)	96.5	0.883	<.001
Pos	6	503		509 (80.9)			
Total	110 (17.5)	519 (82.5)		629			
PR							
Neg	150	28		178 (28.3)	93.0	0.824	<.001
Pos	16	435		451 (71.7)			
Total	166 (26.4)	463 (73.6)		629			
HER2 (IHC)							
Neg	396	1	69	466 (74.1)	81.4	0.591	<.001
Pos	0	73	6	79 (12.6)			
Equi	31	10	43	84 (13.4)			
Total	427 (67.9)	84 (13.4)	118 (18.8)	629			
HER2 (IHC + SISH)							
Neg	532	1		533 (84.7)	99.7	0.988	<.001
Pos	1	95		96 (15.3)			
Total	533 (84.7)	96 (15.3)		629			
Ki67							
	≤20%	>20%			78.7	0.577	<.001
≤20%	225	33		258 (41.0)			
>20%	101	270		371 (59.0)			
Total	326 (51.8)	303 (48.2)		629			

Values are presented as number (%) unless otherwise indicated.

CNB, core needle biopsy; ER, estrogen receptor; PR, progesterone receptor; HER2, human epidermal growth factor receptor 2; Neg, negative; Pos, positive; Equi, Equivocal; IHC, immunohistochemistry; SISH, silver in situ hybridization.

<sup>a</sup>Kappa: <0.20, poor agreement; 0.21–0.40, fair agreement; 0.41–0.60, moderate agreement; 0.61–0.80, good agreement; 0.81–1.00, very good agreement.

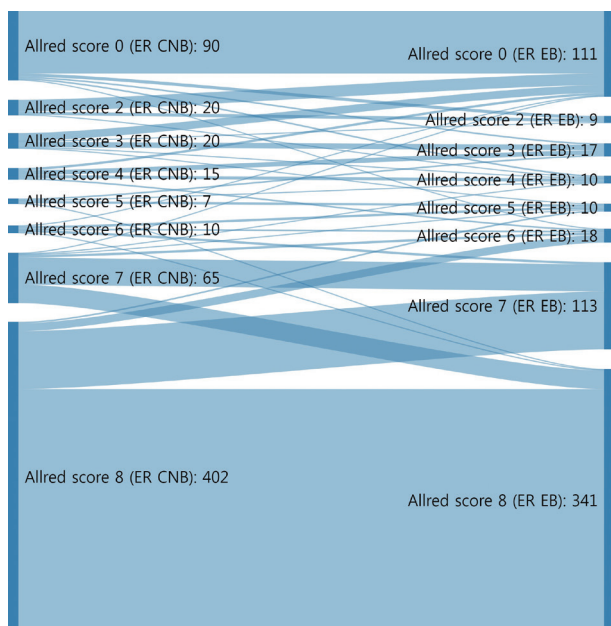


**Fig. 1.** Sankey diagrams depicting changes in Allred scores for estrogen receptor (ER) from core needle biopsy (CNB) to surgical specimen. EB, excisional biopsy (surgical specimen).

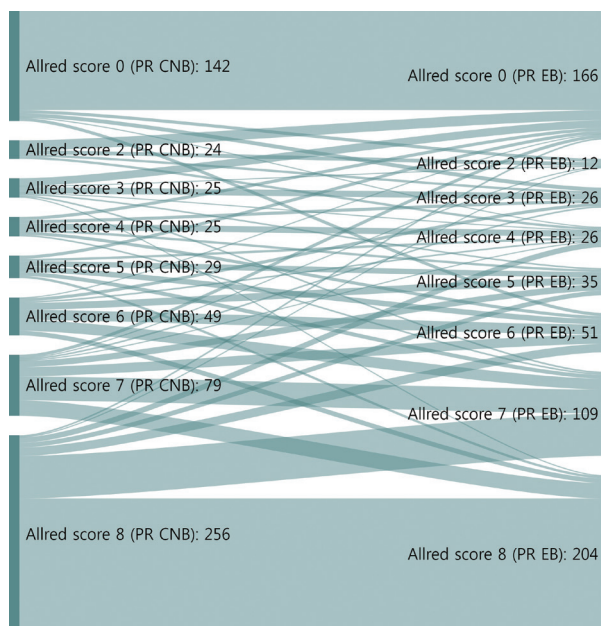


**Fig. 2.** Sankey diagrams depicting changes in Allred scores for progesterone receptor (PR) from core needle biopsy (CNB) to surgical specimen. EB, excisional biopsy (surgical specimen).

with a digital image system and 369 with manual counting. When CNB Ki67s were obtained using the digital image analysis system, the CR for Ki67 was 82.3% (kappa, 0.639;  $p < .001$ ), and when CNB Ki67s were obtained by manual counting, the CR for Ki67 was 76.2% (kappa, 0.534;  $p < .001$ ) (Table 4).

### Concordance of molecular subtypes

Molecular subtypes demonstrated good agreement (kappa, 0.672 in four subtypes and kappa, 0.696 in five subtypes). CRs of surgical specimens with CNBs for luminal A, luminal B, HER2, and triple negative were 89.0%, 70.0%, 82.9%, and 77.2%, respectively (kappa, 0.672; good agreement). The CRs of luminal A and HER2 showed significant agreement; however, luminal B showed the lowest CR among the molecular subtypes. When luminal B was subdivided into luminal B–HER2–negative and –HER2–positive, the CRs for these receptors between CNB and surgical specimens were 61.7% and 95.1%, respectively. Therefore, the especially high discrepancy seen for luminal B–HER2–negative occurred because molecular subtypes changed

from luminal A due to low Ki67 in CNB (75 cases) to luminal B–HER2–negative after high Ki67 was found in surgical specimens (Tables 5, 6).

## DISCUSSION

Neoadjuvant therapy in breast cancer can reduce tumor burden, which facilitates breast conserving surgery, preserves the axilla, and identifies response to systemic therapy before surgery [5–7]. Typically, treatment policies for neoadjuvant systemic therapy are decided according to the molecular subtype determined by ER, PR, HER2, and Ki67 status of CNB. These are also used to predict prognoses of breast cancer patients. In this study, the CRs of ER, PR, HER2, and Ki67 status in CNB specimens prior to surgery and those from surgical specimens were analyzed to confirm the accuracy of molecular classifications performed by CNB. ER and PR status showed high CRs of 96.5% (kappa, 0.883) and 93.0% (kappa, 0.824), respectively (Table 3). However, a greater distribution and bigger change of

**Table 4.** Comparing Ki67 cutoff values between CNB and surgical specimens by digital image analysis and manual scoring assessment

Ki67	Digital image analysis						Manual counting method					
	CNB			Concordance rate (%)	Kappa <sup>a</sup>	p-value	CNB			Concordance rate (%)	Kappa <sup>a</sup>	p-value
	≤20%	>20%	Total				≤20%	>20%	Total			
≤20%	88	28	116	82.3	0.639	<.001	137	73	210	76.2	0.534	<.001
>20%	18	126	144				15	144	159			
Total	106	154	260				152	217	369			

CNB, core needle biopsy.

<sup>a</sup>Kappa: <0.20, poor agreement; 0.21–0.40, fair agreement; 0.41–0.60, moderate agreement; 0.61–0.80, good agreement; 0.81–1.00, very good agreement.

**Table 5.** Concordance between CNB and surgical specimens for molecular subtypes

Surgical specimen	CNB	Luminal A	Luminal B	Triple negative	HER2+	Total	Concordance rate (%)	Kappa
Luminal A		218	26	1	0	245	89.0	0.672
Luminal B		75	189	4	2	270	70.0	
HER2+		0	6	0	29	35	82.9	
Triple negative		2	16	61	0	79	77.2	
Total		295	237	66	31	629	79.0	

CNB, core needle biopsy; HER2, human epidermal growth factor receptor 2.

**Table 6.** Concordance between CNB and surgical specimens for molecular subtypes including the subdivision of luminal B

Surgical specimen	CNB	Luminal A	Luminal B (HER2–)	Luminal B (HER2+)	Triple negative	HER2+	Total	Concordance rate (%)	Kappa
Luminal A		218	26	0	1	0	245	89.0	0.696
Luminal B (HER2–)		75	129	1	4	0	209	61.7	
Luminal B (HER2+)		0	1	58	0	2	61	95.1	
HER2+		0	0	6	0	29	35	82.9	
Triple negative		2	16	0	61	0	79	77.2	
Total		295	172	65	66	31	629	78.7	

CNB, core needle biopsy; HER2, human epidermal growth factor receptor 2.

Allred scores from CNB to surgical specimen were noted for PR than ER (Figs. 1, 2). These findings are consistent with previous reports [16,17] and suggest that the reason behind these findings is heterogeneity of PR expression in tumor cells.

Identifying HER2-positive breast cancer patients by CNB is important, as neoadjuvant HER2-targeted therapy is an effective option for these patients. In this study, the CR for HER2 status, as determined by HER2 IHC or reflex HER2 SISH, was as high as 99.7% (kappa, 0.988), which was higher than most previous reports (ranging from 61%–97.3%) [10,18–29]. The reason for this high CR could partially be due to performing reflex HER2 SISH for all HER2 IHC equivocal cases to determine final HER2 status strictly following ASCO/CAP guidelines. Sufficient CNB specimens were obtained when radiological microcalcifications were noted. In our hospital, at least four core passes in CNB are usually obtained by ultrasound guidance with a 14-gauge needle. However, when radiological calcifications were identified, additional core passes (at least seven) were performed. Sometimes when scattered calcification was noted, ultrasound-guided mammotome biopsy was performed with an 11-gauge needle, and > 12 core passes were obtained. It has been reported that radiologically recognized calcifications in breast cancer are associated with HER2 molecular subtype and pCR after neoadjuvant chemotherapy [30,31]. Another reason for collection of multiple cores in CNB is to overcome tumor heterogeneity. For accurate histologic diagnoses of breast cancer, at least four cores should be obtained using a 14-gauge needle [32]. It has been reported that the accuracy of histologic diagnoses (including tumor grade) plateaus at 74% when four passes are performed, while accuracy is only 32% with one pass [33]. Greer et al. [34] reported that the concordance for ER and PR between CNB and surgical specimen improved with increasing numbers of core passes. However, they also found the concordance of HER2 to be limited when tumor heterogeneity was present [34].

Although ER, PR, and HER2 status showed high CRs between CNB and surgical specimen, Ki67 revealed only moderate agreement. There were 75 cases classified as luminal A from CNB that were moved to luminal B after evaluating surgical specimens, as Ki67 was higher in the surgical specimen than in CNB. Additionally, a higher median value for Ki67 was identified in the surgical specimens (Tables 3, 5, 6). The tendency for a greater Ki67 labeling index in surgical specimens than in CNB has been reported in several studies. The authors explained that it was due to tumor heterogeneity [15,27]. Another study reported that the CR for Ki67 between CNB and surgical specimen improved slightly with increased number of core passes to account

for tumor heterogeneity; however, after more than six core passes, a plateau was reached [34]. In the current study, the Ki67 labeling index was obtained by digital image analysis or manual scoring (Table 4). Digital image analysis of Ki67 in CNB showed better concordance with surgical specimen Ki67 (CR, 82.3% vs. 76.2; kappa, 0.639 vs. 0.534, respectively).

Finally, 21.0% of cases switched molecular subtype between CNB and surgical specimen, mostly because Ki67 changed from low to high; for example, 75 luminal A cases as assessed by CNB were moved to luminal B after evaluating surgical specimens (Table 5). There were also a few cases where hormone status changed from positive to negative, 16 cases of luminal B changed to triple negative, and six cases changed to HER2. The reason for these discrepancies could be fixation conditions such as delayed, under-, or over-fixation with formalin; crush artifacts by needle sampling; or tumor heterogeneity.

In conclusion, CNB with adequate core passes can be reliably used to access molecular subtypes for systemic treatment in invasive breast cancer. Digital image analysis of Ki67 should be used to achieve better, more accurate molecular classifications from CNBs.

## ORCID

Ye Sul Jeong: <https://orcid.org/0000-0003-2952-1662>

Jun Kang: <https://orcid.org/0000-0002-7967-0917>

Jieun Lee: <https://orcid.org/0000-0002-2656-0650>

Tae-Kyung Yoo: <https://orcid.org/0000-0002-5790-353X>

Sung Hun Kim: <https://orcid.org/0000-0003-4478-9720>

Ahwon Lee: <https://orcid.org/0000-0002-2523-9531>

## Author Contributions

Conceptualization: AL.

Data curation: YSJ, TKY.

Formal analysis: YSJ, SHK, AL.

Methodology: YSJ, SHK, JK, AL.

Project administration: YSJ.

Resources: AL.

Supervision: AL.

Validation: YSJ, JL, AL.

Visualization: YSJ.

Writing—original draft: YSJ.

Writing—review & editing: YSJ, SHK, JK, AL.

## Conflicts of Interest

The authors declare that they have no potential conflicts of

interest.

## Funding

No funding to declare.

## REFERENCES

- Cheang MC, Chia SK, Voduc D, et al. Ki67 index, HER2 status, and prognosis of patients with luminal B breast cancer. *J Natl Cancer Inst* 2009; 101: 736-50.
- Goldhirsch A, Winer EP, Coates AS, et al. Personalizing the treatment of women with early breast cancer: highlights of the St Gallen International Expert Consensus on the Primary Therapy of Early Breast Cancer 2013. *Ann Oncol* 2013; 24: 2206-23.
- Goldhirsch A, Wood WC, Coates AS, et al. Strategies for subtypes: dealing with the diversity of breast cancer: highlights of the St. Gallen International Expert Consensus on the Primary Therapy of Early Breast Cancer 2011. *Ann Oncol* 2011; 22: 1736-47.
- Neubauer H, Gall C, Vogel U, et al. Changes in tumour biological markers during primary systemic chemotherapy (PST). *Anticancer Res* 2008; 28: 1797-804.
- Untch M, Konecny GE, Paepke S, von Minckwitz G. Current and future role of neoadjuvant therapy for breast cancer. *Breast* 2014; 23: 526-37.
- Teshome M, Hunt KK. Neoadjuvant therapy in the treatment of breast cancer. *Surg Oncol Clin N Am* 2014; 23: 505-23.
- Loibl S, Denkert C, von Minckwitz G. Neoadjuvant treatment of breast cancer: clinical and research perspective. *Breast* 2015; 24 Suppl 2: S73-7.
- Ge WK, Yang B, Zuo WS, et al. Evaluation of hormone receptor, human epidermal growth factor receptor-2 and Ki-67 with core needle biopsy and neoadjuvant chemotherapy effects in breast cancer patients. *Thorac Cancer* 2015; 6: 64-9.
- Piper GL, Patel NA, Patel JA, Malay MB, Julian TB. Neoadjuvant chemotherapy for locally advanced breast cancer results in alterations in preoperative tumor marker status. *Am Surg* 2004; 70: 1103-6.
- Meattini I, Bicchierai G, Saieva C, et al. Impact of molecular subtypes classification concordance between preoperative core needle biopsy and surgical specimen on early breast cancer management: single-institution experience and review of published literature. *Eur J Surg Oncol* 2017; 43: 642-8.
- Allred DC, Harvey JM, Berardo M, Clark GM. Prognostic and predictive factors in breast cancer by immunohistochemical analysis. *Mod Pathol* 1998; 11: 155-68.
- Wolff AC, Hammond ME, Allison KH, et al. Human epidermal growth factor receptor 2 testing in breast cancer: American Society of Clinical Oncology/College of American Pathologists Clinical Practice Guideline Focused Update. *J Clin Oncol* 2018; 36: 2105-22.
- Wolff AC, Hammond ME, Hicks DG, et al. Recommendations for human epidermal growth factor receptor 2 testing in breast cancer: American Society of Clinical Oncology/College of American Pathologists clinical practice guideline update. *J Clin Oncol* 2013; 31: 3997-4013.
- Cho U, Kim HE, Oh WJ, Yeo MK, Song BJ, Lee A. The long-term prognostic performance of Ki-67 in primary operable breast cancer and evaluation of its optimal cutoff value. *Appl Immunohistochem Mol Morphol* 2016; 24: 159-66.
- Dowsett M, Nielsen TO, A'Hern R, et al. Assessment of Ki67 in breast cancer: recommendations from the International Ki67 in Breast Cancer working group. *J Natl Cancer Inst* 2011; 103: 1656-64.
- Zidan A, Christie Brown JS, Peston D, Shousha S. Oestrogen and progesterone receptor assessment in core biopsy specimens of breast carcinoma. *J Clin Pathol* 1997; 50: 27-9.
- Rakha EA, Ellis IO. An overview of assessment of prognostic and predictive factors in breast cancer needle core biopsy specimens. *J Clin Pathol* 2007; 60: 1300-6.
- Park SY, Kim KS, Lee TG, et al. The accuracy of preoperative core biopsy in determining histologic grade, hormone receptors, and human epidermal growth factor receptor 2 status in invasive breast cancer. *Am J Surg* 2009; 197: 266-9.
- Ricci MD, Calvano Filho CM, Oliveira Filho HR, Filassi JR, Pinotti JA, Baracat EC. Analysis of the concordance rates between core needle biopsy and surgical excision in patients with breast cancer. *Rev Assoc Med Bras (1992)* 2012; 58: 532-6.
- Ozdemir A, Voyvoda NK, Gultekin S, Tuncbilek I, Dursun A, Yamac D. Can core biopsy be used instead of surgical biopsy in the diagnosis and prognostic factor analysis of breast carcinoma? *Clin Breast Cancer* 2007; 7: 791-5.
- Ough M, Velasco J, Hieken TJ. A comparative analysis of core needle biopsy and final excision for breast cancer: histology and marker expression. *Am J Surg* 2011; 201: 692-4.
- Chen J, Wang Z, Lv Q, et al. Comparison of core needle biopsy and excision specimens for the accurate evaluation of breast cancer molecular markers: a report of 1003 cases. *Pathol Oncol Res* 2017; 23: 769-75.
- You K, Park S, Ryu JM, et al. Comparison of core needle biopsy and surgical specimens in determining intrinsic biological subtypes of breast cancer with immunohistochemistry. *J Breast Cancer* 2017; 20: 297-303.
- Ensani F, Omranipour R, Jahanzad I, Jafari A, Nafarzadeh S, Aminishakib P. The core needle and surgical biopsy concordance to detect estrogen, progesterone, and Her-2 receptors in breast cancer: a com-

- parative study. *Iran J Pathol* 2017; 12: 202-8.
25. Liu M, Tang SX, Tsang JY, et al. Core needle biopsy as an alternative to whole section in IHC4 score assessment for breast cancer prognostication. *J Clin Pathol* 2018; 71: 1084-9.
  26. Lorgis V, Algros MP, Villanueva C, et al. Discordance in early breast cancer for tumour grade, estrogen receptor, progesteron receptors and human epidermal receptor-2 status between core needle biopsy and surgical excisional primary tumour. *Breast* 2011; 20: 284-7.
  27. Chen X, Sun L, Mao Y, et al. Preoperative core needle biopsy is accurate in determining molecular subtypes in invasive breast cancer. *BMC Cancer* 2013; 13: 390.
  28. Usami S, Moriya T, Amari M, et al. Reliability of prognostic factors in breast carcinoma determined by core needle biopsy. *Jpn J Clin Oncol* 2007; 37: 250-5.
  29. Robertson S, Ronnlund C, de Boniface J, Hartman J. Re-testing of predictive biomarkers on surgical breast cancer specimens is clinically relevant. *Breast Cancer Res Treat* 2019; 174: 795-805.
  30. Mazari FA, Sharma N, Dodwell D, Horgan K. Human epidermal growth factor 2-positive breast cancer with mammographic microcalcification: relationship to pathologic complete response after neoadjuvant chemotherapy. *Radiology* 2018; 288: 366-74.
  31. Nie Z, Wang J, Ji XC. Microcalcification-associated breast cancer: HER2-enriched molecular subtype is associated with mammographic features. *Br J Radiol* 2018 Jun 21 [Epub]. <https://doi.org/10.1259/bjr.20170942>.
  32. Fishman JE, Milikowski C, Ramsinghani R, Velasquez MV, Aviram G. US-guided core-needle biopsy of the breast: how many specimens are necessary? *Radiology* 2003; 226: 779-82.
  33. McIlhenny C, Doughty JC, George WD, Mallon EA. Optimum number of core biopsies for accurate assessment of histological grade in breast cancer. *Br J Surg* 2002; 89: 84-5.
  34. Greer LT, Rosman M, Mylander WC, et al. Does breast tumor heterogeneity necessitate further immunohistochemical staining on surgical specimens? *J Am Coll Surg* 2013; 216: 239-51.

## Clinicopathologic characteristics of HER2-positive pure mucinous carcinoma of the breast

Yunjeong Jang<sup>1</sup>, Hera Jung<sup>1</sup>, Han-Na Kim<sup>1</sup>, Youjeong Seo<sup>1</sup>, Emad Alsharif<sup>2</sup>, Seok Jin Nam<sup>3</sup>,  
 Seok Won Kim<sup>3</sup>, Jeong Eon Lee<sup>3</sup>, Yeon Hee Park<sup>4</sup>, Eun Yoon Cho<sup>1</sup>, Soo Youn Cho<sup>1</sup>

<sup>1</sup>Department of Pathology and Translational Genomics, Samsung Medical Center, Sungkyunkwan University College of Medicine, Seoul, Korea;

<sup>2</sup>Division of Breast and Endocrine Surgery, Specialized Surgical Unit, King Abdullah Medical City, Makkah, Saudi Arabia;

<sup>3</sup>Division of Breast Surgery, Department of Surgery, <sup>4</sup>Division of Hematology-Oncology, Department of Medicine, Samsung Medical Center, Sungkyunkwan University School of Medicine, Seoul, Korea

**Background:** Pure mucinous carcinoma (PMC) is a rare type of breast cancer, estimated to represent 2% of invasive breast cancer. PMC is typically positive for estrogen receptors (ER) and progesterone receptors (PR) and negative for human epidermal growth factor receptor 2 (HER2). The clinicopathologic characteristics of HER2-positive PMC have not been investigated. **Methods:** Pathology archives were searched for PMC diagnosed from January 1999 to April 2018. Clinicopathologic data and microscopic findings were reviewed and compared between HER2-positive PMC and HER2-negative PMC. We also analyzed the differences in disease-free survival (DFS) and overall survival according to clinicopathologic parameters including HER2 status in overall PMC cases. **Results:** There were 21 HER2-positive cases (4.8%) in 438 PMCs. The average tumor size of HER2-positive PMC was 32.21 mm ( $\pm$ 26.55). Lymph node metastasis was present in seven cases. Compared to HER2-negative PMC, HER2-positive PMC presented with a more advanced T category ( $p < .001$ ), more frequent lymph node metastasis ( $p = .009$ ), and a higher nuclear and histologic grade ( $p < .001$ ). Microscopically, signet ring cells were frequently observed in HER2-positive PMC ( $p < .001$ ), whereas a micropapillary pattern was more frequent in HER2-negative PMC ( $p = .012$ ). HER2-positive PMC was more frequently negative for ER (33.3% vs. 1.2%) and PR (28.6% vs. 7.2%) than HER2-negative PMC and showed a high Ki-67 labeling index. During follow-up, distant metastasis and recurrence developed in three HER2-positive PMC patients. Multivariate analysis revealed that only HER2-positivity and lymph node status were significantly associated with DFS. **Conclusions:** Our results suggest that HER2-positive PMC is a more aggressive subgroup of PMC. HER2 positivity should be considered for adequate management of PMC.

**Key Words:** Breast neoplasms; Receptor, ErbB-2; Pure mucinous adenocarcinoma

**Received:** September 10, 2019 **Revised:** October 23, 2019 **Accepted:** October 24, 2019

**Corresponding Author:** Soo Youn Cho, MD, PhD, Department of Pathology and Translational Genomics, Samsung Medical Center, Sungkyunkwan University School of Medicine, 81 Irwon-ro, Gangnam-gu, Seoul 06351, Korea

Tel: +82-2-3410-2817, Fax: +82-2-3410-0025, E-mail: sooyoun.cho@samsung.com

**Corresponding Author:** Eun Yoon Cho, MD, PhD, Department of Pathology and Translational Genomics, Samsung Medical Center, Sungkyunkwan University School of Medicine, 81 Irwon-ro, Gangnam-gu, Seoul 06351, Korea

Tel: +82-2-3410-2796, Fax: +82-2-3410-0025, E-mail: eunyocho@samsung.com

Breast mucinous carcinoma (MC) is defined as floating tumor clusters within extracellular mucin pools [1]. MC is divided into two subtypes, pure and mixed, according to the proportion of mucinous component in the tumor [1]. Pure MC (PMC) is composed of more than 90% mucinous component, is a rare type of breast cancer accounting for approximately 2% of invasive cancers, and usually occurs in elderly patients (> 55 years) [1,2]. PMC generally has a low nuclear grade and good prognosis [1,3].

Typical PMC is positive for estrogen receptor (ER) and progesterone receptor (PR), whereas it is negative for human epidermal growth factor receptor 2 (HER2) [1,3,4]. While HER2 overexpression occurs in 15%–20% of invasive breast cancers [5], it has been reported in only 2.6–9.0% of PMC [4,6-8]. Clinicopathologic characteristics of HER2-positive PMC have not been studied well because of the rarity of this entity. Herein, we investigate the clinicopathologic characteristics of HER2-positive PMC.

## MATERIALS AND METHODS

### Patients and data

The pathology archives of Samsung Medical Center were searched, and 637 PMC cases were diagnosed from January 1999 to April 2018, which accounted for 2.9% of 22,318 invasive breast cancer cases. Clinicopathologic data were archived from electronic medical records and pathology reports and comprised of sex, age, type of procedure, tumor size, nuclear grade, histologic grade, lymph node status, presence of lymphovascular invasion (LVI), extensive intraductal component (EIC), chemotherapy, hormonal therapy, radiotherapy, recurrence status, distant metastasis, and death. TNM classification was designated according to the 8th edition of the American Joint Committee on Cancer.

Cases were excluded if (1) the tumor were composed of less than 90% MC (i.e., mixed MC), (2) multiple synchronous carcinomas occurred with one or more tumors of non-mucinous histology that were of comparable size or larger than the PMC, (3) tumor size was less than 0.1 cm (microinvasive carcinoma), (4) surgery was not performed, or (5) tumor slides were not available for review. Ultimately, 438 PMC cases were included.

### Histologic review

Tumor slides were re-evaluated by two pathologists (Y.J. Jang and S.Y. Cho). Nuclear grade and histologic grade were classified on the basis of the Bloom-Richardson grading system [1]. EIC was defined as more than 25% ductal carcinoma in situ area within the invasive carcinoma [1]. Cases were subdivided into type A or type B depending on the cellularity of tumor cells,

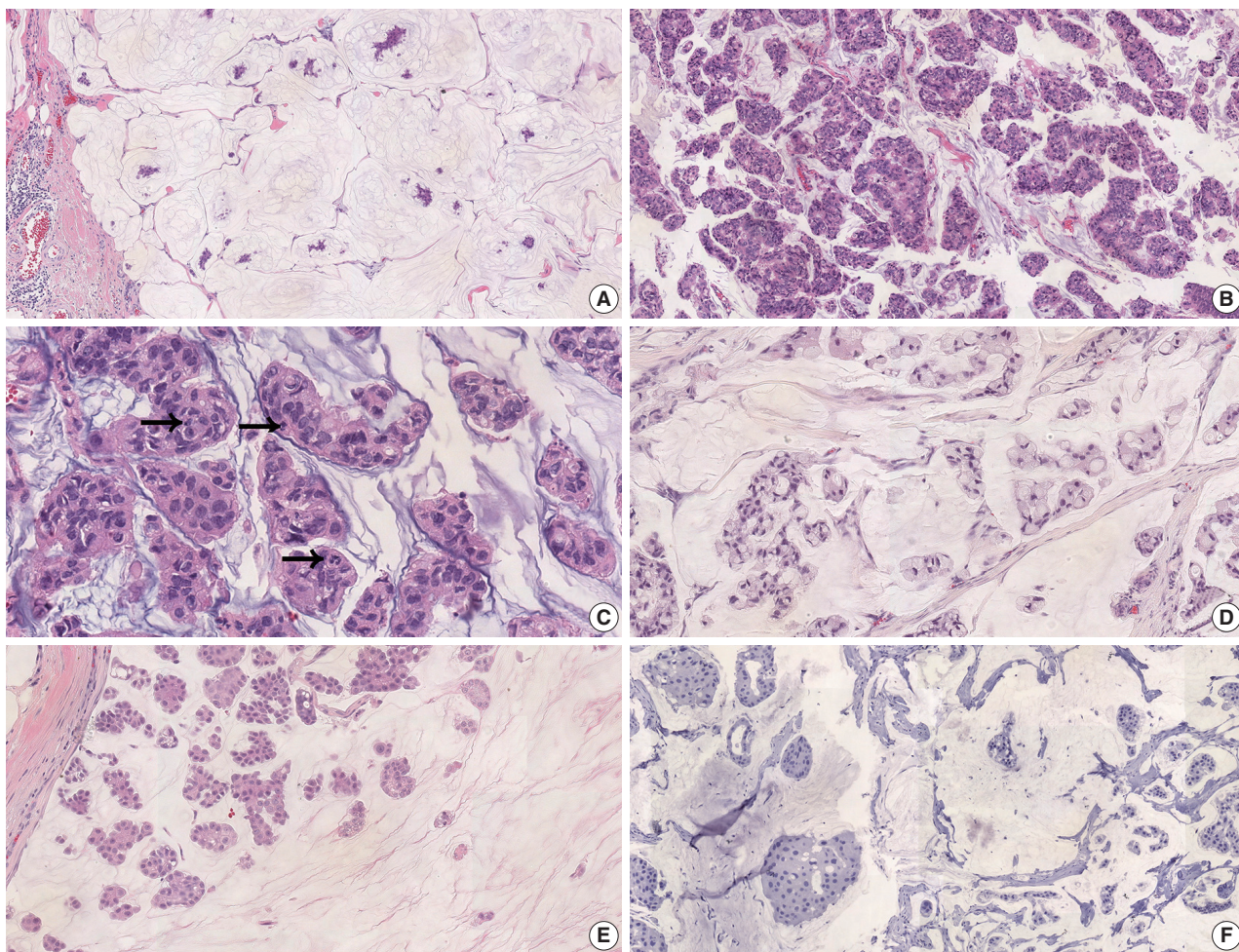


**Fig. 1.** Pure mucinous carcinoma (PMC). (A) Hypocellular type A PMC with abundant extracellular mucin pool. (B) Hypercellular type B pattern. (C) Human epidermal growth factor receptor 2 (HER2)-positive PMC shows high nuclear and histologic grade. There are frequent mitoses (arrows). (D) Some HER2-positive PMC shows extensive signet ring cell differentiation. (E) Some PMC presents a micropapillary pattern. (F) HER2-positive PMC is frequently negative for estrogen receptor.

i.e., classic, hypocellular tumors with more extracellular mucin were classified as type A (Fig. 1A), and hypercellular PMC with large cell clusters were classified as type B (Fig. 1B) [1]. The presence of a micropapillary component or signet ring cells was also evaluated.

### Immunohistochemistry and silver in situ hybridization

Immunohistochemistry (IHC) for ER (1:200, clone 6F11, Bond-Max System, Novocastra, Newcastle upon Tyne, UK), PR (1:800, clone 16, Bond-Max System, Novocastra), HER2 (4B5, BenchMark XT, Ventana, Tucson, AZ, USA), and Ki-67 (1:200, clone MIB-1, Bond-III, Dako, Glostrup, Denmark) was performed on formalin-fixed paraffin-embedded (FFPE) tissue. Silver in situ hybridization (SISH) analysis was performed using INFORM DDISH HER-2 SISH probe kits (BenchMark XT, Ventana) on FFPE tissue. ER and PR were considered positive when at least 1% of tumor cells showed nuclear staining according

to the American Society of Clinical Oncology/College of American Pathologists guidelines [9]. HER2 was considered positive if  $\geq 10\%$  of tumor cells showed 3+ staining by IHC or 2+ staining by IHC with amplification using SISH [10]. The Ki-67 labeling index was determined via automated image analysis. After the Ki-67-stained slide was scanned under  $\times 20$  magnification (Ventana iScan), the percentage of positively stained cells was calculated using image analysis software (Ventana Virtuoso, ver. 5.6).

### Statistical analysis

Categorical variables were analyzed using t tests and chi-square tests. Disease-free survival (DFS) and overall survival (OS) were defined as the duration from pathologic diagnosis to recurrence/progression and death, respectively. DFS and OS were plotted using the Kaplan-Meier method. A log-rank test was used to evaluate differences in survival. Multivariate analyses were performed to assess the prognostic factors for survival using a Cox proportional

**Table 1.** Clinicopathologic features of HER2-positive pure mucinous carcinoma

Case	Age (yr)	Sex	Procedure	Mass size (mm)	T category	No. of positive LNs	N category	Nuclear grade	Histologic grade	ER	PR	Type A/B	Structure	Recurrence	Follow-up	Trastuzumab	
1	60	F	T	A	30.0	2	0	0	3	III	-	-	B	SRC	NED	ND	
2	41	F	B	S	15.0	1	0	0	3	III	+	+	B	None	NED	ND	
3	43	F	T	S	3.0	1	0	0	2	II	+	+	A	None	NED	ND	
4	28	F	B	S	15.0	1	0	0	3	III	+	+	B	SRC	NED	ND	
5	60	F	T	A	70.0	3	1	1	3	III	-	-	A	MP/SRC	NED	ND	
6	43	F	B	S	4.0	1	0	0	2	II	-	+	A	None	NED	ND	
7	53	F	T	S	4.5	1	0	0	2	II	+	-	B	SRC	NED	ND	
8	46	F	T	A	65/60 <sup>a</sup>	3	5	2	2	II	-	-	A	MP/SRC	Local recurrence	DOD	ND
9	39	F	T	A	38.0	2	0	0	2	II	+	+	NA	None	Metastasis to lung and brain	DOC	ND
10	55	F	B	S	15.0	1	0	0	3	III	+	+	A	MP	NED	NA	
11	37	F	B	S	55/0 <sup>b</sup>	3	NA <sup>b</sup>	NA <sup>b</sup>	2	II	-	+	B	SRC	NED	Done <sup>c</sup>	
12	46	F	T	A	85/70 <sup>a</sup>	3	7	2	3	III	+	+	A	None	NED	Done <sup>c</sup>	
13	48	F	B	A	90/80 <sup>a</sup>	3	1	1	2	II	+	+	A	SRC	NED	Done <sup>c</sup>	
14	63	F	B	S	16.0	1	0	0	3	III	+	+	A	SRC	NED	Done	
15	40	F	B	A	30/10 <sup>a</sup>	2	2	1	NA	NA	+	+	NA	NA	NED	Done	
16	38	F	B	S	12.0	1	0	0	2	II	-	-	A	MP	NED	Done	
17	32	F	T	A	16.0	1	0	0	3	III	+	+	A	SRC	NED	Done	
18	34	F	B	S	40.0	2	0	0	2	II	-	-	A	SRC	NED	Done	
19	41	F	T	A	41.0	2	2	1	3	III	+	+	B	SRC	NED	Done	
20	50	F	B	S	16.0	1	0	0	2	II	+	+	A	SRC	NED	Done	
21	54	F	T	A	16/19 <sup>a</sup>	1	22	3	3	III	+	+	A	MP	Metastasis to skin and lung	DOC	Done

HER2, human epidermal growth factor receptor 2; ER, estrogen receptor; PR, progesterone receptor; F, female; T, total mastectomy; A, axillary lymph node dissection; SRC, signet ring cells; NED, no evidence of disease; ND, not done; B, breast conserving surgery; S, sentinel lymph node biopsy; MP, micropapillary; DOD, died of disease; NA, not applicable; DOC, died of other cause.

<sup>a</sup>For cases with neoadjuvant chemotherapy, tumor size before/after treatment were recorded; <sup>b</sup>In this patient, lymph node metastasis was suspected in radiologic images, but pathologic confirmation was not performed due to pathologic complete response; <sup>c</sup>Used trastuzumab for neoadjuvant chemotherapy.

hazards model. A p-value less than .05 was considered statistically significant. All statistical analyses were performed using SPSS software ver. 25.0 (IBM Corp., Armonk, NY, USA).

### Ethics statement

This study was approved by the Institutional Review Board of Samsung Medical Center, and the need for informed consent was waived (IRB No. 2019-08-051).

## RESULTS

### Basic characteristics of HER2-positive pure mucinous carcinoma

Basic clinicopathologic characteristics are summarized in Table 1. Twenty-one HER2-positive cases were included, accounting for 4.8% of 438 PMC. Seventeen cases were HER2 IHC 3+, and the remaining four cases showed equivocal (2+) staining, of which *HER2* amplification were confirmed using SISH. All 21 patients were female, and their mean age was 45 years. Ten patients underwent total mastectomy, and 11 patients underwent conserving surgery. Axillary lymph node dissection was performed in 10 cases, and sentinel node biopsy alone was performed in the remaining 11 cases. Six patients received neoadjuvant chemotherapy, and their T category before treatment was cT1 in one case, cT2 in one case, and cT3 in four cases. Among them, three patients (cases Nos. 11, 12, and 13) received neoadjuvant chemotherapy including trastuzumab. One patient showed pathologic complete response (case No. 11). The T category of the remaining 15 patients was pT1 in 10 cases, pT2 in four cases, and pT3 in one case. Nodal metastasis was present in seven cases (35.0%). Eleven patients received trastuzumab treatment after surgery. Distant metastasis occurred in two patients (9.5%) (lung and brain, one; skin and lung, one each), and local recurrence occurred in one patient (4.8%). Distant metastasis and local recurrence occurred in two of nine patients without trastuzumab treatment (22.2%) and one of 11 patients with trastuzumab treatment (9.1%) ( $p = .421$ ).

### Microscopic findings of HER2-positive pure mucinous carcinoma

Nuclear grade was two in 10 cases (50.0%) and three in 10 cases (50.0%). Histologic grade was II in 10 cases (50.0%) and III in 10 cases (50.0%) (Fig. 1C). EIC was present in 10 cases (50.0%). LVI was present in five cases (25%). Thirteen cases (68.4%) were classified as type A, and six cases (31.6%) were classified as type B. Signet ring cells were present in 12 cases (60.0%) (Fig.

1D). In two cases, the tumor was comprised of >90% of signet ring cells. The micropapillary component was present in five cases (25.0%) (Fig. 1E). ER was positive in 14 cases (66.7%) and negative in seven cases (33.3%) (Fig. 1F). PR was positive in 15 cases (71.4%) and negative in six cases (28.6%).

### Comparison of clinicopathologic characteristics between HER2-positive and HER2-negative pure mucinous carcinoma

Clinicopathologic characteristics of HER2-positive and HER2-negative PMC are summarized in Table 2. Average follow-up duration was 69 months (range, 1 to 227 months). Mean age was younger in the HER2-positive group without statistical significance ( $p = .073$ ). Tumor size was larger ( $p < .001$ ) and axillary lymph node metastasis was more common in the HER2-positive group ( $p = .009$ ). Nuclear and histologic grades were higher in the HER2-positive group than in the HER2-negative group ( $p < .001$  and  $p < .001$ ). Distribution of tumor type (mucinous type A or B) was similar in the two groups ( $p = .940$ ). The micropapillary pattern was more frequent in HER2-negative PMC ( $p = .012$ ), whereas signet ring cells were frequently observed in the HER2-positive PMC ( $p < .001$ ). In HER2-positive PMC, EIC was more common (50.0% vs. 21.9%,  $p = .011$ ), and LVI tended to occur more frequently without statistical significance (25.0% vs. 12.2,  $p = .158$ ). ER was negative in seven HER2-positive PMC (33.3%), while there were only five HER2-negative PMC (1.2%) ( $p < .001$ ). PR was negative in six cases of HER2-positive PMC (28.6%); in contrast, PR was negative in 30 cases of HER2-negative PMC (7.2%) ( $p = .005$ ). HER2-positive PMC cases showed a more frequent high Ki-67 labeling index ( $\geq 20\%$ ) ( $p = .006$ ).

### Prognosis of pure mucinous carcinoma

Recurrence or distant metastasis occurred in 16 cases (3.7%), and 17 deaths were observed. In three cases, the cause of death was breast cancer (HER2-negative PMC, two cases; HER2-positive PMC, one case). Nuclear and histologic grades, T category, lymph node status, LVI, and HER2 status were significantly associated with DFS in univariate analysis using a log-rank test (Table 3). The 10-year DFS was significantly lower in HER2-positive PMC (DFS, 78.1% vs 93.9%,  $p = .001$ ) (Fig. 2). In multivariate analysis, only lymph node status and HER2 positivity were significantly associated with DFS (relative risk [RR], 4.818;  $p = .005$  and RR, 7.822;  $p = .002$ ) (Table 4). In univariate analysis of OS, lymph node status and HER2 positivity had significance. In multivariate analysis, only lymph node status retained significance (RR, 11.72;  $p = .045$ ) (Table 4).

**Table 2.** Clinicopathologic characteristics of patients with HER2-positive and HER2-negative PMC

Variable	Total (n=438)	HER2-negative PMC (n=417)	HER2-positive PMC (n=21)	p-value
Age (yr)	49.92	50.15	45.29	.073
Sex				
Female	431	410	21	
Male	7	7	0	
Tumor size (mm)	21.3±14.41	20.73±13.34	32.21±26.55	<.001
T category				<.001
T1	242	231 (55.5)	11 (52.4)	
T2	174	169 (40.6)	5 (23.8)	
T3	21	16 (3.8)	5 (23.8)	
Lymph node status <sup>a</sup>				.009
Negative	378	365 (88.0)	13 (65.0)	
Positive	57	50 (12.0)	7 (35.0)	
Nuclear grade <sup>a</sup>				<.001
1	200	200 (48.0)	0	
2	217	207 (49.6)	10 (50.0)	
3	20	10 (2.4)	10 (50.0)	
Histologic grade <sup>a</sup>				<.001
I	248	248 (59.5)	0	
II	166	156 (37.4)	10 (50.0)	
III	23	13 (3.1)	10 (50.0)	
ER				<.001
Negative	12	5 (1.2)	7 (33.3)	
Positive	424	410 (98.8)	14 (66.7)	
PR				.005
Negative	36	30 (7.2)	6 (28.6)	
Positive	400	385 (92.8)	15 (71.4)	
KI-67 <sup>a</sup>				.006
<20%	244	236 (84.6)	8 (53.3)	
≥20%	50	43 (15.4)	7 (46.7)	
Type A/B <sup>a</sup>				.940
A	301	288 (69.2)	13 (68.4)	
B	134	128 (30.8)	6 (31.6)	
EIC <sup>a</sup>				.011
Negative	328	318 (78.1)	10 (50.0)	
Positive	99	89 (21.9)	10 (50.0)	
LVI <sup>a</sup>				.158
Absent	346	331 (87.8)	15 (75.0)	
Present	51	46 (12.2)	5 (25.0)	
MP <sup>a</sup>				.012
Absent	207	192 (46.2)	15 (75.0)	
Present	229	224 (53.8)	5 (25.0)	
SRC <sup>a</sup>				<.001
Absent	376	368 (88.5)	8 (40.0)	
Present	60	48 (11.5)	12 (60.0)	
Operation				.182
Excision	7	7 (1.7)	0	
Conserving surgery	299	288 (69.1)	11 (52.4)	
Total mastectomy	132	122 (29.3)	10 (47.6)	
Lymph node dissection				.011
Sentinel biopsy	329	318 (76.8)	11 (52.4)	

(Continued)

Variable	Total (n=438)	HER2-negative PMC (n=417)	HER2-positive PMC (n=21)	p-value
Axillary dissection	106	96 (23.2)	10 (47.6)	
Chemotherapy <sup>a</sup>				<.001
No	320	315 (76.1)	5 (25.0)	
Yes	114	99 (23.9)	15 (75.0)	
Trastuzumab treatment <sup>a</sup>				
No			9 (45.0)	
Yes			11 (55.0)	
Radiotherapy <sup>a</sup>				.199
No	119	111 (26.9)	8 (40.0)	
Yes	314	302 (73.1)	12 (60.0)	
Hormone therapy <sup>a</sup>				.001
No	11	7 (1.7)	4 (20.0)	
Yes	420	404 (98.3)	16 (80.0)	

Values are presented as number (%) or mean ± standard deviation.

HER2, human epidermal growth factor receptor 2; PMC, pure mucinous carcinoma; ER, estrogen receptor; PR, progesterone receptor; EIC, extensive intraductal component; LVI, lymphovascular invasion; MP, micropapillary pattern; SRC, signet ring cell pattern.

<sup>a</sup>There are some missing data.**Table 3.** Univariate analysis of DFS and OS using Kaplan-Meier plot and log-rank test in pure mucinous carcinoma

	p-value	
	DFS	OS
T category	.003	.072
Node metastasis	<.001	.011
Nuclear grade	.003	.548
Histologic grade	.021	.494
ER	.588	.103
PR	.296	.755
HER2	.001	.026
Ki-67 (≥20%)	.395	-
Type A/B	.127	.877
Structure (MP)	.761	.085
Structure (SRC)	.788	.515
EIC	.772	.914
LVI	<.001	.127

DFS, disease-free survival; OS, overall survival; ER, estrogen receptor; PR, progesterone receptor; MP, micropapillary pattern; SRC, signet ring cell pattern; EIC, extensive intraductal component; LVI, lymphovascular invasion.

## DISCUSSION

PMC is a rare subtype of breast cancer characterized by extracellular mucin pools with floating tumor cells [1]. Typical PMC belongs to the luminal A molecular subtype; most PMC is low grade, positive for ER and/or PR, and negative for HER2 [1-4]. PMC generally shows favorable prognosis. However, some studies reported that ER/PR negativity and high grade are associated with a poor prognosis in PMC [11,12].

While HER2 amplification occurs in 15%–20% of invasive

breast cancer [5], it is very rare in PMC and is reported to occur in 2.6%–9% of cases [4,6–8]. In our cohort, 4.8% of PMC showed HER2 positivity, consistent with previous studies. HER2-positive breast cancer is typically poorly differentiated and high grade, has high rates of cell proliferation and lymph node involvement, and is relatively resistant to certain types of chemotherapy [13]. Clinicopathologic characteristics of HER2-positive PMC have not been well investigated because of its very low incidence. This study was the first to describe clinicopathologic features of HER2-positive PMC in a large series. HER2-positive PMC showed higher nuclear and histologic grades, more frequent

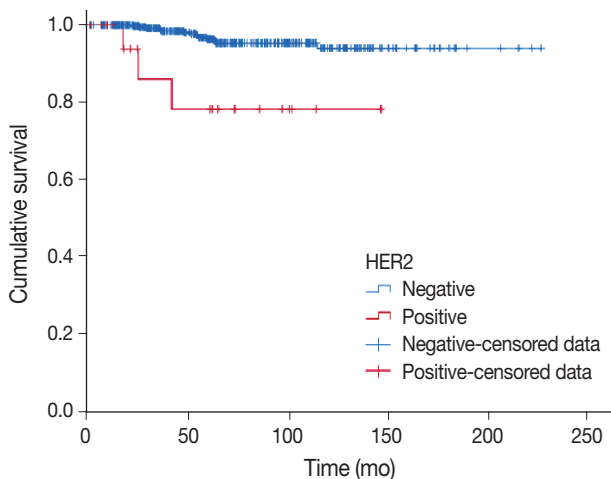


**Fig. 2.** Kaplan-Meier plots for disease-free survival of pure mucinous carcinoma according to human epidermal growth factor receptor 2 (HER2) status.

axillary lymph node metastasis, and a more advanced stage at the time of diagnosis than HER2-negative PMC. HER2 status was significantly associated with DFS in multivariate and univariate analyses. However, this would have to be further validated because of the few events in our series. Recently, Gwark et al. [14] also reported worse prognosis of HER2-positive PMC among PMC cases that were hormone receptor positive and node negative with a tumor size  $\geq 3$  cm.

Clinically, HER2-positive PMC has important implications for patient management. Although there was no difference in recurrence or survival according to trastuzumab treatment in this study, the effects of anti-HER2 agents including trastuzumab on survival of HER2-positive breast cancers are well known [5]. Our result might be due to the limited number of cases. Besides, we experienced a case of HER2-positive PMC with pathologic complete response after neoadjuvant chemotherapy with trastuzumab and pertuzumab (case No. 11) [15]. Gwark et al. [14] also reported better prognosis of patients treated with trastuzumab than without trastuzumab among HER2-positive hormone receptor-positive PMC. In our study population, only 11 patients received trastuzumab as either neoadjuvant or adjuvant treatment. None of the patients who were initially diagnosed before 2009 received trastuzumab, whereas all but three patients who were diagnosed after 2009 received trastuzumab treatment. Tumors of two patients were too small (0.4 cm and 0.45 cm), and in one patient, trastuzumab use was uncheckable because of her referral to an outside hospital. Clinicians should be aware of HER2-positive PMC and manage according to immunophenotype of

**Table 4.** Multivariate analysis of DFS and OS using the Cox proportion hazard model in pure mucinous carcinoma

	DFS		OS	
	Multivariate RR (95% CI)	p-value	Multivariate RR (96% CI)	p-value
T category				
1	1	.535	-	
2	1.069 (0.275–4.156)	.924		
3	2.892 (0.411–20.324)	.286		
Node metastasis	4.818 (1.609–14.424)	.005	11.724 (1.059–129.775)	.045
Nuclear grade				
1	1	.629	-	
2	2.532 (0.345–18.608)	.361		
3	5.113 (0.046–565.687)	.497		
Histologic grade				
I	1	.977	-	
II	1.091 (0.207–5.742)	.918		
III	0.731 (0.008–66.579)	.892		
HER2	7.822 (2.130–28.722)	.002	2.738 (0.189–39.568)	.460
LVI	2.355 (0.559–9.928)	.243	-	

DFS, disease-free survival; OS, overall survival; RR, relative risk; CI, confidence interval; HER2, human epidermal growth factor receptor 2; LVI, lymphovascular invasion.

PMC, as in usual breast cancers.

Previous case reports of our group and others reported signet ring cell components in HER2-positive PMC [15-17]. Micropapillary features have been suggested to have an association with HER2 positivity [18]. Thus, we evaluated micropapilla and signet ring cells in PMC. Interestingly, the presence of signet ring cells was significantly associated with HER2 positivity in PMC, with 12/20 cases showing signet ring cells (60.0%). In contrast, 48 HER2-negative PMC patients (11.5%) showed signet ring cell differentiation. Extracellular mucin pools are a characteristic feature of PMC, and intracellular accumulation of mucin is a feature of signet ring cells. Coexistence of extracellular and intracellular mucin with HER2 positivity remains unexplained. Although carcinomas with signet ring cell differentiation are not a distinct disease entity in the World Health Organization classification [1], our result suggests signet ring cell differentiation may represent a specific histologic feature associated with HER2 positivity in PMC [15-17]. Micropapillary features were quite common in overall PMC (53.8%) and were more frequently observed in HER2-negative PMCs than in HER2-positive PMCs. The prognostic significance of micropapillary features in PMC remains controversial. Some studies suggested more aggressive behavior of PMC with micropapillary features [19], whereas others showed no association [20]. Recently, Xu et al. [21] reported that micropapillary features are common in PMC (80%), and micropapillary features with low nuclear grade are associated with indolent biologic behavior. This might explain the discordant results of previous studies and frequent presence of micropapillary features in HER2-negative PMC in our study.

Typical PMC is a luminal A type breast cancer with low nuclear grade, high ER expression, and HER2 negativity. However, as shown in this study, there is a minor proportion of HER2-positive PMCs, which showed aggressive histologic and clinical features, including high nuclear grade, high histologic grade, large tumor size, a frequent extensive intraductal component, and lymph node metastasis. Signet ring cells were also significantly associated with HER2-positive PMC. Finally, HER2 positivity in PMC was significantly associated with poor DFS in univariate and multivariate analyses. Consideration of HER2 positivity in PMC is important for treatment decisions regarding the use of HER2 target therapy.

## ORCID

Yunjeong Jang: <https://orcid.org/0000-0002-8997-9686>

Hera Jung: <https://orcid.org/0000-0002-4269-1546>

Han-Na Kim: <https://orcid.org/0000-0001-5171-3658>

Youjeong Seo: <https://orcid.org/0000-0003-4595-3836>

Emad Alsharif: <https://orcid.org/0000-0002-6433-4697>

Seok Jin Nam: <https://orcid.org/0000-0003-1072-8954>

Seok Won Kim: <https://orcid.org/0000-0002-6130-7570>

Jeong Eon Lee: <https://orcid.org/0000-0003-0037-2456>

Yeon Hee Park: <https://orcid.org/0000-0003-4156-9212>

Eun Yoon Cho: <https://orcid.org/0000-0001-5849-3600>

Soo Youn Cho: <https://orcid.org/0000-0001-9714-7575>

## Author Contributions

Conceptualization: SYC, EYC, JEL.

Data Curation: YJ.

Formal analysis: YJ, SYC.

Investigation: YJ, HJ, HNK, YS, EA, SJN, SWK, JEL, YHP.

Project administration: YJ, YS.

Supervision: SYC, EYC.

Writing—original draft: YJ, SYC.

Writing—review & editing: YJ, SYC, EYC.

## Conflicts of Interest

The authors declare that they have no potential conflicts of interest.

## Funding

No funding to declare.

## REFERENCES

1. Lakhani SR, Ellis IO, Schnitt SJ, Tan PH, van de Vijver MJ. WHO classification of tumours of the breast. 4th ed. Lyon: IARC Press, 2012.
2. Di Saverio S, Gutierrez J, Avisar E. A retrospective review with long term follow up of 11,400 cases of pure mucinous breast carcinoma. *Breast Cancer Res Treat* 2008; 111: 541-7.
3. Barkley CR, Ligibel JA, Wong JS, Lipsitz S, Smith BL, Golshan M. Mucinous breast carcinoma: a large contemporary series. *Am J Surg* 2008; 196: 549-51.
4. Lacroix-Triki M, Suarez PH, MacKay A, et al. Mucinous carcinoma of the breast is genomically distinct from invasive ductal carcinomas of no special type. *J Pathol* 2010; 222: 282-98.
5. Loibl S, Gianni L. HER2-positive breast cancer. *Lancet* 2017; 389: 2415-29.
6. Bae SY, Choi MY, Cho DH, Lee JE, Nam SJ, Yang JH. Mucinous carcinoma of the breast in comparison with invasive ductal carcinoma: clinicopathologic characteristics and prognosis. *J Breast Cancer*

- 2011; 14: 308-13.
7. Pan B, Yao R, Shi J, et al. Prognosis of subtypes of the mucinous breast carcinoma in Chinese women: a population-based study of 32-year experience (1983-2014). *Oncotarget* 2016; 7: 38864-75.
  8. Ranade A, Batra R, Sandhu G, Chitale RA, Balderacchi J. Clinicopathological evaluation of 100 cases of mucinous carcinoma of breast with emphasis on axillary staging and special reference to a micropapillary pattern. *J Clin Pathol* 2010; 63: 1043-7.
  9. Hammond ME, Hayes DF, Dowsett M, et al. American Society of Clinical Oncology/College Of American Pathologists guideline recommendations for immunohistochemical testing of estrogen and progesterone receptors in breast cancer. *J Clin Oncol* 2010; 28: 2784-95.
  10. Wolff AC, Hammond ME, Hicks DG, et al. Recommendations for human epidermal growth factor receptor 2 testing in breast cancer: American Society of Clinical Oncology/College of American Pathologists clinical practice guideline update. *J Clin Oncol* 2013; 31: 3997-4013.
  11. Fu J, Wu L, Jiang M, et al. Clinical nomogram for predicting survival outcomes in early mucinous breast cancer. *PLoS One* 2016; 11: e0164921.
  12. Avisar E, Khan MA, Axelrod D, Oza K. Pure mucinous carcinoma of the breast: a clinicopathologic correlation study. *Ann Surg Oncol* 1998; 5: 447-51.
  13. Burstein HJ. The distinctive nature of HER2-positive breast cancers. *N Engl J Med* 2005; 353: 1652-4.
  14. Gwark SC, Lee HS, Lee Y, et al. Clinical implication of HER2 status in hormone receptor-positive mucinous breast cancer. *Ann Surg Oncol* 2019; 26: 2166-74.
  15. Jang Y, Cho EY, Cho SY. Human epidermal growth factor receptor 2-positive mucinous carcinoma with signet ring cell differentiation, which showed complete response after neoadjuvant chemotherapy. *J Breast Cancer* 2019; 22: 336-40.
  16. Kim HM, Kim EK, Koo JS. Mucinous carcinoma with extensive signet ring cell differentiation: a case report. *J Pathol Transl Med* 2017; 51: 176-9.
  17. Leung KM, Yeoh GP, Chan JK, Cheung PS, Chan KW. Ductal type signet ring cell carcinoma of breast with growth pattern of pure mucinous carcinoma. *Pathology* 2011; 43: 282-4.
  18. Varga Z, Zhao J, Ohlschlegel C, Odermatt B, Heitz PU. Preferential HER-2/neu overexpression and/or amplification in aggressive histological subtypes of invasive breast cancer. *Histopathology* 2004; 44: 332-8.
  19. Barbashina V, Corben AD, Akram M, Vallejo C, Tan LK. Mucinous micropapillary carcinoma of the breast: an aggressive counterpart to conventional pure mucinous tumors. *Hum Pathol* 2013; 44: 1577-85.
  20. Kim HJ, Park K, Kim JY, Kang G, Gwak G, Park I. Prognostic significance of a micropapillary pattern in pure mucinous carcinoma of the breast: comparative analysis with micropapillary carcinoma. *J Pathol Transl Med* 2017; 51: 403-9.
  21. Xu X, Bi R, Shui R, et al. Micropapillary pattern in pure mucinous carcinoma of the breast: does it matter or not? *Histopathology* 2019; 74: 248-55.

# Expression of female sex hormone receptors and its relation to clinicopathological characteristics and prognosis of lung adenocarcinoma

Jin Hwan Lee, Han Kyeom Kim, Bong Kyung Shin

Department of Pathology, Korea University Guro Hospital, Korea University College of Medicine, Seoul, Korea

**Background:** Adenocarcinoma (ADC) of the lung exhibits different clinicopathological characteristics in men and women. Recent studies have suggested that these differences originate from the expression of female sex hormone receptors in tumor cells. The aim of the present study was to evaluate the immunohistochemical expression of female sex hormone receptors in lung ADC and determine the expression patterns in patients with different clinicopathological characteristics. **Methods:** A total of 84 patients with lung ADC who underwent surgical resection and/or core biopsy were recruited for the present study. Immunohistochemical staining was performed for estrogen receptor  $\alpha$  (ER $\alpha$ ), estrogen receptor  $\beta$  (ER $\beta$ ), progesterone receptor (PR), epidermal growth factor receptor (EGFR), *EGFR* E746-A750 del, and *EGFR* L858R using tissue microarray. **Results:** A total of 39 (46.4%) ER $\alpha$ -positive, 71 (84.5%) ER $\beta$ -positive, and 46 (54.8%) PR-positive lung ADCs were identified. In addition, there were 81 (96.4%) EGFR-positive, 14 (16.7%) *EGFR* E746-A750 del-positive, and 34 (40.5%) *EGFR* L858R-positive cases. The expression of female sex hormone receptors was not significantly different in clinicopathologically different subsets of lung ADC. **Conclusions:** Expression of female sex hormone receptors is not associated with the prognosis and clinicopathological characteristics of patients with lung ADC.

**Key Words:** Adenocarcinoma of lung; Receptors, estrogen; ER $\alpha$ ; ER $\beta$ ; Receptors, progesterone; Prognosis

**Received:** August 2, 2019 **Revised:** September 22, 2019 **Accepted:** October 12, 2019

**Corresponding Author:** Bong Kyung Shin, MD, PhD, Department of Pathology, Korea University Guro Hospital, Korea University College of Medicine, 148 Gurodong-ro, Guro-gu, Seoul 08308, Korea

Tel: +82-2-2626-1472, Fax: +82-2-2626-1486, E-mail: tabrega@korea.ac.kr

Lung cancer is a difficult malignancy to treat and has a high mortality rate worldwide [1]. Smoking was thought to be a major cause of lung cancer, but a large number of lung cancer cases have occurred regardless of smoking status, especially adenocarcinoma (ADC) in women [2,3]. As female sex hormones were demonstrated to be involved in the differentiation and maturation of fetal lung tissue [4], it was suggested that they may also be involved in the development and tissue differentiation of lung cancer. The risk of lung ADC is lower in women with menopause at a relatively young age, and a significant positive correlation has been identified between hormone replacement therapy and the incidence of lung ADC [5,6], suggesting that female sex hormones may serve certain roles in the development of lung ADC. Mollerup et al. [7] demonstrated that estrogen receptor (ER) gene expression was significantly increased in the normal lung tissue of patients with non-small cell lung cancer

and non-small cell lung cancer cell lines; the effects of estrogen on cell proliferation were tissue- and cell type-specific. These results suggested a possible role of ERs in lung carcinogenesis [7].

Studies on the prognostic effects of female sex hormone receptor expression on lung cancer have exhibited inconsistent results. In a study conducted by Kawai et al. [8], patients with non-small cell lung cancer with upregulation of estrogen receptor  $\alpha$  (ER $\alpha$ ) and downregulation of estrogen receptor  $\beta$  (ER $\beta$ ) exhibited poor prognoses. Stabile et al. [9] demonstrated that high expression of ER $\beta$  and low expression of progesterone receptor (PR) were associated with rapid progression of lung cancer. Hsu et al. [10] also reported that the prognosis of patients with ER $\beta$ -positive lung ADC was poor. By contrast, studies by Schwartz et al. [11] and Skov et al. [12] demonstrated that the expression of ER $\beta$  was associated with good prognosis in non-small cell lung cancer.

The aim of the present study was to analyze the association

between female sex hormone receptor expression and clinicopathological characteristics of lung ADC and to determine the clinical significance of female sex hormone receptors and their potential use as prognostic factors.

## MATERIALS AND METHODS

Patients diagnosed with lung ADC at Korea University Guro Hospital (Seoul, Korea) between 2010 and 2012 and treated or followed for > 1 month were included in this study, with the exception of those with a history of cancer or chemotherapy. Hematoxylin and eosin (H&E)-stained glass slides, paraffin tissue blocks, and medical records from 84 patients who underwent surgical resection or biopsy were collected. The medical records included clinical information such as sex, age, smoking history, menopause status, disease relapse, death, and follow-up period, as well as pathological information such as tumor size, stage, histological classification, invasion of vessels/lymph nodes/nerves, and epidermal growth factor receptor (*EGFR*) gene mutation peptide nucleic acid clamping quantitative polymerase chain reaction results. All of the glass slides, paraffin blocks, and clinicopathological information were provided by the Korea University Guro Hospital Biobank, which is a member of the Korea Biobank Network.

In the collected paraffin blocks, representative cancer areas were identified by contrasting with H&E-stained glass slides, and one to three 2-mm cores were obtained and transferred to empty paraffin blocks to construct tissue microarray (TMA) blocks. The TMAs were sectioned in 4- $\mu$ m slices, mounted on glass slides, and stained with H&E. They were also stained immunohistochemically using a Bond-III automatic stainer (Leica Biosystems Nussloch GmbH, Wetzlar, Germany) or a BenchMark ULTRA automatic stainer (Ventana Medical Systems, Inc., Tucson, AZ, USA). The antibodies used were as follows: anti-ER $\alpha$  (Ready-To-Use [RTU], clone SP1, Ventana Medical Systems, Inc.), anti-ER $\beta$  (1:100, clone 14C8, Abcam, Cambridge, UK), anti-PR (RTU, clone 1E2, Ventana Medical Systems, Inc.), anti-androgen receptor (AR; 1:50, clone AR27, Leica Biosystems Nussloch GmbH), anti-EGFR (RTU, clone 3C6, Ventana Medical Systems, Inc.), anti-*EGFR* E746-A750 del (RTU, clone SP111, Ventana Medical Systems, Inc.), and anti-*EGFR* L858R (RTU, clone SP125, Ventana Medical Systems, Inc.).

The results of the immunohistochemical (IHC) staining were assessed independently by two pathologists (J.H.L. and B.K.S.) blinded to clinicopathological information, and the discrepancies were resolved by discussion. ER $\alpha$ , ER $\beta$ , and PR staining results

were interpreted according to the Allred scoring method, which is a commonly used tool for the determination of female sex hormone receptors in breast cancer, and the staining was considered positive when tumor cell nuclei appeared brown [13]. The proportion of stained cells was scored as follows: 0, no positive cells; 1, < 1% positive cells; 2, 1%–10% positive cells; 3, 11%–33% positive cells; 4, 34%–66% positive cells; and 5, 100% positive cells. The staining intensity was scored as follows: 0, cell nuclei were not stained; 1, weakly stained; 2, moderately stained; and 3, intensely stained [13]. Subsequently, the sum of the two scores was calculated, and tissue samples with score > 2 were considered positive for ER $\alpha$ , ER $\beta$ , and/or PR expression. For AR, cell nuclear staining was considered positive regardless of the intensity of staining. For EGFR, *EGFR* E746-A750 del, and *EGFR* L858R, cell membrane staining was considered positive regardless of the intensity of staining [14].

Pearson's chi-square test and Fisher exact test were used to evaluate the association between IHC staining and patient clinicopathological characteristics. Overall survival (OS) was defined as the period between the date of first diagnosis and the date of death or the last follow-up. Progression-free survival (PFS) was defined as the period between the date of first diagnosis and the date when recurrence or progression of lung ADC was confirmed or the last follow-up. A Kaplan-Meier survival curve was used for survival analysis, and the log-rank test was used to determine significant differences. Univariate and multivariate analyses of each factor were performed using the Cox proportional hazards model, and the results were considered statistically significant when the p-value was < 0.05. The Windows version of IBM SPSS ver. 24.0 (IBM Corp., Armonk, NY, USA) was used for statistical analysis.

## Ethics statement

This study was approved by the Institutional Review Board of Korea University Guro Hospital (approval No. 2018GR0387), and all of the glass slides, paraffin blocks, and clinicopathological information were provided by the Korea University Guro Hospital Biobank, who had collected patients' samples and information with their informed consents.

## RESULTS

The detailed clinicopathological information of the study patients is presented in Table 1. The male-to-female ratio was 43:41; 31 patients had a history of smoking. Of the 41 female patients, 32 were in menopause. According to the 8th edition

of the American Joint Committee on Cancer (AJCC) cancer staging manual, stage I or II cancer was identified in 54 patients, whereas advanced stage III or IV cancer was identified in 30 patients. Histological pattern evaluation revealed an acinar pattern in 52 patients, a papillary pattern in 15 patients, a solid pattern

**Table 1.** Clinicopathological characteristics of patients studied for female sex hormones receptor expression

Characteristic	No. (%) (n=84)
Sex	
Male	43 (51.2)
Female	41 (48.8)
Age (yr)	63.9 $\pm$ 8.8
Size (cm)	3.1 $\pm$ 1.5
Stage	
I/II	54 (64.3)
III/IV	30 (35.7)
Smoking	
Never	53 (63.1)
Ever	31 (36.9)
Menopause	
Pre	9 (22.0)
Post	32 (78.0)
Histologic pattern	
Acinar	52 (61.9)
Papillary	15 (17.9)
Solid	10 (11.9)
Lepidic	6 (7.1)
Mucinous	1 (1.2)

in 10 patients, a lepidic pattern in six patients, and a mucinous pattern in one patient. By July 2018, signs of disease recurrence or progression were observed in 36 patients, among which 32 succumbed to disease.

The results of the IHC staining according to clinicopathological features are presented in Table 2. Among the 84 cases, positive staining for ER $\alpha$ , ER $\beta$ , and PR was identified in 39, 71, and 46 cases, respectively. For ER $\alpha$  and PR, the staining was mainly restricted to tumor cell nuclei, whereas for ER $\beta$ , the staining was distributed in the nucleus and the cytoplasm. Microscopic images of the representative hormone receptor staining are presented in Fig. 1. The expression of ER $\beta$  was more frequent in patients  $\geq$ 65 years compared with patients  $<$ 65 years ( $p = .027$ ), whereas that of PR was only weakly associated with old age and sex ( $p = .051$  and  $p = .051$ , respectively). Sex, smoking history, tumor stage, and tumor size were not significantly associated with the expression of female sex hormone receptors, nor did the histological growth pattern exhibit any association with the expression of sex hormone receptors (ER $\alpha$ ,  $p = .566$ ; ER $\beta$ ,  $p = .577$ ; PR,  $p = .857$ ).

Among the 84 cases, positive staining for AR was identified in only one patient, who was a 64-year-old male never-smoker. The associations between the expression of AR and other clinicopathological or molecular characteristics were not further analyzed due to the small number of positive cases.

**Table 2.** The results of IHC staining and clinicopathological characteristics

Characteristic	No. (n=84)	ER $\alpha$ positive (%)	p-value	ER $\beta$ positive (%)	p-value	PR positive (%)	p-value	EGFR 19 positive (%)	p-value	EGFR 21 positive (%)	p-value	EGFR positive (%)	p-value
Age (yr)			.373		.027		.051		.097		.004		>.99
<65	41	17 (41.5)		31 (75.6)		18 (43.9)		4 (9.8)		23 (56.1)		40 (97.6)	
$\geq$ 65	43	22 (51.2)		40 (93.0)		28 (65.1)		10 (23.3)		11 (25.6)		41 (95.3)	
Sex			.184		.109		.051		.283		<.001		>.99
Male	43	23 (53.5)		39 (90.7)		28 (65.1)		9 (20.9)		9 (20.9)		41 (95.3)	
Female	41	16 (39.0)		32 (78.0)		18 (43.9)		5 (12.2)		25 (61.0)		40 (97.6)	
Smoking			.237		.119		.358		.479		.036		.552
Never	53	22 (41.5)		42 (79.2)		27 (50.9)		10 (18.9)		26 (49.1)		52 (98.1)	
Ever	31	17 (54.8)		29 (93.5)		19 (61.3)		4 (12.9)		8 (25.8)		29 (93.5)	
Stage			.161		>.99		.102		>.99		.145		.549
I-II	54	22 (40.7)		46 (85.2)		26 (48.1)		9 (16.7)		25 (46.3)		51 (94.4)	
III-IV	30	17 (56.7)		25 (83.3)		20 (66.7)		5 (16.7)		9 (30.0)		30 (100)	
Size (cm)			.778		.059		.335		.433		.288		>.99
<3	46	22 (47.8)		42 (91.3)		23 (50.0)		9 (19.6)		21 (45.7)		44 (95.7)	
$\geq$ 3	38	17 (44.7)		29 (76.3)		23 (60.5)		5 (13.2)		13 (34.2)		37 (97.4)	
Menopause (n=41)			>.99		>.99		>.99		>.99		>.99		>.99
Pre	9	3 (33.3)		7 (77.8)		4 (44.4)		1 (11.1)		6 (66.7)		9 (100)	
Post	32	13 (40.6)		25 (78.1)		14 (43.8)		4 (12.5)		19 (59.4)		31 (96.9)	

Statistically significant ( $p < .05$ ).

IHC, immunohistochemical; ER, estrogen receptor; PR, progesterone receptor; EGFR, epidermal growth factor receptor; EGFR 19, EGFR E746-A750 del; EGFR 21, EGFR L858R.

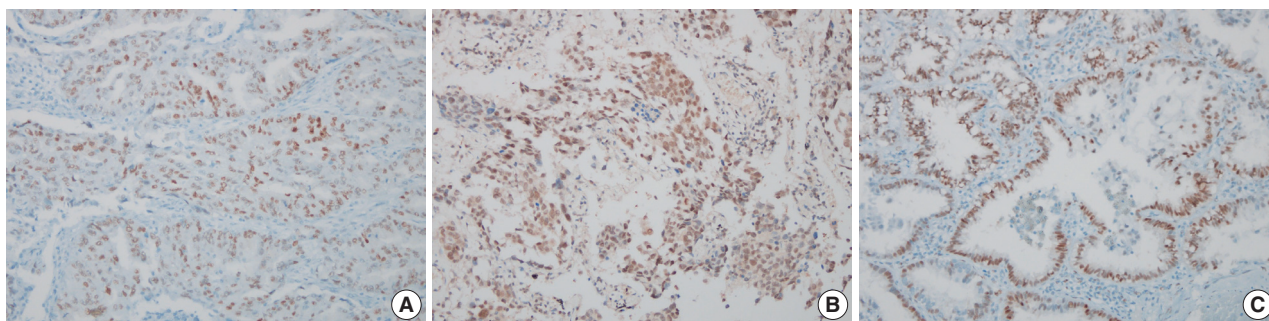


**Fig. 1.** Representative results of immunohistochemical staining. (A) Nuclear staining for estrogen receptor  $\alpha$ . (B) Nuclear staining for estrogen receptor  $\beta$ . (C) Nuclear staining for progesterone receptor.

**Table 3.** Pearson correlation coefficient between the results of IHC staining and *EGFR* mutation PNA clamping real-time PCR study

	ER $\alpha$	ER $\beta$	PR	<i>EGFR</i> 19del mutation	<i>EGFR</i> 20 ins mutation	<i>EGFR</i> L858R mutation
ER $\alpha$	1.00					
ER $\beta$	0.398 <sup>a</sup>	1.00				
PR	0.319 <sup>a</sup>	0.405 <sup>a</sup>	1.00			
<i>EGFR</i> 19del mutation	-0.103	-0.198	0.013	1.00		
<i>EGFR</i> 20 ins mutation	-0.227	-0.086	-0.245	0.011	1.00	
<i>EGFR</i> L858R mutation	-0.257	-0.049	-0.068	-0.499 <sup>a</sup>	-0.185	1.00

IHC, immunohistochemical; EGFR, epidermal growth factor receptor; PNA, peptide nucleic acid; PCR, polymerase chain reaction; ER, estrogen receptor; PR, progesterone receptor.

<sup>a</sup>Statistically significant ( $p < .05$ ).

IHC staining of EGFR, *EGFR* E746-A750 del, and *EGFR* L858R demonstrated that of the 84 cases, 81, 14, and 34 cases were positive for each marker, respectively. No statistically significant associations were identified with clinicopathological features in patients with EGFR- or *EGFR* E746-A750 del-positive tumors. However, *EGFR* L858R-positive tumors were identified to be associated with a younger age ( $< 65$  years vs.  $\geq 65$  years,  $p = .004$ ) and more frequent in women compared with men ( $p < .001$ ) and in patients without any smoking history compared with smokers ( $p = .036$ ) (Table 2).

The expression levels of female sex hormone receptors were associated with one another (ER $\alpha$  and ER $\beta$ ,  $p < .001$ ; ER $\alpha$  and PR,  $p = .003$ ; ER $\beta$  and PR;  $p < .001$ ).

Molecular analysis of *EGFR* mutation status was performed in 51 patients, among which the *EGFR* 19 del mutation was identified in 16 cases (31.4%), the *EGFR* 20 insertion mutation in three cases (5.9%), concurrent *EGFR* 19 del mutation and *EGFR* 20 insertion in one case (2.0%), and the *EGFR* L858R mutation in 18 cases (35.3%). The IHC female sex hormone receptor expression and molecular *EGFR* mutation results appeared to be negatively associated but were not statistically significant (Table 3).

Kaplan-Meier survival curves and the log-rank test were used to analyze the OS and PFS of the patients. The positive or negative staining of ER $\alpha$  was not significantly associated with OS or

PFS. The staining of ER $\beta$  and PR also did not impact survival. In addition, the results of IHC staining associated with EGFR exhibited no significant differences in survival. Patients with tumors expressing ER $\alpha$  or ER $\beta$  were subdivided into groups according to age, sex, and tumor stage; in the subgroup of patients aged  $\geq 65$  years, the ER $\alpha$ -positive group exhibited significantly worse PFS and OS compared with the ER $\alpha$ -negative group (Fig. 2).

The results of the univariate analysis demonstrated that OS was significantly associated with sex, tumor stage, and smoking history, whereas PFS was associated with tumor size, stage, smoking history, and menopause status. However, in the multivariate analysis, only sex and tumor stage were significantly associated with OS, and only tumor size was associated with PFS (Table 4). In the subgroup of patients aged  $\geq 65$  years, ER $\alpha$  expression was associated with PFS and OS in the univariate analysis ( $p = .046$  and  $p = .031$ , respectively), but not in the multivariate analysis ( $p = .522$  and  $p = .475$ , respectively) (Table 5).

## DISCUSSION

The present study investigated the association of female sex hormone receptor expression with clinicopathological features and prognosis in lung ADC. The results demonstrated an association between poor prognosis and ER $\alpha$  expression in the Ka-

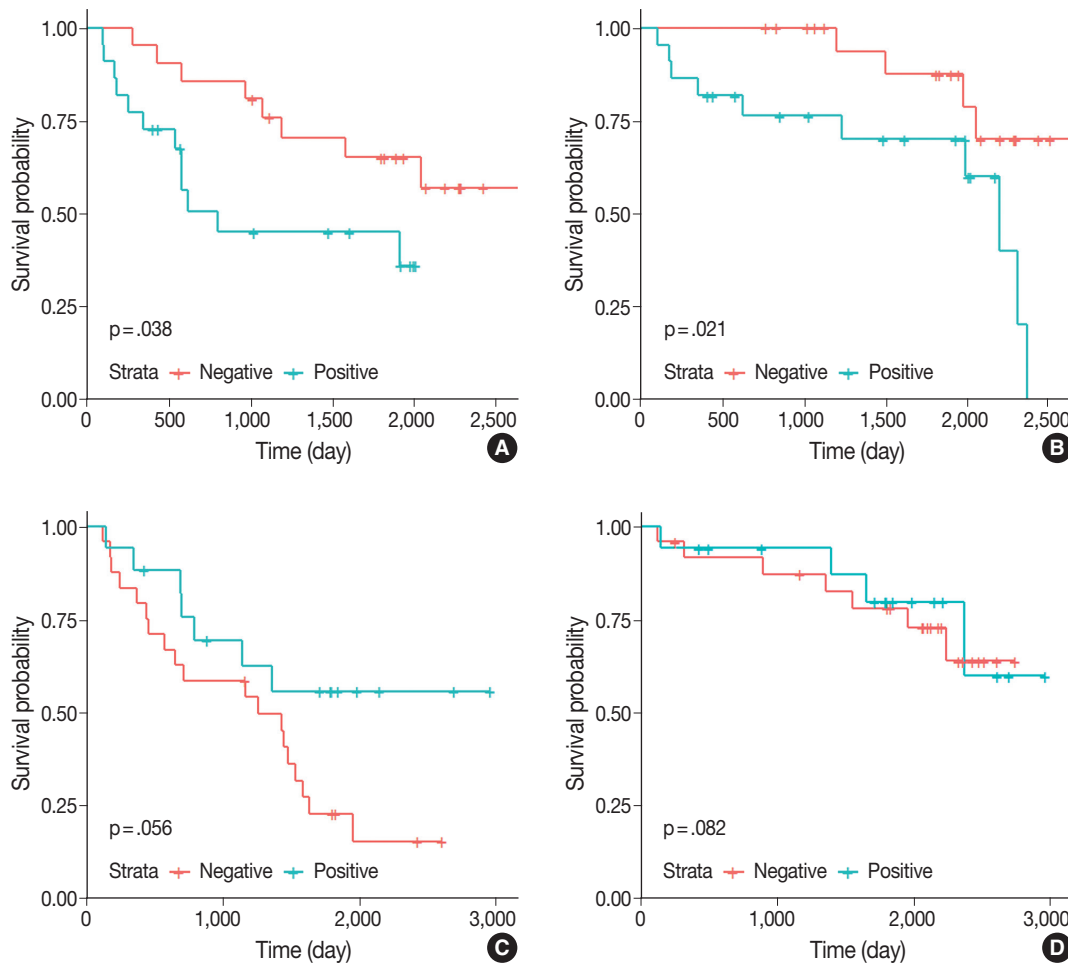


**Fig. 2.** Kaplan-Meier plots of progression-free survival (PFS) and overall survival (OS) in the age subgroups. (A) Estrogen receptor  $\alpha$  (ER $\alpha$ ) expression was associated with poor PFS in the age  $\geq 65$  years subgroup. (B) ER $\alpha$  expression was associated with poor OS in the age  $\geq 65$  years subgroup. (C) ER $\alpha$  expression was not associated with PFS in the age  $< 65$  years subgroup. (D) ER $\alpha$  expression was not associated with OS in the age  $< 65$  years subgroup.

**Table 4.** Cox proportional hazard regression model survival analysis in progression-free survival and overall survival

Variable	Progression-free survival				Overall survival			
	Univariate analysis		Multivariate analysis		Univariate analysis		Multivariate analysis	
	HR (95% CI)	p-value	HR (95% CI)	p-value	HR (95% CI)	p-value	HR (95% CI)	p-value
Age ( $\geq 65$ yr)	0.717 (0.400–1.287)	.265	-	-	1.592 (0.716–3.537)	.254	-	-
Female sex	0.569 (0.317–1.021)	.059	-	-	0.257 (0.107–0.620)	.002 <sup>a</sup>	0.266 (0.089–0.789)	.017 <sup>b</sup>
Size ( $\geq 3$ cm)	4.006 (2.167–7.405)	$< .001^a$	5.447 (1.664–17.837)	.005 <sup>b</sup>	1.925 (0.859–4.310)	.111	-	-
Stage (III, IV)	3.625 (1.969–6.675)	$< .001^a$	1.049 (0.329–3.349)	.935	5.686 (2.488–12.993)	$< .001^a$	4.325 (1.815–10.306)	.001 <sup>b</sup>
Smoking	1.904 (1.047–3.462)	.035 <sup>a</sup>	0.680 (0.113–4.091)	.673	2.933 (1.311–6.559)	.009 <sup>a</sup>	0.943 (0.348–2.551)	.908
Menopause (n=41)	0.304 (0.114–0.813)	.018 <sup>a</sup>	0.803 (0.251–2.565)	.711	0.636 (0.122–3.301)	.590	-	-
ER $\alpha$	0.996 (0.553–1.795)	.990	-	-	1.919 (0.868–4.245)	.107	-	-
ER $\beta$	0.642 (0.318–1.294)	.215	-	-	1.341 (0.400–4.500)	.634	-	-
PR	0.793 (0.444–1.415)	.432	-	-	1.165 (0.528–2.573)	.705	-	-
EGFR E746-A750 del	0.933 (0.435–2.004)	.860	-	-	0.808 (0.275–2.374)	.699	-	-
EGFR L858R	1.137 (0.630–2.050)	.670	-	-	0.737 (0.324–1.675)	.466	-	-

HR, hazard ratio; CI, confidence interval; ER, estrogen receptor; PR, progesterone receptor; EGFR, epidermal growth factor receptor.

<sup>a</sup>Statistically significant in univariate analysis ( $p < .05$ ); <sup>b</sup>Statistically significant in multivariate analysis ( $p < .05$ ).

**Table 5.** Cox proportional hazard regression model survival analysis in progression-free survival and overall survival with the age over 65 subgroup

Variable	Progression-free survival				Overall survival			
	Univariate analysis		Multivariate analysis		Univariate analysis		Multivariate analysis	
	HR (95% CI)	p-value	HR (95% CI)	p-value	HR (95% CI)	p-value	HR (95% CI)	p-value
Female sex	0.341 (0.123–0.947)	.039 <sup>a</sup>	0.494 (0.171–1.424)	.192	0.159 (0.035–0.718)	.017 <sup>a</sup>	0.132 (0.020–0.088)	.037 <sup>b</sup>
Size (≥3 cm)	6.170 (2.196–17.333)	.001 <sup>a</sup>	2.662 (0.725–9.777)	.140	3.208 (1.065–9.660)	.038 <sup>a</sup>	0.911 (0.212–3.915)	.900
Stage (III, IV)	6.504 (2.403–17.609)	<.001 <sup>a</sup>	2.822 (0.825–9.659)	.098	4.684 (1.521–14.427)	.007 <sup>a</sup>	5.080 (0.926–27.874)	.061
Smoking	2.245 (0.906–5.560)	.081	-	-	3.393 (1.130–10.190)	.029 <sup>a</sup>	0.503 (0.095–2.671)	.420
ER $\alpha$	2.605 (1.017–6.674)	.046 <sup>a</sup>	1.383 (0.513–3.733)	.522	3.648 (1.128–11.797)	.031 <sup>a</sup>	1.756 (0.374–8.243)	.475
ER $\beta$	2.018 (0.267–15.242)	.496	-	-	24.255 (0.006–104217.826)	.455	-	-
PR	1.819 (0.687–4.814)	.228	-	-	2.379 (0.655–8.641)	.188	-	-
EGFR E746-A750 del	0.965 (0.349–2.665)	.945	-	-	1.257 (0.384–4.118)	.706	-	-
EGFR L858R	1.159 (0.416–3.224)	.778	-	-	0.982 (0.270–3.574)	.979	-	-

HR, hazard ratio; CI, confidence interval; ER, estrogen receptor; PR, progesterone receptor; EGFR, epidermal growth factor receptor.

<sup>a</sup>Statistically significant in univariate analysis ( $p < .05$ ); <sup>b</sup>Statistically significant in multivariate analysis ( $p < .05$ ).

plan-Meier survival analysis with a log-rank test, but the association was not statistically significant in the multivariate analysis. The remaining hormone receptor expression results did not identify statistically significant associations.

ERs are categorized into two subgroups, ER $\alpha$  and ER $\beta$  [15]. ER $\alpha$ , first identified in 1986, is coded by the *ESR1* gene and mainly distributed in the breast, ovary, and endometrium. ER $\beta$ , identified in 1996, is coded by the *ESR2* gene and distributed in various cells and tissues, including the bone, brain, colon, vascular endothelial cells, kidney, lung, ovary, prostate, and testes. In normal lung tissue, ER $\beta$  is highly expressed in alveolar and bronchial epithelial cells and involved in the maintenance of the extracellular matrix. In addition, studies using ER $\beta$ -knockout mice have reported hypoxia in the mice caused by a decrease in alveolar formation and surfactant secretion [15]. ERs contribute to intracellular signaling [16]. The complex of estrogen and ER directly acts on the estrogen response element in the nucleus and promotes gene expression through the activation of the RAS/RAF signaling pathway or the phosphoinositide 3-kinase (PI3K)/Akt signaling pathway [17].

Studies on the significance of ERs as risk and/or prognostic factors of lung ADC have produced inconsistent results. Certain studies reported that ER $\alpha$  expression in the cytoplasm was associated with poor prognosis [8,18]. A previous study reported that ER $\alpha$  expression in tumor cell nuclei was associated with good prognosis [19], whereas another study identified an association with poor prognosis [20]. Studies on the expression of ER $\beta$  also produced variable and inconsistent results with different prognosis depending on the sex of the patients and the site of expression in tumor cells [8,12,21,22].

The expression patterns and rates of ERs have also been in-

consistent in previous studies. The expression rate of ER $\alpha$  has been reported as ranging from 0%–80% and that of ER $\beta$  as ranging from 9%–98% [23]; these wide ranges may have been due to the various types of antibodies used for evaluation. Antibodies against ER $\alpha$  include mouse monoclonal antibodies 1D5 targeting the amino-terminal domain, 6F11 recognizing the full-length receptor, and rabbit monoclonal antibodies SP1 and HC20, both recognizing the carboxy-terminal domain. A study on ER $\alpha$  expression in lung ADC reported a positive rate of 7.6% with 1D5, 14.1% with 6F11, and 27% with SP1, respectively [24]. In another study, the HC20 antibody exhibited a similar positive rate to that of 1D5 [23]. Generally, antibodies targeting the amino terminal domain exhibit a positive rate of 0%–40% [11,25], those against the carboxyl terminal domain exhibit a positive rate of 36%–79% [22,26], and those recognizing the full-length receptor exhibit a positive rate of 0%–80% [11, 27,28]. Antibodies against ER $\beta$  also have various types recognizing full-length receptor and splicing variants; a previous study reported that those targeting the amino-terminal exhibited a positive rate of 49%, and the antibody against the carboxyl-terminal exhibited a positive rate of 48%–51%, demonstrating relatively consistent expression, regardless of the target domain, compared with the ER $\alpha$  antibodies [23]. The absence of consensus on the criteria for “positivity” in IHC evaluation may also have caused the inconsistent results. Although most of the previous studies used both the proportion of stained cells and the staining intensity, the specific methods were inconsistent. In addition, the criteria for determining the positive results were divided into nuclear and cytoplasmic staining in certain studies, which led to further confusion and discrepancy.

Expression of PR has been demonstrated to increase the se-

cretion of vascular endothelial growth factor (VEGF), which promotes tumor angiogenesis and contributes to tumorigenesis [29,30]. A previous study in which ER and PR were concurrently administered to lung cancer cell lines revealed that lung tumor cells can produce angiogenetically active VEGF. As these were inhibited by anti-progesterone treatment, the authors concluded that these cancer-promoting effects were mediated by progesterone [30]. In chemically-induced lung ADCs in mice, the expression levels of PR and EGFR were associated with each other, as well as with tumor progression [31]. However, other studies evaluating the association among the expression of PR, tumorigenesis, and prognosis of lung ADC demonstrated that PR expression was present in 8%–63% of tumors and exhibited no significant association with disease prognosis [19,22,32].

The expression of AR and its relevance to lung ADC have not been well characterized yet. Several studies demonstrated AR expression in non-small cell carcinomas, which suggested the role of AR status in lung cancer [33,34]. However, the results of studies conducted through this theoretical background were inconsistent. Berardi et al. [35] demonstrated a better OS in female non-small cell carcinoma patients with AR expression in carcinoma cells compared to those with tumors showing no AR expression. In contrast, Grant et al. [36] demonstrated that AR expression has no association with recurrence or survival in modification with the Ki-67 labeling index. In the present study, only one case expressed AR receptor positivity and therefore cannot be interpreted because of the small number.

EGFR has been identified to be upregulated in > 60% of non-small cell carcinomas [37] and is considered to serve an important role in the survival and proliferation of tumor cells. The EGFR signaling pathway is influenced by estrogen-activated ER $\beta$  signaling on the cell membrane. Estrogen activates the PI3K/AKT and the MEK/ERK signaling pathways, which are downstream pathways of EGFR activation, and facilitates lung cancer metastasis through epithelial-mesenchymal transition [38,39]. However, a study evaluating the association between the expression of ERs and EGFR mutation in lung ADC failed to demonstrate a significant result [32].

In the present study, the expression of EGFR and female sex hormone receptors was evaluated. The IHC evaluation for receptor expression revealed no significant association between female sex hormone receptors and EGFR in lung ADCs. This result was different from the negative association that has generally been observed between the expression of female sex hormone receptors and EGFR in breast cancer [40–42]; further studies with a larger sample size may be required to validate this result.

The present study also aimed to demonstrate the association between female sex hormone receptor expression and EGFR mutation; however, although a negative association was observed, statistical significance could not be achieved.

When the expression patterns of ER $\alpha$  and ER $\beta$  were subdivided into groups according to age, sex, or tumor stage, and Kaplan-Meier plotting with the log-rank test was performed, the association between ER $\beta$ -expressing tumors in men and better prognosis that was previously reported in some studies [11,12] was not observed in the present study. PR expression was detected in 54.8% of cases in tumor cell nuclei. PR expression exhibited no significant association with any of the clinicopathological features, and in the survival analysis, no significant differences were observed. The EGFR L858R mutation detected by immunohistochemistry was significantly associated with certain clinicopathological features such as age < 65 years, female sex, and no smoking history, which also exhibited well-known associations with molecularly detected EGFR mutation.

In conclusion, the present study investigated the expression of the female sex hormone receptors ER $\alpha$ , ER $\beta$ , and PR in lung ADCs. The expression of each receptor exhibited associations with certain clinicopathological features and prognostic factors; however, in multivariate analysis, none of the female sex hormone receptors were significantly associated with patient survival.

## ORCID

Jin Hwan Lee: <https://orcid.org/0000-0003-3647-7487>

Han Kyeom Kim: <https://orcid.org/0000-0001-6750-8528>

Bong Kyung Shin: <https://orcid.org/0000-0001-9017-2831>

## Author Contributions

Conceptualization: JHL, BKS.

Data curation: JHL, BKS.

Formal analysis: JHL.

Investigation: JHL, BKS.

Methodology: JHL.

Project administration: HKK, BKS.

Resources: BKS.

Supervision: HKK.

Validation: JHL, BKS.

Visualization: JHL.

Writing—original draft: JHL.

Writing—review & editing: BKS.

## Conflicts of Interest

The authors declare that they have no potential conflicts of interest.

## Funding

No funding to declare.

## REFERENCES

- Torre LA, Bray F, Siegel RL, Ferlay J, Lortet-Tieulent J, Jemal A. Global cancer statistics, 2012. *CA Cancer J Clin* 2015; 65: 87-108.
- Omoto Y, Kobayashi Y, Nishida K, et al. Expression, function, and clinical implications of the estrogen receptor beta in human lung cancers. *Biochem Biophys Res Commun* 2001; 285: 340-7.
- Yano T, Miura N, Takenaka T, et al. Never-smoking nonsmall cell lung cancer as a separate entity: clinicopathologic features and survival. *Cancer* 2008; 113: 1012-8.
- Torday JS, Nielsen HC, Fencel Mde M, Avery ME. Sex differences in fetal lung maturation. *Am Rev Respir Dis* 1981; 123: 205-8.
- Taioli E, Wynder EL. Re: Endocrine factors and adenocarcinoma of the lung in women. *J Natl Cancer Inst* 1994; 86: 869-70.
- Henderson BE, Ross RK, Pike MC, Casagrande JT. Endogenous hormones as a major factor in human cancer. *Cancer Res* 1982; 42: 3232-9.
- Mollerup S, Jørgensen K, Berge G, Haugen A. Expression of estrogen receptors alpha and beta in human lung tissue and cell lines. *Lung Cancer* 2002; 37: 153-9.
- Kawai H, Ishii A, Washiya K, et al. Combined overexpression of EGFR and estrogen receptor alpha correlates with a poor outcome in lung cancer. *Anticancer Res* 2005; 25: 4693-8.
- Stabile LP, Dacic S, Land SR, et al. Combined analysis of estrogen receptor beta-1 and progesterone receptor expression identifies lung cancer patients with poor outcome. *Clin Cancer Res* 2011; 17: 154-64.
- Hsu LH, Liu KJ, Tsai MF, et al. Estrogen adversely affects the prognosis of patients with lung adenocarcinoma. *Cancer Sci* 2015; 106: 51-9.
- Schwartz AG, Prysak GM, Murphy V, et al. Nuclear estrogen receptor beta in lung cancer: expression and survival differences by sex. *Clin Cancer Res* 2005; 11: 7280-7.
- Skov BG, Fischer BM, Pappot H. Oestrogen receptor beta over expression in males with non-small cell lung cancer is associated with better survival. *Lung Cancer* 2008; 59: 88-94.
- Allred DC, Bustamante MA, Daniel CO, Gaskill HV, Cruz AB Jr. Immunocytochemical analysis of estrogen receptors in human breast carcinomas: evaluation of 130 cases and review of the literature regarding concordance with biochemical assay and clinical relevance. *Arch Surg* 1990; 125: 107-13.
- Wen YH, Brogi E, Hasanovic A, et al. Immunohistochemical staining with EGFR mutation-specific antibodies: high specificity as a diagnostic marker for lung adenocarcinoma. *Mod Pathol* 2013; 26: 1197-203.
- Patrone C, Cassel TN, Pettersson K, et al. Regulation of postnatal lung development and homeostasis by estrogen receptor beta. *Mol Cell Biol* 2003; 23: 8542-52.
- Swedenborg E, Power KA, Cai W, Pongratz I, Rüegg J. Regulation of estrogen receptor beta activity and implications in health and disease. *Cell Mol Life Sci* 2009; 66: 3873-94.
- Kato S, Endoh H, Masuhiro Y, et al. Activation of the estrogen receptor through phosphorylation by mitogen-activated protein kinase. *Science* 1995; 270: 1491-4.
- Nose N, Sugio K, Oyama T, et al. Association between estrogen receptor-beta expression and epidermal growth factor receptor mutation in the postoperative prognosis of adenocarcinoma of the lung. *J Clin Oncol* 2009; 27: 411-7.
- Rouquette I, Lauwers-Cances V, Allera C, et al. Characteristics of lung cancer in women: importance of hormonal and growth factors. *Lung Cancer* 2012; 76: 280-5.
- Kadota K, Eguchi T, Villena-Vargas J, et al. Nuclear estrogen receptor-alpha expression is an independent predictor of recurrence in male patients with pT1aN0 lung adenocarcinomas, and correlates with regulatory T-cell infiltration. *Oncotarget* 2015; 6: 27505-18.
- Karlsson C, Helenius G, Fernandes O, Karlsson MG. Oestrogen receptor beta in NSCLC: prevalence, proliferative influence, prognostic impact and smoking. *APMIS* 2012; 120: 451-8.
- Raso MG, Behrens C, Herynk MH, et al. Immunohistochemical expression of estrogen and progesterone receptors identifies a subset of NSCLCs and correlates with EGFR mutation. *Clin Cancer Res* 2009; 15: 5359-68.
- Baik CS, Eaton KD. Estrogen signaling in lung cancer: an opportunity for novel therapy. *Cancers (Basel)* 2012; 4: 969-88.
- Gomez-Fernandez C, Mejias A, Walker G, Nadji M. Immunohistochemical expression of estrogen receptor in adenocarcinomas of the lung: the antibody factor. *Appl Immunohistochem Mol Morphol* 2010; 18: 137-41.
- Di Nunno L, Larsson LG, Rinehart JJ, Beissner RS. Estrogen and progesterone receptors in non-small cell lung cancer in 248 consecutive patients who underwent surgical resection. *Arch Pathol Lab Med* 2000; 124: 1467-70.
- Sun HB, Zheng Y, Ou W, et al. Association between hormone receptor expression and epidermal growth factor receptor mutation in patients operated on for non-small cell lung cancer. *Ann Thorac*

- Surg 2011; 91: 1562-7.
27. Mauro LV, Dalurzo M, Carlini MJ, et al. Estrogen receptor beta and epidermal growth factor receptor as early-stage prognostic biomarkers of non-small cell lung cancer. *Oncol Rep* 2010; 24: 1331-8.
  28. Abe K, Miki Y, Ono K, et al. Highly concordant coexpression of aromatase and estrogen receptor beta in non-small cell lung cancer. *Hum Pathol* 2010; 41: 190-8.
  29. Trotter A, Kipp M, Schrader RM, Beyer C. Combined application of 17beta-estradiol and progesterone enhance vascular endothelial growth factor and surfactant protein expression in cultured embryonic lung cells of mice. *Int J Pediatr* 2009; 2009: 170491.
  30. Marquez-Garban DC, Mah V, Alavi M, et al. Progesterone and estrogen receptor expression and activity in human non-small cell lung cancer. *Steroids* 2011; 76: 910-20.
  31. Kishi S, Yokohira M, Yamakawa K, Saoo K, Imaida K. Significance of the progesterone receptor and epidermal growth factor receptor, but not the estrogen receptor, in chemically induced lung carcinogenesis in female A/J mice. *Oncol Lett* 2014; 8: 2379-86.
  32. Toh CK, Ahmad B, Soong R, et al. Correlation between epidermal growth factor receptor mutations and expression of female hormone receptors in East-Asian lung adenocarcinomas. *J Thorac Oncol* 2010; 5: 17-22.
  33. Beattie CW, Hansen NW, Thomas PA. Steroid receptors in human lung cancer. *Cancer Res* 1985; 45: 4206-14.
  34. Kaiser U, Hofmann J, Schilli M, et al. Steroid-hormone receptors in cell lines and tumor biopsies of human lung cancer. *Int J Cancer* 1996; 67: 357-64.
  35. Berardi R, Morgese F, Santinelli A, et al. Hormonal receptors in lung adenocarcinoma: expression and difference in outcome by sex. *Oncotarget* 2016; 7: 82648-57.
  36. Grant L, Banerji S, Murphy L, et al. Androgen receptor and Ki67 expression and survival outcomes in non-small cell lung cancer. *Horm Cancer* 2018; 9: 288-94.
  37. Gazdar AF. Epidermal growth factor receptor inhibition in lung cancer: the evolving role of individualized therapy. *Cancer Metastasis Rev* 2010; 29: 37-48.
  38. Hsu LH, Chu NM, Kao SH. Estrogen, estrogen receptor and lung cancer. *Int J Mol Sci* 2017; 18: E713.
  39. Zhao XZ, Liu Y, Zhou LJ, Wang ZQ, Wu ZH, Yang XY. Role of estrogen in lung cancer based on the estrogen receptor-epithelial mesenchymal transduction signaling pathways. *Onco Targets Ther* 2015; 8: 2849-63.
  40. Fitzpatrick SL, Brightwell J, Wittliff JL, Barrows GH, Schultz GS. Epidermal growth factor binding by breast tumor biopsies and relationship to estrogen receptor and progesterin receptor levels. *Cancer Res* 1984; 44: 3448-53.
  41. Rimawi MF, Shetty PB, Weiss HL, et al. Epidermal growth factor receptor expression in breast cancer association with biologic phenotype and clinical outcomes. *Cancer* 2010; 116: 1234-42.
  42. Masuda H, Zhang D, Bartholomeusz C, Doihara H, Hortobagyi GN, Ueno NT. Role of epidermal growth factor receptor in breast cancer. *Breast Cancer Res Treat* 2012; 136: 331-45.

# Comparison of papanicolaou smear and human papillomavirus (HPV) test as cervical screening tools: can we rely on HPV test alone as a screening method? An 11-year retrospective experience at a single institution

Myunghee Kang, Seung Yeon Ha, Hyun Yee Cho, Dong Hae Chung, Na Rae Kim,  
Jungsuk An, Sangho Lee, Jae Yeon Seok, Juhyeon Jeong

Department of Pathology, Gil Medical Center, Gachon University College of Medicine, Incheon, Korea

**Background:** The decrease in incidence of cervical dysplasia and carcinoma has not been as dramatic as expected with the development of improved research tools and test methods. The human papillomavirus (HPV) test alone has been suggested for screening in some countries. The National Cancer Screening Project in Korea has applied Papanicolaou smears (Pap smears) as the screening method for cervical dysplasia and carcinoma. We evaluated the value of Pap smear and HPV testing as diagnostic screening tools in a single institution. **Methods:** Patients co-tested with HPV test and Pap smear simultaneously or within one month of each other were included in this study. Patients with only punch biopsy results were excluded because of sampling errors. A total of 999 cases were included, and the collected reports encompassed results of smear cytology, HPV subtypes, and histologic examinations. **Results:** Sensitivity and specificity of detecting high-grade squamous intraepithelial lesion (HSIL) and squamous cell carcinoma (SCC) were higher for Pap smears than for HPV tests (sensitivity, 97.14%; specificity, 85.58% for Pap smears; sensitivity, 88.32%; specificity, 54.92% for HPV tests). HPV tests and Pap smears did not differ greatly in detection of low-grade squamous intraepithelial lesion (85.35% for HPV test, 80.31% for Pap smears). When atypical glandular cells were noted on Pap smears, the likelihood for histologic diagnosis of adenocarcinoma following Pap smear was higher than that of high-risk HPV test results (18.8 and 1.53, respectively). **Conclusions:** Pap smears were more useful than HPV tests in the diagnosis of HSIL, SCC, and glandular lesions.

**Key Words:** Uterine cervical neoplasms; Papanicolaou test; Human papillomavirus DNA tests; Early detection of cancer; Sensitivity

**Received:** August 13, 2019 **Revised:** November 28, 2019 **Accepted:** November 28, 2019

**Corresponding Author:** Seung Yeon Ha, MD, Department of Pathology, Gachon University Gil Medical Center, 21 Namdong-daero 774beon-gil, Namdong-gu, Incheon 21565, Korea  
Tel: +82-32-460-3078, Fax: +82-32-460-2394, E-mail: syha@gilhospital.com

Uterine cervical cancer is a well-understood malignancy. Information about the carcinogenesis, diagnosis, and vaccine prevention of cervical cancer is now available [1]. However, cervical cancer remains the third most common cause of death among females worldwide [2]. The incidence and mortality rates are diverse and are influenced by screening tests and public health infrastructure [2]. The incidence and mortality rates in Eastern Africa are about ten times higher than in Western Asia [2]. However, the incidence of cervical dysplasia and carcinoma have not decreased dramatically in areas with well-established public health programs. In developed countries, the estimated number of new cases has not decreased in four years, while the estimated number of deaths has increased from 33,500 cases in GLOBOCAN 2008 to 34,700 cases in GLOBOCAN 2012 [2,3].

For detection and treatment in the early stages, nationwide screening tests are needed. The Papanicolaou smear (Pap smears) was adopted as a screening test in 1999 for the National Cancer Screening Project in Korea. The Pap smear is performed biyearly in females over the age of thirty [4]. However, the use of human papillomavirus (HPV) DNA test as a screening method has been considered more helpful for protection against invasive cervical carcinomas in some studies [5]. The HPV DNA test has also been suggested as a screening method in some countries [6-8]. In the United States, some institutions proposed co-testing with Pap smears and HPV as a screening method [9]. In this study, we evaluated the value of Pap smears and HPV testing at a single institution.

## MATERIALS AND METHODS

### Case selection

The medical records of 204,588 Pap smear cases at Gil Medical Center during the 11-year period from May 2006 to September 2017 were collected and retrospectively studied. Among these, 15,762 cases were HPV/Pap smear co-testing. Patients underwent HPV testing and Pap smears at the same time or within one month of each other. A total of 2,491 cases additionally underwent histologic evaluation. Patients with only punch biopsy results were excluded because of sampling errors. Inclusion criteria of the histologic results were reports of biopsies performed within 3 months of Pap smears and HPV testing. A total of 999 cases were included to include the results of smear cytology, HPV subtypes, and histologic examinations. Information on patient age, Pap smear results, HPV subtypes, surgical procedures, and pathologic results were collected.

### Pap smear evaluation

Both conventional smear and liquid base preparations (Thin Prep Pap test, Cytoc Corporation, Boxborough, MA, USA) were included. Each case was reviewed by one cytotechnologist and one pathologist. The results were reported using the Bethesda system [10].

### HPV subtype testing

During the 11-year period, the MyHPV chip kit (from March 2006 to February 2012, MyGene Co., Seoul, Korea), HPV DNA Chip (from March 2012 to February 2014, BioMedLab Inc., Chuncheon, Korea), and BMT HPV 9G DNA KIT (from March 2014 to September 2017, Biometrix Technology Inc., Chuncheon, Korea) were used to detect HPV. HPV tests were performed according to the manufacturer's instructions. Results were reported as positive or negative and as high-risk (HPV-16, 18, 26, 31, 33, 34, 35, 39, 45, 51, 52, 53, 56, 58, 59, 66, 67, 68, 69, 70, 73) or low-risk (HPV-3, 6, 10, 11, 27, 32, 40, 42, 43, 44, 54, 55, 57, 61, 62, 72, 74) subtypes. Cases showing HPV-negativity on the chip scanner but positivity under electrophoresis, i.e., not specified, were categorized as "other" after one repeat examination.

### Histologic evaluation

When abnormal results were noted on cytology and/or HPV test, additional surgical procedures were performed after considering patient age, childbearing plans, and associated gynecologic diseases. If any patient had more than two pathologic results,

the higher degree of abnormality was selected.

### Statistical analysis

To evaluate the diagnostic accuracy, sensitivity, specificity, positive/negative likelihood ratio, and odds ratio were calculated along with their 95% confidence intervals (CI) [11]. Cohen's kappa coefficient ( $\kappa$ ) was calculated using SPSS ver. 21.0 software (IBM Corp., Armonk, NY, USA). The  $\kappa$  was interpreted categorically following the Fleiss guidelines of poor ( $\kappa < 0.4$ ), fair/good ( $\kappa = 0.40$  to  $0.75$ ), and perfect ( $\kappa > 0.75$ ) [12].

### Ethics statement

This study was reviewed and approved by the Institutional Review Board (IRB) of Gil Medical Center (No. GBIRB2019-015). Formal written informed consent was not required due to a waiver from the appropriate IRB.

## RESULTS

### Characteristics of cases

A total of 999 cases fulfilled the inclusion criteria. Mean age was 46 years (range, 16 to 92 years). High-grade squamous intraepithelial lesion (HSIL) was the most common cytologic finding (473 cases, 46.7%), followed by low-grade intraepithelial lesion (LSIL) (137 cases, 13.5%) and negative for intraepithelial lesion or malignancy (NILM) (131 cases, 12.9%). There were about five times more HPV positive cases than HPV-negative cases (830 cases, 83.1%). Cervical conization was performed more commonly than hysterectomy (723 cases, 72.4%). Severe dysplasia/squamous carcinoma in situ (CIS) were the most common histologic findings (424 cases, 42.2%). Clinicopathologic characteristics of patients are summarized in Table 1.

### Detection of squamous cell carcinomas and HSIL

When HSIL cells were present on smear cytology, i.e., in cases of atypical squamous cells, cannot exclude HSIL (ASC-H), HSIL, and squamous cell carcinoma (SCC), the sensitivity was 97.14% (95% CI, 95.41 to 98.23) and specificity was 85.58% (95% CI, 77.56 to 91.06). The sensitivity and specificity of high-risk HPV type test (sensitivity, 88.32%; specificity, 54.92%) were lower than that of Pap smears. These results are shown in Table 2. Sixteen cases showed benign cellular changes in the Pap smears (16/654, 2.45%), and 69 cases gave negative results on HPV tests (69/654, 10.55%). Seven cases gave negative results on both the Pap smears and the HPV tests (7/654, 1.07%).

**Table 1.** Clinicopathologic characteristics

Characteristic	No. (%)
Age (yr), mean (range)	46 (16–92)
Pap smear <sup>a</sup>	
NILM	131 (12.9)
ASCUS	98 (9.7)
ASC-H	70 (6.9)
LSIL	137 (13.5)
HSIL	473 (46.7)
SCC	52 (5.1)
Atypical glandular cells	24 (2.4)
AIS, adenocarcinoma	26 (2.6)
Other malignant neoplasms	3 (0.3)
HPV test	
Negative	169 (16.9)
Positive	830 (83.1)
High-risk	704 (84.8)
Low-risk	14 (1.7)
Others	112 (13.5)
Surgical procedures	
Conization	723 (72.4)
Hysterectomy	276 (27.6)
Histologic results <sup>b</sup>	
Normal	150 (14.9)
Koilocytosis	55 (5.5)
Mild dysplasia	102 (10.2)
Moderate dysplasia	116 (11.5)
Severe dysplasia, CIS	424 (42.2)
SCC	114 (11.3)
AIS	10 (1.0)
Adenocarcinoma	20 (2.0)
Adenosquamous cell carcinoma	11 (1.1)
Others (malignant Mullerian mixed tumor)	3 (0.3)
Total	999

NILM, negative for intraepithelial lesion or malignancy; ASCUS, atypical squamous cells of unknown significance; ASC-H, atypical squamous cells, cannot exclude HSIL; LSIL, low-grade squamous intraepithelial lesion; HSIL, high-grade squamous intraepithelial lesion; SCC, squamous cell carcinoma; AIS, adenocarcinoma in situ; CIS, carcinoma in situ.

<sup>a</sup>Fifteen cases presented as two categorized results; <sup>b</sup>Six cases presented as two categorized results.

### Detection of LSIL, including koilocytosis

When atypical squamous cells of undetermined significance (ASCUS) or LSIL were identified in Pap smears, the sensitivity for LSIL detection was 80.31% (95% CI, 72.55 to 86.30) and the specificity was 68.46% (95% CI, 60.04 to 75.82). High and low-risk HPV tests (83.35%; 95% CI, 78.98 to 90.04) had higher sensitivity for detection of LSIL lesions than Pap smears; however, the CI overlapped. These results are shown in Table 2. Twenty-five cases had negative results on Pap smears (25/157, 15.92%), and 23 cases showed non-HPV infection (23/157, 14.65%). Four cases were negative by both Pap smear and HPV test (4/157, 2.55%).

### Detection of glandular lesions

For detection of adenocarcinoma in situ (AIS) or adenocarcinoma, Pap smears were an excellent diagnostic tool. The sensitivity of the Pap smear was 100% (95% CI, 86.68 to 100) and specificity was 94.68% (95% CI, 88.15 to 97.71). The sensitivity of high-risk type HPV test was 68.97% (95% CI, 50.77 to 82.72) and specificity was 54.92% (95% CI, 46.07 to 63.46). Nine cases were negative for HPV (9/30, 30%). No cases were normal on Pap smears. Among nine HPV-negative cases, four revealed adenocarcinomas of endometrial origin and five were endocervical adenocarcinomas or AIS. One endocervical AIS case was accompanied by CIS.

### False positivity of Pap smears and HPV tests

A total of 150 cases showed normal histologic results. Among them, 22 cases were diagnosed as abnormal by Pap smears (22/150, 14.67%), and high-risk HPV was detected in 44 cases (44/150, 29.33%). LSIL was the most common diagnosis from Pap smears (16 cases), followed by HSIL (three cases), atypical glandular cells (two cases), and ASC-H (one case). Of 999 total cases in this study, 16 cases had positive results on Pap smears and high-risk HPV but negative histologic results (16/999, 1.6%).

### Comparison of discrepancies between Pap smears and HPV test

Among 999 cases, 180 showed discrepancies between cytology and HPV tests. The proportion of positivity on Pap smears was higher than that in HPV tests (86.89% and 83.08%, respectively), and  $\kappa$  was 0.30 (95% CI, 0.22 to 0.37). The  $\kappa$  between Pap smears and histologic results was 0.57 (95% CI, 0.50 to 0.65). The  $\kappa$  between HPV test and histologic results was 0.31 (95% CI, 0.23 to 0.39). These results are shown in Table 3.

## DISCUSSION

The present study was performed at a single institution in Korea to evaluate the value of Pap smears and HPV DNA tests for diagnosing cervical neoplasms. Pap smears had higher sensitivity and specificity than HPV DNA tests for HSIL, SCC, and glandular lesions. The sensitivity of HPV tests for LSIL was higher than that of Pap smears; however, the difference was not significant because of overlapping CI. Odds ratios of Pap smears were higher than that of HPV tests for all histologic categories. This study showed higher sensitivity and specificity for Pap smears compared with previously reported studies (sensitivity,

**Table 2.** Sensitivity, specificity, positive LR, negative LR and OR with histologic confirmation

Histologic results	Sensitivity	Specificity	Positive LR	Negative LR	OR
SCC/HSIL					
ASC-H/HSIL/SCC on Pap smear	97.14 (95.41–98.23)	85.58 (77.56–91.06)	6.74 (4.22–10.76)	0.03 (0.02–0.05)	201.73 (96.33–422.48)
hrHPV+	88.32 (85.48–90.67)	54.92 (46.07–63.46)	1.96 (1.61–2.39)	0.21 (0.16–0.28)	9.22 (5.96–14.25)
LSIL					
ASCUS/LSIL on Pap smear	80.31 (72.55–86.30)	68.46 (60.04–75.82)	2.55 (1.95–3.33)	0.29 (0.20–0.42)	8.86 (4.99–15.71)
HPV+ <sup>a</sup>	85.35 (78.98–90.04)	44.67 (36.94–52.66)	1.54 (1.32–1.81)	0.33 (0.22–0.50)	4.7 (2.72–8.13)
AIS, adenocarcinoma					
Glandular cell abnormality on Pap smear	100 (86.68–100)	94.68 (88.15–97.71)	18.8 (8.01–44.11)	NA	NA
hrHPV+	68.97 (50.77–82.72)	54.92 (46.07–63.46)	1.530 (1.12–2.09)	0.57 (0.32–0.99)	2.71 (1.14–6.42)

Numbers in parentheses indicate 95% confidence interval.

LR, likelihood ratio; OR, odds ratio; SCC, squamous cell carcinoma; HSIL, high-grade squamous intraepithelial lesion; ASC-H, atypical squamous cells, cannot exclude HSIL; hr, high-risk; LSIL, low-grade intraepithelial lesion; ASCUS, atypical squamous cells of undetermined significance; Pap smear, Papanicolaou smear; HPV, human papillomavirus; AIS, adenocarcinoma in situ; NA, not available.

<sup>a</sup>HPV included low- and high-risk HPV types.

**Table 3.** Kappa coefficients of Pap smear, HPV and histology

	$\kappa$	Standard error of $\kappa$	95% confidence interval	The strength of agreement <sup>a</sup>
Pap smear HPV	0.30	0.04	0.22–0.37	Poor
Pap smear Histology	0.57	0.04	0.50–0.65	Fair/good
Pap smear Histology	0.31	0.04	0.23–0.39	Poor
Pap smear and/or HPV Histology	0.42	0.04	0.33–0.50	Fair/good

Pap smear, Papanicolaou smear; HPV, human papillomavirus.

<sup>a</sup>These categories were classified by Fleiss guidelines.

49%–84%; specificity, 45%–84%) [13–16]. Sensitivity and specificity of high-risk HPV tests were similar in previous studies (sensitivity, 74%–96%; specificity, 59%–80%) [13–16]. This is explained by the multiple review systems used in this study. Rules of the Clinical Laboratory Improvement Amendments (CLIA) 1988 mandated 10% random rescreening process in cases of NILM category of the Bethesda system were applied. However, many slides were actually reviewed to train pathology residents or cytotechnologists. More than one pathologist, each with more than five years of experience, reviewed almost all cases.

Most cases in this study were from the period without HPV vaccination. Quadrivalent HPV vaccines were approved in Korea in 2006, and a nationwide vaccination program was adopted in 2016. Vaccine effects require more time to stop carcinogenesis [17]. In addition, the prevalence of LSIL or HSIL in this specific hospital was higher than that in most other institutions, as reported in nationwide screening results [18]. Between 2009 and 2014, the diagnostic rates of LSIL and HSIL were 1.32% and 0.62%, respectively, at our hospital. In the Korea nationwide survey, the diagnostic rates of LSIL and HSIL were 0.24% and 0.14%, respectively [18]. There is a higher chance of encountering squamous intraepithelial lesions in the clinical field at

tertiary referral hospitals. The thorough slide review might have led to the high specificity and sensitivity of Pap smears. Furthermore, the number of detectable HPV subtypes increased with changes in HPV test kits three times, from 24 subtypes in 2006 to 38 subtypes in 2017.

The false-negative rates of HPV tests were higher than those of Pap smears for SCC, HSIL, and glandular lesions. In cases of negative HPV detection results and HSIL/SCC in surgical specimens, HPV DNA test samples were re-examined through formalin-fixed paraffin embedded blocks. In this study, 10.55% of HSIL/SCC cases (69/654) were not detected through HPV tests. Among these, 51 cases were diagnosed as ASC-H/HSIL/SCC (51/69, 73.91%) from Pap smears and 11 were diagnosed as LSIL/ASCUS (11/69, 15.94%). Only seven cases were NILM on Pap smears (7/69, 10.15%). This might have been due to a low viral load or HPV-negative squamous cell carcinoma [19–21]. It has been suggested that progression of cervical dysplasia does not require continuous HPV replication. Therefore, the degree of dysplasia does not correlate with HPV load. About 5% of SCCs are HPV-negative [21]. In the present study, HPV-negative SCCs constituted 9.65% (11/114) of SCCs. Among these, only one case showed normal cytology on Pap smear. When us-

ing Pap smear to detect SCC, the false-negative rate was 0.88%.

In this study, Pap smears proved more promising than HPV tests to detect glandular lesions. In addition, 16.6% of endocervical AIS or adenocarcinoma cases (5/30) were negative on HPV tests. These findings are in agreement with previous observations on the existence of HPV-negative endocervical adenocarcinoma (about 15%) [22]. The Pap smears and histologic slides of five cases of HPV-negative endocervical AIS/adenocarcinoma were reviewed. Three cases were endometrioid type adenocarcinoma and one was gastric type adenocarcinoma [23]. Gastric type adenocarcinoma is an HPV-unrelated cancer, and endometrioid type adenocarcinoma is commonly associated with cervical endometriosis. We did not identify cervical endometriosis in these three cases. The relationship between endocervical adenocarcinoma, endometrioid adenocarcinoma, and HPV infection is not fully understood [22-24]. One case diagnosed as cervical AIS was accompanied by squamous CIS. The negative HPV test result may have been a false-negative. Among the nine cases of HPV-negative adenocarcinoma in this study, four cases revealed an endometrial origin. These cases presented with vaginal bleeding, and Pap smears and HPV tests were initially performed with colposcopic examination. Ultrasonography and endometrial biopsy or curettage usually follow in the routine clinical setting. Endometrial dilation and curettage are performed under anesthesia; however, Pap smears are easily performed. Similar to previously reported results, we found that Pap smears were useful in detection of glandular lesions [25].

Co-testing of Pap smears and HPV yielded higher sensitivity and specificity in detection of HSIL than one test alone in some previous studies [26-28]. In the present study, sensitivity (98.91%; 95% CI, 97.75 to 99.47) was higher but specificity (44.55%; 95% CI, 35.60 to 53.86) was lower than with a single test alone. This may result from high false-positive rates in this study pool. Transient HPV infection was considered one reason for the high false-positive rate. About 90% of infections were eliminated within three years [29]. Additionally, some previously treated lesions showed atypical cells on Pap smears during the wound healing period, which may be diagnosed as ASCUS or LSIL on Pap smear. Among 20 cases of false positives on Pap smears and HPV tests, three cases were diagnosed as HSIL, and two cases demonstrated glandular cell abnormality on cytology. One case of HSIL presented with marked inflammatory cells and red blood cells on the smear; therefore, misinterpretation could have occurred due to artifact. In the two other cases of HSIL, the patient had previously undergone conization. The Pap smears and HPV tests in this study were follow-up examina-

tions, and two patients underwent repeat conization. Specimens after a second conization were small and fragmented. In addition, they had ambiguous orientation and cautery artifact, resulting in questionable histologic results. One patient diagnosed with atypical glandular cells underwent hysterectomy to treat a large leiomyoma. No grossly abnormal lesions were noted in the cervix. Therefore, only two representative sections of cervix were submitted. If all cervical tissues had been submitted and reviewed by microscopy, atypical glandular lesion may have been diagnosed. The other case of glandular cell abnormality presented as adenocarcinoma cells on Pap smear. This patient underwent conization, and additional treatment was proposed. However, the patient refused treatment. Based on these cases, the false-positive rate might be due to misdiagnosis on Pap smear or under-diagnosis on histologic examination or clinical procedures.

In this study, we found that Pap smears are still more useful than HPV DNA tests in diagnosing HSIL, SCC, and glandular lesions. Pap smears are indicated for diagnosis of non-HPV related cervical adenocarcinomas or endometrial lesions. Additionally, Pap smears may provide information on the degree of squamous dysplasia, i.e., high grade versus low grade. There are some limitations because the present study did not consider disease progression or elimination of HPV infections.

## ORCID

Myunghee Kang: <https://orcid.org/0000-0003-4083-888X>

Seung Yeon Ha: <https://orcid.org/0000-0001-7071-1623>

Hyun Yee Cho: <https://orcid.org/0000-0003-3603-5750>

Dong Hae Chung: <https://orcid.org/0000-0002-4538-0989>

Na Rae Kim: <https://orcid.org/0000-0003-2793-6856>

Jungsuk An: <https://orcid.org/0000-0003-0312-2460>

Sangho Lee: <https://orcid.org/0000-0003-4636-7521>

Jae Yeon Seok: <https://orcid.org/0000-0002-9567-6796>

Juhyeon Jeong: <https://orcid.org/0000-0002-8665-0295>

## Author Contributions

Conceptualization: SYH.

Data curation: JJ.

Formal analysis: SL.

Investigation: JYS.

Methodology: DHC.

Project administration: NRK.

Supervision: SYH, HYC.

Validation: JA.

Visualization: JYS.

Writing—original draft: MK, SYH.

Writing—review & editing: MK, SYH.

### Conflicts of Interest

S.Y.H., a contributing editor of the *Journal of Pathology and Translational Medicine*, was not involved in the editorial evaluation or decision to publish this article. All remaining authors have declared no conflicts of interest.

### Funding

This research was supported by The Korean Society for Cytopathology Grant.

## REFERENCES

- Snijders PJ, Steenbergen RD, Heideman DA, Meijer CJ. HPV-mediated cervical carcinogenesis: concepts and clinical implications. *J Pathol* 2006; 208: 152-64.
- Torre LA, Bray F, Siegel RL, Ferlay J, Lortet-Tieulent J, Jemal A. Global cancer statistics, 2012. *CA Cancer J Clin* 2015; 65: 87-108.
- Jemal A, Bray F, Center MM, Ferlay J, Ward E, Forman D. Global cancer statistics. *CA Cancer J Clin* 2011; 61: 69-90.
- Kim Y, Jun JK, Choi KS, Lee HY, Park EC. Overview of the National Cancer screening programme and the cancer screening status in Korea. *Asian Pac J Cancer Prev* 2011; 12: 725-30.
- Polman NJ, Snijders PJ, Kenter GG, Berkhof J, Meijer CJ. HPV-based cervical screening: Rationale, expectations and future perspectives of the new Dutch screening programme. *Prev Med* 2019; 119: 108-17.
- Sangrajrang S, Laowahutanont P, Wongsena M, et al. Comparative accuracy of Pap smear and HPV screening in Ubon Ratchathani in Thailand. *Papillomavirus Res* 2017; 3: 30-5.
- Ronco G, Dillner J, Elfstrom KM, et al. Efficacy of HPV-based screening for prevention of invasive cervical cancer: follow-up of four European randomised controlled trials. *Lancet* 2014; 383: 524-32.
- Tota JE, Bentley J, Blake J, et al. Introduction of molecular HPV testing as the primary technology in cervical cancer screening: acting on evidence to change the current paradigm. *Prev Med* 2017; 98: 5-14.
- US Preventive Services Task Force, Curry SJ, Krist AH, et al. Screening for cervical cancer: US Preventive Services Task Force recommendation statement. *JAMA* 2018; 320: 674-86.
- Nayar R, Wilbur DC. The Bethesda system for reporting cervical cytology: definitions, criteria, and explanatory notes. 3rd ed. Cham: Springer, 2015.
- Brown LD, Cai TT, DasGupta A. Interval estimation for a binomial proportion. *Stat Sci* 2001; 16: 101-33.
- Fleiss JL. *Statistical methods for rates and proportions*. 2nd ed. New York: John Wiley, 1981.
- Tracht J, Wrenn A, Eltoun IE. Primary HPV testing verification: a retrospective ad-hoc analysis of screening algorithms on women doubly tested for cytology and HPV. *Diagn Cytopathol* 2017; 45: 580-6.
- Costa S, Sideri M, Negri G, et al. The predictive value of human papillomavirus testing for the outcome of patients conservatively treated for stage IA squamous cell cervical carcinoma. *J Clin Virol* 2015; 70: 53-7.
- McKenna M, McMenamin MM. Human papillomavirus testing in young women: clinical outcomes of human papillomavirus triage in a UK cervical screening program. *Cancer Cytopathol* 2014; 122: 702-10.
- Pileggi C, Flotta D, Bianco A, Nobile CG, Pavia M. Is HPV DNA testing specificity comparable to that of cytological testing in primary cervical cancer screening? Results of a meta-analysis of randomized controlled trials. *Int J Cancer* 2014; 135: 166-77.
- Garland SM, Kjaer SK, Muñoz N, et al. Impact and effectiveness of the quadrivalent human papillomavirus vaccine: a systematic review of 10 years of real-world experience. *Clin Infect Dis* 2016; 63: 519-27.
- Shim SH, Kim H, Sohn IS, et al. Nationwide cervical cancer screening in Korea: data from the National Health Insurance Service Cancer Screening Program and National Cancer Screening Program, 2009-2014. *J Gynecol Oncol* 2017; 28: e63.
- Sherman ME, Wang SS, Wheeler CM, et al. Determinants of human papillomavirus load among women with histological cervical intraepithelial neoplasia 3: dominant impact of surrounding low-grade lesions. *Cancer Epidemiol Biomarkers Prev* 2003; 12: 1038-44.
- Jastania R, Geddie WR, Chapman W, Boerner S. Characteristics of apparently false-negative digene hybrid capture 2 high-risk HPV DNA testing. *Am J Clin Pathol* 2006; 125: 223-8.
- Cancer Genome Atlas Research Network, Albert Einstein College of Medicine; Analytical Biological Services, et al. Integrated genomic and molecular characterization of cervical cancer. *Nature* 2017; 543: 378-84.
- Stolnicu S, Barsan I, Hoang L, et al. International Endocervical Adenocarcinoma Criteria and Classification (IECC): a new pathogenetic classification for invasive adenocarcinomas of the endocervix. *Am J Surg Pathol* 2018; 42: 214-26.
- Hodgson A, Park KJ, Djordjevic B, et al. International endocervical adenocarcinoma criteria and classification: validation and interob-

- server reproducibility. *Am J Surg Pathol* 2019; 43: 75-83.
24. Kurman RJ, Carcangiu ML, Herrington CS, Young RH. WHO classification of tumours of female reproductive organs. 4th ed. Lyon: IARC Press, 2014.
25. Nasser H, AlAyyaf M, Atallah A, et al. Eleven-year review of data on Pap smears in Saudi Arabia: we need more focus on glandular abnormalities! *Ann Saudi Med* 2017; 37: 265-71.
26. Patanwala IY, Bauer HM, Miyamoto J, Park IU, Huchko MJ, Smith-McCune KK. A systematic review of randomized trials assessing human papillomavirus testing in cervical acancer screening. *Am J Obstet Gynecol* 2013; 208: 343-53.
27. Kitchener HC, Almonte M, Thomson C, et al. HPV testing in combination with liquid-based cytology in primary cervical screening (ARTISTIC): a randomised controlled trial. *Lancet Oncol* 2009; 10: 672-82.
28. Luyten A, Buttman-Schweiger N, Luyten K, et al. Early detection of CIN3 and cervical cancer during long-term follow-up using HPV/Pap smear co-testing and risk-adapted follow-up in a locally organised screening programme. *Int J Cancer* 2014; 135: 1408-16.
29. Sasagawa T, Takagi H, Makinoda S. Immune responses against human papillomavirus (HPV) infection and evasion of host defense in cervical cancer. *J Infect Chemother* 2012; 18: 807-15.

# Morule-like features in pulmonary adenocarcinoma associated with epidermal growth factor receptor mutations: two case reports with targeted next-generation sequencing analysis

Yoo Jin Lee, Harim Oh, Eojin Kim, Bokyung Ahn, Jeong Hyeon Lee, Youngseok Lee, Yang Seok Chae, Chul Hwan Kim

Department of Pathology, Korea University Anam Hospital, Seoul, Korea

Morules, or morule-like features, can be identified in benign and malignant lesions in various organs. Morular features are unusual in pulmonary adenocarcinoma cases with only 26 cases reported to date. Here, we describe two cases of pulmonary adenocarcinoma with morule-like features in Korean women. One patient had a non-mucinous-type adenocarcinoma *in situ* and the other had an acinar-predominant adenocarcinoma with a micropapillary component. Both patients showed multiple intra-alveolar, nodular, whorled proliferative foci composed of atypical spindle cells with eosinophilic cytoplasm. Targeted next-generation sequencing was performed on DNA extracted from formalin-fixed paraffin-embedded samples of the tumors. Results showed unusual epidermal growth factor receptor (EGFR) mutations, which are associated with drug resistance to EGFR tyrosine kinase inhibitors, revealing the importance of identifying morule-like features in pulmonary adenocarcinoma and the need for additional study, since there are few reported cases.

**Key Words:** Morule-like features; Pulmonary adenocarcinoma; Next-generation sequencing; Epidermal growth factor receptor

**Received:** April 30, 2019 **Revised:** August 28, 2019 **Accepted:** September 26, 2019

**Corresponding Author:** Chul Hwan Kim, MD, PhD, Department of Pathology, Korea University Anam Hospital, 73 Incheon-ro, Seongbuk-gu, Seoul 02841, Korea  
 Tel: +82-2-920-5595, Fax: +82-2-927-6576, E-mail: [chkap@korea.ac.kr](mailto:chkap@korea.ac.kr)

Morules, or morule-like features, can be identified in both benign and malignant lesions in various organs [1]. A subset of pulmonary adenocarcinomas show morule-like features, particularly papillary-predominant adenocarcinoma [2]. Morules can also be identified in adenocarcinoma *in situ* (AIS); previously known as bronchioloalveolar carcinoma [3]. One case in this report showed morule-like features in AIS and the other case showed these features in invasive adenocarcinoma. Using next-generation sequencing (NGS), we attempted to identify the molecular characteristics of these rare morular features in the two cases.

## CASE REPORT

The Institutional Review Board of Korea University Anam Hospital (2018AN0182) approved this study, and we received informed consent from both patients.

### Case 1

A healthy, 78-year-old Korean woman was admitted to the

hospital with an incidental mass in the left lung. The computed tomography (CT) scan of the left upper lung showed a sub-solid nodule measuring 23 mm in diameter, suggestive of AIS or minimally invasive adenocarcinoma. The patient had no surgical history, had never smoked, and was relatively healthy. A segmentectomy was performed to remove the pulmonary mass. Grossly, the resected lung measured 10.3×5.3×4.5 cm and weighed 30 g in total. The pleural surface of the mass was smooth. The tumor measured 2.2×1.8 cm, was fibrotic and whitish and grey colored without hemorrhage or necrosis, and did not involve the pleura. Hematoxylin and eosin-stained histology sections showed lepidic growth of atypical columnar cells with enlarged nuclei and irregular nuclear contours (Fig. 1A). There were multiple intra-alveolar nodular proliferative foci composed of atypical spindle cells with eosinophilic cytoplasm (Fig. 1B). Cells in the nodular proliferative lesions were arranged in a whorled pattern, normally interpreted with a squamoid appearance, yet obvious squamous differentiation was not seen. The underlying pulmonary architecture was preserved, which suggested that stromal invasive foci

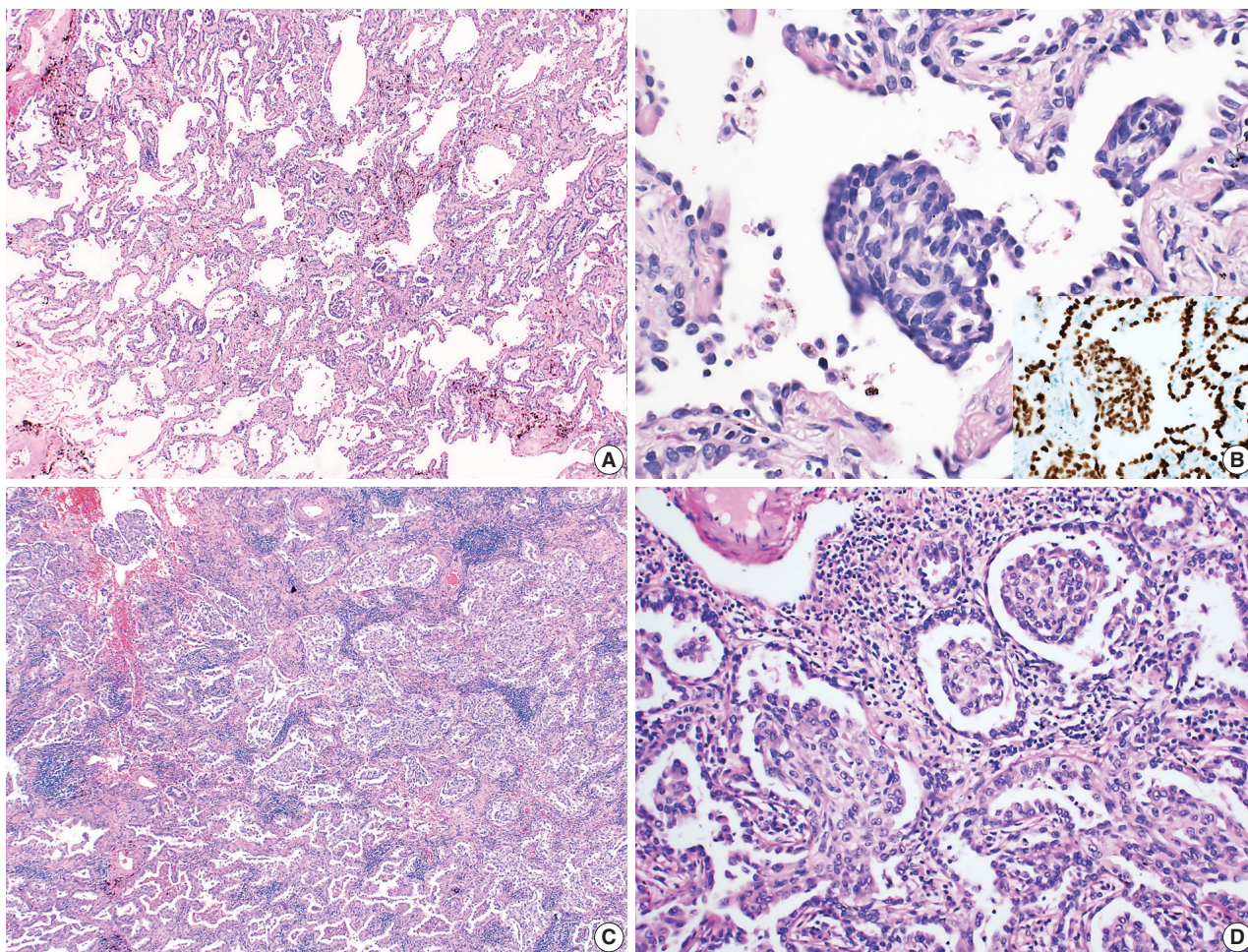


**Fig. 1.** Microscopic findings of the tumor. (A) The case of adenocarcinoma in situ shows lepidic growth of atypical columnar cells without definite evidence of stromal invasion. (B) Multiple nodular proliferative lesions in intra-alveolar spaces. The cells in those structures are atypical spindle cells that are positive for thyroid transcription factor 1 immunostaining (inset). (C) The acinar-predominant adenocarcinoma case shows multiple foci of morule-like components (D) floating within the intra-alveolar space.

were not present. Neither lymphovascular nor pleural invasion was evident; therefore, the final diagnosis was non-mucinous type AIS. Upon immunohistochemistry, the cells forming morule-like features were positive for thyroid transcription factor 1 (TTF-1) and cytokeratin (CK), but negative for p40, CDX-2, neuron-specific enolase, chromogranin, and synaptophysin (Fig. 1B, inset). There were no remarkable features in normal lung tissue. We also performed NGS analysis and revealed an insertion in epidermal growth factor receptor (*EGFR*) exon 20 (NM\_001346897.1: c.2180\_2185dup) with 35.5% mutation abundance. There was no evidence of recurrence or metastasis at 1-year follow-up.

## Case 2

A healthy, 46-year-old Korean woman was admitted to the

hospital with an incidental mass in one lung. The CT scan of the right lower lung showed a sub-solid nodule measuring 29 mm in diameter with a 12-mm-sized solid portion. The mass was associated with apical pleural thickening, suggestive of a malignant tumor with pleural invasion. The patient had no surgical history, had never smoked, and was relatively healthy. A lobectomy was performed to remove the sub-solid nodule from the right lower lung. Grossly, the resected lung specimen was 16.9×14.5×4.3 cm. The pleural surface showed umbilicated foci, suggestive of pleural invasion. Upon sectioning, the cut surface showed an ill-demarcated, whitish-grey, fibrotic mass measuring 2.7×1.3 cm with pleural invasion. Upon microscopic examination, the tumor was identified as an acinar-predominant adenocarcinoma with a micropapillary component. In the region of the acinar-predominant adenocarcinoma, multiple

morule-like foci were identified floating within the intra-alveolar space without clear evidence of squamous differentiation (Fig. 1C, D). In accordance with the gross findings, visceral pleural invasion was confirmed by microscopy. Lymphatic invasion was also evident, yet there was no lymph node metastasis. Additional studies were performed to determine molecular characteristics of the morule-like component. Fluorescent in situ hybridization for anaplastic lymphoma kinase (*ALK*) gene rearrangement was performed on a preoperative diagnostic needle biopsy specimen and showed split signals in four out of 100 analyzed cancer cells, indicating the absence of *ALK* rearrangement. We performed NGS analysis on a formalin-fixed paraffin-embedded section of a surgical specimen, and a L747S missense mutation was detected in *EGFR* exon 19 (NM\_005228.3: c.2240T > C) with 24.8% mutation abundance. There was no recurrence or metastasis at 1-year follow-up.

## DISCUSSION

Adenocarcinoma with morule-like features is a rare variant of lung adenocarcinoma, accounting for 1.9% of all adenocarcinomas [2]. To date, 26 cases of lung adenocarcinoma with morule-like features have been reported [1-5] that were reported as papillary (15 cases), micropapillary (3 cases), acinar (3 cases), and solid-predominant adenocarcinoma (3 cases). The remaining two cases were adenocarcinoma with a lepidic pattern [2], and bronchioloalveolar carcinoma (AIS) [3].

Histologically, the cells comprising the morular feature were spindle shaped and distinct from the other cancer cells. There are several possibilities to explain the pathophysiology of this unusual morular component. Traditionally, morules have been reported in pulmonary blastoma and well-differentiated fetal adenocarcinoma, and are regarded as non-epithelial cell clusters showing neuronal differentiation [1,6]. However, morular cells in the cases reported here were positive for pulmonary epithelial markers, including CK and TTF-1, but negative for neuroendocrine markers, consistent with several other reports [1-3,5]. As such, they can be considered a complex glandular component, or epithelial cell nodules. Therefore, the presence of a morular component in small biopsy specimens does not, by itself, indicate pulmonary blastoma and immunohistochemistry can help to determine the likelihood of epithelial carcinoma. Furthermore, although the morular cells are spindle shaped, Moran et al. [5] reported that negative results for muscle markers and human melanoma black-45 reduce the probability of smooth muscle tumor and lymphangioliomyomatosis.

Fornelli et al. [3] reported the first case of AIS with morule-like features as a non-invasive tumor because both architectural complexity and stromal desmoplasia were not apparent. Fornelli's case is the only report currently available in the literature, making our reported cases the second study of AIS showing morule-like features. Tsuta et al. [2] found that lung adenocarcinomas with morule-like features have lower 5-year overall survival rates, suggesting that morule-like features are an invasive component similar to an aggressive histologic micropapillary pattern. On the other hand, one report suggested that the morular feature itself might not have prognostic significance [7], and the invasion criteria for the pulmonary adenocarcinoma used in World Health Organization 2015 classification of tumors of the lung, pleura, thymus, and heart does not include morular features. Therefore, if there is no other evidence of stromal invasion, AIS with morular features should be evaluated separately from the invasive adenocarcinoma. This case of AIS did not show any evidence of recurrence or metastasis at 1-year follow-up; however, further studies of AIS with morule-like features are needed.

Depending on the observer, morular like components filling the intra-alveolar space can be considered as an invasive lesion, or an airspace invasion forming a solid nest. From that point of view, case 1 described here can be diagnosed as lepidic predominant adenocarcinoma, as morular portion size is 0.7 cm in maximum diameter. However, further research will be needed as some argue that there is no prognostic significance [7].

The molecular characteristics of the morular component are not fully understood. However, several studies have revealed that this feature is associated with *EGFR* mutations. In a previous report that analyzed two common *EGFR* mutations, including deletions in exon 19 and a point mutation at codon 858 in exon 21 (L858R), the presence of morule-like components correlated with *EGFR* mutations, particularly deletions, and was reported to be an independent predictive factor of *EGFR* mutation status [2]. Another report by Tajima and Koda [4] found that morule-like features were associated with a deletion mutation at exon 19 in *EGFR*. Ours is the first report in which NGS was used to identify the molecular characteristics of morule-like features in pulmonary adenocarcinoma. Our results revealed unusual *EGFR* mutations that have not been previously reported in pulmonary adenocarcinoma with morule-like features. The rare mutation in *EGFR* exon 19 and the insertion mutation in *EGFR* exon 20 can be associated with drug resistance to *EGFR* tyrosine kinase inhibitors [8-10], implying the importance of identifying morule-like features in pulmonary adenocarcinoma.

Morule-like components are a rare histologic feature of pulmonary adenocarcinoma, which may be associated with rare *EGFR* mutations, such as the L747S missense mutation of exon 19 or an insertion mutation in exon 20. The presence of morule-like features without definite invasive components led to the diagnosis of AIS in one of these cases, as it is not yet clear whether this feature needs to be considered as an invasive component. Additional studies are needed to clarify the significance of this rare histologic variant in pulmonary adenocarcinoma.

### ORCID

Yoo Jin Lee: <https://orcid.org/0000-0003-3830-7051>  
 Harim Oh: <https://orcid.org/0000-0003-4904-4015>  
 Eojin Kim: <https://orcid.org/0000-0003-3111-6754>  
 Bokyoung Ahn: <https://orcid.org/0000-0002-0229-2276>  
 Jeong Hyeon Lee: <https://orcid.org/0000-0003-2041-4617>  
 Youngseok Lee: <https://orcid.org/0000-0002-9762-4957>  
 Yang Seok Chae: <https://orcid.org/0000-0002-8801-0910>  
 Chul Hwan Kim: <https://orcid.org/0000-0003-2026-8824>

### Author Contributions

Conceptualization: YJL, CHK.  
 Data curation: EK, BA.  
 Investigation: YJL, HO.  
 Project administration: YJL, JHL.  
 Resources: YL, YSC.  
 Supervision: YSC, CHK.  
 Validation: YL, YSC.  
 Visualization: YJL, JHL.  
 Writing – original draft: YJL.  
 Writing – review & editing: CHK.

### Conflicts of Interest

The authors declare that they have no potential conflicts of interest.

### Funding

No funding to declare.

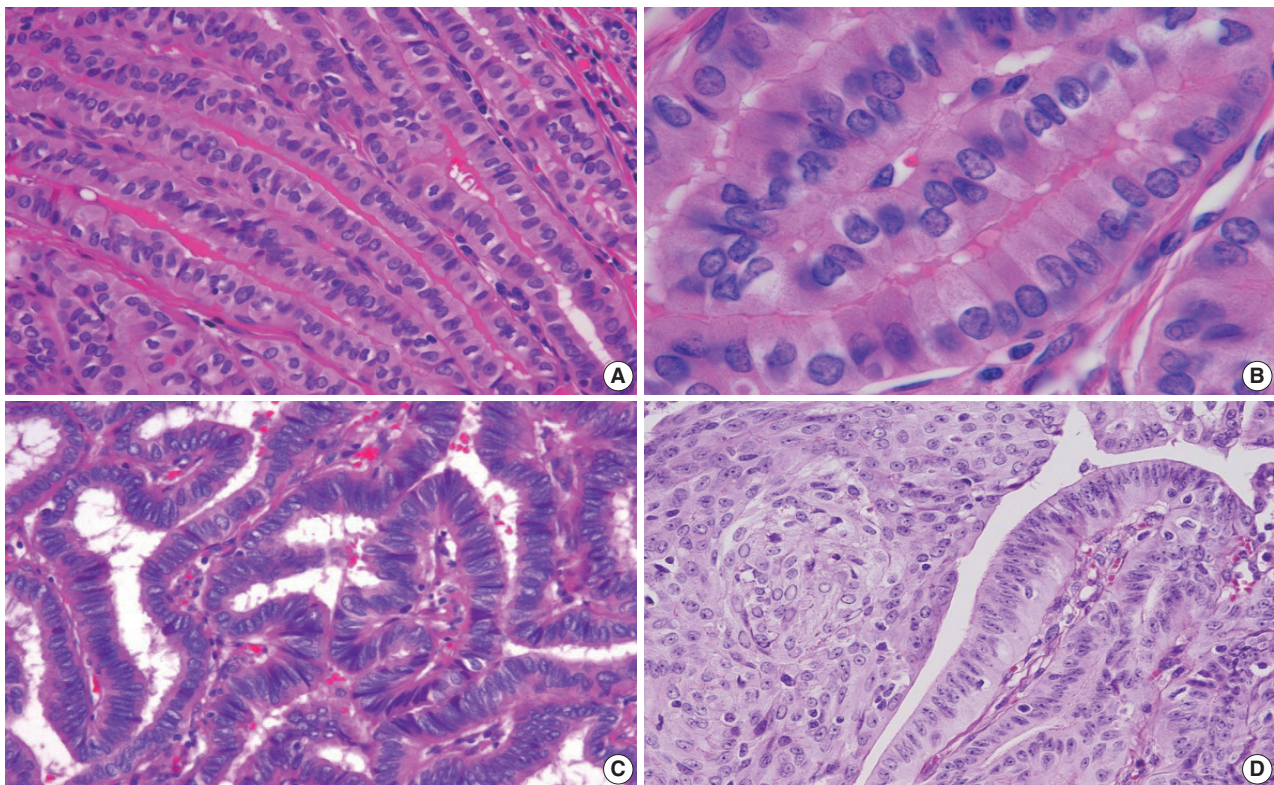
## REFERENCES

1. Makishi S, Kinjo T, Sawada S, et al. Morules and morule-like features associated with carcinomas in various organs: report with immunohistochemical and molecular studies. *J Clin Pathol* 2006; 59: 95-100.
2. Tsuta K, Kawago M, Yoshida A, et al. Primary lung adenocarcinoma with morule-like components: a unique histologic hallmark of aggressive behavior and *EGFR* mutation. *Lung Cancer* 2014; 85: 12-8.
3. Fornelli A, Cavazza A, Cancellieri A, Rossi G, De Marco L. Bronchioloalveolar carcinoma with nodular ("morule-like") features. *Virchows Arch* 2003; 442: 407-8.
4. Tajima S, Koda K. Transition between morule-like and solid components may occur in solid-predominant adenocarcinoma of the lung: report of 2 cases with *EGFR* and *KRAS* mutations. *Int J Clin Exp Pathol* 2015; 8: 7475-81.
5. Moran CA, Jagirdar J, Suster S. Papillary lung carcinoma with prominent "morular" component. *Am J Clin Pathol* 2004; 122: 106-9.
6. Nakatani Y, Masudo K, Miyagi Y, et al. Aberrant nuclear localization and gene mutation of beta-catenin in low-grade adenocarcinoma of fetal lung type: up-regulation of the Wnt signaling pathway may be a common denominator for the development of tumors that form morules. *Mod Pathol* 2002; 15: 617-24.
7. Matsukuma S, Obara K, Kato K, et al. Non-sarcomatous spindle cell morphology in conventional lung adenocarcinoma: a clinicopathological study. *Virchows Arch* 2014; 465: 165-72.
8. Suda K, Mizuuchi H, Maehara Y, Mitsudomi T. Acquired resistance mechanisms to tyrosine kinase inhibitors in lung cancer with activating epidermal growth factor receptor mutation: diversity, ductility, and destiny. *Cancer Metastasis Rev* 2012; 31: 807-14.
9. Yamaguchi F, Fukuchi K, Yamazaki Y, et al. Acquired resistance L747S mutation in an epidermal growth factor receptor-tyrosine kinase inhibitor-naive patient: a report of three cases. *Oncol Lett* 2014; 7: 357-60.
10. Yasuda H, Kobayashi S, Costa DB. *EGFR* exon 20 insertion mutations in non-small-cell lung cancer: preclinical data and clinical implications. *Lancet Oncol* 2012; 13: e23-31.

## Papillary thyroid carcinoma variants with tall columnar cells

Chan Kwon Jung

Department of Hospital Pathology, College of Medicine, The Catholic University of Korea, Seoul, Korea



Tall columnar cells can be seen in different variants of papillary thyroid carcinoma (PTC). Tall cell variant of PTC shows elongated and closely packed follicles lined by a single layer of tall cells producing a so-called “tram-track” appearance (A). High-power view showing tall cells (at least twice as tall as wide) with nuclear features of PTC, intensely eosinophilic cytoplasm, and sharply delineated cell borders. The nuclei are basally located (B). Columnar cell variant of PTC shows tightly packed papillae lined by pseudostratified tall columnar cells with elongated dark nuclei. The nuclear features of PTC are not evident (C). Cribriform-morular variant of PTC showing pseudostratified tall columnar cells with abundant eosinophilic cytoplasm and elongated dark nuclei. The solid area shows a small whorl (morule) of squamoid tumor cells with peculiar nuclear clearing (D).

Received: December 15, 2019 Accepted: December 17, 2019

**Corresponding Author:** Chan Kwon Jung, MD, PhD  
 Department of Hospital Pathology, Seoul St. Mary's Hospital, College of Medicine,  
 The Catholic University of Korea, 222 Banpo-daero, Seocho-gu, Seoul 06591, Korea  
 Tel: +82-2-2258-1622, Fax: +82-2-2258-1627, E-mail: ckjung@catholic.ac.kr

### ORCID

Chan Kwon Jung: <https://orcid.org/0000-0001-6843-3708>

### Conflicts of Interest

C.K.J. is the editor-in-chief of *Journal of Pathology and Translational Medicine*.

